



694
2016

Berichte

zur Polar- und Meeresforschung

Reports on Polar and Marine Research

The Expedition PS92 of the Research Vessel POLARSTERN to the Arctic Ocean in 2015

Edited by

Ilka Peeken

with contributions of the participants

Die Berichte zur Polar- und Meeresforschung werden vom Alfred-Wegener-Institut, Helmholtz-Zentrum für Polar- und Meeresforschung (AWI) in Bremerhaven, Deutschland, in Fortsetzung der vormaligen Berichte zur Polarforschung herausgegeben. Sie erscheinen in unregelmäßiger Abfolge.

Die Berichte zur Polar- und Meeresforschung enthalten Darstellungen und Ergebnisse der vom AWI selbst oder mit seiner Unterstützung durchgeführten Forschungsarbeiten in den Polargebieten und in den Meeren.

Die Publikationen umfassen Expeditionsberichte der vom AWI betriebenen Schiffe, Flugzeuge und Stationen, Forschungsergebnisse (inkl. Dissertationen) des Instituts und des Archivs für deutsche Polarforschung, sowie Abstracts und Proceedings von nationalen und internationalen Tagungen und Workshops des AWI.

Die Beiträge geben nicht notwendigerweise die Auffassung des AWI wider.

Herausgeber

Dr. Horst Bornemann

Redaktionelle Bearbeitung und Layout

Birgit Reimann

Alfred-Wegener-Institut
Helmholtz-Zentrum für Polar- und Meeresforschung
Am Handeshafen 12
27570 Bremerhaven
Germany

www.awi.de

www.reports.awi.de

Der Erstautor bzw. herausgebende Autor eines Bandes der Berichte zur Polar- und Meeresforschung versichert, dass er über alle Rechte am Werk verfügt und überträgt sämtliche Rechte auch im Namen seiner Koautoren an das AWI. Ein einfaches Nutzungsrecht verbleibt, wenn nicht anders angegeben, beim Autor (bei den Autoren). Das AWI beansprucht die Publikation der eingereichten Manuskripte über sein Repositorium ePIC (electronic Publication Information Center, s. Innenseite am Rückdeckel) mit optionalem print-on-demand.

The Reports on Polar and Marine Research are issued by the Alfred Wegener Institute, Helmholtz Centre for Polar and Marine Research (AWI) in Bremerhaven, Germany, succeeding the former Reports on Polar Research. They are published at irregular intervals.

The Reports on Polar and Marine Research contain presentations and results of research activities in polar regions and in the seas either carried out by the AWI or with its support.

Publications comprise expedition reports of the ships, aircrafts, and stations operated by the AWI, research results (incl. dissertations) of the Institute and the Archiv für deutsche Polarforschung, as well as abstracts and proceedings of national and international conferences and workshops of the AWI.

The papers contained in the Reports do not necessarily reflect the opinion of the AWI.

Editor

Dr. Horst Bornemann

Editorial editing and layout

Birgit Reimann

Alfred-Wegener-Institut
Helmholtz-Zentrum für Polar- und Meeresforschung
Am Handeshafen 12
27570 Bremerhaven
Germany

www.awi.de

www.reports.awi.de

The first or editing author of an issue of Reports on Polar and Marine Research ensures that he possesses all rights of the opus, and transfers all rights to the AWI, including those associated with the co-authors. The non-exclusive right of use (einfaches Nutzungsrecht) remains with the author unless stated otherwise. The AWI reserves the right to publish the submitted articles in its repository ePIC (electronic Publication Information Center, see inside page of verso) with the option to "print-on-demand".

Titel: FS Polarstern, wie es langsam während der 4ten Eisstation vom Meereis eingeschlossen wird. (Foto von Ilka Peeken, Alfred-Wegener-Institut, 7. Juni 2015).

Cover: RV Polarstern slowly enclosed by sea ice during the 4th ice station. (picture taken by Ilka Peeken, Alfred Wegener Institute, 7 June 2015).

Cover: RV Polarstern

The Expedition PS92 of the Research Vessel POLARSTERN to the Arctic Ocean in 2015

Edited by

Ilka Peeken

with contributions of the participants

Please cite or link this publication using the identifiers

hdl:10013/epic.46750 or <http://hdl.handle.net/10013/epic.46750>

doi:10.2312/BzPM_0694_2016

ISSN 1866-3192

PS92

(ARK-XXIX/1)

19 May 2015 – 28 June 2015

Bremerhaven – Longyearbyen

**Chief scientist
Ilka Peeken**

**Coordinator
Rainer Knust**

Contents

1.	Zusammenfassung und Fahrtverlauf	3
	Summary and Itinerary	11
2.	Weather Conditions	15
3.	Activities of the Sea Ice Physics Group during PS92	18
3.1	AEM bird ice thickness measurements	18
3.2	Ground-based ice thickness and snow measurements	21
3.3	Airborne digital video camera survey of surface properties	23
3.4	Snow temperature and grain size evolution	25
3.5	ROV work and optical properties of sea ice	26
3.6	Ice observations	28
4.	Physical Oceanography	29
5.	Trace Gases and Carbonate Chemistry	44
5.1.	Trace gases	44
5.2	Water column carbonate chemistry	47
6.	Geochemistry	49
6.1	Organic biomarkers in suspended particles	49
6.2.	Water mass signatures ($\delta^{18}\text{O}$, $\delta^{13}\text{C}_{\text{DIC}}$)	51
6.3.	Suspended particulate matter (SPM)	53
6.4.	Dissolved neodymium isotopes and rare earth elements	54
6.5	Source and transformations of chromophoric dissolved organic matter and its role in surface ocean heating	57
7.	Sea Ice Biota	65
7.1	Ecological consequences of climate change in the Transpolar Drift region	65
7.2	Heterotrophic microbial activity and the fate of ice associated production	77
8.	Sea Ice Ecology, Pelagic Food Web and Copepod Physiology - Iceflux / PEBCAO	81
9.	Ecosystems	91
9.1	Nutrients, primary production and nitrogen cycling (GREENEDGE)	91
9.2	Distribution patterns of protists with special emphasis on toxic dinoflagellates in the North Atlantic and Arctic Waters	96

9.3	Nitrogen cycling and microbial ecology in the Arctic: measurements of dinitrogen fixation rates, characterization of diazotroph assemblages, and nifH gene expression	102
9.4	Vertical export	106
9.5	Watercolumn biogeochemistry	109
9.6	Benthos ecology	110
10.	Geology and Paleoceanography	113
10.1	Parasound and Hydrosweep	116
10.2	Sediment coring	118
10.3	Multi-sensor core logging	123
10.4	Inorganic geochemistry	125
10.5	Water column and sea ice studies	128
	Appendix	135
A.1	Teilnehmende Institute / Participating Institutions	136
A.2	Fahrtteilnehmer / Cruise Participants	140
A.3	Schiffsbesatzung / Ship's Crew	142
A.4	Stationsliste PS92 / Station List	144

1. ZUSAMMENFASSUNG UND FAHRTVERLAUF

Ilka Peeken

AWI

Am 19. Mai verließ das Forschungsschiff *Polarstern* Bremerhaven, um eine sechswöchige Expedition im arktischen Ozean durchzuführen. Diese Expedition wurde von dem ART Team initiiert, ART steht für „Arctic in Rapid Transition“. Die Expedition PS92 (ARK-XXIX/1) „TRANSSIZ“ („Transitions in the Arctic Seasonal Sea Ice Zone“, Abb. 1.1) hat Prozessstudien zur Produktivität, sowie zur Dynamik des Ökosystems und biogeochemischer Stoffkreisläufe im Frühjahr vom Schelf bis in die Tiefsee am Kontinentalrand der Europäischen Arktis und auf dem Yermak Plateau durchgeführt. Ziel war es, die Veränderungen der Meereisausdehnung im Arktischen Ozean in der Vergangenheit mit denen der Gegenwart zu verknüpfen. Auf der Expedition waren WissenschaftlerInnen aus 11 Ländern vertreten, die gemeinsam mit Forschergruppen aus allen Forschungsbereichen des AWI und WissenschaftlerInnen des BMBF-Projektes „Transdrift“, sowie des französisch-kanadischen Projektes „GreenEdge“ Prozessstudien durchführten. Während der Expedition hat das Schiff 3.665 sm zurückgelegt und es wurden 68 Stationen mit insgesamt 242 Geräteinsätzen durchgeführt. Einige Arbeitsgruppen hatten bereits die Anfahrt in das Untersuchungsgebiet genutzt, um die meridionalen Unterschiede von Spurengasen, Algen und Nährstoffen entlang unserer Fahrtroute von den gemäßigten zu den eisbedeckten polaren Breiten hin zu untersuchen.



Abb. 1.1: Das Expeditionslabel TRANSSIZ (@Ilias Nasis, modified Hauke Flores)

Fig. 1.1: The expedition label TRANSSIZ (@Ilias Nasis, modified Hauke Flores)

Nach dem Erreichen des Untersuchungsgebiets wurden Prozessstudien durchgeführt, die Ratenmessungen von Produktivität und Wechselbeziehungen zwischen Ökosystemen und den Kreisläufen von Kohlenstoff- und Stickstoff beinhalteten. Durch den Vergleich der Daten vom Schelf über die Schelfkante bis in die arktischen Tiefseebecken wurde der Kohlenstoffexport von pelagischen und Meereisgemeinschaften bestimmt. Ziel war es, Produktivitätsregime zu vergleichen, um mögliche Eigenschaften der Primärproduktion und des Kohlenstoffexportes nach Ähnlichkeiten und Unterschieden entlang von topographie- und wassermassenbezogenen Gradienten zu identifizieren.

Auf den Meereisstationen wurde ein Standard-Set von Meereiskernen sowohl für biologische, physikalische und chemische Variablen und Spurengase, als auch für die Validierung von geologischen Proxys genommen. Des Weiteren wurden die Meereiseigenschaften untersucht und das Untereiswasser beprobt. Im Wasser wurden Spuren- und Treibhausgase sowie Biodiversität untersucht, sowie die primäre und bakterieller Produktion und Aspekte des Stickstoffkreislaufs bestimmt. Kurzzeitverankerungen wurden unter dem Eis eingesetzt, um den vertikalen Kohlenstofffluss zu bestimmen. Ein kabelgesteuerter Tauchroboter („Remotely Operated Vehicle“, ROV) wurde unter dem Eis eingesetzt, um spektrale Strahlungsmessungen durchzuführen. Zusätzlich wurden weitere Umweltparameter (z.B. Eisdicke, Salzgehalt, Temperatur) gemessen und mit Hilfe einer Video-Kamera am ROV wurde die Untereistopographie aufgezeichnet. Die unter dem Eis lebenden Tiere und andere Umweltparameter wurden mit Hilfe eines Untereis-Schleppnetzes („Surface and Under-Ice Trawl“, SUIT) an verschiedenen Stationen auf und zwischen den Eisstationen beprobt.



Abb. 1.2: Aktivitäten während einer Eisstation; im Vordergrund die ROV-Hütte und das Dreibein für die Kurzzeitverankerung (@ Sascha Willmes)

Fig. 1.2: Activities during an ice station; in the front the ROV-hut and the tripod for the short term mooring. (@ Sascha Willmes)

Ergänzend zu den Arbeiten auf den Meereisstationen wurde mit Hilfe eines EM-Birds die Meereisdicke entlang der Fahrtroute bestimmt. Mit durchschnittlich nur 1,4 m war die Eisdicke für das Frühjahr vergleichsweise gering; ähnliche Eisdicken wurden in der Framstrasse im Sommer gemessen. Parallel zu den Eisstationen wurden Proben zur Untersuchung der pelagischen und benthischen Lebensgemeinschaften genommen und ein geologisches Messprogramm durchgeführt. Lichtspektren wurden mit einem Hyperspektral

Radiometer gemessen, um die Eindringtiefe der ultravioletten Strahlung in unterschiedliche Wasserschichten zu bestimmen. Das Gerät wurde vom Schlauchboot aus eingesetzt. Der Kranwasserschöpfer wurde eingesetzt, um chemische und biologische Proben zu gewinnen, sowie um Proben für die Kalibrierung geologischer Proxys zu erhalten. Ein Unterwasser-Video-Aufnahmegerät wurde eingesetzt, um detaillierte Vertikalprofile der Partikelverteilung, der Größe und der Zusammensetzung zu erhalten sowie um Zooplankton zu bestimmen. Quantitative Untersuchungen der Mesozooplanktongemeinschaft sowie der Foraminiferen, die auch als Paläo-Proxys dienen, wurden mit Multi-Netzen durchgeführt. Für Studien an der Makrozooplankton- und Nektongemeinschaft wurde ein mehrfach schließendes pelagisches Schleppnetz („Multiple-closing Rectangular Midwater Trawl“, MRMT) eingesetzt. Die Verteilung des Makrozooplanktons und der pelagischen Fische wurde im Untersuchungsgebiet kontinuierlich mit dem EK60 Echolot der *Polarstern* aufgezeichnet. Benthos Organismen wurden mit Hilfe eines Kastengreifers gesammelt und die Sedimentproben auch weiterhin für Experimente und für biogeochemische Analysen einschließlich der Bestimmung von Meereis- und Paläo-Proxys verwendet. Benthische Organismen zeigten eine Abnahme der Respiration vom Schelf zu den Tiefseegemeinschaften.



Abb. 1.3. Eine Momentaufnahme des Meeresbodens nördlich von Spitzbergen aufgenommen mit dem Online-Kamerasystem des Multicorers (@Jutta Wollenburg).

Fig. 1.3: A snapshot of the sea floor north of Spitzbergen, taken by the online camera system attached to the Multicorer (@Jutta Wollenburg).

Ungestörte Oberflächensedimente für die Geologie wurden mit Hilfe des TV-Multicorers gewonnen (Abb. 1.3). Die geologischen Kernpositionen wurden anhand von detaillierten Kartierungen (Hydrosweep und Parasound) ausgewählt. Die durchgeführten bathymetrischen Messungen haben für bisher unbekannte Regionen neue hochauflösende Meeresboden Karten und Informationen zur Sedimentbeschaffenheit entlang der Fahrtroute und von den Kernpositionen geliefert. Kerne wurden mit Hilfe des Kastenlotes und Schwerelots gewonnen. Ein besonderer Wert wurde bei dieser Expedition auf die Bestimmung und Quantifizierung der Umweltbedingungen (z.B. Nährstoffe, Schichtung) für die Produktivität gelegt, um die potenzielle jährliche Primärproduktion in einem zukünftigen eisfreien Arktischen Ozean vorherzusagen zu können. Diese Expedition wird weiterhin dazu beitragen, Veränderungen in der Produktivität, des

Meereises und der Ozean-Zirkulation während des letzten Glazialzyklus zu untersuchen. Ein weiterer Schwerpunkt war die Untersuchung der Wechselwirkungen der Ökosystemfunktionen und der Stoffkreisläufe während des Überganges vom Frühjahr zum Sommer. Die Expedition endete am Morgen des 28. Juni 2015 in Longyearbyen.

Fahrtverlauf

Die Expedition „Transitions in the Arctic Seasonal Sea Ice Zone“ PS92 (ARK-XXIX/1) begann am 19.05.2015 in Bremerhaven. Nach 3 Tagen wurde die Norwegen See erreicht, wo bei 65° 12,52' N, 3° 36,91' E der erste Test für eine U-CTD(Underway-CTD) durchgeführt wurde.

Auf dem Weg nach Norden wurde das hydrographische Programm mit weiteren U- und XCTDs fortgesetzt. Am Abend des 23.05 verließen wir unseren Kurs und begaben uns Richtung Tromsø, um ein krankes Besatzungsmitglied zur medizinischen Weiterbehandlung in ein Krankenhaus auszufliegen. Bereits einen Tag später konnten wir unseren Kurs nach Norden weiter fortsetzen. Ab $70^{\circ} 51,90' \text{ N}$, $13^{\circ} 41,46' \text{ E}$ wurde das Programm aus U- und XCTDs weiter fortgesetzt, bis wir am 26.05. den ersten Test-Kranzwasserschöpfer auf der Position $77^{\circ} 4,35' \text{ N}$, $9^{\circ} 31,20' \text{ E}$ durchgeführt haben. Die U- und XCTD Messungen wurden dann bis zum Erreichen des Untersuchung Gebiets nördlich von Svalbard fortgesetzt, bis wir am 27.05. auf dem Barents-See Schelf die erste Eisstation bei $81^{\circ} 0,48' \text{ N}$, $19^{\circ} 54,49'$ bei einer Wassertiefe von 200 m erreicht hatten. Während der Nacht wurde der Einsatz der geschleppten Netze wie SUIT und RMT getestet (Abb. 1.4), und danach eine Aufnahme der Sedimentbeschaffenheit mit Hydrosweep und Parasound gefahren.

Die erste Eisstation fand an einer großen Eisscholle bei $81^{\circ} 10,43' \text{ N}$, $19^{\circ} 8,07' \text{ E}$ und bei einer Wassertiefe von 370 m bis zum 29. Mai statt. Prozessstudien, bei denen *Polarstern* über ca. 36 Stunden an einer Eisscholle verankert war, bildeten einen Schwerpunkt dieser Expedition. Ca. 70 % der WissenschaftlerInnen an Bord waren daran mit ihren Forschungen beteiligt. Während das Schiff mit der Scholle gedriftet war, fanden parallel die Probennahme für ozeanographische, chemische, pelagische, benthische und geologische Variablen aus dem Wasser mit Hilfe des Kranzwasserschöpfers (CTD) statt. Weiterhin kamen ein Compact Optical Profiling System, ein Underwater Video Profiler, eine *in-situ* Pumpe, sowie Plankton-Netze und ein Kastengreifer zum Einsatz. Zu Beginn einer Station wurde eine CTD gefahren, um Wasserproben für Experimente zur Untersuchung des Nährstoffkreislaufes zu erhalten. Diese Proben wurden dann in eine Kurzzeit-Verankerung integriert, die am Rand der Eisscholle mit einem Schlauchboot ausgebracht wurden. Die Arbeiten auf dem Meereis liefen in der Regel wie folgt ab: Das physikalische Meereissteam setzte ein Unterwasserfahrzeug (ROV) ein, mit dem die optischen Eigenschaften des Meereises untersucht wurden. Außerdem wurden Eis und Schneeeigenschaften dokumentiert. Das hydrographische Team hatte ein ADCP für die Messungen von Strömungen während der ganzen Eisstation verankert. Eine Mikrostruktursonde wurde benutzt, um Vermischungsprozessen im Wasser zu studieren. Da das Gerät manuell bedient wurde, wurde in der Regel mindestens ein Tidenzyklus beprobt. Das Meereis-Eiskernteam hatte die Probennahme für die verschiedenen Forschungsgruppen koordiniert und die Eiskerne gebohrt und zusätzlich das Untereiswasser beprobt. Auf der ersten Eis-Station dominierten Diatomeen mit einer vergleichsweise hohen Phytoplankton Biomasse. Da wir durch das Driften der Scholle während der Expedition eine Wassertiefe von 600 m erreicht hatten, wurde noch eine zusätzliche südlichere Station bei $81^{\circ} 1,86' \text{ N}$, $19^{\circ} 21,71'$ durchgeführt, um Benthosproben vom flachen Schelf zu erhalten. Nach dieser Station wurde der erste Versuch unternommen, das Zielgebiet bei 30° Ost zu erreichen, was leider durch eine massive Eisscholle blockiert wurde. Diese Scholle erlaubte es auch nicht, einen geraden Schnitt bei 20° Ost durchzuführen, so dass wir nachfolgend nur noch Tiefen für den darauffolgenden hydrographischen Schnitt und das RMT benutzt haben, bis wir die nächste Eisstation bei $81^{\circ}23.18' \text{ N}$ $17^{\circ} 35,66' \text{ E}$ (850 m Tiefe) erreichten.



Abb. 1.4: Das RMT as it is being hauled in. All nets are closed. (@ Fokje Schaafsma)

Fig. 1.4.: Das RMT wird eingeholt. Alle Netze sind geschlossen. (@ Fokje Schaafsma).



Abb. 1.5: Blick auf eine Sedimentfalle, die in 90 m Wassertiefe verankert war. Auf dem Boden des Gefäßes sind die herab gesunkenen Partikel zu erkennen (@SChristine Dybwad)

Fig. 1.5.: A sediment trap, deployed at 90 m after recovery. On the bottom of the cylinder the trapped sinking particles are visible (@ Christine Dybwad)

Die zweite Eisstation begann am 31.5. und wurde zuvor mit einem SUIT begonnen. Ab dieser Station wurde die Kurzzeitverankerung (Abb. 1.5) durch ein Eisloch ausgebracht.

Interessanterweise war hier die Phytoplanktongemeinschaft von der Schaumalge *Phaeocystis* dominiert. Um die Drift der Scholle auszugleichen, wurde das Schiff noch einmal verholt und die benthischen Arbeiten am 1.6. beendet. Ab dem 2.6. wurde die Expedition Richtung Norden fortgesetzt und unterwegs CTD und Netzfänge durchgeführt. Die Eissituation ließ leider nur ein mäßiges Vorankommen auf unserem Schnitt entlang des Schelfhanges zu, so dass wir die nächste Eisstation am 3.6. auf der Position $81^{\circ} 37,37' N$, $19^{\circ} 26,92' E$ bei einer Wassertiefe von 2000 m durchgeführt haben. Um unsere ursprüngliches Ziel - nach Osten vorzudringen- hatten wir anhand von Eiskarten eine mögliche Route im Süden bei $81^{\circ} 10' N$ identifiziert. Nachdem wir am Anfang gut voran kamen, schlug das Wetter um und wir kamen letztendlich nicht weiter als 22° Ost. Wir hatten daraufhin die vierte Eisstation am Nachmittag des 6.6. erreicht. Die Position war $81^{\circ} 14,16' N$, $19^{\circ} 25,52' E$ (450 m Tiefe). Auf dieser Station hatten wir die höchste Eisalgenbiomasse gefunden, wobei viele Algen schon in Form von kleinen Aggregaten unter dem Eis vorlagen. Die guten Wetterbedingungen während dieser Station konnten für viele Helikopterflüge mit dem EM-Bird zur Bestimmung der Eisdicke genutzt werden (Abb. 1.6). Die guten Flugbedingungen wurden weiterhin dazu genutzt, die Passierbarkeit des Eises in östlicher Richtung zu erkunden. Nach dem Erkundungsflug, wurde klar, dass die Region östlich von unserer Station durch große Eisschollen, die unter extremen Druck standen, charakterisiert war und dass nirgends genügend große Kanäle vorhanden waren, die für das Vorankommen von *Polarstern* notwendig gewesen wären.

Eine Veränderung der Windrichtung zwang uns dazu, die Eisstation am 7.6. vorzeitig abzubrechen, um nicht zwischen zwei massiven Eisschollen eingeschlossen zu werden. Wir verließen die Gefahrenregion, und setzen das Programm fort. Letztendlich mussten wir erneut

die Position wechseln, bevor das benthische Programm am 9.6 bei 81° 6,05' N, 19° 35,34' E (200 m Wassertiefe) beendet wurde. Zu diesem Zeitpunkt wurden nach Abwägen aller Optionen festgelegt, dass wir keine weiteren Vorstöße nach Osten mehr durchführen und das Yermak Plateau wurde als neue Zielregion identifiziert.

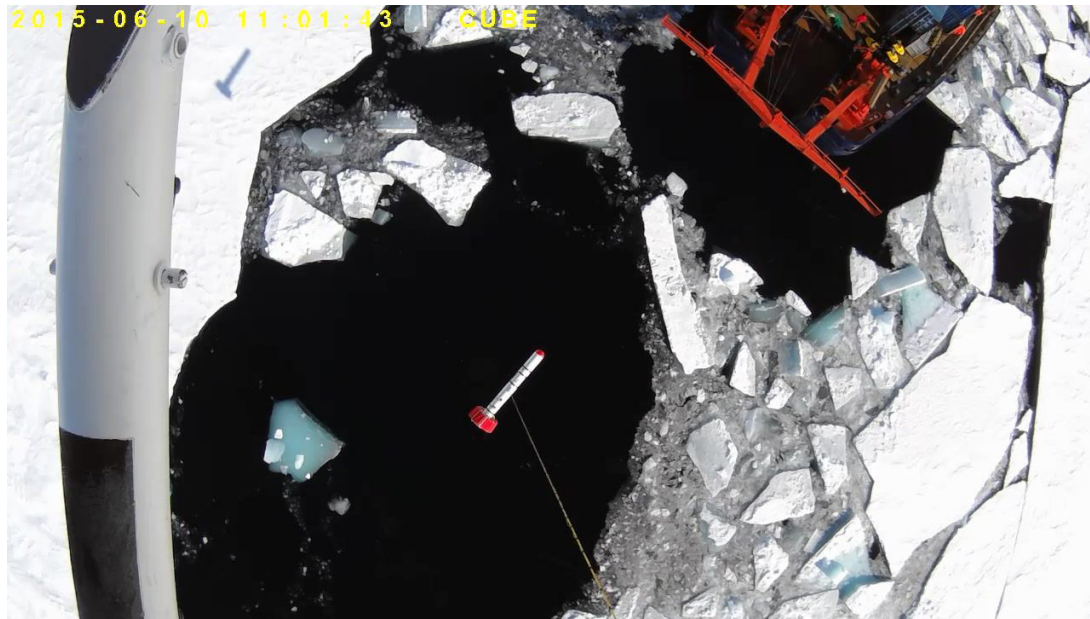


Abb. 1.6: Luftaufnahme aus dem Helikopter vom Meereis während einer Electromagnetic (EM) Bird Untersuchung ((@ Sacha Willmes).

Fig. 1.6.: Aerial photo of sea ice from the helicopter during an Electromagnetic (EM) Bird survey ((@ Sacha Willmes.)

Die guten Wetterbedingungen am 8.6. erlaubten eine Fortführung der EM-Bird Flüge und einer der Messflüge konnte dazu genutzt werden unsere norwegischen und zwei Kollegen vom AWI, die sich auf dem norwegischen Forschungsschiff *Lance* befanden, dahingehend zu unterstützen, dass wir Meereis Messungen von ihrem Eis Camp durchgeführt haben, das sich nur wenige Seemeilen von unserer Position befand. Der Weg zum Yermak Plateau wurde zusätzlich dazu genutzt, einen hydrographischen Schnitt hangabwärts ins Sophia Becken am 9.6. durchzuführen. Dieser Schnitt wurde durch Netzfänge bei 81° 19,07' N, 16° 18,78' E vervollständigt.

Während wir am Anfang unseres Transfers zum Plateau sehr gut vorankamen, wurden wir ab dem 10.6. durch die erneut schweren Eisbedingungen behindert, so dass wir das Untersuchungsgebiet erst in der Nacht zum 11.6. erreichten. Das Programm wurde hier mit einer Sedimentkartierung gestartet, um eine gute Position für das Kastenlot zu finden, welches dann bei 81° 56,99' N, 13° 50,28' E eingesetzt wurde (Abb. 1.7) und mit allen weiteren geologischen und benthischen Beprobungen ergänzt wurde, bevor die 5. Eisstation (Wassertiefe 1.500 m) am selben Tag mittags gestartet wurde.

Insgesamt wardiese Region durch deutlich niedrigere Phytoplankton Biomassen gekennzeichnet und auch die Biomasse im Meereis war nicht so stark entwickelt wie auf früheren Stationen. Die Eisstation wurde mit einem SUIT am Abend des 12.6 beendet und von dort wurde die Expedition in Richtung westlichen Hang des Yermak Plateaus fortgesetzt und auf dem Weg drei Multicorer Stationen durchgeführt, die der Kultivierung von Foraminiferen dienten. Der nördlichste Punkt dieser Route wurde am 14.6. erreicht, weil ein weiteres Vordringen durch

die Eisbedingungen verhindert wurde. Die GeowissenschaftlerInnen nutzen diese Region, um bestimmte Foraminiferen Arten mit Hilfe des Multicorers bei $82^{\circ} 11,63' N$, $7^{\circ} 45,69' E$ zu beproben. Dieses Programm wurde mit der benthischen Probennahme vervollständigt und die 6. Eisstation begann am 15.6. um 4 Uhr an der Position $82^{\circ} 12,70' N$, $7^{\circ} 35,03' E$ (800 m



Abb. 1.7: Das geöffnete Kastenlot nach der ersten Probennahme (@ Kirstin Werner)

Fig. 1.7: The opened Kastenlot after a first round of sampling (@ Kirstin Werner.)

Wassertiefe). Am 16.6. wurde die Station mit einem SUIT Fang beendet. Als nächstes wurden weitere geologische Kernpositionen am östlichen Hang des Yermak Plateau angesteuert und auf dem Weg dorthin weitere SUIT Fänge durchgeführt.

Das geologische Kern-Programm wurde dann am 17.6. bei $81^{\circ} 56,08' N$, $9^{\circ} 15,30' E$ und $81^{\circ} 53,66' N$, $9^{\circ} 46,32' E$ durchgeführt, gefolgt von der 7. Eisstation (900 m Wassertiefe) am Nachmittag des 17.6. Auf dieser Eisstation wurden zum ersten Mal Schmelzprozesse des Schnees auf dem Eis durch die Ausbildung dunklerer Regionen sichtbar, die die Vorstufe für sich später entwickelnden Schmelztümpel bilden. Aufgrund veränderter Wetterbedingungen drohten wir am Ende der Eisstation zwischen mehreren großen Schollen eingeschlossen zu werden, so dass wir einen der geplanten Kastengreifer Einsätze nicht mehr durchführen konnten.

Durch die veränderten Wetterbedingungen war es dann auch angezeigt, das Untersuchungsgebiet umgehend in Richtung Sophia Becken zu verlassen, wo am frühen Morgen des 19.6. die letzte Eisstation mit dem gesamten Programm durchgeführt wurde. Auf dieser Station war das Eis insbesondere durch ein Abschmelzen der Eis-Unterseiten gekennzeichnet. Diese 8. Eisstation wurde in der Nacht zum 20.6. mit einem SUIT beendet. Als nächstes Ziel, insbesondere für geologische Kerne, wurde die Sverdrup Bank angesteuert und auf dem Weg weitere SUIT Fänge durchgeführt. Hangaufwärts wurde dann ein erneuter hydrographischer Schnitt am 21.6. bei $81^{\circ} 1,07' N$, $11^{\circ} 26,43' E$ begonnen. Am 22.6. wurde das erste Schwerelot bei $81^{\circ} 7,47' N$, $8^{\circ} 27,98' E$ (1145 m Tiefe) genommen. Da erneut die Eisbedingungen das Vorankommen erschwert hatten, erreichten wir unsere letzte Station mit biogeochemischer Ausrichtung am 23. 6. am späten Morgen. Die Station wurde mit einem Schwerelot begonnen, das Programm musste aber aufgrund der widrigen Eisbedingungen verkürzt werden. Am Abend des 23.6. hatten wir diesen Untersuchungsgebiet nach Süden verlassen, um eine sichere Passage der *Polarstern* durch das Eis zu gewährleisten. Gut passierbares Eis wurde am Mittag des 24.6. erreicht, wo die verbleibende Zeit der Expedition zu einer Sedimentkartierung (Hydrosweep/ Parasound) in der Region $80^{\circ} 14,83' N$, $11^{\circ} 2,33' E$ bis $80^{\circ} 3,82' N$, $11^{\circ} 2,10' E$ durchgeführt wurde, die am Morgen des 27.6. endete. Während der Kartierung wurden zusätzlich ozeanographische Messungen mit einer U-CTD im eisfreien Bereich sowie mit XCTDs in der Region mit Meereisbedeckung eingesetzt. Im Anschluss an die bathymetrischen Messungen

nahmen wir Kurs auf Longyearbyen, wo die Expedition am 28.6. um 10 Uhr endete. Obwohl die angestrebten Schnitte bei 20°E und 30°E nicht wie geplant durchgeführt werden konnten, kann diese Expedition insgesamt als sehr erfolgreich eingestuft werden, da trotz der widrigen Bedingungen die wesentlichen Forschungsziele erreicht werden konnten. Im Namen aller FahrtteilnehmerInnen (Abb. 1.8) möchten wir uns herzlich bei Kapitän und Besatzung der *Polarstern* für die hervorragende Unterstützung und die freundliche Arbeitsatmosphäre auf der TRANSSIZ Expedition PS92 (ARK-XXIX/1) bedanken.



Abb. 1.8: Gruppenphoto der Expedition (@Ilias Nasis)

Fig. 1.8.: Expedition group photo (@Ilias Nasis)

SUMMARY AND ITINERARY

On May 19, 2015, the German research icebreaker *Polarstern* began a six-week expedition to the Arctic Ocean initiated by the “ART” team, which stands for “Arctic in Rapid Transition”. The expedition PS92 (ARK-XXIX/1) “TRANSSIZ” (Transitions in the Arctic Seasonal Sea Ice Zone, Fig. 1.1) conducted ecological and biogeochemical early spring process studies from the shelf to the basins of the European Arctic margin and on the Yermak Plateau, in order to link past and present sea-ice transitions in the Arctic Ocean. The cruise involved scientists from eleven countries in collaboration with research groups from divisions of the Alfred Wegener Institute Helmholtz Centre for Polar and Marine Research together with scientists from the German BMBF-project ‘Transdrift’, as well as from the French-Canadian projects ‘GreenEdge’. Overall the vessel travelled 3,665 sm and carried out 68 stations with a total of 242 casts. Some groups also used the transit to the research area to study meridional variability of trace gases, algae species and nutrients from temperate regions of the North Atlantic and into the ice-covered Arctic Ocean by using the surface online water system. Once reaching the investigation area, the science parties conducted process studies for rate measurements of productivity, ecosystem interactions and carbon- and nitrogen cycling. By comparing data from the shelf, data from across the shelf-break into the deep basin it was possible to compare carbon export from plankton and sea ice communities as well as identifying the potential characteristics in carbon production, the fate and export, and to identify similarities and differences in ecosystem functioning along topography-, sea ice- and water mass-related gradients. The ice stations (Fig. 1.2) involved coring of a standard set of sea-ice cores for biological, physical and chemical variables as well as for trace gases and geological proxy validation. It further involved the study of sea ice properties and under-ice water and covered the study of trace and greenhouse gases, biodiversity, primary and bacterial production as well as a detailed study of the nitrogen cycle. Short-term moorings were deployed under the ice to determine the vertical carbon flux. A small Remotely Operated Vehicle (ROV) was operated under the ice to focus on spectral radiation measurements, but also to record environmental parameters (e.g. ice thickness, salinity, temperature) and video imaging of the under-ice environment. Light transmission measured with the ROV showed an increase of light penetration during the course of our expedition. The under-ice fauna and other environmental parameters were investigated by using the towed “Surface Under Ice Trawl” (SUIT). Helicopter flights were used to determine the large-scale distribution of sea-ice thickness with an EM-bird along the cruise track, which overall revealed that the average sea-ice thickness was 1.4 m, that is, comparatively thin and similar to summer values previously observed in Fram Strait. During the sea-ice stations, parallel sampling of pelagic and benthic ecosystems and geological cores were conducted. Light spectra of hyper-spectral radiometers were used to establish the penetration depth of ultraviolet radiation into the different types of oceanic waters from the zodiac and under the ice. Water samples were taken from the water bottles of the CTD rosette to study the chemistry, biology and various geological proxies. A UVP (Underwater Video Profiler System) was deployed to provide detailed vertical profiles of particle distribution, size composition and the zooplankton community. Quantitative sampling of the mesozooplankton, and also foraminifera, which are used as paleo-proxies, were carried out by using multi-nets. For macrozooplankton and nekton, a Multiple-closing Rectangular Midwater Trawl (MRMT) was used. The distribution

of macrozooplankton and pelagic fish was monitored continuously on selected transects with *Polarstern's* EK60 echosounder. Benthic communities were collected by box corers and the material was further used for experimental and biogeochemical analyses of the benthic surface sediment layers, including sea ice- and paleo proxies. Benthic communities show a clear shelf to basin decrease in the oxygen demand. Overall, the communities also show a clear North South gradient in our study area. TV-Multi-corers for geological measurements were used to get undisturbed core tops of near-surface sediments (Fig. 1.3). For the geological coring, detailed bathymetric mapping and sub-bottom profiling systems (Hydrosweep and Parasound) were used to find suitable coring positions for Kastenlot and Gravity cores. Special emphasis on this cruise was taken to quantify the environmental preconditions for productivity (e.g. nutrients, stratification) which will allow us to be able to improve predictions of the potential annual primary production in a future ice-free Arctic Ocean, as well as improving reconstructions of productivity, sea ice and ocean circulation across the last 1-2 last glacial cycles. Results from the cruise will further improve the understanding of ecosystem functioning and biogeochemical cycles during the transition from spring to summer. The expedition ended on the morning of the 28th June 2015 in Longyearbyen.

Narrative

The expedition „ Transitions in the Arctic Seasonal Sea Ice Zone “PS92 (ARK-XXIX/1) started in Bremerhaven, Germany, in the afternoon of 19th May. We steamed 3 days north into the Norwegian Sea, where at 65° 12.52' N, 3° 36.91' E the first test for an underway CTD was performed. Proceeding north, more XCTDs and underway CTDs were carried out. From the evening of 23rd May until the afternoon of the 24th, we had to deviate from our course to transport a sick crew member for onshore treatment in Tromsø. The person was eventually transported by helicopter, and one day later we were back on our course heading North. Starting at 70° 51.90' N 13° 41.46' E, we conducted further XCTDs and Underway CTDs until we reached the first CTD test station on the 26th May at 77° 4.35' N, 9° 31.20' E. Underway CTD and XCTD sampling was continued until we reached the investigation area North of Svalbard where we started out first long-term ice station at 81° 0.48' N, 19° 54.49' E on the Barents Sea Shelf at a water depth of 200 m on May, 27th. The evening and night were used to test the towed net samplers (RMT, Fig. 1.4 and SUIT) and was followed by bathymetric surveys. We identified a large ice floe at 81° 10.43' N, 19° 8.07' E and performed our first shallow ice station at 370 m lasting from 28-29 May. Ice stations were the main focus of the expedition, involving 2/3 of the science party. During the ice station, the ship was anchored at the ice floe and drifted as the other winches operated instruments in parallel to the work on the ice. Oceanographic, chemical, pelagic, benthic and geological sampling of the water column and sediments were carried out using CTD/ Rosette, Compact Optical Profiling System, Underwater Video Profiler, *in-situ* pumps, net, plankton nets and box corer. The station was started with a CTD to collect water at various depths, which was spiked for nutrient measurements and thereafter hooked on a mooring array of small sediment traps. The mooring was deployed at the edge of the floe using a zodiac. The work on the ice consisted of a sea ice physics team working with an ROV for optical properties of the ice and several devices to determine ice and snow properties. The hydrographic team studied velocity and mixing by deploying an ADCP for the entire station time and operating a microstructure probe for at least one tidal cycle. The coring team took sea-ice cores for different research parties and sampled the under-ice water. The phytoplankton biomass at this station was high and dominated by diatoms. During the first ice station we drifted to a deeper water depth, so we steamed back South to 81° 1.86' N, 19° 21.71' E to perform an additional benthic sampling station at 200 m. After the station we made the first attempt to reach our 30°E position but had to give up due to a large ice floe blocking our way. Even our 20°E downslope transect was blocked by this flow so we carried out a depth dependent downslope hydrographic survey, and towed instruments such as the rectangular

midwater trawl (RMT) until we reached the next ice station further to the west at 23.18' N, 17° 35.66' E (850 m water depth).

The second ice station started on 31st May, and was preceded by an under-ice trawl. During this station we started to deploy the small mooring (Fig. 1.5) through a hole in the ice. The phytoplankton community at this station had already changed to a more *Phaeocystis* dominated community. After repositioning for the benthic and geologic work on 1st June, we proceeded further north on 2nd June carrying out nets and CTD stations on the way. Again we were stopped by the ice from continuing the down-slope transect and we therefore performed our next ice station on 3rd June at 81° 37.37' N, 19° 26.92' E (2,000 m water depth). Based on ice maps we saw a chance to move to our 30°E transect by going south to 81° 10' N and proceed from there east ward, but this attempt brought us only to 22° E and we were not able to proceed further east. We started our fourth ice station in the afternoon of 6th June at 81° 14.16' N, 19° 25.52' E (450 m depth) at a large ice floe. This station turned out to be the station where the highest ice algae biomass was observed and the algae had already started to build aggregates. During this station the weather was extremely sunny and numerous EM-bird observations could be carried out (Fig. 1.6). The good weather further gave us a chance to evaluate any opportunity to proceed to the east. After the helicopter flight it was evident that the situation to the east was characterized by large ice floes that were under pressure and impenetrable. Additionally, a change in wind direction forced us to evacuate the floe at noon on 7th June, since over night the lead started closing in and we were worried about being trapped between two giant floes. We repositioned and finished part of the measurement programme, but had to reposition again to finish with the benthic work on the morning of 9th June at 81° 6.05' N, 19° 35.34' E (200 m water depth). After evaluating all options we gave up on trying to proceed further to the east and instead aimed for the Yermak Plateau as a new target area to accommodate the research needs of the various groups. While transecting to the plateau on the 8th, weather conditions allowed us to continue the helicopter based ice thickness surveys with the EM-Bird. During one operation we were able to support our Norwegian and two AWI colleagues onboard the Norwegian research vessel *Lance* who were just a few miles away, by mapping their ice camp with our EM-Bird. On the way to the Yermak Plateau we conducted a down slope hydrographic survey on 9th June, followed by some towed net-sampling in the deep Sophia Basin at 81° 19.07' N, 16° 18.78' E. While at the beginning of this transect we made extremely good progress in the ice, on the 10th we were substantially slowed down by severe ice conditions and reached the designated area on the night of June 11th. Here a bathymetric survey was started in order to find a suitable location for a Kastenlot core, which was taken at 81° 56.99' N, 13° 50.28' E (Fig. 1.7) and followed by all other benthic sampling for geology and benthic fauna. The fifth ice station started at noon of the same day (water depth of 1,500 m). Overall this region had a less developed phytoplankton standing stock and additionally the ice algae were less developed. Instead, large numbers of jellyfish were seen under the ice with the ROV and also found in the towed nets. This ice station ended with a SUIT in the evening of 12th June and from there we aimed to get to a downslope transect on the western slope of the Yermak Plateau. On the way 3 MUC's were taken for cultivation purposes of foraminifera. On the 14th of June it was evident that we reached the northern most point on our transect and the geological party interested in collecting specific foraminifera continued collecting samples with a MUC at 82° 11.63' N, 7° 45.69' E. This programme was followed by benthic sampling and thereafter the sixth ice station started on 15th June at 4 pm at 82° 12.70' N, 7° 35.03' E (water depth of 800 m). The station ended in the afternoon of the 16th with a series of SUIT sampling while heading east to two geological sites selected for gravity coring on the eastern slope of the plateau. These were carried out on 17th June at 81° 56.08' N, 9° 15.30' E and 81° 53.66' N, 9° 46.32' E, respectively. The seventh ice station was started at this position in the afternoon of the 17th of June (water depth of 900 m). The ice of this station already showed clear signs of melting, evident by the darker patches on the surface where melt ponds would

soon appear. At the end of the station, we were about to get trapped by several large ice floes and had to omit one box core from the regular program. Due to changing wind conditions, the entire area started to get dangerous so we moved back to the Sophia Basin without delay in order to carry out the last ice station on the 19th of June. It started early in the morning with net sampling and we eventually anchored at the ice at noon, when the general sea-ice programme began. Contrary to the previous stations, this ice station showed signs of extensive melting from below. This ice station was finished on the night of the 20th of June and was followed by net sampling as we moved westward towards the Sverdrup Bank, another target area for geological coring. Upslope towards the bank a hydrographic transect was carried out starting in the evening of the 21st at 81° 1.07' N, 11° 26.43' E. On the 22nd the first gravity core in this region was taken from 81° 7.47' N, 8° 27.98' E (1,145 m). Again it became more difficult to break through the ice so we reached our last biogeochemical station on the 23rd in the late morning. The station started with a gravity core and due to time limitation we could only perform a reduced measurement programme. We left this region on the evening of the 23rd in order to find a safe passage out of the ice by moving south. We reached moderate ice conditions at noon on 24th of June where we started a Hydrosweep/Parasound bathymetric survey in a rectangular area starting at 80° 14.83' N 11° 2.33' E and ending at 80° 3.82' N, 11° 2.10' E. The programme was accompanied by hydrographic studies using XCTDs and the underway CTD. This bathymetric survey ended in the early morning of 27th and from there we took our course to Longyearbyen, where the cruise ended on the 28th June at 10 am. Overall the cruise can be considered as a great success since most major research aims were fulfilled although the we had not been able to reach some of our targeted areas around 20°E and 30°E. On behalf of all cruise participants (Fig. 1.8) we like to thank captain and crew of *Polarstern* for the excellent support during work at sea, and the friendly cooperation during expedition TRANSISZ PS92 (ARK-XXIX/1).

2. WEATHER CONDITIONS

Max Miller, Hartmut Sonnabend DWD

Grant No AWI_PS92_00

On Tuesday, May 19, 2015, 2:00 pm *Polarstern* left Bremerhaven for the campaign PS92 (ARK-XXIX/1). A heavy shower crossed the harbour and caused gusts up to Bft 8 from southwest and the temperature dropped from 13° to 8 °C.

The accompanying low over northern North Sea weakened, but showers were present until Wednesday (May 20). During Wednesday afternoon south-westerly winds abated to wind force 2.

A new low had formed and intensified northeast of Cape Farvel. From Thursday (May 21) on it moved east and southerly winds increased steadily up to Bft 7. Friday evening we arrived at the west side of the low. Winds veered northwest, reached their peak at Bft 8 during the night to Saturday (May 23) and forced a sea state of 4 m. But already on Saturday afternoon winds abated clearly while the low moved away.

Heading north we crossed a ridge at light and variable winds. But during the night to Wednesday (May 27) we could observe an increase of wind speed caused by coastal effects. At the north-western end of Svalbard we measured easterly winds at Bft 5 to 6, but Bft 3 to 4 would have been the regular wind force.

During the following days *Polarstern* operated between a high north of Bering Strait and several lows over Barents Sea but north-easterly winds didn't exceed wind force 5.

On Wednesday (June 03) a new low over Norway moved to Barents Sea at first and further east later on. Now winds from north to northeast increased and peaked at Bft 7 on Thursday (June 04). Until Saturday (June 06) winds veered northwest and abated to Bft 4. On Sunday a weak ridge created sunny skies.

Meanwhile above mentioned low had reached the International Date Line. It built a trough towards Fram Strait which moved slowly east. Light southerly winds caused temporarily a lee situation and clear skies north of Svalbard. During the night to Tuesday (June 09) light winds veered north and the well-known colour grey got prevailing again.

On Wednesday (June 10) a low over the mouth of Ob River moved towards Barents Sea and intensified to storm. *Polarstern* got at its northwest side. North-easterly winds reached their maximum at Bft 7 to 8 between Thursday (June 11) evening and noon on Friday. Until Sunday winds abated slowly to Bft 3 to 4 and veered east.

During the following week the pressure gradient over our area was weak. Mist and fog got the dominant features.

On Monday (June 22) a low north of Bering Strait built a trough towards Fram Strait and caused noticeable south-westerly winds up to Bft 5. But the trough weakened soon and therefore winds, too.

On Friday (June 26th) a small low formed over north-eastern Greenland and moved east. On Saturday the wind veered north and increased gradually. Along the west coast of Svalbard winds peaked at Bft 6 during the evening.

On Sunday morning, June 28 2015, *Polarstern* reached Longyearbyen at moderate north-easterly winds.

Further statistics can be found in Fig. 2.1 to Fig. 2.4.

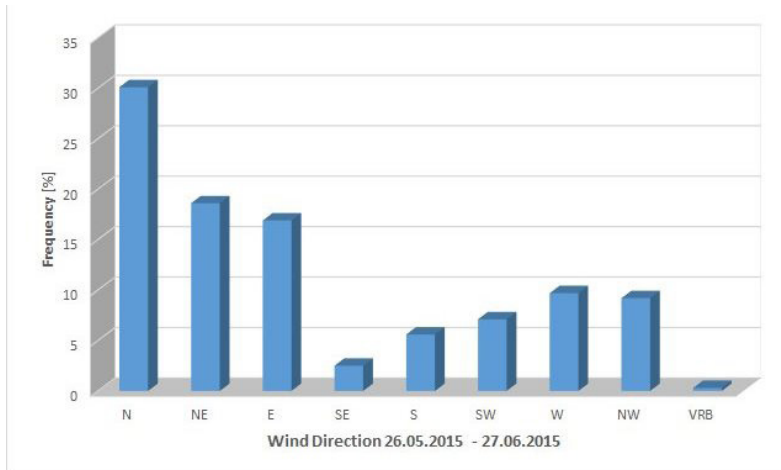


Fig. 2.1: Distribution of wind direction

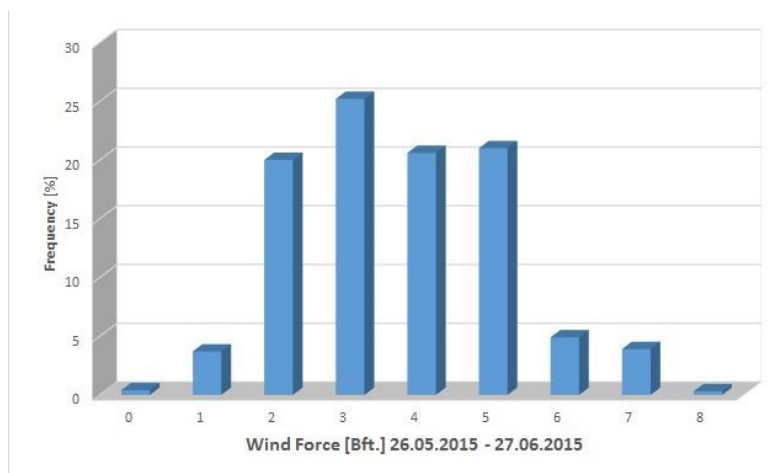


Fig. 2.2: Distribution of wind force

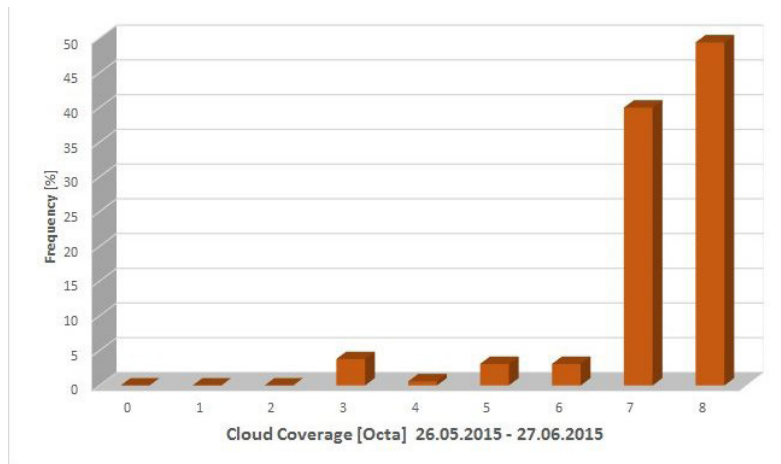


Fig. 2.3: Distribution of cloud coverage

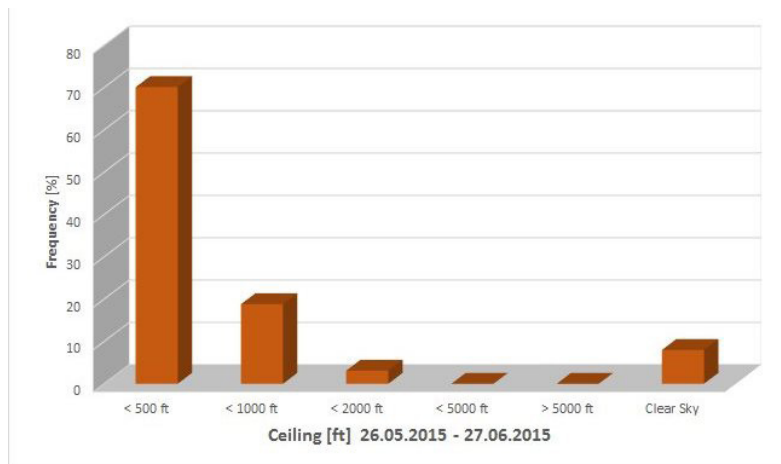


Fig. 2.4: Cloud coverage

3. ACTIVITIES OF THE SEA ICE PHYSICS GROUP DURING PS92

Jakob Belter¹, Christian Katlein², Thomas Krumpfen, Sebastian Schulte-Kortnack³ and Sascha Willmes⁴

¹CAU, ²AWI
³HS-B, ⁴UTR

Grant No AWI_PS92_00

3.1 AEM bird ice thickness measurements

Objectives

Climate models agree that the sea ice extent and thickness will further decline through the 21st century in response to atmospheric greenhouse gas loading (Zhang et al. 2006, Massonnet et al., 2012). Furthermore, ice drift and deformation increase and net ice growth rates decrease (Spreen et al., 2011, Rampal et al., 2009). To determine associated changes in the Arctic sea ice volume requires consideration of changes in ice volume fluxes that appear at the major gates of the Arctic, such as the Fram Strait and along the pathways feeding the exit gates. Given the importance of the Fram Strait sea ice fluxes for the Arctic sea ice volume changes, aim of the sea ice physics group is to measure ice thickness of sea ice in the southern Transpolar Drift. The ice thickness surveys complement earlier measurements made by moorings, drifters and from ships. It is a continuation of the large scale airborne sea ice surveys in March/April 2015 (NETCARE) and July/August 2015 (MELTEX/TIFAX).

Work at sea

We used airborne electromagnetic (AEM) induction sounding to measure sea ice thickness by helicopter surveys. The instrumentation consists of 4 m long sensor which is towed on a 20 m long cable at an altitude between 10 and 15 m above the ice surface. The method utilizes the difference of electrical conductivity between sea ice and sea water to estimate the thickness of sea ice including the snow layer if present.

Preliminary results

The flight operations were significantly hampered by weather conditions with low clouds and low contrast during the entire cruise. Therefore, only 8 flights were successfully performed in the vicinity of *Polarstern*, covering predominantly first-year and second year sea ice. Fig. 3.1 and Table 3.1 provide an overview of AEM flights made during PS92. Ice thickness data based on the "Orphan" sensor has been fully processed during the cruise and is available upon request as point data with an average spacing of 3 to 4 meters and a footprint of approximately 40 m. The mean thickness of sea ice for all flights made between May 27 and June 19 amounts to 1.7 m. The modal thickness is 1.4 m (compare Fig. 3.2).

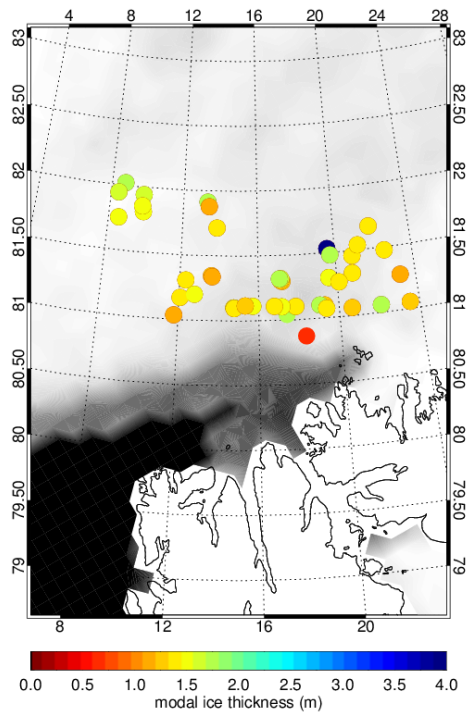


Fig. 3.1: Overview of all airborne sea ice thickness surveys performed between May 27 and June 19 2015 in the area north of Svalbard. Each dot represents 25 km of sea ice thickness measurements. The color coding corresponds to the modal thickness.

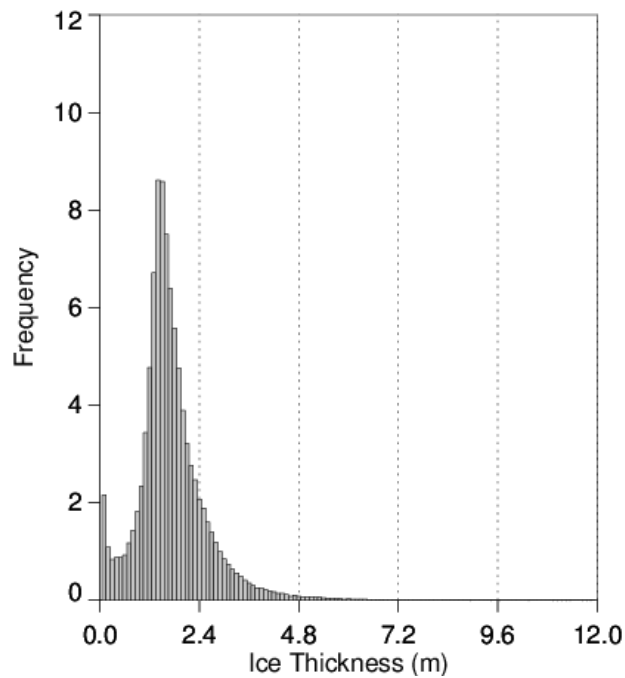


Fig. 3.2: Frequency distribution of sea ice thickness measurements made between May 27 and June 19. The mean thickness amounts to 1.8 m, the modal thickness is 1.4 m.

3.1 AEM bird ice thickness measurements

Tab. 3.1: List of airborne sea ice thickness surveys during *Polarstern* cruise PS92

Platform/Device	Date	Lat/Lon	Station Number	Flight Pattern	Comment
EM-Bird ,Orphan'	2015/05/27	80.86287 N 18.35893 E	PS92_HELI_HEM01	Straight line	<i>Straight line north. Flight had to be interrupted because of icing</i>
EM-Bird ,Orphan'	2015/06/01	81.31827 N 17.23537 E	PS92_HELI_HEM02	Floe survey	<i>Ice thickness survey in the vicinity of the ship only.</i>
EM-Bird ,Orphan'	2015/06/07	81.21202 N 19.60135 E	PS92_HELI_HEM03	Triangle	<i>No comment</i>
EM-Bird ,Orphan'	2015/06/08	81.09977 N 19.64383 E	PS92_HELI_HEM04	Straight line	<i>Flight to RV Lance and back to RV Polarstern</i>
EM-Bird ,Orphan'	2015/06/08	81.05717 N 19.29678 E	PS92_HELI_HEM05	Triangle	<i>Continuation of the early morning flight to Lance in eastern direction</i>
EM-Bird ,Orphan'	2015/06/10	81.74650 N 13.58867 E	PS92_HELI_HEM07	Straight line	<i>Bad visibility made flight operation difficult</i>
EM-Bird ,Orphan'	2015/06/18	81.86137 N 9.82327 E	PS92_HELI_HEM08	Triangle	<i>Floe survey at the end of the flight</i>
EM-Bird ,Orphan'	2015/06/19	81.34313 N 13.60688 E	PS92_HELI_HEM09	Triangle	<i>Floe survey at the end of the flight</i>

Data management

The sea ice thickness data will be released following final processing after the cruise in the PANGAEA database and international databases like the Sea Ice Thickness Climate Data Record (Sea Ice CDR).

References

- Massonnet F, T Fichet, H Goosse, C M Bitz, G Philippon-Berthier, M M Holland, and P Y Barriat (2012) Constraining projections of summer Arctic sea ice. *Cryosphere* 6: 1383-1394.
- Rampal P, J Weiss, and D Marsan (2009) Positive trend in the mean speed and deformation rate of Arctic sea ice, 1979-2007. *J Geophys Res-Oceans* 114: -.
- Spren G, R Kwok and D Menemenlis (2011) Trends in Arctic sea ice drift and role of wind forcing: 1992-2009. *Geophys Res Lett* 38.
- Zhang XD, and J E Walsh (2006) Toward a seasonally ice-covered Arctic Ocean: Scenarios from the IPCC AR4 model simulations. *Journal of Climate* 19: 1730-1747.

3.2 Ground-based ice thickness and snow measurements

Objectives

Characterization of the sea ice cover is crucial for an assessment of the state of the polar climate system. Sea ice thickness datasets are sparse and rarely combine high resolution thickness information and high spatial coverage. Furthermore instrument design and processing techniques are usually based on a simple 1D representation of the sea ice layer and the ice cover is interpreted as level ice. A multi-frequency device (GEM-2) was used during this expedition. Similar to the AEM measurements, GEM-2 surveys during PS92 are made to resolve with different sounding depths complex and small-scale sea ice thickness and conductivity structures. Snow and sea ice thickness were measured to resolve the thickness distributions on individual floes. Data from the small footprint instrument GEM-2 will be compared to the larger footprint device EM-Bird. A focus is on the identification of ice and snow thickness values over the 100 x 100 m² transect grid that is surveyed by the ROV from under the ice. In doing so, a later assessment of light transmission through the ice, which is highly dependent on sea-ice and (mainly) snow thicknesses, can be ensured.

Work at sea

We used the ground-based electromagnetic device GEM-2 to measure sea ice plus snow thickness. The method is based on the contrast of electrical conductivity between ocean water and sea ice (including snow). The instrumentation consists of two coils with separation of 1.67 m. The device was used by pulling it over the sea ice mounted in a plastic sled. For calibration purpose a wooden ladder was used. The snow thickness during GEM-2 surveys was measured with a MagnaProbe instrument with approximately 2 m spacing. The device measures the snow depth and records it on a data logger for later downloading to a computer. The measurement is made by means of a sliding basket and magneto-strictive device. The combined GEM-2 and MagnaProbe measurements were started immediately after the ROV light transmission measurements were finished to ensure that the snow surface remains undisturbed.

Preliminary results

GEM-2 surveys were made during all 8 ice stations along and across the ROV transects, but also on the entire floe. Due to an instrument failure of the MagnaProbe after ice station 6, snow thickness could not be measured during ice stations 7 and 8. With the recorded GPS position data points were corrected for drift and rotation of the floe relative to the ship's position. The resulting grid data as total thicknesses (ice+snow) are shown in Fig. 3.3. After the MagnaProbe measurements are interpolated to the nearest respective GEM-2 data point the total thickness can be separated into snow and ice thicknesses. In general, the frequency distributions for snow and ice thickness differed substantially between the ROV sites on the ice stations, reaching from a mean total thickness of 1.01 m on ice station 1 to 1.95 m on ice station 5 (Fig. 3.4).

Data management

The MagnaProbe and GEM-2 data will be released following final processing after the cruise in the PANGAEA database.

3.2 Ground-based ice thickness and snow measurements

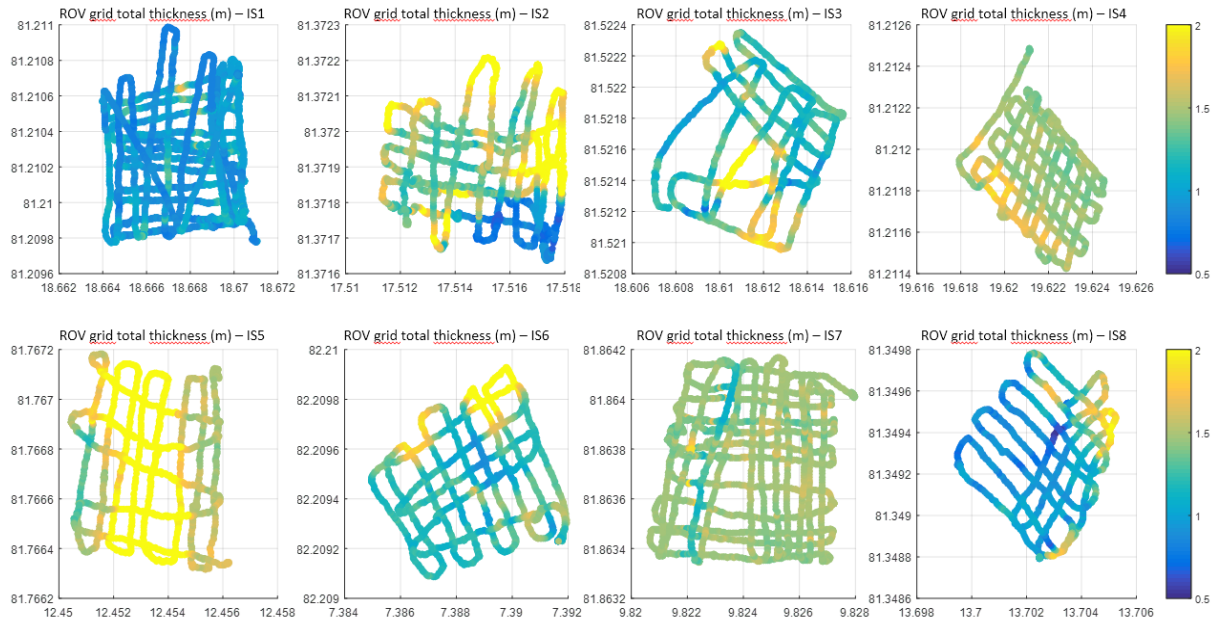


Fig. 3.3: Drift- and rotation-corrected transect grid of GEM-2 measurements (ice+snow thickness) at the ROV sites for ice station 1 – 8.

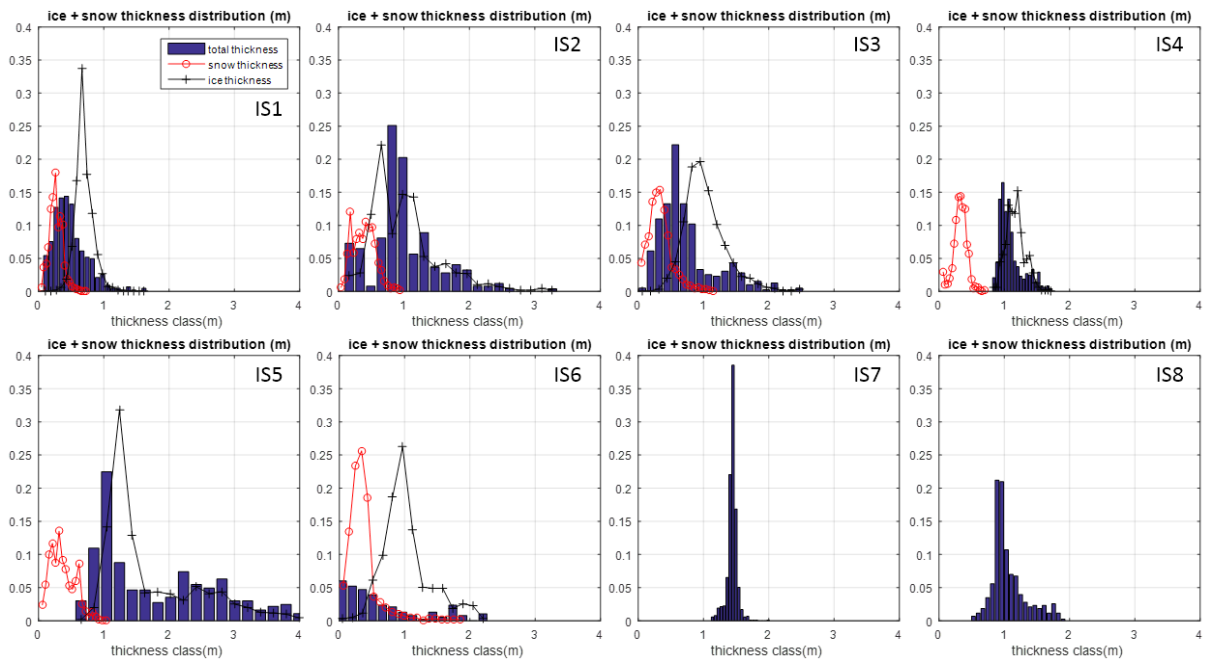


Fig. 3.4: Histograms of total thickness (ice+snow, blue bars), snow thickness (red line) and ice thickness (black line). Only the total thickness is shown for ice stations 7 and 8 due to an instrument failure of the MagnaProbe.

3.3 Airborne digital video camera survey of surface properties

Objectives

The surface properties of sea ice are subject to pronounced changes in the transition from spring to summer. The snow starts to undergo repeated melt-freeze cycles before continuous and strong melt takes over and causes the formation of melt ponds. Across the marginal ice zone, which was covered by the PS92 research area, gradients can be expected from North to South with enhanced melt towards the sea-ice edge. Additionally, the break-up of large ice floes causes a shift in floe size distributions that impact the local sea-ice concentration and supports lateral melting. Since PS92 was meant to conduct measurements along North-South transects in the marginal ice zone, a high-resolution airborne digital camera survey was aimed at by the sea-ice physics group to serve two main scientific goals: First, it should help with detecting transitions of lead width and floe size distributions within the marginal ice zone. Second, the evolution and spatial variability of surface melting (i.e. melt pond occurrence, and properties) was to be determined. Both of these goals can help to interpret and validate SAR imagery and satellite sea-ice concentration data. Extracted video image frames can be used to run automatic image segmentation techniques and a retrieval of associated object features, e.g. sea-ice concentration within frame, floe area, floe perimeter, etc.

Work at sea

A Polaroid CubeCAM was mounted to the lateral helicopter stepping bars before each flight of the EM-Bird (Fig. 3.5, Tab. 3.2). The CubeCAM records HD video data for approximately 90 Minutes. After each flight recorded data were read out and image frames extracted. Preliminary processing was implemented to extract basic features from each frame. The prevailing presence of low level clouds and fog, however, complicated a dense survey in terms of spatial and temporal coverage.

Preliminary results

The image frames from the camera videos have proven to be useful for an automatic segmentation of sea ice and ocean, and partly also melt ponds. In most cases the evolution of melt ponds had not yet proceeded very far. The segmented floes can be used to calculate floe perimeter, major axis length, floe area and associated parameters. A correction for panoramic distortion and the handling of objects exceeding image frames is yet to be implemented before a quantitative analysis of video transects can be performed.

Tab. 3.2: List of airborne sea-ice surface surveys during *Polarstern* cruise PS92

Platform/ Device	Date	Lat/Lon	Occasion	Flight pattern	Video time
Polaroid CubeCAM	2015/05/27	80.86287 N 18.35893 E	With AEM Bird	Straight line	45 min., (interrupted AEM flight)
Polaroid CubeCAM	2015/06/07	81.21202 N 19.60135 E	PS92_HELI_HEM03	Triangle	45 min.
Polaroid CubeCAM	2015/06/08	81.09977 N 19.64383 E	With AEM Bird; Transect to LANCE	Straight line	70 min.
Polaroid CubeCAM	2015/06/10	81.74650 N 13.58867 E	With AEM Bird	Straight line	45 min

3.2 Ground-based ice thickness and snow measurements

Platform/ Device	Date	Lat/Lon	Occasion	Flight pattern	Video time
Polaroid CubeCAM	2015/06/18	81.86137 N 9.82327 E	With AEM Bird	Triangle	20 min.
Polaroid CubeCAM	2015/06/24	80.4874 N 8.2313 E	NONE	Triangle	50 min.

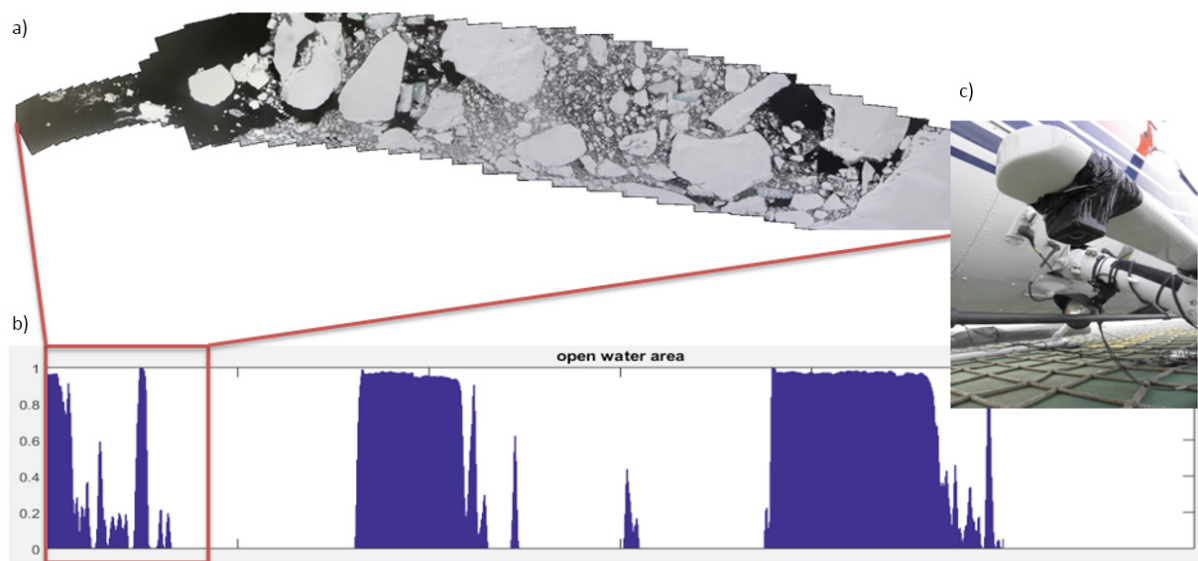


Fig. 3.5: a) Flight transect as stitched from single image frames, b) derived open water area and c) Polaroid CubeCAM attached to the helicopter

Data management

The videos and extracted image frames will undergo further processing after the expedition. Obtained transects of image frame properties will be made available after final processing in the PANGAEA database.

3.4 Snow temperature and grain size evolution

Objectives

The temporal setting of the TRANSSIZE cruise fell right into the transition from spring conditions to intensive summer melt. The onset of strong and continuous melt can occur very abrupt, especially in the marginal ice zone. The transition from early melt, characterized by diurnal melt-freeze cycles is rather short in the Arctic, compared to the Antarctic. Therefore, a measurement of daily cycles of vertical snow temperature profiles can help to identify the stage of melt conditions in which the ice station work was conducted. Associated changes in snow grain sizes and their vertical stratification is a further asset for an interpretation of spatial and temporal variability of satellite SAR data, e.g. Sentinel-1 and TerraSAR-X. Moreover, a comparison with satellite thermal infrared imagery helps to set local measurements also into a larger regional context.

Work at sea

Starting from ice station 3, vertical snow temperature profiles were measured approximately every 2 hours with a focus on capturing the daily maximum temperatures. Additionally, the vertical distribution of snow grain sizes was determined at least once per ice station. Different snow regimes were chosen for the grain size survey to identify potential lateral inhomogeneity. To provide a regional context of the in-situ snow measurements MODIS surface temperature maps (MOD/MYD29 product) were acquired and investigated for the region covering the ship's position during clear-sky conditions. Due to the prevailing overcast conditions, mostly consisting of low cloud cover and fog, the thermal infrared satellite data could provide, however, only limited additional information.

Preliminary results

The obtained snow temperatures reveal that ice stations 3-7 were conducted on floes in an early melt stage with non-isothermal snow conditions but with temperatures close to 0°C (Fig. 3.6). Grain size investigations showed the presence of melt clusters for every ice station, indicating the snow has previously undergone temporarily limited melt (Tab. 3.3). Ice Station 8 (19 to 20 June 2015) differs from the previous stations such that the snow was isothermal and melting after 1700 LT.

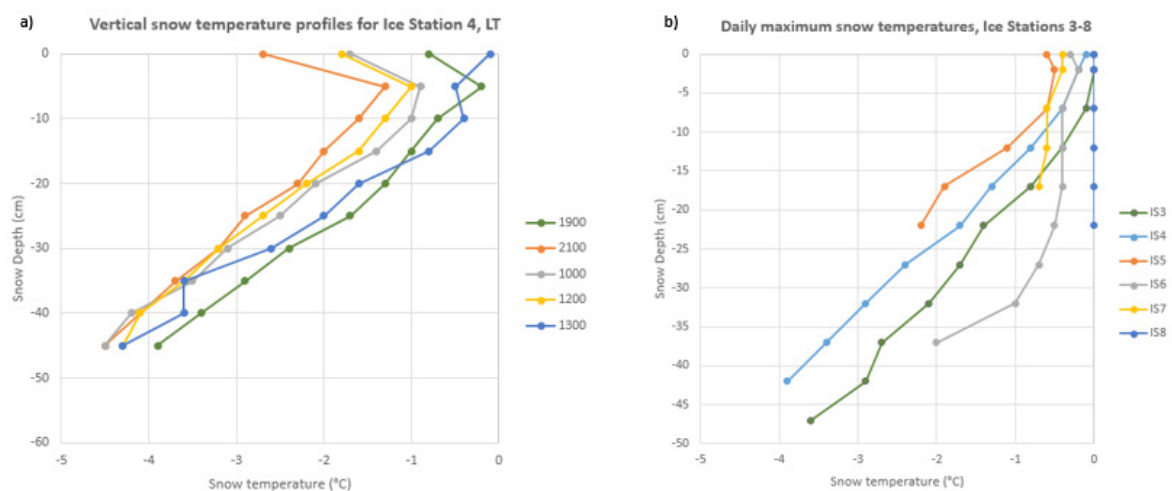


Fig. 3.6: a) Vertical snow temperature profiles acquired on ice station 4 (6 June 2015) for different local times (LT); b) Maximum daily snow temperatures for ice stations 3 to 8.

3.5 ROV work and optical properties of sea ice

Tab. 3.3: Vertical profiles of snow grain sizes and associated compactness for ice stations 4 -7

depth layer (cm)	Ice Station 4		Ice Station 5		Ice Station 6		Ice Station 7				
	grain size	compactness	grain size	compactness	grain size	compactness	grain size	compactness			
-1	0.5	loose	1	loose	3	refrozen melt cluster	0.5	new snow			
-3	3	loose	3	refrozen melt cluster			2.5	loose	1.5	refrozen melt cluster	
-5									3	refrozen melt cluster	2.5
-7					3	refrozen melt cluster					
-10					2.5	compacted			2-3	loose	ice layer (sup. Ice)
-15	2.5	compact									
-20	1.5	compacted	ice layer (sup. Ice)	ice layer (sup. Ice)	ice layer (sup. Ice)						
-25						2.5	compacted	ice layer (sup. Ice)			
-30									1.5	compacted	ice layer (sup. Ice)
-35						slush	ice layer (sup. Ice)				
-40	slush	ice layer (sup. Ice)									
-45			slush	ice layer (sup. Ice)							
-50	slush	ice layer (sup. Ice)									

Data management

The measured snow properties will be released following final processing after the cruise in the PANGAEA database.

3.5 ROV work and optical properties of sea ice

Objectives

Sunlight is the most important energy source on earth. It is crucial for eco-systems and geochemical processes, especially in the ocean. The most influencing factor of this interaction in the Arctic Ocean is sea ice. The interactions between light and sea ice control the amount of energy that passes through the ice and therefore have great impact on the mass- and energy-balances in the ice-covered Arctic Ocean. The main goal of the optical work during this cruise was to measure the distribution of short-wave radiation directly underneath the sea ice and in the uppermost ocean. Therefore measurements were conducted along horizontal and vertical transects with a remotely operated vehicle (ROV).

Additionally, solar irradiance was measured on the sea ice during stations using RAMSES spectral radiometers. This study continues work from previous expeditions (ARK-XXVI/3 (TransArc, 2011), ARK-XXVII/3 (IceArc, 2012)), but focuses on a different time of the year (May to June).

Work at sea

The optical measurements during the 8 ice stations (Tab. 3.4) of TRANSSIZ consisted of:

- Surface measurements of solar irradiance with RAMSES spectral radiometers above the sea ice during ice stations and along the entire route of the RV *Polarstern*.
- Under-ice irradiance and radiance measurements along horizontal (at least 80x80m) and vertical transects. These measurements were performed with two RAMSES spectral radiometers (320-950 nm, Trios GmbH, Rastede, Germany) operated on a V8Sii ROV (remotely operated vehicle from Ocean Modules, Åtvidaberg, Sweden).
- The optical ROV data are supported by sea ice thickness and snow depth measurements, as well as aerial photography from each ice station. Finally, 15 optical cores were

taken directly at the ROV transects for calibration of hyperspectral retrieval of the in ice chlorophyll content.

Preliminary results

The combination of all optical measurements will be used to derive characteristic optical properties for different sea-ice conditions. Due to the comparably early time of the measurements, the main focus for the analysis lies on the difference between different melt stages and the degrees of snow coverage and ice thickness. While the first ice stations had a very low light transmittance, the beginnings of surface melt lead to higher light transmittance on the last two stations (Fig. 3.7).

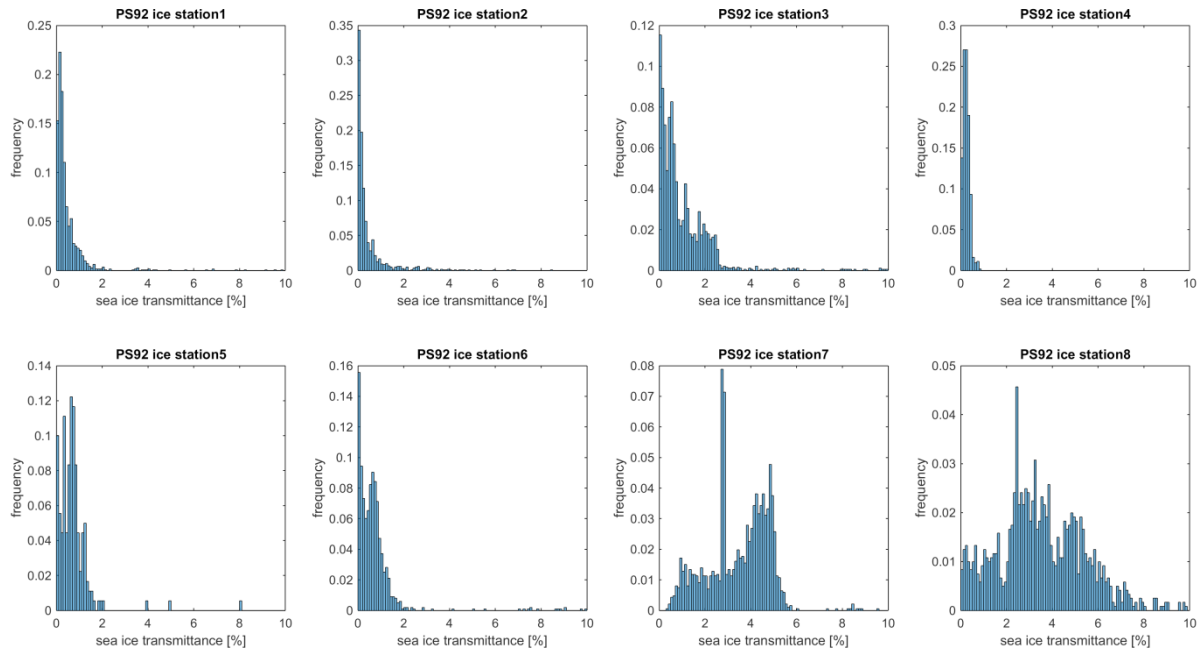


Fig. 3.7: Sea ice light transmittance as measured during the 8 ice stations

Tab. 3.4: Overview about the ROV measurements conducted on the ice stations during PS92

Ice station number	PS station number	Start date	End date
1	PS92-019	28.05.	29.05.
2	PS92-027	31.05.	01.06.
3	PS92-031	03.06.	04.06.
4	PS92-032	06.06.	07.06.
5	PS92-039	11.06.	12.06.
6	PS92-043	15.06.	16.06.
7	PS92-046	17.06.	18.06.
8	PS92-047	19.06.	20.06.

Data management

All optical data will be published on Pangaea following the cruise. This also includes the meta data and related sea-ice properties. The available data set is going to be identical to similar data from the expedition ARK-XXVI/3 (TransArc, 2011).

3.6 Ice observations

Objectives

Ice observations from the bridge, using the software based protocol ASSIST were performed during the cruise. The observations are continuations of earlier ice observations made on board of *Polarstern* and are available via the ASSIST database. The aim of the observations is to assist sample and satellite data interpretation and reconstruct ice conditions during the cruise at a later stage.

Work at sea

Ice observations started after the first ice station. During the cruise observations were carried out from the bridge between 08 am to 11 pm. During station work, ice observations were made twice daily only (10 am and 2 pm).

Preliminary results

Preliminary results of the ice observations are summarized in Table 3.5.

Tab. 3.5: Preliminary summary of ice observations made during PS 92

Number of observations	192	
Observation hours	During cruise	<i>08 am – 10 pm</i>
	During ice station	<i>10 am & 2 pm</i>
Parameter	Mean	STDDEV
Total ice concentration	76 %	+ - 2.1 %
Ice thickness	96.4 cm	+ - 34.9 cm
Snow thickness	26.2 cm	+ - 14.3 cm

Data management

The ice observation data will be released following final processing and quality checks after the cruise in the ASSIST databases.

4. PHYSICAL OCEANOGRAPHY

Anna Nikolopoulos¹, Markus Janout²,
Jens Hölemann², Meri Korhonen³,
Bennet Juhls⁴, Achim Randelhoff⁵

¹ABWR
²AWI
³FMI/UH
⁴GEOMAR
⁵NPI/UiT

Grant No AWI_PS92_00

Objectives

The physical oceanography component of this interdisciplinary TRANSSIZ-cruise aimed to map the physical properties (temperature, salinity, currents and turbulence) of the study region during the little-studied early summer period. Based on the collected data information will be gained on the properties and pathways of the Atlantic water (AW), on shelf-to-basin fluxes, and on the vertical mixing of energy and matter under the sea ice in a key region of the Arctic Ocean. The AO currently progresses toward a seasonally ice-free ocean with several record-low ice extents within the last decade. The seasonal ice retreat occurs in the season of maximum biological productivity and is hence of special interest for biology, oceanography and sea ice dynamics. The mechanisms responsible for these changes are not yet fully understood. Furthermore, despite the obvious potential importance, the contribution of warm subsurface waters to the ice reduction is even less understood. Hence, further efforts are required to understand the oceanic heat fluxes, in particular during the transition seasons when sea ice melts and forms.

In this sector of the Arctic Ocean, the dominant feature is the AW inflow along the West Spitsbergen Current and the Fram Strait inflow branch; one of the two prominent pathways for AW from the Nordic Seas. Even if this AW inflow is of comparable magnitude as the Barents Sea branch, the Fram strait branch is estimated to carry the bulk of the oceanic sensible heat into the Arctic Ocean, (Rudels, 1987; Blindheim, 1989; Rudels, 2013). Since 1997 observations by the mooring array in Fram Strait have revealed several pulses of warmer AW flowing into the Arctic Ocean with a general trend towards higher temperatures, having a maximum in 2006 and slightly decreasing temperatures thereafter (Hughes et al., 2011). The complex topography in Fram Strait forces a bifurcation of the inflow around 80°N, where one part propagates eastward, and another part follows the topography around the sickle-shaped Yermak Plateau. The partitioning of the inflow, and the associated spatial and temporal variability are yet to be fully deciphered. Before reaching 30°E, both portions of the Fram Strait branch reunite and follow the continental slope eastward as a well-defined boundary current distributing heat and nutrients along its way around, mainly, the Nansen Basin (Rudels 2013).

In most AO regions the ice-covered surfaces are separated from the warm Atlantic (or Pacific) derived waters by a pronounced halocline layer (i.e. a layer of strong stratification due to vertical salinity differences), which is a crucial feature for protecting the sea ice from the warm AW (Rudels et al., 2004). However, in the inflow region north of Svalbard Atlantic AW is found near the surface contributing to seasonal ice melt as well as delays in the fall freeze-up relative to other regions.

Earlier hydrographic observations extending from north of Spitsbergen, across the Sofia Deep, and over the Yermak Plateau have earlier been made on the CEAREX expedition in March-April 1989 (Muench et al. 1992), the ARK-XIII-2 cruise of RV *Polarstern* in July 1997 (Rudels et al., 2000), and on the AO-02 cruise by I/B Oden in May 2002 (Rudels et al. 2005, Marnela et al. 2008). Hence, there are important comparisons to be made between these earlier observations and the data collected during the PS92 expedition.

Work at sea

The oceanographic objectives included a detailed data collection on the properties of the Arctic Boundary Current in several cross-continental slope transects north of Svalbard and over the Yermak Plateau as well as to measure currents, turbulence and vertical exchange under the sea ice. Unfortunately, parts of the planned programme along 30°E and across the north-western flank of the Yermak Plateau had to be aborted due to heavy ice conditions. Also, the initially planned measurements by lowered-ADCP on the CTD/RO casts were cancelled since this ADCP-system was under repair and not installed at that time.

Nevertheless, we managed to collect data from a decent number of locations over the continental shelf and slope north of Svalbard as well as over the Yermak Plateau and its southern flank. Velocities down to ~250 m, are supplied by the vessel mounted ADCP.

CTD measurements

Vertical profiles of temperature and salinity were obtained using three Conductivity Temperature Depth (CTD) systems (Fig. 4.1). Two of these systems, the underway CTD (uCTD) and eXpendable CTD (XCTD), could be used during transit (although requiring relatively open waters).

In total, 86 CTD profiles were taken. Among these, 54 casts were carried out with the onboard standard CTD/rosette water sampler system (CTD/RO) from Sea-Bird Electronics Inc. The SBE911+ CTD was equipped with duplicate temperature (SBE3; SN5101/5112) and conductivity sensors (SBE4; SN3570/3597), a pressure sensor (SBE9+; SN0937) as well as an altimeter (Benthos; SN1229), and was connected to a SBE32 Carousel Water Sampler with 24 bottles á 12 liters. Additional sensors for fluorescence (WETLabs ECO-AFL/FL; SN1853), dissolved oxygen (SBE43; SN0467) and beam transmission (WETLabs C-Star; SN1229) were also mounted on the carousel. At a later stage of the cruise (ice station #5-8), a Satlantic MBARI *in-situ* Ultraviolet Spectrophotometer (ISUS-V3) sensor for nitrate was also used on casts to a depth less than 1,000 m.

The majority of the CTD/RO casts (32 in total) were made in connection to the eight ice stations. During each of these stations, four casts were carried out to accommodate the water sampling required for the biogeochemistry. Typically, the first cast was taken to 200 m depth for high-resolution sampling of the upper water column, the second to a maximum depth of 200-1,000 m for sampling of larger volumes, the third cast down to bottom depth for “feature” sampling (e.g. from surface, Chl-max, AW T/S-max, or bottom), and finally, the fourth cast to the bottom in connection to the benthos work programme.

The remaining 22 CTD/RO casts were taken across the Svalbard continental slope and the southern flank of the Yermak Plateau in an effort to perform a hydrographic transect with as little time between stations as possible. The locations of these transects, and the individual stations were often dictated by the harsh ice conditions. Two transects covered more or less the entire shelf and slope (see T4 and T5 in Fig. 4.1.), while the remaining transects were shorter and/or interrupted by ice station activities.

The CTD/RO data were preliminary processed on board promptly after acquisition with help of the *ManageCTD* software, which is a collection of the SBE data processing scripts intervened with custom-made matlab scripts (Gadeberg and Rohardt 2009). This processing routine, resulting in data in ODV spreadsheet format, made it possible to directly share the data with several working groups onboard, e.g. the group for volatile compounds (fluorescence data) as well as the parasound/hydrosweep group (sound velocity data).

For calibration of the conductivity sensors salinity samples were taken from the rosette bottles at 29 stations (duplicate samples from 2-3 depths per cast). The samples were analyzed during the cruise with an Optimare Sensorsysteme AG salinometer.

XCTD probes were used underway from the ship for 16 temperature and salinity profiles (maximum depth 1 100 m) in the Yermak Plateau region and during the hydrosweep/parasound profile survey around 80°N/10°E at the end of the cruise (see Fig. 4.1). The initial plan to utilize the helicopter for additional XCTD casts for increasing the spatial resolution within transects or extending transects was obscured by weather conditions not permitting helicopter flights. The profiles measured during the hydrosweep profiling were first-hand used to calculate the sound velocity profiles for immediate use in the bathymetric mapping.

The UCTD was used in open water in 17 casts (to a maximum depth of 600 m) during the northward transit from Bremerhaven and also at the end of the cruise (see Fig. 4.1).

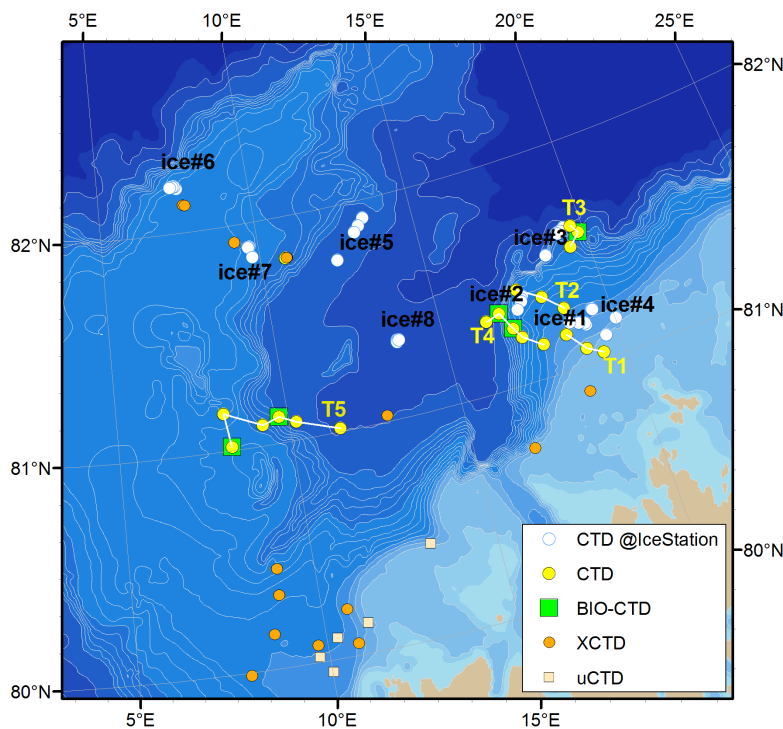


Fig. 4.1: The locations of the CTD stations during PS92. White symbols indicate repeated ice station casts (ice#1-8) while yellow symbols indicate CTD “transect” measurements (T1-5). Five locations during these transect casts were dedicated to extensive biological sampling from the rosette bottles (BIO-CTD).

Physical oceanographic on-ice activities

Our main activities during the 8 ice stations were centered around microstructure measurements through the sea ice. The objective was to determine dissipation rates of turbulent kinetic energy and fluxes of heat (and nutrients). The structure of the water column is characterized by a near-freezing surface mixed layer above a sharp pycnocline separating the cold ice covered layer from the warm Atlantic waters below.

We operated an MSS90L profiler (MSS, Fig. 4.2 and 4.3) in free-fall mode. The MSS samples with a rate of 1,024 Hz and is equipped with two shear sensors, as well as with fast response temperature, conductivity, acceleration, and turbidity sensors. Data are transmitted via an online cable in real time. During ice stations 1-5, we operated a manual winch with 200 m cable (SWM-200), during stations 6-8, we used a motorized winch with 400 m cable (SWM-400), which was powered with a generator. Due to the patchiness of turbulence in the ocean, a statistically meaningful sampling strategy requires a greater number of casts to average them into one profile. Mixing rates are further strongly dependent on shear that may be forced by sea ice motion, wind-driven currents or tides, which is why the goal was to resolve at least one full semidiurnal tidal cycle during each ice station.

During the ice stations, we followed a general routine, where a site was chosen as a function of ice topography and of a safe distance from the ship, which means far enough to be away from ship-induced turbulence, but close enough to the ship to remain within good sight for the bridge bear watch. Throughout the ice station, we operated a 300 kHz Acoustic Doppler Current Profiler (ADCP) under the ice (Fig. 4.4), in order to measure the current velocities and shear in the upper ~80 m as background information for the MSS work. Sea ice thicknesses varied between ~1.0 m and 1.6 m.

Underway measurements

Underway measurements with a vessel-mounted narrow-band 150 kHz ADCP from TRD Instruments and with two Sea-Bird SBE45 thermosalinographs were conducted to supply water current velocity and temperature and salinity data, respectively. The thermosalinographs are installed in 6 m depth in the bow thruster tunnel and in 11 m depth in the keel.



Fig. 4.2: The MSS in the ice hole (Photo M. Janout)

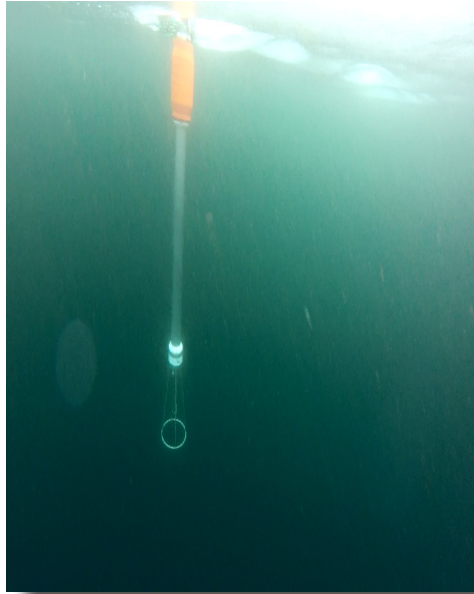


Fig. 4.3: The MSS under the ice (Photo, B. Juhls)



Fig. 4.4: The ADCP under the ice (Photo, B. Juhls)

Preliminary results

All data are subject to final post-cruise processing but some first results follow below.

CTD/RO measurements

Fig. 4.5 summarizes the θS_{σ} -properties found during PS92. The lowest temperature measured was -1.81 °C (Halocline Water) at stations 43-1/ice#6 and 53-1/T5 (both at ~ 35 m depth), while the maximum temperature was 3.75 °C (Atlantic Water core) at station 33-1/T4 (~ 55 m depth, cf. Fig. 4.18 and 4.19). The salinity ranged from 33.65 (Polar Surface Water) at surface levels of station 47-19/ice#8 to 35.05 (Atlantic Water) at stations 33-1/T4 (~ 55 m depth) and 26-1/T2 (~ 250 m depth). When present, the bend at minimum temperature indicates that the halocline waters do not form through direct mixing between the polar mixed layer and the underlying AW, but created elsewhere and advected to these locations (Rudels, 2004).

Winter convection in the Nansen Basin generally reaches to about 100 m depth, and somewhat less, to 50-100 m, closer to the continental slope. The salinity of the homogenized winter mixed layer is typically 34.2-34.4, before being overlaid by a thin low salinity meltwater layer during summer (Rudels, 2004). During PS92 the θ/S -profiles for the eight ice stations showed varying mixed layer depths (ML; defined here by the minimum potential temperature), see Fig. 4.6 and 4.8-4.15. The shallowest ML were found to be around 15-20 m at ice stations #1 and #2 (individual casts), on the shallow continental shelf north of Spitsbergen. The deepest ML was more than 60 m at ice station #5, and for individual casts also at ice station #6, on the Yermak Plateau. The salinity at the stations with a pronounced mixed layer varied between 34.1 and 34.4, see Fig. 4.6. The freshest surface waters (33.65), however, were found at ice station #8 over the Sofia Deep in connection to increased temperatures, relatively to the overall ML temperature, down to ca. 25 m (Fig. 4.16). Station 50-1, the deepest station of transect T5 over the southern flank of the Yermak Plateau, showed similar features, which indicates that melting of the sea ice had been initiated.

Over the continental shelf and slope (ice stations #1, 2, 4), as well as over the Sofia basin (ice#8) the chlorophyll distribution was characterized by pronounced Chl-maxima at 10-25 m depth, see Fig. 4.6. On the contrary, we found only very low chlorophyll values, and very weak or non-existing Chl-maxima, over the Yermak Plateau (ice stations #5-7). Ice station #3 fell somewhere in between these two "groups" with a moderate chlorophyll signal and a maximum at 25-30 m depth. The chlorophyll profile at ice station #2 may be noted for its bimodal structure with a second maximum at 50 m depth (visible at all four casts during this station). Except from the ice stations, extensive biological sampling was also undertaken at some of the transect stations (denoted BIO-CTD), reflecting a range of water-mass configurations both within and outside the strong influence of the AW inflow, Fig. 4.17.

In general, the AW core became colder, less saline, and deeper as we moved from the continental slope region towards the Yermak Plateau (Fig. 4.7). The relatively warm and saline θS -characteristics of the AW at ice station #8, in the centre of the Sofia Deep, resembles those over the continental slope (ice#2 and #3), rather than those further west. Also station 50-1 shows core temperatures of nearly 3 °C (Fig. 4.20), supporting the findings of Rudels et al. (2000) and Rudels et al. (2005); that the AW in the Sofia Deep mainly seems to be supplied by the eastern inflow pathway of the Fram Strait branch, rather than from the outer branch circulating around the Yermak Plateau.

At stations 33-1 of transect T4, the Atlantic core was observed at rather high temperatures ($\theta \sim 3.75$ °C, at 50-100 m depth), see Figs 4.5, 4.18 and 4.19 (cf. Rudels et al. 2005). At the other continental slope stations, the maximum AW temperature was nearly 3 °C, and the core

was typically found somewhat deeper, at 150 m depth. The $\theta S\sigma$ -characteristics of T4/33-1 ($\theta \sim 3.749$ °C, $S=35.051$, $\sigma=27.853$ kgm⁻³) indicate that this patch of the inflow may have travelled along the slope rather unaffected from e.g. entrainment and mixing by shelf waters.

On-ice measurements

Preliminary station post-processing was done after each sampling day using Matlab routines. Upon processing of station 1, we noted that one shear sensor was corrupted, due to humidity in the sensor’s shaft. Therefore, we replaced the sensor, dried the shaft and electronics, and replaced the O-rings, which solved the problem. Preliminary analysis overall indicates a good data quality. Dissipation was highest at ice station 5 (Fig. 4.22), due to the strong ice drift during and after a strong wind event (8 Bft), followed by station 2 above the continental slope, where currents were considerably stronger (Fig. 4.23). Overall, a wide spectrum of different sea ice and wind conditions was present during the 8 ice stations, which provides excellent opportunities to investigate vertical mixing rates in different locations under various environmental conditions.

Please note that full processing of the MSS casts is time-intense and was not finished at the time of writing.

Tab. 4.1: Ice station overview

Ice Station	Date	Lat. °N	Lon. °E	Depth (m)	Drift (kt)	Wind (m/s)	MSS Casts
1	5/28 07:00 - 5/29 15:00	81° 10.43'	19° 8.07'	376	0.1	6	45
2	5/31 07:00 - 6/01 16:00	81° 23.18'	17° 35.66'	876	0.2	7	50
3	6/3 11:00 - 6/4 15:00	81° 37.35'	19° 26.77'	2034	0.3	9	36
4	6/6 17:00 - 6/6 13:00	81° 14.16'	19° 25.52'	461	0.2	8	25
5	6/11 13:00 - 6/12 16:00	81° 56.23'	13° 34.20'	1570	0.6	15	51
6	6/15 04:00 – 6/16 10:00	82° 12.70'	7° 35.70'	806	0.0	0	35
7	6/17 17:00 – 6/18 16:00	81° 50.65'	9° 45.76'	887	0.1	4	30
8	6/19 12:00 – 6/20 16:00	81° 20.54'	13° 38.19'	2164	0.2	3	58

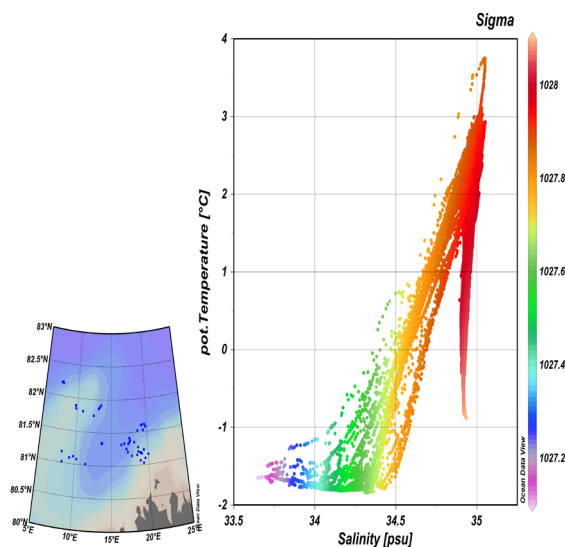


Fig. 4.5: Temperature, salinity and density of all CTD/RO data collected during PS92 showing the fresh polar surface waters, the halocline waters at minimum temperatures, the warm Atlantic Water at maximum temperatures, as well as the dense deep water masses.

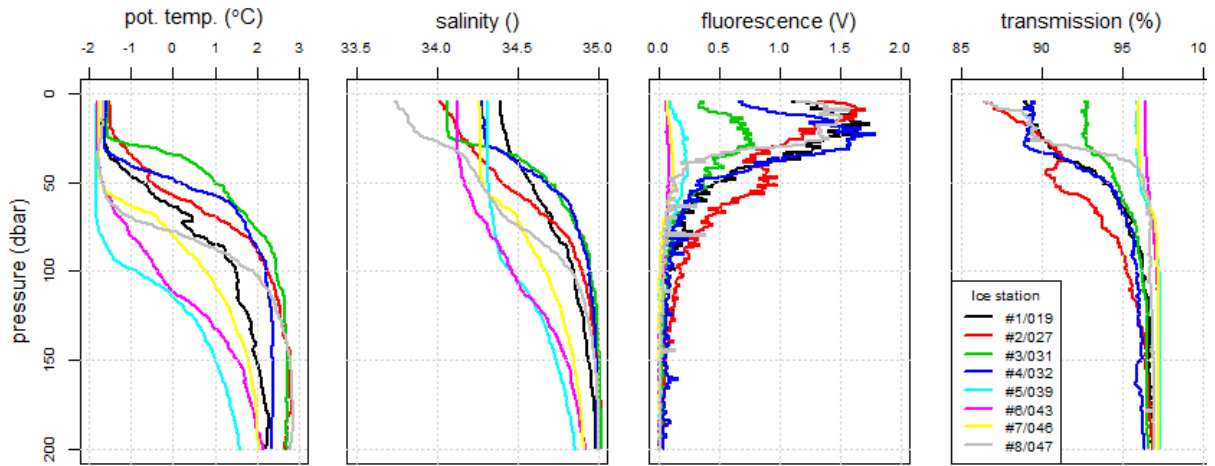


Fig. 4.6: CTD/RO profiles of (a) potential temperature, (b) salinity, (c) fluorescence and (d) beam transmission for the upper 200 m. Legend in (d) valid for all graphs. The values shown are average values of all casts made during each ice station. Plots for each individual ice station are shown below in Figs 4.8-4.15.

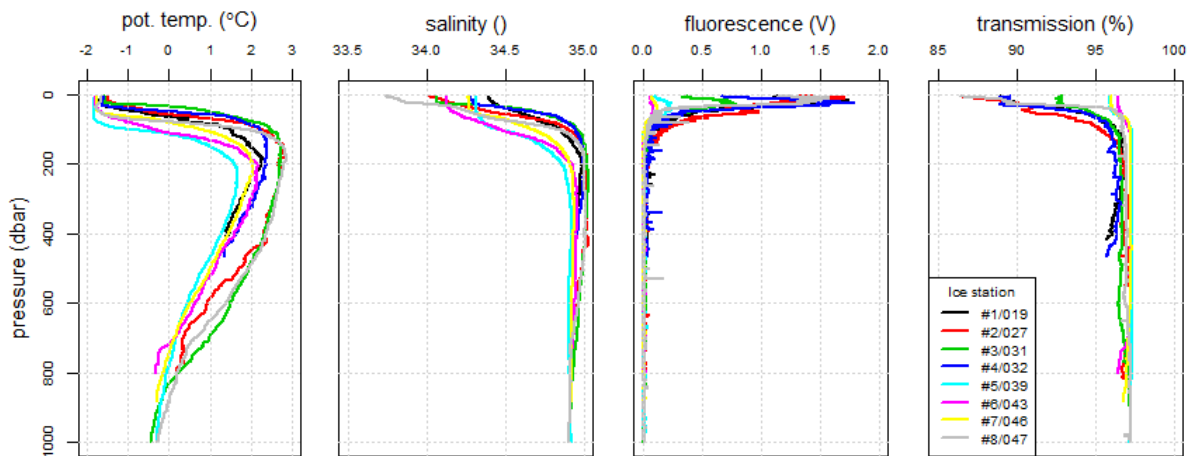


Fig. 4.7: As in Fig. 4.3 but down to 1,000 dbar

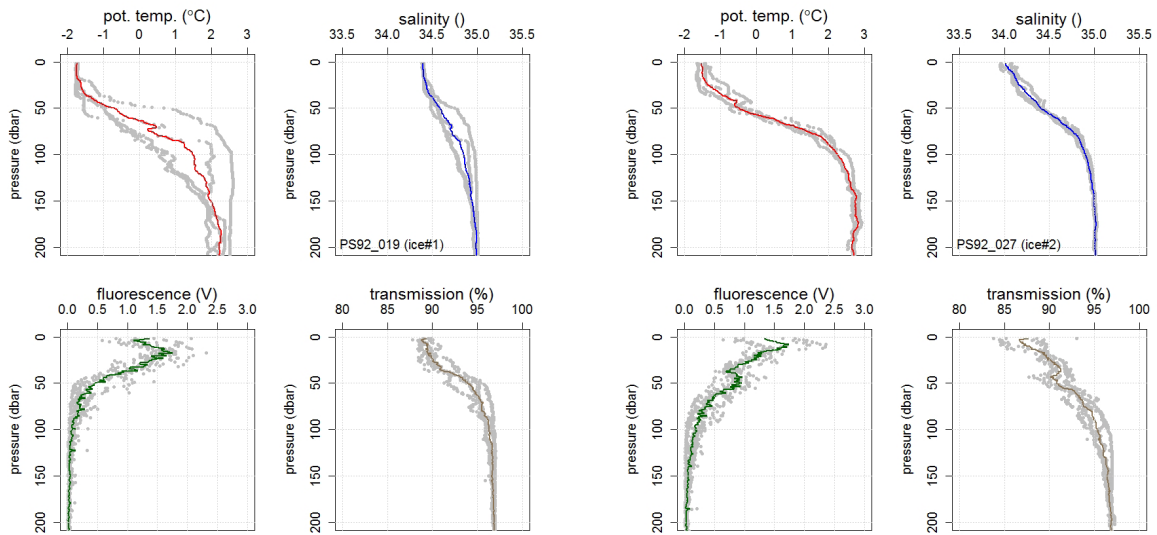


Fig. 4.8 and 4.9: CTD/RO profiles of potential temperature, salinity, fluorescence and beam transmission for the upper 200 m at ice stations #1 (left panel) and #2 (right panel). Grey dots show data from individual casts, while thick solid lines show the averages for each ice station (also shown in Fig. 4.6).

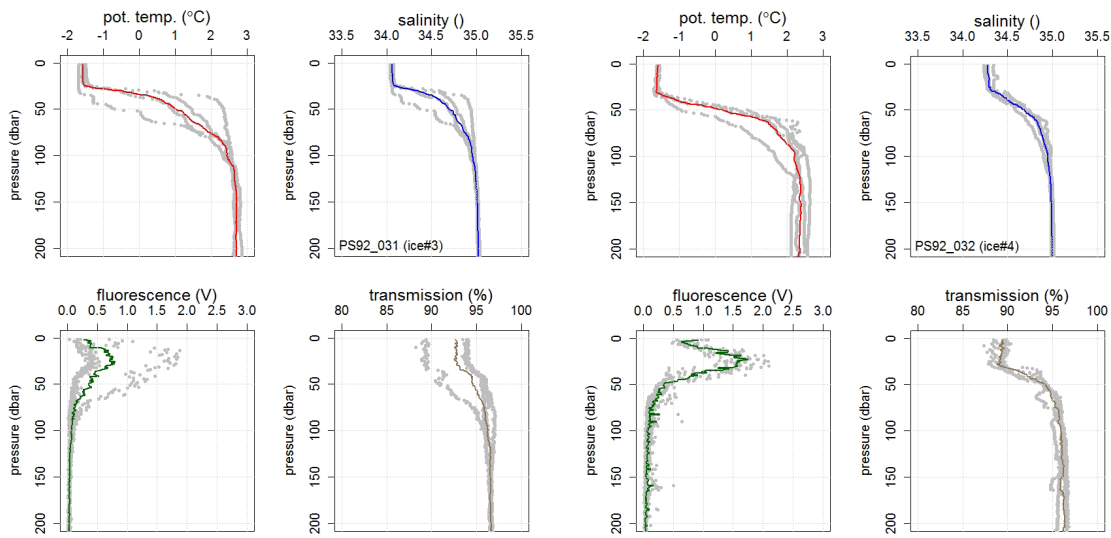


Fig. 4.10 and 4.11: As in Fig. 4.8, but for ice stations #3 (left panel) and #4 (right panel)

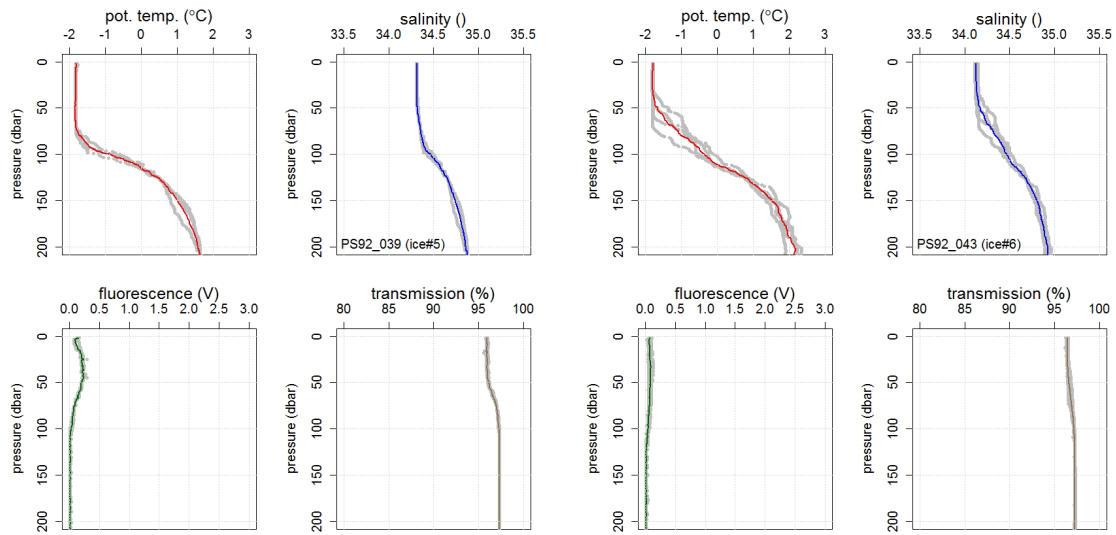


Fig. 4.12 and 4.13: As in Fig. 4.8, but for ice stations #5 (left panel) and #6 (right panel)

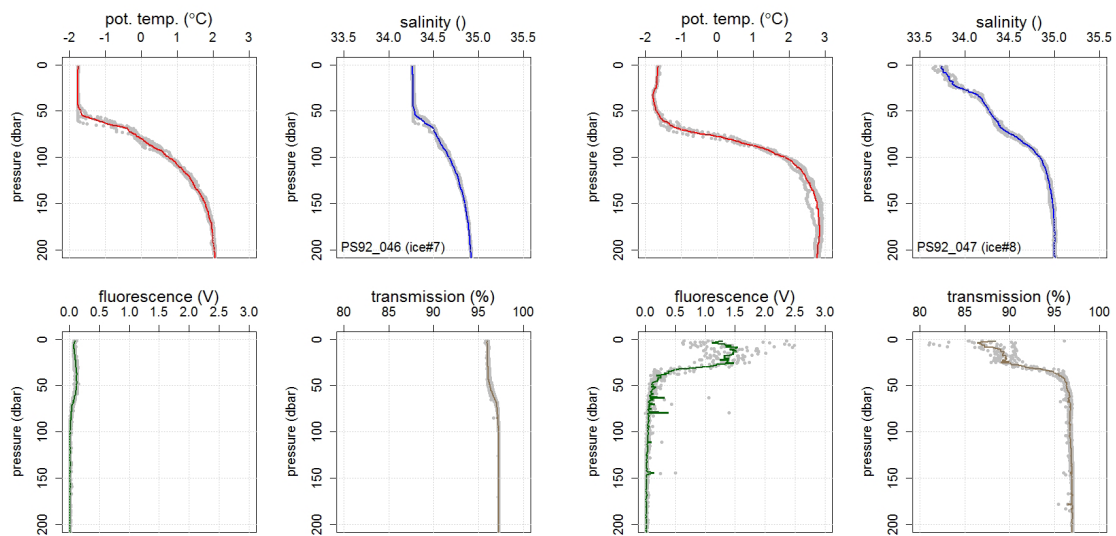


Fig. 4.14 and 4.15: As in Fig. 4.8, but for ice stations #7 (left panel) and #8 (right panel)

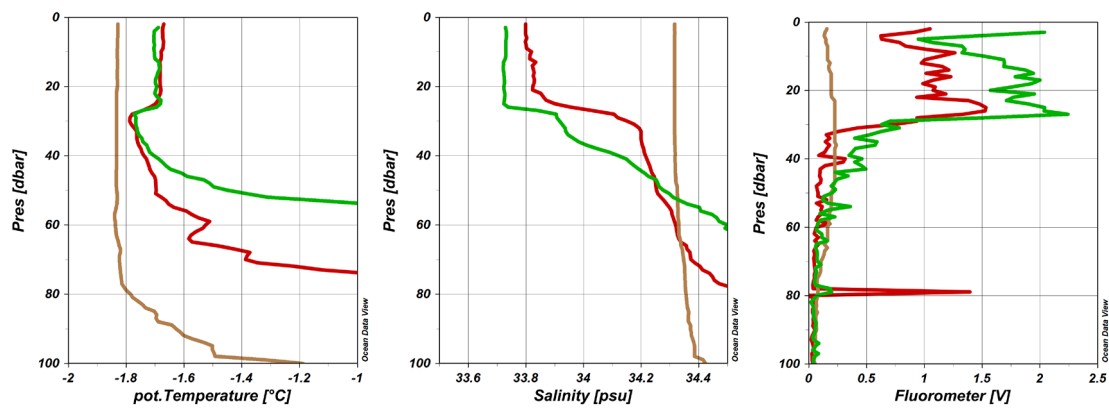


Fig. 4.16: Profiles of temperature, salinity and fluorescence for the upper 100 dbar of cast ice#5/39-8 (brown), ice#8/47-4 (red), and 50-1 (green), of which the latter two indicate a warming, and freshening, of the surface layers (ice#5 shown as reference).

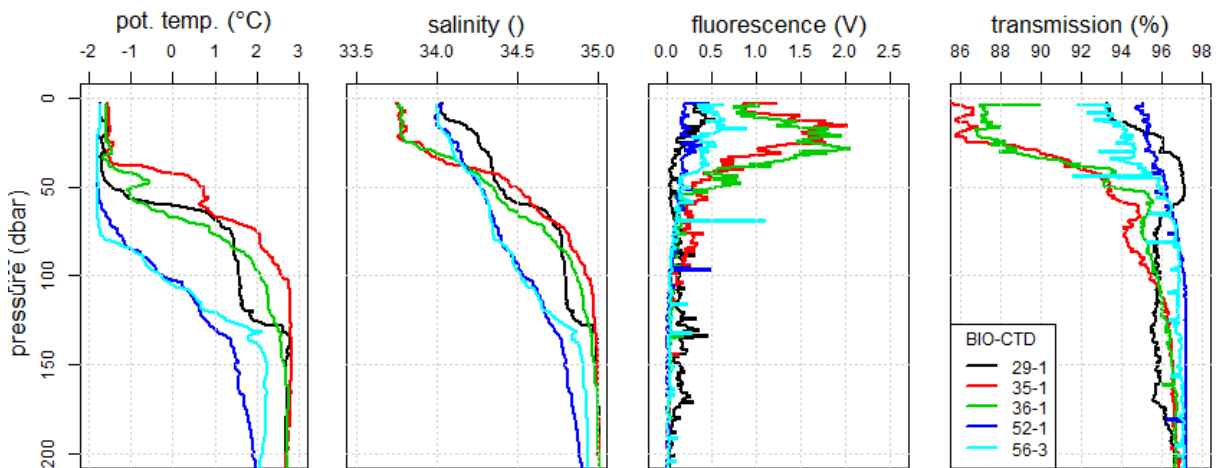


Fig. 4.17: Profiles of temperature, salinity and fluorescence for the upper 200 dbar of the transect casts with extensive biogeochemical sampling (legend in (d) valid for all graphs).

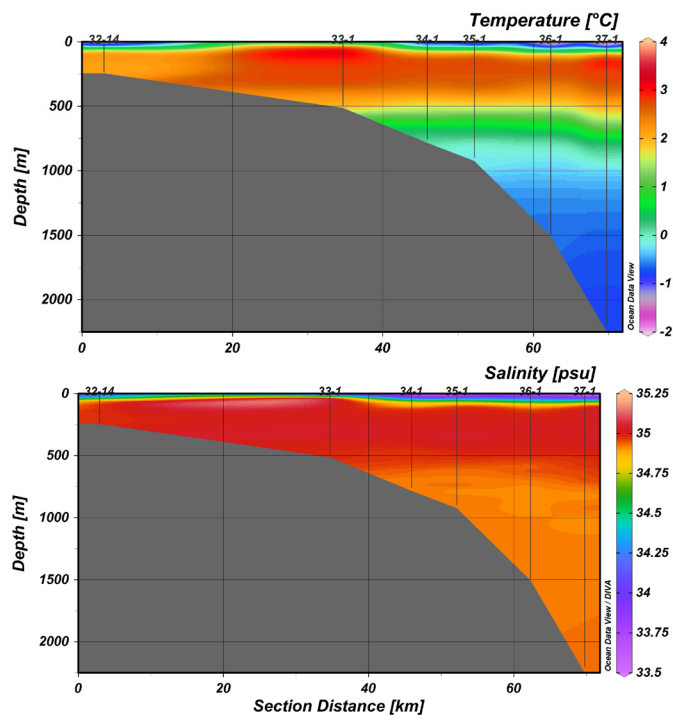


Fig. 4.18: Temperature (a) and salinity (b) along the cross-slope transect T4 north of Svalbard, measured 9 June 2015

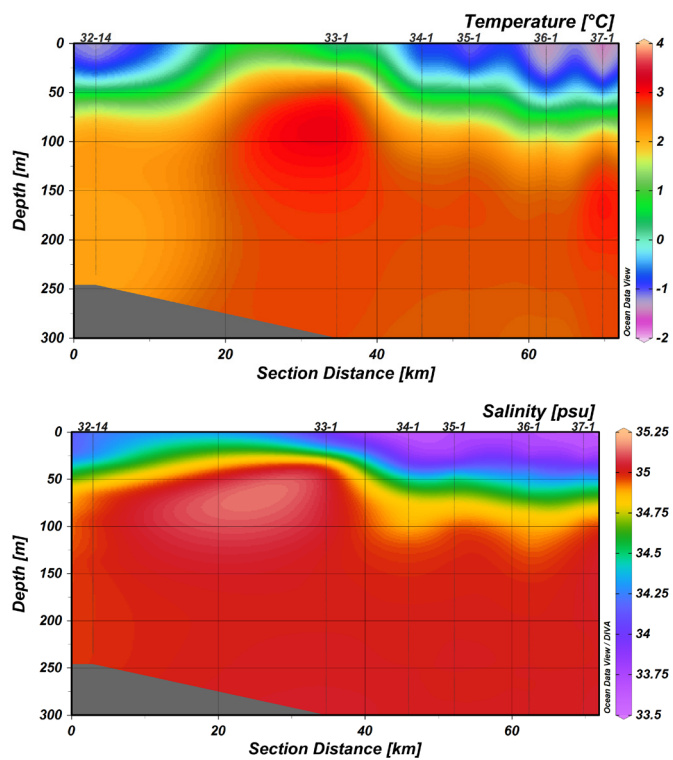


Fig. 4.19: As in Fig. 4.18 but for the upper 300 m

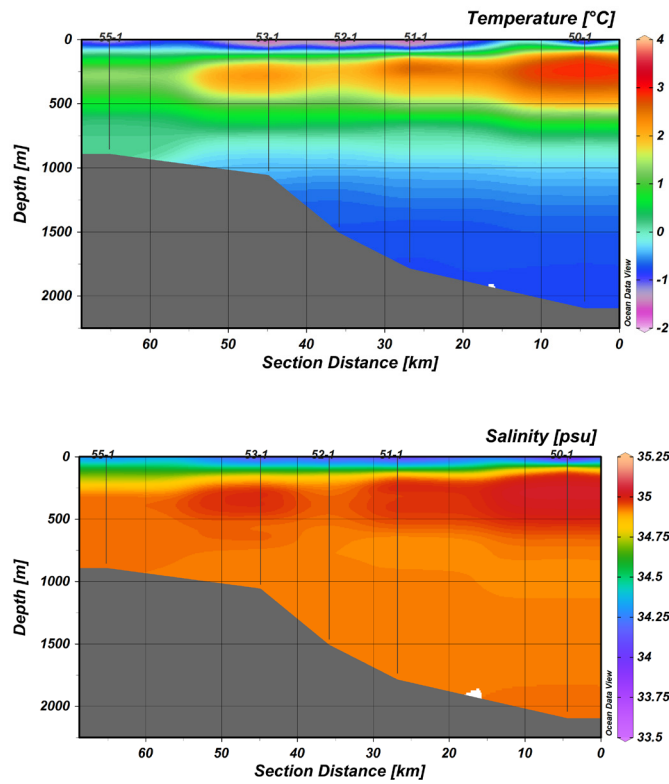


Fig. 4.20: Temperature (a) and salinity (b) along the cross-slope transect T5 over the southern flank of the Yermak Plateau, measured 21-22 June 2015

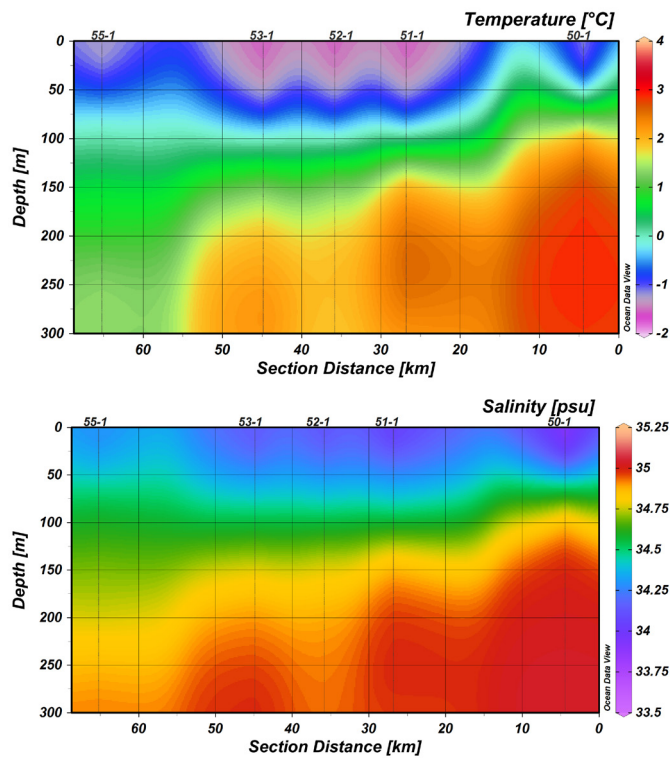


Fig. 4.21: As in Fig. 4.20 but for the upper 300 m

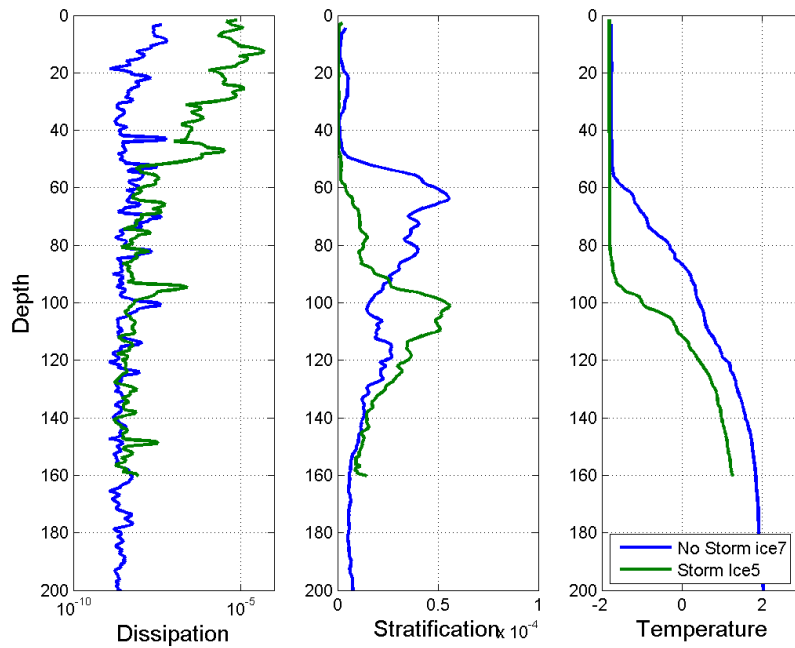


Fig. 4.22: Example of dissipation [$W\ kg^{-1}$], stratification [s^{-2}] and temperature [$^{\circ}C$] from two MSS profiles (ice stations 5 and 7). Note that station 5 was during a strong wind event, which resulted in considerably higher dissipation rates and a deeper mixed layer than station #7.

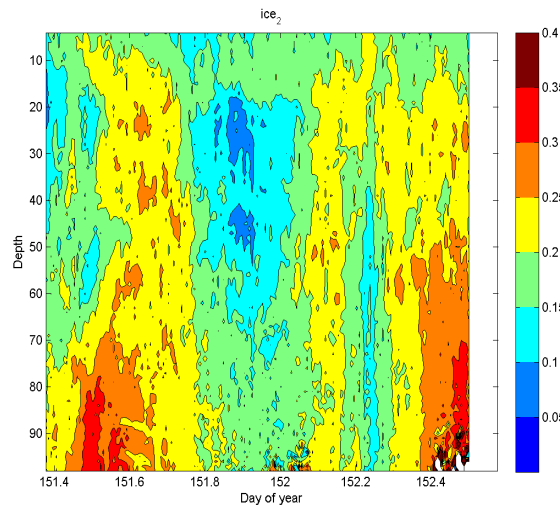


Fig. 4.23: ADCP current magnitude [ms^{-1}] during ice station 2. Note that ice station 2 was located above the continental slope.

Data management

Until August 2016, the oceanographic data are subject of post-cruise calibration, processing and quality assessment. During that time frame the data will be presented at the post-cruise workshop and may be available to cruise participants in their current preliminary state.

At completion, processed and post-cruise calibrated data will be uploaded to the PANGAEA database and available mainly for cruise and project participants. After publication or, at

the latest, five years after the cruise the data will be made openly available to the scientific community via PANGAEA, and other relevant national data centres.

References

- Blindheim J, (1989) Cascading of Barents Sea bottom water into the Norwegian Sea. *ICES Journal of Marine Science*, 188, 49–58.
- Gadeberg S, Rohardt G (2009) Manual for processing CTD-Profiles measured with Seabird CTD SBE911plus, Revision 1.1.
- Hughes S L, Holliday N P, Beszczynska-Möller A (editors) (2011) ICES Report on Ocean Climate 2010, ICES Cooperative Research Report, No. 309, International Council for the Exploration of the Sea, Copenhagen, 69 pp.
- Marnela M, Rudels B, Olsson A, Anderson L G, Jeansson E, Torres D, Messias M-J, Swift J, Watson A (2008) Transports of Nordic Seas water masses and excess SF₆ through Fram Strait to the Arctic Ocean. *Progress in Oceanography* 78, 1–11, doi: 10.1016/j.pocean.2007.06.004.
- Muench R D, McPhee M G, Paulson C A, Morison J H (1992) Winter oceanographic conditions in the Fram Strait-Yermak Plateau region. *Journal of Geophysical Research*, 97, 3469-3483.
- Rudels B (1987). On the mass balance of the Polar Ocean, with special emphasis on the Fram Strait. *Norsk Polarinstitutt Skrifter* 188, 53.
- Rudels B, Meyer R, Fahrbach E, Ivanov V, Østerhus S, Quadfasel D, Schauer U, Tverberg V, Woodgate R A (2000) Water mass distribution in Fram Strait and over the Yermak Plateau in summer 1997. *Annales Geophysicae* 18, 687-705.
- Rudels B, Jones E P, Schauer U, Eriksson P (2004) Atlantic sources of the Arctic Ocean surface and halocline waters. *Polar Research*, 23, 181–208.
- Rudels B, Björk G, Nilsson J, Winsor P, Lake I, Nohr C (2005). The interactions between waters from the Arctic Ocean and the Nordic Seas north of Fram Strait and along the East Greenland Current: results from the Arctic Ocean-02 Oden expedition. *Journal of Marine Systems* 55, 1–30, doi:10.1016/j.jmarsys.2004.06.00.
- Rudels B, Schauer U, Björk G, Korhonen M, Pisarev S, Rabe B, Wisotzki A (2013). Observations of water masses and circulation with focus on the Eurasian Basin of the Arctic Ocean from the 1990s to the late 2000s *Ocean Science*, 9, 147–169, doi:10.5194/oos-9-147-2013

5. TRACE GASES AND CARBONATE CHEMISTRY

5.1. Trace gases

Valérie Gros¹, Roland Sarda-Estève¹
not on board: Bernard Bonsang¹

¹LSCE

Grant No AWI_PS92_00

Objectives

The polar areas are very sensitive to global warming and particularly the Arctic Ocean which is dramatically subject to rapid changes in the extent of ice cover with short and long term consequences on complex feedback processes including climatic, physical, biological, and chemical aspects. These changes affect the distribution of nutrients and impact the distribution of primary producers, phytoplankton, at the base of the reservoir's total biomass. The reduction of sea ice cover and thickness through positive feedback processes lead to the extension of the free oceanic surface. As a consequence, the retreating of sea ice and the subsequent increase of light penetration in different wavelengths in the ocean surface layers will deeply modify both photosynthesis and photochemical processes, and the production of trace gases through photosynthesis of planktonic biomass and photolytic degradation of dissolved organic matter. Such effects can result in variation of trace gases emission by phytoplankton, strongly dependent on available radiation, with subsequent impact on the atmospheric chemistry of boreal zones through the tropospheric ozone cycle and its precursors.

Results obtained during the previous arctic campaigns on board *Polarstern* (ARK-XXV and ARK-XXVI campaigns in summers 2010 and 2011) show that all the newly ice free ocean surface acts as a more intense source of volatile organic compounds (VOCs) to the atmosphere. These first studies have shown also the presence of enhanced concentrations of carbon monoxide, alkenes and isoprene at the bottom of ice cores. These facts have raised emerging questions on the role of photolytic processes and photosynthetic activity for VOCs production in sea ice and the magnitude of the turnover of the biogenic gases in the ice cover and the upper part of the ocean.

Considering that oceanic emissions processes of these different VOCs might be tightly coupled and have never been simultaneously investigated, the objective is to understand and to quantify the impact of the various physical processes sensitive to climate change on the emissions of trace gases in the Arctic areas, waters and ice pack. The focus has been placed on the gases having possible important feedbacks for the chemistry of the atmosphere and climate: dimethylsulphide, carbon monoxide, and volatile organic compounds in the group of polyunsaturated (isoprene) and oxygenated hydrocarbons. Among these species unsaturated hydrocarbons (such as isoprene) and carbon monoxide (CO) have a strong impact on the OH radical and ozone budget. Isoprene and DMS act also as a secondary source of the fine and ultra-fine fraction of the marine aerosols with a direct effect on the radiation balance.

Scientific questions to be addressed are:

What is the distribution of oxygenated VOCs, isoprene, dimethylsulphide and carbon monoxide dissolved in the surface seawater as a function of latitude and different parameters including

physical (i.e. sea water temperature, radiation) and biological parameters: chlorophyll, planktonic abundance, dissolved inorganic and organic carbon?

How does the vertical distribution of the concentration of dissolved gases in seawater reflect the different production processes? What is the role of direct emission by plankton metabolism (under PAR) versus photoproduction processes by DOC degradation (under UV)?

What is the budget of these gases in the ice and in the water column; particularly is it possible to establish a balance between the production rates in seawater and ice and the losses by exchanges with the atmosphere and other bio-chemical or physical losses processes (oxidation, microbial consumption)?

Work at sea

During the transit time (from May 20 to 27), on-line seawater measurements were performed. Surface seawater delivered by the ship membrane pump was continuously injected in an on-line water extraction device. Compounds of interest were extracted from the water into the gas-phase and then injected into the analysers. The instruments consist in a gas chromatograph (for carbon monoxide –CO- measurement) and in a mass spectrometer (for Volatile Organic Compounds –VOCs- measurement). The latter instrument is a state-of the art analyser (PTR-MS for Proton Transfer Mass Spectrometry, Ionicon, Austria) allowing on-line fast measurements of selected VOCs (including oxygenated, aromatics and biogenic compounds). For this campaign, compounds of particular interest were isoprene, dimethyl sulphide (DMS) and oxygenated compounds (acetone, acetaldehyde...). During the transit period, surface seawater measurements were performed every 2.5 minutes. During the rest of the campaign, surface seawater measurements were performed during four additional short periods (less than 1 day) corresponding to streaming time of the ship.

The main part of the work was focussed on measurements on the ice stations. It consisted in a first stage by measuring the compounds vertical gradient (from the surface ocean to 100 m) and it was performed during the CTD cast 1 (for which biogeochemical parameters will be available, Tab. 5.1.1). Samples from eight depths were collected in 1L flasks (light protected) for this purpose and were directly processed on our analytical system. Therefore, all the samples were always analysed within a few hours after their collection. In a second stage, measurements from water under the ice (at the surface and chlorophyll maximum) as well from snow and from sack-hole were performed and also processed within a few hours after collection (Tab. 5.2.2). Finally, two ice cores were taken in the main coring grid, then stored and prepared at -20°C. Only the inside part of the ice cores was used for measurement, to avoid any contamination from the ice in contact with the air. One ice-core was divided in two duplicates which were analysed using two different protocols (one where the ice was melting at room temperature, the other one when the ice melting was accelerating by warming it through the flask immersion within a bucket filled of warm water). The second core was divided into three parts, corresponding to the surface (20 cm), mid and bottom part (20 cm) of the ice core.

Tab. 5.1.1: CTD station – measurements of trace gases: CO and VOC (including DMS, Methanethiol, Isoprene, Acetaldehyde, Acetone, Acetonitrile, Methanol)

Station	Depth (m)	CO	VOC
PS92/19_05	0,5,10,20,30,40,50,100	X	X
PS92/27_03	0,5,10,20,30,40,50,100	X	X
PS92/31_03	0,5,10,25,30,40,50,100	X	X
PS92/32_06	0,5,10,25,30,40,50,100	X	X
PS92/39_11	0,5,10,30,35,40,50,100	X	X
PS92/43_05	0,5,10,20,30,40,50,100	X	X

5.1. Trace gases

Station	Depth (m)	CO	VOC
PS92/46_04	0,5,10,20,30,40,50,100	X	X
PS92/47_04	0,5,10,20,30,40,50,100	X	X

Tab. 5.1.2: Ice station water and ice cores samples: measurements of trace gases: CO and VOC (including DMS, Methanethiol, Isoprene, Acetaldehyde, Acetone, Acetonitrile, Methanol); UIW surf = water under the ice surface; UIW chl a max = water under the ice at the chlorophyll maximum, SH = sack hole, IC = ice cores, MP = Melt pond

Station Nr	Depth	CO	VOC
PS92/19	UIW surf; UIW 20m, SH, IC	X	X
PS92/27	UIW surf; UIW chl a max., SH, IC	X	X
PS92/31	UIW surf; UIW chl a max., SH, IC	X	X
PS92/32	UIW surf; UIW chl a max., SH, IC	X	X
PS92/39	UIW surf; UIW chl a max., SH, IC	X	X
PS92/43	UIW surf; UIW chl a max., SH, IC	X	X
PS92/46	UIW surf; UIW chl a max., SH, IC, snow	X	X
PS92/47	UIW surf; UIW chl a max. ~10m., MP, IC	X	X

Preliminary (expected) results

Results obtained during the transect surface seawater measurement show a high degree of variability for CO and VOCs. Preliminary calibrations of these data suggest quite low values (ranging from 0.2 to 6 nmol L⁻¹ for CO and from 0.05 to 6 nmol L⁻¹ for isoprene), in the lowest range of the concentrations measured in 2010 (Tran et al. 2013). DMS showed also a large degree of variability (with amplitude up to 10). These results will be studied in relation with variations of physical (radiation...) and biological (chlorophyll content...) parameters.

Vertical gradients determined from CTD samples show significant variations between the different ice stations. CO vertical profile seems to be mainly driven by the light penetration (as previously seen before, Tran et al. 2013, except for one profile entirely controlled by the biology (to our knowledge for the first time). DMS vertical gradient shows generally a co-variation with the one from chlorophyll, in agreement with its biological source. Results from ice cores measurements need to be further processed and investigated as well with other measured parameters.

Data management

The data will be available 18 months after the cruise and they will be made available for all project partners in the Pangaea data base (pass word protected). Data will subsequently be made available to the scientific community through the data base after publication and latest 5 years after the cruise.

References

Tran S, B. Bonsang, V. Gros, I. Peeken, R. Sarda-Estevé, A. Bernhardt, S. Belviso (2013), A survey of carbon monoxide and non-methane hydrocarbons in the Arctic Ocean in summer 2010: assessment of the role of phytoplankton, *Biogeosciences*, 10, 1909-1935.

5.2 Water column carbonate chemistry

Sarah Zwicker¹
not on board: Helen Findlay²

¹AWI
²PML

Grant No AWI_PS92_00

Objectives

Carbon dioxide (CO₂) levels are increasing as a result of human activities. The oceans naturally absorb CO₂, however the rate at which CO₂ is being added to the oceans is altering ocean carbonate chemistry. These changes in the carbonate chemistry are causing the surface ocean to become more acidic: a process termed “Ocean acidification” (Caldiera & Wickett, 2003). The Arctic Ocean also has the potential for enhanced ocean acidification in the future because of the increase input of freshwater as sea ice retreats and the planet warms (Steinacher et al. 2009). It is thought that the addition of freshwater into the Arctic will dilute the ocean’s ability cope with increases in acidity, but this is yet to be tested by observations. Several factors can additionally influence seawater carbonate chemistry, other than the ice and freshwater, such as biological productivity or calcification (Findlay et al. 2008). These various drivers change on both temporal and spatial scales. Understanding these dynamics and the drivers are critical for fully understanding what physicochemical conditions Arctic marine organisms’ experience, both presently and what they could experience in the future. This is especially important for setting baselines, as well as informing both experiments and models that look to assess the future Arctic marine ecosystems.

Key questions:

1. How does the ice-edge bloom affect the uptake of CO₂ into the ocean;
2. How does the bloom affect the carbonate system, and what are the implications for seasonality of ocean acidification;
3. How does the carbonate system change across the ice-edge and shelf-to-basin transitions?

Work at sea

At 9 stations (see table 1), samples were collected from the water column from the biogeochemistry CTD/rosette. A minimum of 5 depths were sampled, but whole water columns sampling was carried out, so more depth samples were included at stations with a larger water depth. A minimum of surface (2 m), chlorophyll maximum, 50 m, 100 m and bottom water, were sampled at each station.

Tab. 5.2.1: Water column sampling for DIC (dissolved inorganic carbon) and TA total alkalinity

Station	Depth [m]	DIC	TA
PS92/19-05	2, 20, 50, 100, 354	x	x
PS92/21-01	2, 20, 50, 100, 193	x	x
PS92/24-01	2, 25, 50, 100, 200, 496	x	x

5.2 Water column carbonate chemistry

Station	Depth [m]	DIC	TA
PS92/27-02	2, 25, 50, 100, 200, 500, 805	x	x
PS92/31-03	2, 25, 50, 100, 500, 1000, 1500	x	x
PS92/32-05	2, 25, 50, 100, 458	x	x
PS92/39-08	2, 10, 35, 50, 100, 200, 1000, 1536	x	x
PS92/43-05	2, 20, 50, 100, 200, 500, 780	x	x
PS92/46-02	2, 20, 50, 100, 500, 872	x	x

The basic sampling procedure was to wash and fill two 50 mL boreosilicate glass bottles using Tygon tubing from the niskin water bottle for each depth and preserve the water sample using mercuric chloride following standard procedures outlined in Dickson et al. (2007). Samples were then stored (not frozen) to be returned to Plymouth Marine Laboratory for analysis.

Preliminary results

Samples had been shipped back to Plymouth Marine Laboratory, UK for analysis for DIC and alkalinity. Therefore no results are yet available. Results are expected to be available February 2016.

Data management

Data will be published in peer reviewed journals and presented on international conferences. Final data will be submitted to a public data center (PANGAEA) after publication, latest after 5 years. Before this, for any data request, please contact H Findlay.

References

- Caldeira K, Wickett ME (2003) Anthropogenic carbon and ocean pH. *Nature* 425:365.
- Dickson A G, Sabin C L & Christian J R (2007). Guide to Best Practices for Ocean CO₂ Measurements. PICES special publication 3, IOCC Report No. 8.
- Findlay H S, Tyrrell T, Bellerby R G J, Merico A & Skjelvan I (2008) Carbon and nutrient mixed layer dynamics in the Norwegian Sea. *Biogeosciences* 5, 395 -1410.
- Steinacher M, Joos F, Froelicher TL, Plattner G & Doney SC (2009) Imminent ocean acidification in the Arctic projected with the NCAR global coupled carbon cycle-climate model. *Biogeosciences* 6, 51-533.

6. GEOCHEMISTRY

6.1 Organic biomarkers in suspended particles

Eunmi Park¹

¹AWI

not on board: Gesine Mollenhauer¹

Grant No AWI_PS92_00

Objectives

Organic biomarkers are often used to reconstruct sea-surface temperatures. In particular, the biomarker index TEX_{86} is increasingly applied in regions where other techniques do not yield reasonable estimates. However, the depth at which the precursor organisms for the glycerol dialkyl glycerol tetraether (GDGT) lipids, on which the index is based, thrive is poorly known. Efforts to calibrate the index in the Arctic have resulted in overestimation of sea surface temperature, which may be related to the special ecological conditions in this region (Ho et al. 2014). The goal of our study therefore is to investigate TEX_{86} on (suspended) particles collected from the surface waters, from water column profiles, and from in and under the sea-ice, and compare these data with results from underlying surface sediments. The results will help address the following research questions:

- Does TEX_{86} in the Arctic record sea-surface temperature?
- Is there a sub-surface maximum in GDGT concentration suggesting a sub-surface habitat of the precursor organisms?
- Do sea-ice associated communities have a distinct TEX_{86} signature, which might alter the pelagic signal?

Work at sea

During cruising and station work, surface waters taken from the ship's seawater inlet were filtered onto glass fiber filters (pore size 0.7 μm). At all of the ice stations, *in-situ* pumps (ISP) were deployed to filter large volumes of water (200-370 L/filter) at turbidity maximum depths, which were determined according to CTD transmissometer (Tab. 6.1.1). To collect particles from in and under the sea-ice, sea-ice cores (Tab. 6.1.2) as well as particles from the water under the ice (Tab. 6.1.1) were collected at each ice stations Additionally, multi-corer (MUC) sediments were collected and sliced at 1 cm interval and stored in pre-combusted glass petri dishes at -20 °C container (Tab. 6.1.3).

6.1 Organic biomarkers in suspended particles

Tab. 6.1.1: Suspended particulate matter sampling efforts during PS92 (ARK-XXIX/1)

Station	Surface water	Water column using <i>in-situ</i> pump		Water column using CTD			Water under sea ice	
		Turbidity max.	Below turbidity max.	Chl-a max.	Below Chl-a max.	Deep	Below sea ice	Chl-a max.
	Depth [m]							
PS92/19-08	5	90	180	15	50	100	1	17
PS92/27-12	5	90		23	58	100	1	7
PS92/31-10	5		150	25	75	150	1	13
PS92/32-06	5	70						
PS92/32-19	5	80		25	50	100	1	27
PS92/39-16	5	80		25	50	100	1	-
PS92/43-17	5	110		20	110	250	1	-
PS92/46-07	5	100						
PS92/47-03	5			40	100	199	1	25
S92/47-16	5	60	100	10	50	100	1	11

Tab. 6.1.2: Sea ice sampling efforts during PS92 (ARK-XXIX/1)

Station	Core length [cm]	Core section [cm]
PS92/19	108	68 + 40
PS92/27	108	90 + 18
PS92/31	117	84 + 33
PS92/32	115	62 + 52
PS92/39	127	69 + 58
PS92/43	112	62 + 49
PS92/46	132	67 + 65
PS92/47	93	93

Tab. 6.1.3: Sediment sampling efforts during PS92 (ARK-XXIX/1)

TV-MUC		Box core		
Station	Core length [cm]	Station	Core top	Archive [cm]
PS92/19-19	52.5	PS92/28-02	x	40.5
PS92/27-14	25.0	PS92/32-15	x	
PS92/31-13	30.5	PS92/39-93	x	
PS92/32-15	9.0			
PS92/39-05	35.3			
PS92/40-01	34.0			
PS92/43-20	31.5			
PS92/46-15	34.0			
PS92/47-20	35.0			
PS92/56-05	32.0			

Preliminary (expected) results

The results expected address the above mentioned research questions. They will help to further refine the calibration of the proxy. All analysis will be performed in home laboratories.

Data management

Data to be obtained from samples collected during the cruise will be archived on Pangaea and published in international peer-reviewed journals.

References

Ho S L et al., (2014) Appraisal of TEX_{86} and TEX_{86}^L thermometries in subpolar and polar regions. *Geochimica et Cosmochimica Acta*, 131, 213–226.

6.2. Water mass signatures ($\delta^{18}\text{O}$, $\delta^{13}\text{C}_{\text{DIC}}$)

Kirstin Werner¹

not on board: Dorothea Bauch²

¹ BPCRC

²GEOMAR

Grant No AWI_PS92_00

Objectives

The overall purpose of the stable oxygen isotope analysis ($\delta^{18}\text{O}$) and stable carbon isotopes of the total dissolved organic carbon ($\delta^{13}\text{C}_{\text{DIC}}$) is to provide an assessment of water mass signatures and freshwater composition within the Arctic Ocean and to understand the seasonal variation of these signals.

Work at sea

Water samples for $\delta^{18}\text{O}$ and $\delta^{13}\text{C}_{\text{DIC}}$ were taken at CTD (Tab. 6.2.1) and ice stations (Tab. 6.2.2).

Tab. 6.2.1: Water samples obtained from CTD casts

Station	Depth (m)
PS92/19-05	bottom, 150, 100, 75, 50, chl-max, surface
PS92/19-15	bottom, 100, 50, chl-max, surface
PS92/20-01	bottom, 150, 100, 75, 50, chl-max, surface
PS92/27-03-1	bottom, 150, 100, 75, 50, chl-max, surface
PS92/27-07-3	800, 600, 500, 400, 300, 250
PS92/27-13	bottom, 100, 50, chl-max, surface
PS92/28-01	bottom, 800, 600, 500, 400, 300, 250, 200, 150, 100, 75, 50, 15, surface
PS92/31-12	bottom, 800, 600, 500, 400, 300, 250, 200, 150, 100, 75, 50, chl-max, surface
PS92/32-14	bottom, 200, 150, 100, 75, 50, chl-max, surface
PS92/39-10	bottom, 800, 600, 500, 400, 300, 250, 200, 150, 100, 75, 50, 45, surface
PS92/40-01	bottom, 600, 500, 400, 300, 250, 200, 150, 100, 75, 60, 50
PS92/43-01	bottom, 600, 500, 400, 300, 250, 200, 150, 100, 75, 50, 18, surface
PS92/46-14	bottom, 600, 500, 400, 300, 250, 200, 150, 100, 75, 50, surface
PS92/47-19	bottom, 800, 600, 500, 400, 300, 250, 200, 150, 100, 75, 50, chl-max, surface
PS92/56-CTD	bottom, 500, 400, 300, 200, 150, 100, 50, chl-max, surface

Tab. 6.2.2: Water samples obtained during ice stations

Station	Depth (m)
PS92/19-06-ICE1	sackhole, underice chl-max, underice surface
PS92/27-02-ICE2	sackhole, underice chl-max, underice surface
PS92/31-02-ICE3	sackhole, underice chl-max, underice surface
PS92/32-ICE4	sackhole, underice chl-max, underice surface
PS92/39-ICE5	sackhole, underice chl-max, underice surface
PS92/43-ICE6	sackhole, underice chl-max, underice surface
PS92/46-ICE7	sackhole, underice chl-max, underice surface
PS92/47-ICE8	meltpond, sackhole, underice chl-max, underice surface

Expected results

Samples for $\delta^{18}\text{O}$ and $\delta^{13}\text{C}_{\text{DIC}}$ analysis will be transported to Kiel. Analysis will be conducted at the Leibniz Laboratory at Kiel University, Kiel, Germany and at the Stable Isotope Facility at CEOAS at Oregon State University, Oregon, USA within 1 year.

Based on hydrological data and stable oxygen isotope analysis ($\delta^{18}\text{O}$) the influence of mainly shelf-derived meteoric waters and modification by sea-ice processes (melting or formation) can be quantified (Bauch et al., 1995).

From previous investigations in the Central Arctic Ocean e.g. in summer 2007 we know that there is spatial and temporal variation of freshwater distribution within the Arctic Ocean halocline on an interannual to potentially seasonal timescale (Bauch et al., 2011). With the planned work on PS92 we expect to learn more about the potential seasonal variation of freshwater within the different layers of the Arctic Ocean halocline

Data management

Data will be stored at the Pangaea data repository and will be made public after publication at Pangaea Data Repository.

References

- Bauch D, Schlosser P, Fairbanks R F (1995) Freshwater balance and the sources of deep and bottom waters in the Arctic Ocean inferred from the distribution of H_2^{18}O . *Progress in Oceanography*, 35, 53-80.
- Bauch D, M Rutgers van der Loeff, N Andersen, S Torres-Valdes, K Bakker, and E P Abrahamsen (2011) Origin of freshwater and polynya water in the Arctic Ocean halocline in summer 2007, *Progress in Oceanography*, 482-495, doi:10.1016/j.pocean.2011.1007.1017.

6.3. Suspended particulate matter (SPM)

Stefan Büttner¹
not on board:Carolyn Wegner¹

¹GEOMAR

Grant No AWI_PS92_00

Objectives

The overall goal is to study the particle flux from the Barents shelf to the Nansen Basin to improve our understanding of the pathways of suspended particulate matter (SPM), which is critical in order to draw the connection between sediment dynamics, optical properties and ecosystem dynamics under a changing climate on the one hand. Furthermore quantifying the abundance and composition of SPM, and comparing these to sea ice and surface sediment samples is required to understand the significance of large-scale lateral transport, and how this may affect the reconstruction of ice conditions in the geologic past.

Work at sea

To investigate shelf-to-basin particle flux process studies in the water column were carried out by deriving SPM concentration in the water column from direct measurements (water samples) and indirect measuring devices (transmissometer). In general, losses of light propagating through water can be attributed to two primary causes: scattering and absorption. By projecting a collimated beam of light through the water and placing a focused receiver at a known distance away, one can quantify these losses. The ratio of light gathered by the transmissometer's receiver to the amount originating at the source is known as the beam transmittance (T_r), which provides an indication of total.

In order to estimate the SPM concentration from the transmissometer signal 34 water samples of 1l at 5 stations were collected and directly filtered through pre-weighed HVLP filters by MILLIPORE (0.45microns), and washed carefully with distilled water after filtering. All the filters were dried for 24hours and packed for further analyses at GEOMAR.

Tab. 6.3.1: Direct SPM-sampling in the water column during PS92

Station	Sampling depth [m]	Sampling size [l]
PS92/19-05	2, 50, 75, 100, 150, 355	1
PS92/19-14	5, 50, 100, 200, 300, 390	1
PS92/21-1	2, 10, 50, 100, 150, 192	1
PS92/23-1	2, 10, 50, 100, 150, 192	1
PS92/32-14	2, 10, 50, 100, 150, 192	1

Expected results

All filters will be analysed in GEOMAR, Kiel (concentration, grain size). All transmissometer measurements will be correlated with corresponding in situ water samples to obtain accuracy by taking the effects of different mineralogy, varying particle darkness, and salinity of ambient water on the response of the turbidity meter into account.

The results expected address the mentioned research questions above and will improve our knowledge on shelf-to-basin particle fluxes and add to the quantification of the environmental preconditions for productivity.

Data management

Final post-cruise data will be made public available in due time in the open access library PANGAEA (<http://www.pangaea.de>) at the World Data Center for Marine Environmental Sciences (WDC-MARE) operated by the Alfred Wegener Institute for Polar and Marine Research, Bremerhaven (AWI) and the MARUM, Bremen.

6.4. Dissolved neodymium isotopes and rare earth elements

Stefan Büttner¹,

¹GEOMAR

not on board: Georgi Laukert¹ Martin Frank¹

Grant No AWI_PS92_00

Objectives

Neodymium (Nd) isotopes (expressed as ϵ_{Nd}) and rare earth element (REE) patterns are powerful geochemical tracers of water masses introduced into seawater through weathering of the rocks in the source areas of the water masses (Frank, 2002). The source rock composition and age of the continental crust are geographically variable and characteristic for particular groups and ages of rocks providing a geochemical “finger-print”. The global average residence time of Nd in seawater is about 400-1000 years (Arsouze et al., 2009). Thus typical isotopic signatures of water masses can be preserved and transported over large distances. While changes in weathering inputs from land (rivers, exchange with shelf sediments) influence the surface water signatures, changes of the Nd isotope signatures in the open ocean are only controlled by mixing of water masses with different signatures, which can also be extracted from sediments and have been used for reconstruction of past water mass mixing and ocean circulation in the Arctic ocean (e.g. Haley et al., 2008).

The overall purpose of the project is to provide an assessment of dissolved water mass, sea ice and snow signatures based on these tracers. Seawater sampling along two shelf-to-basin transects of the European Arctic margin allows to capture Atlantic-derived water (AW) entering the Arctic Ocean through Fram Strait and the Barents Sea and its interaction with overlying and underlying waters of different origin. The modification of the AW signature ($\epsilon_{Nd} \sim -12$) through admixture of other water masses is of particular interest. Surface waters above the AW layer are expected to have high REE concentrations and Nd isotope signatures representative of a Siberian River and shelf origin (Andersson et al., 2008; Porcelli et al., 2009), whereas intermediate waters below the AW most likely are similar to those from the eastern Fram Strait and characterized by low Nd concentrations and Nd isotopic signatures of $\epsilon_{Nd} \sim -10$ (Laukert et al., in prep.). Local Nd input from Svalbard shelf sediments might also contribute to a change in Nd characteristics in the upper water column north of Svalbard (e.g. Andersson et al., 2008).

The dissolved Nd signatures in sea ice should be similar to those of the (sea)water from which the sea ice has formed and thus provide information on the origin area of the sea ice, while dissolved Nd in snow most likely is of atmospheric origin (e.g. from eolian dust). The behavior of REEs during sea ice/snow formation and melting is as yet not completely understood and requires particular attention.

Work at sea

Water samples of different depths were collected in 10L and 20L acid-cleaned plastic cubitainers and filtered immediately through AcroPak™ 500 Capsules with Supor® Membrane (pore size: 0.8/0.2 μ m) to avoid exchange of dissolved Nd/REE and Nd/REE in the suspended particles. A total of 37 seawater samples (~630L) from 10 stations (Tab. 6.4.1) were collected and stored for

further treatment at the GEOMAR home laboratory. Additionally, 14 snow samples (~20L each) were collected under clean conditions and put into the freezer (Tab. 6.4.2). In collaboration with the sea ice biology team 8 ice cores were collected and also stored in the freezer (Tab. 6.4.2).

Tab. 6.4.1: Water column sampling of Neodymium (Nd) isotopes (expressed as eNd) and rare earth element (REE)

Station	Depth [m]	eNd	REE
PS92/19-08	2, 210, 370	x	x
PS92/27-07	2, 250, 500, 805	x	x
PS92/31-06	7, 50, 150, 400, 1000, 1383	x	x
PS92/32-14	2, 235	x	x
PS92/37-1	2, 150, 500, 1000, 2220	x	x
PS92/39-9	2, 250, 1000, 1552	x	x
PS92/43-9	2, 250, 790	x	x
PS92/46-4	2, 200, 890	x	x
PS92/47-7	2, 200, 2120	x	x
PS92/56-3	2, 150, 500, 820	x	x

Tab. 6.4.2: Snow sampling on ice stations for Neodymium (Nd) isotopes (expressed as eNd) and rare earth element (REE).

Station	Amount [L]	eNd	REE
PS92/19-08	40	x	x
PS92/27-07	40	x	x
PS92/31-06	40	x	x
PS92/32-14	20	x	x
PS92/39-9	40	x	x
PS92/43-9	20	x	x
PS92/46-4	40	x	x
PS92/47-7	40	x	x

Tab. 6.4.3: Collection of ice cores stations for Neodymium (Nd) isotopes (expressed as eNd) and rare earth element (REE)

Station	Length [m]	Amount of sub-cores	eNd	REE
PS92/19	1.08	2	x	x
PS92/27	1.12	2	x	x
PS92/31	1.25	2	x	x
PS92/32	1.12	2	x	x
PS92/39	1.28	2	x	x
PS92/43	1.09	2	x	x
PS92/46	1.3	2	x	x
PS92/47	1.18	2	x	x

Expected results

First results can be evaluated after the samples will have been transported to the home laboratory at GEOMAR in Kiel, and analyzed by multicollector (MC) ICP-MS. Strong Nd signals from different water masses, especially in the upper water column and at intermediate depths, are expected. AW entering the Arctic Ocean through Fram Strait is characterized by $\epsilon\text{Nd} \sim -12$ and Nd concentrations of ~ 16 pmol/kg (Laukert et al., in prep.). During its transport along the continental slope a modification towards more radiogenic signatures is expected through admixture of other water masses. A release of Nd from Svalbard shelf sediments might also modify the Nd signatures of AW north of Svalbard (e.g. Andersson et al., 2008). Surface waters above the AW layer in general are expected to have higher Nd concentrations and different isotopic compositions, reflecting the different freshwater sources (e.g. riverine runoff). Intermediate and deep waters below are expected to have more radiogenic Nd isotopic signatures of $\epsilon\text{Nd} \sim -10$, similar to values observed for Arctic Intermediate Water in the eastern Fram Strait (Laukert et al., in prep.). Dissolved Nd characteristics of sea ice should be similar to those of the seawater from which the sea ice originally has formed, whereas dissolved Nd concentrations and isotopic compositions of snow might be similar to those of eolian dust present in the snow.

Data management

Final post-cruise data will be made public available in due time in the open access library PANGAEA (<http://www.pangaea.de>) at the World Data Center for Marine Environmental Sciences (WDC-MARE) operated by the Alfred Wegener Institute for Polar and Marine Research, Bremerhaven (AWI) and the MARUM, Bremen.

References

- Andersson PS, Porcelli D, Frank M, Björk G, Dahlqvist R, Gustafsson Ö (2008) Neodymium isotopes in seawater from the Barents Sea and Fram Strait Arctic-Atlantic gateways. *Geochimica et Cosmochimica Acta*, 72, 2854-2867.
- Arsouze T, Dutay JC, Lacan, F, Jeandel, C (2009) Reconstructing the Nd oceanic cycle using a coupled dynamical – biogeochemical model. *Biogeosciences* 6, 2829-2846.
- Frank M (2002) Radiogenic isotopes: Tracers of past ocean circulation and erosional input. *Rev. Geophys.* 40(1), 1001, 10.1029/2000rg000094.
- Haley BA, Frank M, Spielhagen RF and Eisenhauer A (2008) Influence of brine formation on Arctic Ocean circulation over the past 15 million years. *Nature Geoscience* 1, 68-72.
- Porcelli D, Andersson PS, Baskaran M., Frank M, Björk, G, Semiletov I (2009) The distribution of neodymium isotopes in the Arctic Ocean basins. *Geochimica et Cosmochimica Acta*, 73, 2645-2659.

6.5 Source and transformations of chromophoric dissolved organic matter and its role in surface ocean heating

Monika Zabłocka¹, Justyna Meler¹
not on board: Piotr Kowalczyk¹

¹ IOPAN

Grant No AWI_PS92_00

Objectives

The retreating sea ice, and changes in the fresh water balance, has major implications on ecosystems and biogeochemical processes attributed to variable light conditions. Increased exposure of the upper ocean layer to sunlight occurs as sea ice retreats in summer. While these dynamics allow more photosynthetically active radiation (PAR) to become available for photosynthesis, increased ultraviolet (UV) radiation might in turn inhibit primary production. Apart from changing boundary conditions, underwater light availability and spectral quality are largely defined by spatial, temporal and vertical distribution of the main optically active substances such as coloured dissolved organic matter (CDOM), phytoplankton and non-algal matter. CDOM plays a key role in the biogeochemistry and radiant heating of the upper layer in the Arctic Ocean (Granskog et al. 2007).

The scientific objectives of the Institute of Oceanology Polish Academy of Sciences (IOPAS) project were:

- Identify individual components of chromophoric dissolved organic matter (CDOM) in the oceanic waters and ice cores in the Central Arctic and characterize them by spectral properties of excitation/emission fluorescence and absorption
- Identify processes that control distribution of specific component in time and space and find those component, which distribution is controlled by physical conservative mixing of water masses with distinctly different optical and hydrological properties
- Derive empirical relationships between specific CDOM components and inherent and apparent optical properties of marine waters and salinity
- Derive empirical relationships between spectral properties of fluorescent dissolved organic matter (FDOM) and light absorption by particles aCDOM with dissolved organic carbon (DOC) concentration. Investigate the temporal and spatial variability of aCDOM/DOC and FDOM/DOC
- Establish the zonal variation of the depth integrated action spectra (the product of the CDOM absorption spectrum and spectral distribution of underwater irradiance at given depth) of the CDOM photodegradation

Work at sea

Water samples for determining CDOM absorption, particulate absorption, CDOM fluorescence and DOC concentration were collected at fixed depths with Niskin bottles attached to CTD rosette during 8 ice stations and 4 bio-stations. Water samples depths were determined upon features of the vertical profiles of the chlorophyll a fluorescence: at all ice stations following depths were sampled: 10 m, above Chlorophyll Maximum, at Chlorophyll Maximum, under Chlorophyll Maximum, 50 m, 100m, 10 m above the bottom. Table 6.5.1 lists names of CTD stations during the cruise together with collected water samples for determined water depths. The surface water was collected from zodiac motor boat to 10 liter HDPE container. Table 6.5.2 lists surface water samples collected from the Zodiak board during COPS measurements.

Additionally, water samples for determining CDOM absorption, particulate absorption, CDOM fluorescence and DOC concentration were collected on 8 ice stations from under the ice water column from „surface“ and Chlorophyll Maximum depth. Table 6.5.3 lists collected water samples from under the ice cover on every of 8 ice stations.

On each from 8 ice stations, two ice cores („salinity“ and „PAB“) were collected. for determining CDOM absorption and fluorescence, particulate absorption and DOC concentration. Salinity core was divided into 10 cm long pices and kept in dark in +4 C for 36 hours until melted. From PAB core only bottom 5 cm were collected and kept in dark in +4 C for 36 hours until melted.

Water samples for determination of CDOM absorption, fluorescence EEM and DOC concentrations underwent a filtration with use of flow-through Sartorius filter (nominal pore size 0.2 μm).

Water from ice samples from salinity core were integrated into 20 cm sections and then underwent a two-step filtration process. The first filtration was through Whatman glass fiber filters (GF/F, nominal pore size 0.7 μm). The particulate material retained of filters was stored for further laboratory measurements of particulate absorption. Portion of the filtered water was then passed through Sartorius 0.2 μm pore cellulose membrane filters to remove fine-sized particles. This water was used for spectrophotometric and spectrofluorometric scans for determination of CDOM absorption spectra, CDOM fluorescence Excitation-Emission Matrix spectra, and the DOC concentration.

Last 5 cm from PAB core underwent a filtration through Whatman glass fiber filters (GF/F, nominal pore size 0.7 μm) for particulate absorption analysis. Table 6.5.4 lists all samples collected from ice cores. Table 6.5.5 contains summary about number of samples taken for each parameter from open waters, under ice waters, surface waters collected from Zodiak and from melted ice cores.

Spectroscopic analysis of CDOM absorption has been done in the laboratory on board *Polarstern* using a double-beam Perkin-Elmer Lambda-35 spectrophotometer with a 10-cm quartz cell in the spectral range of 200–700 nm. MilliQ water was used as the reference for all measurements.

The absorption of light by CDOM can be parameterized as an exponential function as follows:

$$a_{CDOM}(\lambda) = a_{CDOM}(\lambda_{ref}) * e^{-S(\lambda - \lambda_{ref})} + K$$

where $a_{CDOM}(\lambda)$ is the absorption coefficient at wavelength λ (m^{-1}), λ_{ref} is a reference wavelength, and S is the CDOM absorption spectrum slope parameter coefficient (nm^{-1}). K is a background constant that allow any baseline shift caused by residual scattering by fine size particle fractions, micro-air bubbles or colloidal material present in the sample, refractive index differences between sample and the reference, or attenuation not due to organic matter.

Samples for fluorescence measurements were stored in +4°C for further laboratory measurements. Those analyses will be done at laboratory on land in the Institute of Oceanology, Polish Academy of Sciences, Sopot, Poland. CDOM fluorescence measurements will be made on an Aqualog Horriba scientific scanning spectrofluorometer. Collected Excitation Emission Matrix spectra will be further processed using DOM fluorescence toolbox developed by Stedmon and Bro (2007). Samples will be spectrally corrected with set of instrument dependent correction coefficients and calibrated against the water Raman scatter peak (excitation wavelength of 350 nm) of a Milli-Q water sample, run the same day. The Raman normalization and correction procedures will result in spectra that are in Raman units (R.U., nm^{-1}) and are directly comparable to corrected spectra measured on other machines. The corrected and calibrated EEM spectra will be statistically analyzed with the method described by Stedmon et

al., (2003), and the PARAFAC model will be derived with use of the in MATLAB using the “N-way toolbox for MATLAB ver. 2.0”(Andersson and Bro, 2002). PARAFAC aids the characterization of fluorescent DOM by decomposing the fluorescence matrices into different independent fluorescent components.

Samples for DOC measurements were acidified with 150 μ l 0.1 M HCl and stored in the dark at 4°C until laboratory analysis. Samples will be shipped in the conditioned container to the Institute of Oceanology, Polish Academy of Sciences, Sopot, Poland for estimation of the DOC concentration in the laboratory. These will be done in a ‘HyPerTOC’ analyser (Thermo Electron Corp., The Netherlands) using UV/persulphate oxidation and non-dispersive infrared detection (Sharp 2002). Measurements of each sample using the standard addition method (potassium hydrogen phthalate) will be performed in triplicate. Quality control of DOC concentrations will be performed with reference material supplied by Hansell Laboratory, University of Miami. The methodology will ensure satisfactory accuracy.

Water samples for determination of particulate absorption underwent a filtration process through Whatman glass fiber filters (GF/F, nominal pore size 0.7 μ m). Immediately after collection the particulate material retained of filters was stored deep frozen for further laboratory measurements of particulate absorption. Those analyses will be done at laboratory on land in the Institute of Oceanology, Polish Academy of Sciences, Sopot, Poland. The absorption spectrum of particles, $a_p(\lambda)$, retained on a filter will be determined using the transmittance-reflectance (T-R) spectrophotometric method (Tassan and Ferrari, 1995). Transmittance and reflectance will be measured in spectral range between 380 and 750 nm with a 1 nm resolution. A formula derived by (Kaczmarek et al., 2003) will be applied for correction for pathlength amplification factor (β).

In addition to collecting water samples for laboratory spectroscopic measurements of inherent optical properties on every ice station vertical profiles of spectral underwater radiation were recorded with use of profiling underwater free fall radiometer – the Compact Optical Profiling System COPS, (Biospherical Instruments Inc., San Diego, USA). This small instrument consist with the submersible radiometer that measures the solar radiation at 12 spectral bands: 305, 320, 340, 380, 412, 443, 490, 555, 625, 665, 683, 710 nm and pressure sensors attached to profiling vehicle connected with telemetry cable with the deck power supply and telemetry control unit and was manually deployed from the ice edge. This instrument measures the intensity of the solar radiation that propagates through the water column into a deep in the function of depth and wavelength. The measurements of underwater light field were consistent with The Ocean Optics Protocols (Mueller, 2003b). On three ice stations (no. 5, 6 and 8) we were able to make additional vertical profiles of spectral underwater radiation under the ice by deploying COPS through the hole made in the ice. On two of those stations (no. 6 and 8) we were able to deploy COPS from the ice edge on first and second day of the station.

Tab. 6.5.1: List of samples collected from CTD during the cruise PS92; EEM = excitation–emission matrix, a_p (EEM), absorption spectrum of particles (a_p)

Station	Depth [m]	DOC	EEM	aCDOM	a_p
PS92/019-5	0, 5.7, 20.5, 30, 50	x	x	x	x
PS92/019-5	75, 100, 365	x	x	x	
PS92/021-1	2, 10.5, 20, 50	x	x	x	x
PS92/021-1	100, 192	x	x	x	
PS92/027-3	5, 20, 40, 50	x	x	x	x
PS92/027-3	100	x	x	x	

6.5 Source and transformations of chromophoric dissolved organic matter

Station	Depth [m]	DOC	EEM	aCDOM	ap
PS92/029-1	1.5, 10, 20, 30, 50	x	x	x	x
PS92/029-1	100	x	x	x	
PS92/031-3	5, 25, 40, 50	x	x	x	x
PS92/031-3	100	x	x	x	
PS92/032-5	5, 25, 40, 50	x	x	x	x
PS92/032-5	75, 100	x	x	x	
PS92/036-1	10, 20, 30, 50	x	x	x	x
PS92/036-1	100	x	x	x	
PS92/039-8	5, 35, 50	x	x	x	x
PS92/039-8	100	x	x	x	
PS92/043-5	10, 30, 50	x	x	x	x
PS92/043-5	75, 100, 780	x	x	x	
PS92/046-2	10, 20, 30, 50	x	x	x	x
PS92/046-2	100, 872	x	x	x	
PS92/047-4	10, 15, 30, 50	x	x	x	x
PS92/047-4	50, 100, 1000	x	x	x	
PS92/052-1	1.8, 10, 20, 30, 50	x	x	x	x
PS92/052-1	100, 1464	x	x	x	
PS92/056-3	10, 17, 30, 50	x	x	x	x
PS92/056-3	100, 820	x	x	x	

Tab. 6.5.2: List of surface water samples collected from the zodiak during COPS measurements

Station	Depth [m]	DOC	EEM	aCDOM	ap	Ca
PS92/027-5	0	x	x	x	x	x
PS92/031-11	0	x	x	x	x	x
PS92/036-2	0	x	x	x	x	x
PS92/039-7	0	x	x	x	x	x
PS92/043-8	0	x	x	x	x	x
PS92/043-19	0	x	x	x	x	x
PS92/046-10	0	x	x	x	x	x
PS92/047-5	0	x	x	x	x	x
PS92/047-15	0	x	x	x	x	x
PS92/056-4	0	x	x	x	x	x

Tab. 6.5.3: List of collected water samples from under the ice cover on every of the 8 ice stations

Station	Depth [m]	DOC	EEM	aCDOM	ap
PS92/019-6	0, 20	x	x	x	x
PS92/027-2	0, 8	x	x	x	x
PS92/031-2	0, 15	x	x	x	x

Station	Depth [m]	DOC	EEM	aCDOM	ap
PS92/032-4	0, 25	x	x	x	x
PS92/039-6	0, 3	x	x	x	x
PS92/043-4	0, 25	x	x	x	x
PS92/046-1	0, 25	x	x	x	x
PS92/047-3	0, 10	x	x	x	x

Tab. 6.5.4: List all samples collected from ice cores

Station	Core section[cm]	DOC	EEM	aCDOM	ap
PS92/019-6	0-10, 10-20, 20-30, 30-40, 40-50, 50-60, 60-70, 70-80, 80-90, 90-100, last 10 cm	x	x	x	x
PS92/027-2	0-10, 10-20, 20-40, 40-60, 60-80, 80-100, 100-115, last 5 cm	x	x	x	x
PS92/031-2	0-20, 20-40, 40-60, 60-80, 80-100, 100-130,	x	x	x	x
PS92/031-2	last 5 cm		x	x	x
PS92/032-4	0-20, 20-40, 40-60, 60-80, 80-107	x	x	x	x
PS92/032-4	last 5cm		x	x	x
PS92/039-6	0-20, 20-41, 41-61, 61-80, 80-100, 100-126	x	x	x	x
PS92/039-6	last 5cm		x	x	x
PS92/043-4	0-20, 20-40, 40-60, 60-80, 80-100, 100-106	x	x	x	x
PS92/043-4	last 5cm		x	x	x
PS92/046-1	0-20, 20-40, 40-60, 60-80, 80-100, 100-131	x	x	x	x
PS92/046-1	last 5cm		x	x	x
PS92/047-3	0-20, 20-39, 39-59, 59-79, 79-106	x	x	x	x
PS92/047-3	last 5 cm		x	x	x

Tab. 6.5.5: Summary of all samples taken for each parameter from open waters, under ice waters, surface waters collected from the zodiak and from melted ice cores

	Zodiak	CTDRO	UIW	ICE	Total
DOC	10	76	16	53	155
EEM	10	76	16	59	161
aCDOM	10	76	16	59	161
ap	10	54	16	59	139

Preliminary (expected) results

Our measurements enable us to measure light intensity and its spectral quality at given depths and that way we can estimate how quickly light is diminished in the ocean in open waters and under the ice (only on stations: 5,6,8), and which part of the solar radiation spectrum penetrate deepest. The light conditions in the water are essential for phytoplankton to grow and produce the biomass in the process of photosynthesis. We were particularly interested in penetration of the UV radiation in to the ocean's depths and through the ice cover. This part of solar radiation spectrum is harmful for marine organisms but also it interacts with particulate and soluble material contributing to its degradation through photoreactions.

Figs 6.5.1 and 6.5.2 present the distribution of downwelling spectral irradiance in the function of depth in selected spectral bands at selected stations during the cruise (raw data). The slope of the lines represents the attenuation of specific light band. The higher the slope, the faster the light is being attenuated. Depending on the optically significant sea water constituents dissolved (e.g. CDOM) and suspended in the water column, light at different wavelengths can reach different depths. Different light wavelengths are being attenuated by different water constituents in different ways. As it is shown, the most efficiently attenuated is ultraviolet radiation. The irradiance at 305 nm band (UV-ultraviolet light, brown line) is present only in a few first meters of the water column. In most cases this light is absent deeper than 10 meters. In investigated arctic waters the least attenuated light bands lay in the blue and green part of the sunlight spectrum (443, 490, 555 nm). The euphotic zone in arctic waters can reach up to 140 m.

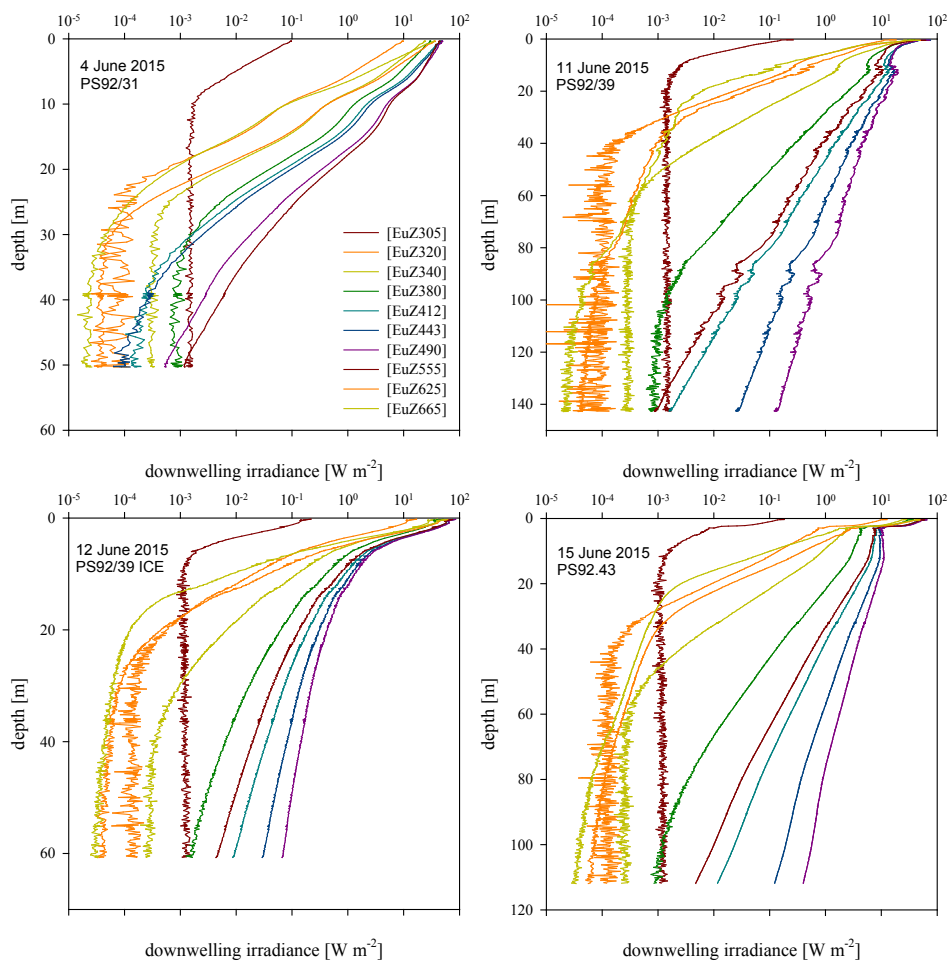


Fig. 6.5.1: Distribution of downwelling spectral irradiance in the function of depth in 10 spectral channels: 305, 320, 340, 380, 412, 443, 490, 555, 625 and 665 on selected stations of the PS92 cruise

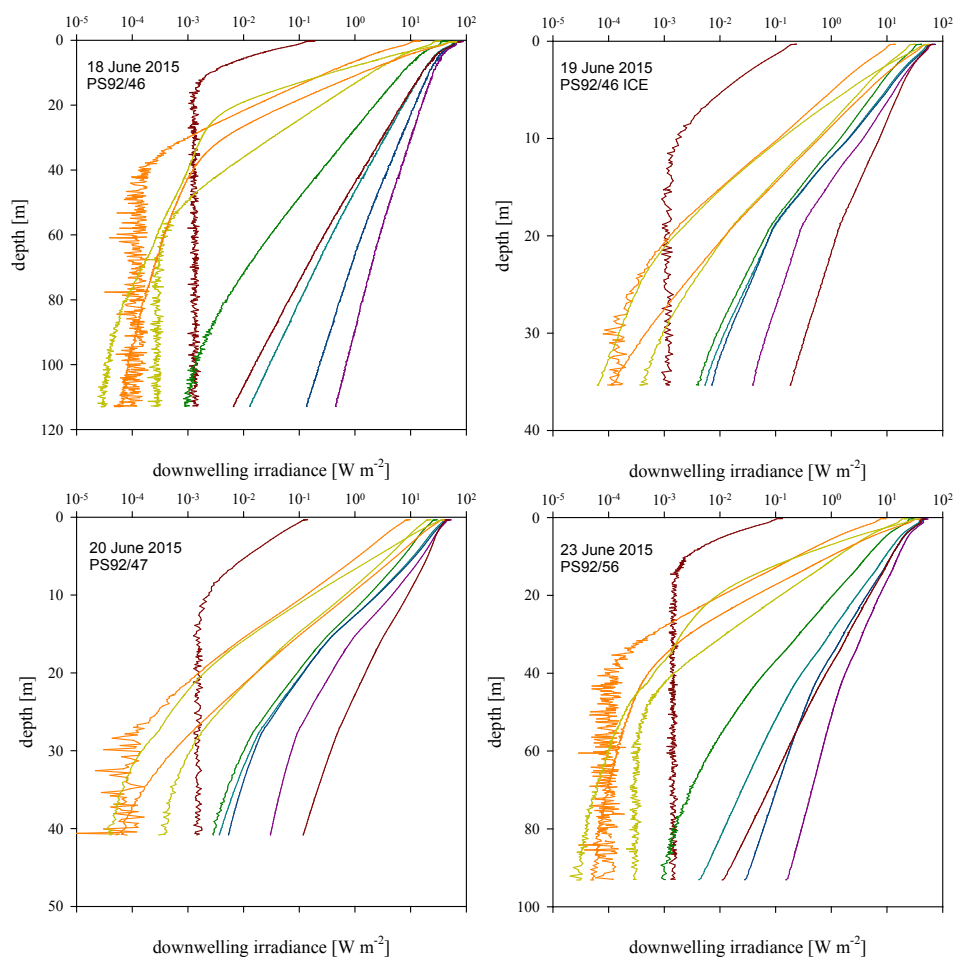


Fig. 6.5.2: Distribution of downwelling spectral irradiance in the function of depth in 10 spectral channels: 305, 320, 340, 380, 412, 443, 490, 555, 625 and 665 nm on selected stations of the PS92 cruise.

Data management

Almost all sample processing and data post processing will be carried out in the home laboratory at IOPAS. As soon as the data sets are available they can be used by other cruise participants on request. The data will be submitted to PANGAEA in December 2017.

References

- Andersson C A and R Bro (2000) The N-way toolbox for MATLAB. Chemometrics Intelligent Laboratory System 52, 1–4.
- Granskog MA, Macdonald RW, Mundy CJ, Barber DG (2007) Distribution, characteristics and potential impacts of chromophoric dissolved organic matter (CDOM) in Hudson Strait and Hudson Bay, Canada. Cont Shelf Res 27:2032–2050. doi:10.1016/j.csr.2007.05.001.
- Kaczmarek S, D Stramski, and M Stramska (2003), The new pathlength amplification factor investigation, Abstract Publication 149, Baltic Sea Sciences Congress, Helsinki.

6.5 Source and transformations of chromophoric dissolved organic matter

- Mueller J L, R W Austin, A Morel, G S Fargion and C R McClain (2003a) Ocean optics protocols for satellite ocean color sensor validation, Revision 4, Volume I: Introduction, background, and conventions. Greenbelt, MD: Goddard Space Flight Center. 50 p.
- Mueller J L, C Pietras, S B Hooker, R W Austin, M Miller, K D Knobelspiesse, R Frouin, B Holben and K Voss (2003b) Ocean optics protocols for satellite ocean color sensor validation, Revision 4, Volume II: Instrument specifications, characterisation and calibration. Greenbelt, MD: Goddard Space Flight Center.
- Stedmon C A, Markager, S, Kaas, H (2000) Optical properties and signatures of chromophoric dissolved organic matter (CDOM) in Danish coastal waters Estuarine, Coastal and Shelf Science 51, 267–278.
- Stedmon C A, S Markager and R Bro (2003) Tracing dissolved organic matter in aquatic environments using a new approach to fluorescence spectroscopy Marine Chemistry 82, 239–254.
- Stedmon C A and R Bro (2008) Characterizing dissolved organic matter fluorescence with parallel factor analysis: a tutorial Limnology and Oceanography: Methods 6, 572–579.
- Tassan S and G M Ferrari (1995) An alternative approach to absorption measurements of aquatic particles retained on filters, Limnology and Oceanography, 40, 1358– 1368.

7. SEA ICE BIOTA

7.1 Ecological consequences of climate change in the Transpolar Drift region

Ulrike Dietrich¹, Shannon MacPhee², Mischa
Ungermann¹, Ilka Peeken¹
not on board: Gunnar Gerds¹, Georgi Laukert³

¹AWI
²DFO
³GEOMAR

Grant No AWI_PS92_00

Objectives

Sea ice is of major importance in the polar oceans since it affects the solar radiation fluxes due to its reflective properties and it is a habitat and feeding ground for various organisms of the polar ecosystem. The Arctic Ocean is now in a state of rapid transition that is best exemplified by the marked reduction in age, thickness and extent of the sea ice cover, at least in summer. The European Arctic margin is largely influenced by drift ice formed on the Siberian shelves and carried to the Fram Strait via the Transpolar Drift. Sea ice thickness for the various regions of the Transpolar Drift between 1991 and 2007 showed a reduction in modal ice thickness from 2.5 m towards 0.9 m. A long-term trend towards thinner sea ice has profound implications for the timing and position of the Seasonal Ice Zone and the anticipated ice free summers in the future will have major implication for the entire ecosystem and thus alter current biogeochemical cycles in the Arctic.

Due to the generally low solar elevation, light is considered to be the key factor for primary production in the ice covered oceans. Light penetration in the Arctic is generally reduced by the sea ice cover and additionally snow greatly reduces light transmission through the ice. In the framework of climate warming, the atmospheric moisture budget in the Arctic is forecast to change, resulting in an increasing snow cover and thus reducing the light for primary production. However, the reduction from multi year ice (MYI) to seasonal ice and additional increase of melt ponds on first year ice (FYI) will substantially increase light transmission through ice.

A systematic inventory of ice-algae biomass collected by Russian colleagues and on various *Polarstern* cruises in the 80ties until recently could show that in the 1980s the biomass concentrations of sea ice algae in the Central Arctic were in general very low. However, the massive reduction in sea ice thickness in recent decades has apparently led to increasing biomass in the central Arctic e.g. during the record low 2012. Contrary to the assumption that the phytoplankton benefits from the reduction of sea ice, it was shown that sea ice algae have the largest benefit in the changing central Arctic (Fernández-Méndez et al 2015). Due to the decrease of the sea ice thickness, evolving habitats for sea ice algae have been observed in surface melt ponds (Fernández-Méndez et al 2014) and under the ice (Assmy et al 2013). New evolving ice aggregates, resulting from these changes in Arctic melt ponds and under the ice might have consequences for the carbon budget, and might have major implications for the cryo-benthic and cryo-pelagic coupling of the Arctic Ocean. It involves the export of large biomass much further north in the Central Arctic as was previous the case (Boetius et al 2013). Changes in sea ice habitat structure and ice algal production will affect the trophic transfer of sea ice-derived carbon through the under-ice community into pelagic food webs, with unknown consequences for biodiversity, ecosystem functioning and resource availability.

7.1 Ecological consequences of climate change in the Transpolar Drift region

PS92 (ARK-XXIX/1) aimed to study the following topics:

- Investigate sea ice biota on shelf to basin transects in the Transpolar Drift region and compare this with historic data.
- Study the biodiversity of the various ice habitats in comparison to the under ice water.
- Study the optical properties of sea ice for the growth conditions of ice algae.
- Reveal the role of melt pond associated communities for the ecosystem.
- Improve estimates of spatial variability of sea ice algae.

In cooperation with G Gerdt and co-workers (AWI) we continued to study the occurrence of micro plastic in sea ice cores from different regions along the Transpolar Drift as well as rare earth elements and Neodymium isotopes in cooperation with G Laukert (GEOMAR, more details in 6.4).

Work at sea

At each of the 8 ice stations a set of ice cores for sampling by various cruise participants was taken at one main coring site. Environmental parameters as sea ice temperature, snow depth, free board and ice thickness were measured for each core and the metadata of those cores are summarized in Table 7.1.1, while the general coring setup of each coring sites is shown in Table 7.1.2. Under ice water (UIW) was sampled at the surface and at the depth of the chlorophyll maximum in cooperation with V Gros and R Sarda-Estevé for sampling by multiple groups. Additionally there were two meltponds sampled at the last ice station and occasionally brown ice was collected (Tab 7.1.3).

Tab. 7.1.1: Summary of all collected ice cores during PS 92 including environmental parameters as length of the core, ice thickness, free board and snow depth Abbreviation and responsible Principal investigator: SAL=Salinity, Peeken; BIO1=Biology I, Peeken; BIO2=Biology II, Peeken; PP=Primary production, Fradette; ARC=Archive, Krumpen; VOC1=Volatile Organic compounds 1, Gros; VOC2=Volatile Organic compounds 2, Gros; GEO=Geology, O'Regan; MEI1=Meiofauna 1, Flores, MEI2=Meiofauna 2, Flores; LSI1=Lipid Isotopes, Flores, LSI2=Lipid Isotopes, Flores; PAB=Particulate absorption, Zablocka; BP5=Bacteria Production, Michel; DNA=Bacteria DNA, Fong; RNA=Bacteria RNA, Fong; NIF=Nif Genes, Fong; NEO=Neodymium, Peeken/Laukert; MIC=Micro plastic, Peeken/Gerdt; T86=TEX 86, Mollenhauer/ Müller.

Station	Date	Core Name	Time [UTC+2]	Length [m]	Ice Thickness [m]	Free-board [m]	Snow Thickness [m]
PS92 - 19	28/05/2015	VOC1	13:05	1.08	1.06	0	0.14
PS92 - 19	28/05/2015	VOC2	13:10	1.09	1.08	0	0.13
PS92 - 19	28/05/2015	GEO	13:20	1.05	1.07	0.01	0.11
PS92 - 19	28/05/2015	MEI1	13:25	1.11	1.07	0.01	0.9
PS92 - 19	28/05/2015	MEI2	13:35	1.08	1.07	0.01	0.9
PS92 - 19	28/05/2015	LSI1	13:45		1.08	0.03	0.1
PS92 - 19	28/05/2015	LSI2	13:55		1.08	0.03	0.1

Station	Date	Core Name	Time [UTC+2]	Length [m]	Ice Thickness [m]	Free-board [m]	Snow Thickness [m]
PS92 - 19	28/05/2015	PAB	14:10	1.09	1.08	0.02	0.12
PS92 - 19	28/05/2015	BP5	14:15	1.095	1.08	0.02	0.12
PS92 - 19	28/05/2015	DNA	14:30	1.05	1.05	-0.01	0.13
PS92 - 19	28/05/2015	RNA	14:40	1.04	1.04	-0.02	0.12
PS92 - 19	28/05/2015	NIF	14:55	1.08	1.04	-0.02	0.13
PS92 - 19	28/05/2015	NEO	15:10	1.08	1.06	0	0.14
PS92 - 19	28/05/2015	MIC	15:15	1.08	1.06	0.01	0.13
PS92 - 19	28/05/2015	T86	15:25	1.08	1.06	0.02	0.11
PS92 - 27	31/05/2015	SAL	11:30	1.18	1.18	0.03	0.31
PS92 - 27	31/05/2015	BIO1	11:50	1.23	1.19	0.05	0.29
PS92 - 27	31/05/2015	BIO2	12:10		1.2	0.4	0.26
PS92 - 27	31/05/2015	ARC	12:30	1.29	1.26	0.11	0.25
PS92 - 27	31/05/2015	VOC1	12:50	1.25	1.2	0.04	0.24
PS92 - 27	31/05/2015	VOC2	13:10	1.13	1.19	0.05	0.28
PS92 - 27	31/05/2015	GEO	13:30	1.24	1.21	0.04	0.28
PS92 - 27	31/05/2015	BP5	13:45	1.2	1.19	0.025	0.28
PS92 - 27	31/05/2015	MEI1	14:00	1.21	1.16	0.04	0.3
PS92 - 27	31/05/2015	MEI2	14:20	1.23	1.14	0.04	0.31
PS92 - 27	31/05/2015	LSI1	14:50	1.17	1.1	0.04	0.25
PS92 - 27	31/05/2015	LSI2	14:35		1.15	0.04	0.3
PS92 - 27	31/05/2015	PAB	15:30	1.16	1.11	0.02	0.28
PS92 - 27	31/05/2015	DNA	16:00	1.18	1.13	0.02	0.24
PS92 - 27	31/05/2015	RNA	16:15	1.17	1.11	0.02	0.24
PS92 - 27	31/05/2015	NIF	16:25	1.19	1.1	0.01	0.23
PS92 - 27	31/05/2015	NEO	16:50	1.12	1.11	0.01	0.22
PS92 - 27	31/05/2015	MIC	17:00	1.22	1.09	0.01	0.23
PS92 - 27	31/05/2015	T86	17:30	1.08	1.14	0	0.35
PS92 - 27	01/06/2015	PB5	11:00	0.52	0.49	-0.01	
PS92 - 27	03/06/2015	PB1	11:00	0.46	0.49	-0.01	
PS92 - 31	03/06/2015	SAL	15:20	1.34	1.22	-0.01	0.34
PS92 - 31	03/06/2015	BIO1	15:35	1.24	1.22	0	0.34
PS92 - 31	03/06/2015	BIO2	15:45	1.21	1.19	0.01	0.34
PS92 - 31	03/06/2015	ARC	16:10	1.17	1.16	0	0.34
PS92 - 31	03/06/2015	GEO	16:30	1.17	1.16	0	0.34
PS92 - 31	03/06/2015	BP5	16:50	1.15	1.13	0	0.32
PS92 - 31	03/06/2015	DNA	17:05	1.19	1.17	-0.01	0.28
PS92 - 31	03/06/2015	RNA	17:15	1.21	1.19	0	0.25
PS92 - 31	03/06/2015	NIF	17:25	1.22	1.21	0	0.3
PS92 - 31	04/06/2015	PP5a	9:45	1.22	1.18	-0.07	0.36
PS92 - 31	04/06/2015	PP5b	9:55	1.22	1.19	-0.08	0.38

7.1 Ecological consequences of climate change in the Transpolar Drift region

Station	Date	Core Name	Time [UTC+2]	Length [m]	Ice Thickness [m]	Free-board [m]	Snow Thickness [m]
PS92 - 31	04/06/2015	PP1a	10:05	1.24	1.21	-0.08	0.4
PS92 - 31	04/06/2015	PP1b	10:10	1.27	1.2	-0.05	0.41
PS92 - 31	04/06/2015	MIC	10:35	1.26	1.22	-0.08	0.43
PS92 - 31	04/06/2015	MEI1	10:55	1.2	1.22	-0.07	0.4
PS92 - 31	04/06/2015	MEI2	11:00	1.25	1.21	-0.09	0.4
PS92 - 31	04/06/2015	LSI1	11:15	1.19	1.2	-0.09	0.4
PS92 - 31	04/06/2015	LSI2	11:25	1.23	1.2	-0.8	0.39
PS92 - 31	04/06/2015	VOC1	12:00	1.28	1.26	0.02	0.32
PS92 - 31	04/06/2015	VOC2	12:10	1.3	1.19	0.02	0.37
PS92 - 31	04/06/2015	PAB	12:20	1.3	1.19	-0.05	0.37
PS92 - 31	04/06/2015	NEO	12:30	1.25	1.14	-0.05	0.38
PS92 - 31	04/06/2015	T86	12:35	1.17	1.16	-0.06	0.39
PS92 - 32	06/06/2015	SAL	9:10	1.1	1.11	0.01	0.29
PS92 - 32	06/06/2015	BIO1	9:30	1.13	1.1	0.02	0.27
PS92 - 32	06/06/2015	BIO2	9:40	1.11	1.08	0.02	0.27
PS92 - 32	06/06/2015	PAB	9:50	1.13	1.11	0.03	0.26
PS92 - 32	06/06/2015	GEO	10:00	1.13	1.12	0.03	0.26
PS92 - 32	06/06/2015	ARC	10:05	1.13	1.11	0.02	0.26
PS92 - 32	06/06/2015	NIF	10:30	1.13	1.11	0.02	0.27
PS92 - 32	06/06/2015	RNA	10:40	1.13	1.11	0.02	0.27
PS92 - 32	06/06/2015	DNA	10:50	1.12	1.11	0.02	0.27
PS92 - 32	06/06/2015	MEI_1	11:00	1.12	1.11	0.02	0.27
PS92 - 32	06/06/2015	MEI_2	11:05	1.13	1.11	0.03	0.27
PS92 - 32	06/06/2015	LSI_1	11:10	1.14	1.12	0.03	0.27
PS92 - 32	06/06/2015	LSI_2	11:20	1.13	1.12	0.02	0.27
PS92 - 32	06/06/2015	VOC1	11:25	1.16	1.1	0.02	0.28
PS92 - 32	06/06/2015	VOC2	11:35	1.13	1.1	0.02	0.3
PS92 - 32	06/06/2015	OPT	11:50	1.18	1.16	0.06	0.13
PS92 - 32	06/06/2015	BP5	12:05	1.14	1.11	0.02	0.28
PS92 - 32	06/06/2015	PP1a	12:30	1.13	1.1	0.02	0.27
PS92 - 32	06/06/2015	PP1b	12:35	1.12	1.1	0.02	0.27
PS92 - 32	06/06/2015	NEO	12:45	1.12	1.1	0.03	0.26
PS92 - 32	06/06/2015	MIC	13:15	1.11	1.1	0.02	0.26
PS92 - 32	06/06/2015	T86	13:30	1.15	1.1	0.01	0.26
PS92 - 39	11/06/2015	SAL	17:15	1.32	1.29	0.04	0.21
PS92 - 39	11/06/2015	GEO	17:30	1.34	1.3	0.04	0.18
PS92 - 39	11/06/2015	NIF	17:45	1.34	1.32	0.05	0.16
PS92 - 39	11/06/2015	RNA	17:50	1.37	1.33	0.05	0.16
PS92 - 39	11/06/2015	DNA	18:00	1.34	1.32	0.04	0.17
PS92 - 39	11/06/2015	ARC	18:10	1.28	1.23	0.05	0.14

Station	Date	Core Name	Time [UTC+2]	Length [m]	Ice Thickness [m]	Free-board [m]	Snow Thickness [m]
PS92 - 39	11/06/2015	MEI1	18:30	1.3	1.25	0.03	0.18
PS92 - 39	11/06/2015	MEI2	18:40	1.31	1.3	0.03	0.18
PS92 - 39	11/06/2015	LSI1	18:50	1.31	1.3	0.03	0.17
PS92 - 39	11/06/2015	LSI2	19:00	1.31	1.28	0.03	0.16
PS92 - 39	12/06/2015	MIC	19:15	1.29	1.26	0.03	0.14
PS92 - 39	12/06/2015	NEO	19:25	1.28	1.26	0.03	0.17
PS92 - 39	12/06/2015	BIO1	9:27	1.28	1.26	0.02	0.17
PS92 - 39	12/06/2015	BIO2	9:40	1.3	1.27	0.03	0.18
PS92 - 39	12/06/2015	BP5	9:45	1.27	1.26	0.04	0.21
PS92 - 39	12/06/2015	BP1	9:50	1.28	1.25	0.02	0.2
PS92 - 39	12/06/2015	PAB	10:05	1.26	1.23	0.02	0.17
PS92 - 39	12/06/2015	PP1a	10:15	1.27	1.22	0.01	0.17
PS92 - 39	12/06/2015	PP1b	10:25	1.27	1.22	0.02	0.17
PS92 - 39	12/06/2015	VOC1	10:45	1.24	1.22	0.02	0.19
PS92 - 39	12/06/2015	VOC2	11:00	1.25	1.23	0.02	0.2
PS92 - 39	12/06/2015	VOC3	11:10	1.26	1.23	0.02	0.21
PS92 - 39	12/06/2015	T86	11:30	1.27	1.24	0.02	0.19
PS92 - 043	15/06/2015	SAL	10:40	1.12	1.08	0	0.2
PS92 - 043	15/06/2015	BIO1	11:10	1.12	1.09	0	0.2
PS92 - 043	15/06/2015	BIO2	11:15	1.11	1.09	0	0.19
PS92 - 043	15/06/2015	ARC	11:20	1.12	1.09	0	0.19
PS92 - 043	15/06/2015	GEO	11:30	1.11	1.1	0.01	0.19
PS92 - 043	15/06/2015	VOC1	11:35	1.09	1.08	0	0.19
PS92 - 043	15/06/2015	VOC2	11:40	1.09	1.09	0	0.18
PS92 - 043	15/06/2015	VOC3	11:45	1.1	1.08	0	0.18
PS92 - 043	15/06/2015	BP1	11:50	1.11	1.09	0.01	0.2
PS92 - 043	15/06/2015	BP5	11:55	1.1	1.08	0.01	0.22
PS92 - 043	15/06/2015	PAB	12:05	1.1	1.08	0.01	0.24
PS92 - 043	15/06/2015	NEO	12:30	1.09	1.08	0.01	0.21
PS92 - 043	15/06/2015	MIC	12:35	1.09	1.08	0	0.17
PS92 - 043	15/06/2015	LSI1	12:45	1.08	1.07	-0.01	0.18
PS92 - 043	15/06/2015	LSI2	12:55	1.09	1.07	-0.01	0.18
PS92 - 043	15/06/2015	MEI1	13:00	1.12	1.09	0	0.24
PS92 - 043	15/06/2015	MEI2	13:15	1.13	1.1	0.01	0.26
PS92 - 043	15/06/2015	DNA	13:45	1.11	1.08	-0.01	0.26
PS92 - 043	15/06/2015	NIF	14:00	1.09	1.06	-0.02	0.25
PS92 - 043	15/06/2015	RNA	14:05	1.07	1.08	0	0.25
PS92 - 043	15/06/2015	T86	14:15	1.12	1.08	0	0.25
PS92 - 043	16/06/2015	PP1a	9:25	1.14	1.12	-0.01	0.14
PS92 - 043	16/06/2015	PP1b	9:35		1.12	0	0.14

7.1 Ecological consequences of climate change in the Transpolar Drift region

Station	Date	Core Name	Time [UTC+2]	Length [m]	Ice Thickness [m]	Free-board [m]	Snow Thickness [m]
PS92 - 043	16/06/2015	GEO1	10:05	1.42	1.4	0.13	0.07
PS92 - 043	16/06/2015	GEO2	10:45	0.87			
PS92 - 043	16/06/2015	GEO3	10:55	0.71			
PS92 - 046	18/06/2015	SAL	9:45	1.37	1.38	0.05	0.1
PS92 - 046	18/06/2015	BIO1	10:00	1.39	1.38	0.05	0.08
PS92 - 046	18/06/2015	BIO2	10:15	1.39	1.35	0.06	0.07
PS92 - 046	18/06/2015	GEO	10:20	1.37	1.34	0.07	0.08
PS92 - 046	18/06/2015	ARC	10:30	1.34	1.3	0.05	0.1
PS92 - 046	18/06/2015	NIF	10:40	1.3	1.33	0.08	0.08
PS92 - 046	18/06/2015	RNA	10:50	1.35	1.31	0.05	0.1
PS92 - 046	18/06/2015	DNA	11:00	1.27	1.34	0.08	0.08
PS92 - 046	18/06/2015	BP5	11:10	1.37	1.34	0.08	0.1
PS92 - 046	18/06/2015	BP1	11:15	1.39	1.33	0.07	0.11
PS92 - 046	18/06/2015	VOC1	11:20	1.32	1.31	0.06	0.12
PS92 - 046	18/06/2015	VOC2	11:30	1.35	1.31	0.06	0.11
PS92 - 046	18/06/2015	VOC3	11:40	1.32	1.3	0.05	0.1
PS92 - 046	18/06/2015	NEO	11:50	1.3	1.3	0.06	0.08
PS92 - 046	18/06/2015	MIC	11:55	1.28	1.29	0.09	0.06
PS92 - 046	18/06/2015	PAB	12:00	1.25	1.24	0.05	0.1
PS92 - 046	18/06/2015	T86	12:15	1.32	1.28	0.05	0.1
PS92 - 046	18/06/2015	MEI1	12:25	1.19	1.11	0.06	0.14
PS92 - 046	18/06/2015	MEI2	12:45	1.32	1.18	0.05	0.12
PS92 - 046	18/06/2015	PP1a	12:55	1.29	1.25	0.07	0.12
PS92 - 046	18/06/2015	PP1b	13:00	1.26	1.29	0.06	0.14
PS92 - 047	19/06/2015	SAL	15:00	1.13	1.1	0.03	0.1
PS92 - 047	19/06/2015	MIC	15:20	1.12	1.12	0.03	0.11
PS92 - 047	19/06/2015	NEO	15:40	1.18	1.12	0.03	0.11
PS92 - 047	19/06/2015	PAB	16:00	1.21	1.19	0.05	0.12
PS92 - 047	19/06/2015	MEI1	16:10	1.24	1.22	0.02	0.17
PS92 - 047	19/06/2015	MEI2	16:24	1.22	1.15	0.04	0.16
PS92 - 047	19/06/2015	GEO	16:40	1.27	1.25	0.03	0.15
PS92 - 047	19/06/2015	ARC	16:45	1.12	1.1	0.03	0.13
PS92 - 047	19/06/2015	DNA	16:50	1.02	1.05	0.01	0.15
PS92 - 047	19/06/2015	RNA	17:00	1.18	1.15	0.03	0.16
PS92 - 047	19/06/2015	NIF	17:10	1.18	1.16	0.01	0.17
PS92 - 047	20/06/2015	BIO1	9:40	0.82	0.79	0.07	0.11
PS92 - 047	20/06/2015	BIO2	9:50	0.89	0.88	0.07	0.13
PS92 - 047	20/06/2015	T86	10:00	0.93	0.9	0.07	0.15
PS92 - 047	20/06/2015	VOC1	10:15	1.05	1.01	0.02	0.15
PS92 - 047	20/06/2015	VOC2	10:20	0.78	0.67	0.07	0.15

Station	Date	Core Name	Time [UTC+2]	Length [m]	Ice Thickness [m]	Free-board [m]	Snow Thickness [m]
PS92 - 047	20/06/2015	VOC3	10:25	0.69	0.85	0.06	0.12
PS92 - 047	20/06/2015	PP1a	10:35	0.87	0.9	0.06	0.12
PS92 - 047	20/06/2015	PP1b	10:40	0.91	0.92	0.05	0.13
PS92 - 047	20/06/2015	BP5	10:45	0.86	0.83	0.06	0.12
PS92 - 047	20/06/2015	BP1	10:50	0.88	0.86	0.07	0.13

Tabl. 7.1.2: General set up of each coring grid for the eight ice stations to collocate neighbor ice cores Special features of the ice station are in the remarks; abbreviation as in Tab 7.1.1

Station No	Remarks	Coring Grid				
PS92-19 ICE 1	under average snow depth for this floe, very slushy surface	RNA	NIF	NEO	MIC	T86
		DNA	BP5	PAB	LSI1	LSI2
		VOC1	VOC2	GEO	MEI1	MEI2
		SAL	BIO1	BIO2	PP	ARC
PS92-27 ICE 2	Ice at coring site has already undergone multiple fracture processes	T86	MIC	NEO	NIF	RNA
		LSI2	LSI1	PAB		DNA
		MEI2	MEI1	BP5	GEO	VOC2
		SAL	BIO1	BIO2	ARC	VOC1
PS92-31 ICE 3	First coring site		NIF	RNA	DNA	BP5
		SAL	BIO1	BIO2	ARC	GEO
	Second coring site, very slushy + strong negative freeboard				T86	NEO
		MEI1	MEI2	LSI1	LSI2	PAB
PS92-32 ICE 4		MIC	PP1b	PP1a	PP5b	PP5a
		NEO	MIC	T86		
				PP1b	PP1a	BP5
		MEI2	LSI1	LSI2	VOC1	VOC2
PS92-39 ICE 5	First coring site				MIC	NEO
					LSI2	MEI2
		ARC			LSI1	MEI1
		SAL	GEO	NIF	RNA	DNA
PS92-43 ICE 6	Second coring site	VOC1	VOC2	VOC3	T86	
		PP1b	PP1a	PAB	BP1	BP5
					BIO1	BIO2
		T86	RNA	NIF	DNA	MEI1
PS92-43 ICE 6		PAB	NEO	MIC	LSI1	LSI2
		BP5	BP1	VOC3	VOC2	VOC1
		SAL	BIO1	BIO2	ARC	GEO

7.1 Ecological consequences of climate change in the Transpolar Drift region

Station No	Remarks	Coring Grid				
PS92-46 ICE 7	Very crusty with slush underneath (first layer is watered + refrozen snow?)		PP1b	PP1a	MEI2	MEI1
				T86	PAB	
		VOC1	VOC2	VOC3	NEO	MIC
		BP1	BP5	NIF	RNA	DNA
		SAL	BIO1	BIO2	GEO	ARC
PS92-47 ICE 8s	First coring site	DNA	RNA	NIF		
		ARC	GEO	MEI2	MEI1	
		SAL	MIC	NEO	PAB	
	Second coring site	BP5	BP1			
		VOC2	VOC3	PP1a	PP1b	
		BIO1	BIO2	T86	VOC1	

From the Salinity (SAL) ice core the temperature was measured every 5 cm directly on the ice, after which it was cut into 10 cm pieces which were stored in plastic containers for further melting on the ship. From these samples the salinity was measured in cooperation with M Zablocka who also measured for CDOM and PAB profiles. The bottom 5 cm were sampled separately and measured for DOC by S MacPhee. From each of the undiluted melted pieces samples for nutrients and ammonium were taken to be measured by M -A Blais. The BIO core was also cut into 10 cm pieces with exception of the bottom 5 cm, which were pooled with the bottom 5 cm of the BIO2 core. All those samples were melted in filtered sea water (0.2 µm) and later filtered for POC and PON ($\delta^{13}C_{POC}$ and $\delta^{15}N_{PON}$), pigments (HPLC), BPSi, fractionated (10 – 0.2 µm) as well as unfractionated (0.2 µm) DNA and chlorophyll A fractionated for particles larger or smaller than 10 µm. Finally samples for flow cytometry and Microscopy were taken. For the under ice water and aggregates the same variables were sampled.

Tab. 7.1.3: Sample list for ice cores (BIO), under ice water (UIW), melt ponds (MP) and aggregates (agg); *indicate sampling of brown ice

Station	Ice core	UIW(m)	MP	Agg
PS92/19-	x	0, 2, 20		
PS92/22*	x*			
PS92/27	x	0, 8		
PS92/31	x	0, 15		
PS92/32	x	0, 25		x
PS92/39	x	0, 3		
PS92/43	x	0, 25		
PS92/46	x	0, 46		
PS92/47	x	0, 10	x	x

Tab. 7.2.4: Variables sampled for ice cores, under ice water, melt ponds and aggregates
 HPLC: pigments, Frac Chl a: chlorophyll a <10 µm and > 10µm, DNA, Frac DNA: Eukaryote biodiversity, POC/PON Istop: Particulate Organic Carbon/Nitrogen isotopes, UT: Utermöhl samples, PNP: pico-nanoplankton, bPSi: Biogenic particulate silica, Nuts: nutrients * in collaboration with Tremblay group.

Station	HPLC	Frac Chl a	DNA Frac DNA	POC PON Istop	UT	PNP	bPSi	Nuts*
PS92/19	x	x	x	x	x	x	x	
PS92/22	x	x	x	x	x	x	x	
PS92/27	x	x	x	x	x	x	x	
PS92/31	x	x	x	x	x	x	x	
PS92/32	x	x	x	x	x	x	x	
PS92/39	x	x	x	x	x	x	x	
PS92/43	x	x	x	x	x	x	x	
PS92/46	x	x	x	x	x	x	x	
PS92/47	x	x	x	x	x	x	x	

Preliminary (expected) results

The aim of this study is to understand the variability and biodiversity of the sea ice-associated biomass with respect to the sea ice conditions and nutrient availability, to access the role of sea-ice biota for the cryo-pelagic, cryo-benthic coupling under different environmental scenarios from the shelf to the deep sea basin. Special emphasis is on understanding the role of melt ponds in the carbon cycling of the Arctic Ocean. These data can be used for modelling approaches to access the role of climate change on the carbon cycle of the Arctic Ocean.

In total 172 sea ice cores were collected during the eight ice stations. The length of the ice cores varied between 0.5 and 1.4 m and the calculated average of all cores was 1.15 m (Tab 7.1.1; Fig 7.1.1), which is slightly thinner compared to the average 1.4 m based on from EM-flight operations. Average snow depth was 22 cm varying between 6 cm and a maximum of 90 cm (Tab 7.1.1).

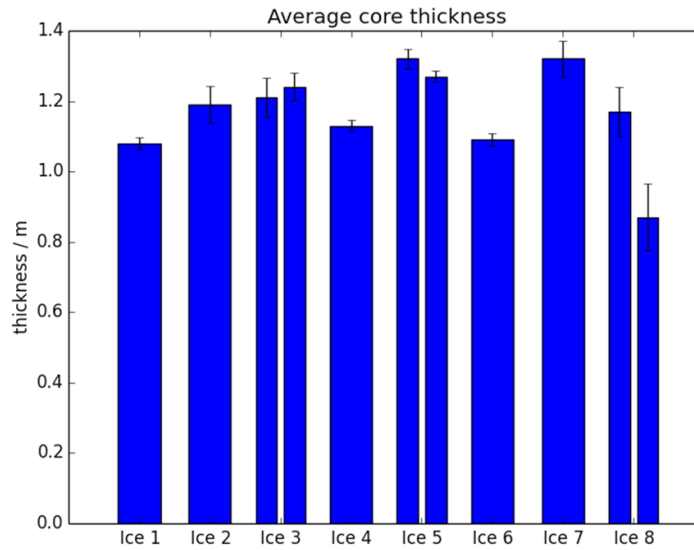


Fig. 7.1.1: Average length and standard deviation of all ice cores sampled during the 8 ice stations

Sea ice temperature showed a clear seasonal trend during the observation with low values below -2°C on the first ice station and a more or less continuous warming of the ice which reached the warmest temperature during ice station 8 with values varying between 0°C and -1°C . Salinity profiles (Fig 7.1.2) on the contrary showed no seasonal trend, but overall high salinities were observed particular on stations, where we also found a negative free board (Tab 7.1.1)

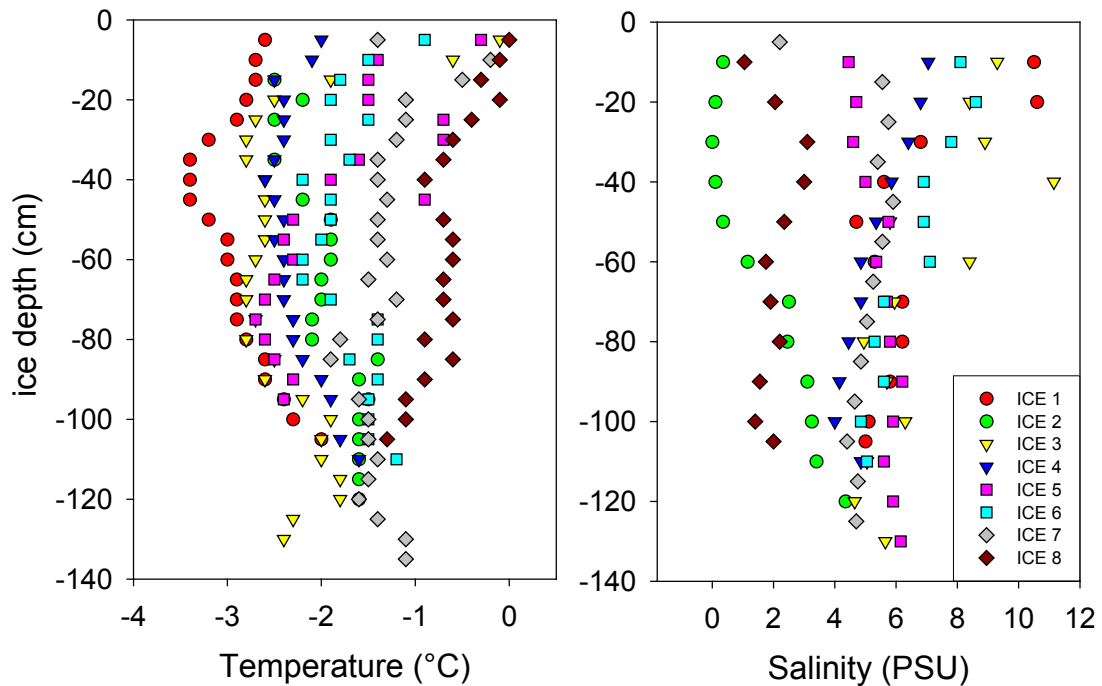


Fig.7.2.2: Temperature (left) and salinity (right) of the ice cores from the 8 ice stations

Chlorophyll profiles show except for station 8 in general low values in the top of the ice core, while all cores have their maximum at the bottom of the ice cores (Fig 7.2.3). No clear seasonal trend is obvious with station 1, 2, and 6 having less than 2 $\mu\text{g/L}$ ice of chl a, while maximum values were found for station 3, 4, and 5 with concentration around 7 $\mu\text{g/L}$ ice.

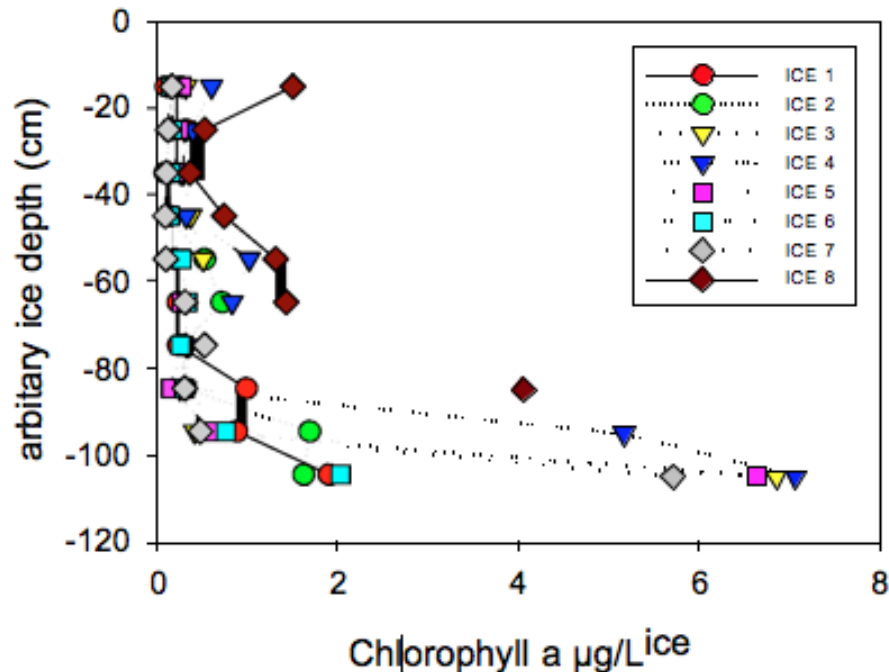


Fig.7.2.3: Preliminary chlorophyll profiles from the various ice stations, Note: the depth are not adjusted to the actual depths

Highest chl a concentrations of phytoplankton in the under ice water were found during the shelf station (ICE 1), with around 7 $\mu\text{g/L}$ Chlorophyll directly under the ice and in the chlorophyll maximum (Fig 7.2.4). There is a downslope tendency of decreasing chlorophyll values, but the lowest chlorophyll concentrations with values below 0.3 $\mu\text{g/L}$, both directly under the ice and at greater depths, were found on the Yermak Plateau. Towards the end of the cruise, the samples from the Sophia basin reach again relative high concentrations, particular in the deeper water column (Ice station 8).

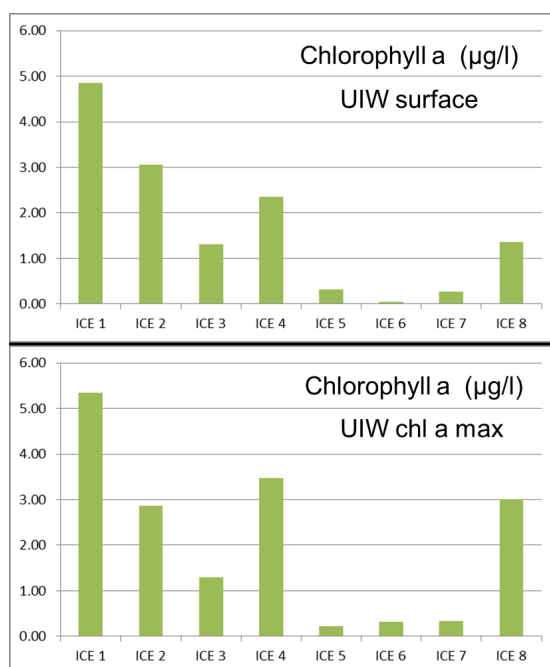


Fig. 7.2.4: Chlorophyll concentrations from the under ice water (UIW) directly measured under the ice (above) and from the chlorophyll max (below)

Data management

Samples

Except for the microscopic samples (Utermöhl samples), all other variables taken during the cruise will be processed during or after the cruise (1 year). Leftovers of the microscopic samples and the DNA will be stored at the Polar Biological Oceanography at the AWI for approximately 10 years.

Data

Data from ice work will be collected during and after the cruise. As soon as the data are available they will be accessible to other cruise participants and research partners on request. The entire data set will be submitted to PANGAEA within 2-3 years.

References

- Assmy P, J K Ehn, M Fernandez-Mendez, H Hop, C Katlein, S Sundfjord, K Bluhm, M Daase, A Engel, A Fransson, M A Granskog, S R Hudson, S Kristiansen, M Nicolaus, I Peeken, A H H Renner, G Spreen, A Tatarek, and J Wiktor (2013) Floating ice-algal aggregates below melting Arctic sea ice PLOS ONE 8: DOI:10.1371/journal.pone.0076599.
- Boetius A , S Albrecht, K Bakker, C Bienhold, J Felden, M Fernández-Méndez, S Hendricks, C Katlein, C Lalande, T Krumpen, M Nicolaus, I Peeken, B Rabe, A Rogacheva, E Rybakova, R Somavilla, F Wenzhöfer, and R P a - -S S Party (2013) Export of Algal Biomass from the Melting Arctic Sea Ice Science 339: 1430-1432.
- Fernández-Méndez M , C Katlein, B Rabe, M Nicolaus, I Peeken, K Bakker, H Flores, and A Boetius (2015) Photosynthetic production in the Central Arctic during the record sea-ice minimum in 2012 Biogeosciences Discussion 12: 2897–2945.
- Fernández-Méndez M , F Wenzhöfer, I Peeken, H Sørensen, R N Glud, and A Boetius (2014) Composition, buoyancy regulation and fate of ice algal aggregates in the Central Arctic Ocean PLoS ONE 9.

7.2 Heterotrophic microbial activity and the fate of ice associated production

Shannon MacPhee¹, Ilka Peeken²
not on board: Christine Michel¹,
(Principal investigator)
Andrea Niemi¹, Anke Reppchen¹

¹DFO
²AWI

Grant No AWI_PS92_00

Objectives

Arctic ecosystems are changing as sea ice extent, thickness and distribution patterns are altered with climate change. As the physical structure of the Arctic changes there is evidence that the foundational components of marine food-webs are shifting with potential cascading impacts throughout the ecosystem. The magnitude of ice-associated productivity is expected to change and shifts in the seasonal progression from ice algae to phytoplankton can already be observed. In the central Arctic Ocean it is possible that the reduction in ice thickness could enhance the growth of ice algae and their early season support of pelagic and benthic communities. Scenarios of increased primary productivity in the Arctic Ocean have already spawned interest in the potential for new or expanded fisheries. However, it is not clear that increased primary production would support higher trophic levels or alternatively be processed and cycled within the microbial food-web.

Within the changing Arctic, the central role of heterotrophic microbes in biogeochemical cycles needs to be understood to determine food-web efficiency and the capacity of the Arctic Ocean to sequester or release CO₂. The transformation, recycling and remineralization of particulate material by bacteria and other heterotrophic microbes, influence the magnitude and composition of sea-ice, surface water and sinking organic carbon pools. Therefore, these processes directly impact cryo-pelagic-benthic coupling and the signal of ice-associated productivity in other species and habitats.

The main objective of this project is to investigate microbial transformations of ice-associated organic material in the ice-covered Arctic Ocean. The activity of autotrophic and heterotrophic microbial communities was assessed and the dissolved and particulate organic carbon pools were quantified. Rates of primary and bacterial (including archaea) production and community respiration rates were measured and protist and bacterial cell abundances were determined. Together, these measurements will provide insights into the microbial carbon fluxes and support the development of organic carbon budgets. This project will also compare heterotrophic processes between the bottom ice, waters near the ice-water interface and waters at 1 m depth and sedimenting particles from the sediment traps (30 m and 200 m).

Work at sea

Sea ice and water at the ice interface and at 1 m were planned for collection along two shelf-to-basin transects. Heavy sea ice restricted access to planned sampling areas, but a total of 8 ice stations were successfully sampled for bottom ice, under-ice water and sinking material (sediment traps). In addition, two melt ponds were opportunistically sampled for bacterial production, dissolved organic carbon concentration and cell size and abundances at station PS92 – 047. Basic sea ice and snow properties were collected at each station in collaboration with the sea ice biology group.

7.2 Heterotrophic microbial activity and the fate of ice associated production

Sample processing and production/respiration measurements were conducted onboard the *Polarstern*. For sea ice and sediment trap samples, the relative importance of attached versus free-living bacteria was investigated using a 3 µm size fractionation for bacterial production. Flow cytometry samples were frozen (-80°C) and dissolved organic carbon samples were kept refrigerated until later analyses. In addition, CDOM and nutrients were collected from the bottom 5cm of the salinity core for project collaborators.

Analyses and linkages to group collaborators (indicated by *) for sea ice and surface water samples include:

- Bacterial production (3H-leucine incorporation)
- Community respiration (dissolved oxygen measurements)
- Protist and microbial abundance (flow cytometry)
- Cell size estimate (flow cytometry)
- Dissolved organic carbon (DOC)
- Dissolved nitrogen (DN)
- Primary production (14C uptake)*
- Particulate organic carbon (POC)*
- Algal biomass (chlorophyll a)*

Sample collections for under ice and melt pond water, ice cores, and sediment traps are summarized in Tables 7.2.1-7.2.3, respectively. Unfortunately planned analyses of photosynthetic parameters were not completed due to technical issues related to the Pulse Amplitude Modulated fluorescence (Phyto-PAM).

A 3H-leucine saturation curve and incubation time curve were conducted at station PS92 – 31 with a second time curve performed at station PS92 – 47.

Tab. 7.2.1: Summary of variables measured from under ice and melt pond water samples collected for the study of heterotrophic microbial activity and the fate of ice-associated production during the PS92 cruise. UIW surf = under ice surface; UIW 1m = 1m under ice surface; MP = melt pond.

Station	Sample Type	DOC/ DON	Flow Cytometry	Respi- ration	Bacterial Production (total)	Bacterial Production (<3µm)
PS92 – 19	UIW surf UIW 1m	x	x	x		
PS92 – 27	UIW surf UIW 1m	x	x	x	x	x
PS92 – 31	UIW surf UIW 1m	x	x	x	x	x
PS92 – 32	UIW surf UIW 1m	x	x	x	x	x
PS92 – 39	UIW surf UIW 1m	x	x	x	x	x

Station	Sample Type	DOC/ DON	Flow Cytometry	Respi- ration	Bacterial Production (total)	Bacterial Production (<3µm)
PS92 – 043	UIW surf UIW 1m	x	x	x	x	x
PS92 – 046	UIW surf UIW 1m	x	x	x	x	x
PS92 - 047	UIW surf UIW 1m	x	x	x	x	x
PS92 - 047	Clear MP Green MP	x	x		x	x

Tab. 7.2.2: Summary of variables measured from ice cores collected for the study of heterotrophic microbial activity and the fate of ice-associated production during the PS92 cruise.

Station	Core Depth (cm from bottom)	DOC/ DON	Flow Cytometry	Respirat- ion	Bacterial Production (total)	Bacterial Production (<3µm)
PS92 – 19	5	x	x	x		
PS92 – 27	5	x	x	x	x	x
PS92 – 31	5	x	x	x	x	x
PS92 – 32	5	x	x	x	x	x
PS92 – 39	5	x	x	x	x	x
	1		x		x	x
PS92 – 43	5	x	x	x	x	x
	1		x		x	x
PS92 – 46	5	x	x	x	x	x
	1		x		x	x
PS92 - 47	5	x	x	x	x	x
	1		x		x	x

Tab. 7.2.3: Summary of variables measured from sediment trap water collected for the study of heterotrophic microbial activity and the fate of ice-associated production during the PS92 cruise.

Station	Sediment Trap Depth (m)	Flow Cytometry	Bacterial Production (total)	Bacterial Production (<3µm)
PS92 – 27	30, 200	x	x	x
PS92 – 31	30, 200	x	x	x
PS92 – 32	30, 200	x	x	x
PS92 – 39	30, 200	x	x	x
PS92 – 43	30, 200	x	x	x
PS92 - 47	30, 200	x	x	x

Preliminary (expected) results

Results are not available at this time. However, it is expected that the sea ice samples will contain higher microbial biomass and activity than surface waters. The magnitude of biomass and production will depend on the stage of ice algal development during the time of sampling, i.e., pre-bloom, bloom or post-bloom. We hypothesize that heterotrophic production and activity will be commensurate to ice algal production and higher over the shelf than in the central basin.

Data management

Integrated datasets for all measurements will be compiled and verified following the analyses of all samples. Meta-data will be available shortly after the completion of the cruise and could be posted on the Polar Data Catalogue or other appropriate site. Following the publication of the results, the data will be made available on BIOCHEM, a national archive of biogeochemical data for Fisheries and Oceans Canada. The data will also be made available in the PANGAEA database after data quality verification and within one year of sample analysis.

8. SEA ICE ECOLOGY, PELAGIC FOOD WEB AND COPEPOD PHYSIOLOGY - ICEFLUX / PEBCAO

Hauke Flores^{1,2}, Giulia Castellani¹,
Fokje Schaafsma³, Martina Vortkamp¹,
Antonia Immerz^{1,4}, Sarah Zwicker^{1,5},
Michiel van Dorssen⁶, Henrieke Tonkes¹,
not on board: Barbara Niehoff¹, Jan Andries van
Franecker³

¹AWI
²UHH
³IMARES
⁴UHB
⁵HS-BRV
⁶v D Met

Grant No AWI_PS92_00

Objectives

Pelagic food webs in the Arctic sea ice zone can depend significantly on carbon produced by ice-associated microalgae. Future changes in Arctic sea ice habitats will affect sea ice primary production and habitat structure, with unknown consequences for Arctic ecosystems. Under-ice amphipods, polar cod *Boreogadus saida* and other species feeding in the ice-water interface layer can play a key role in transferring carbon from sea ice into the pelagic food web, up to the trophic level of birds and mammals (David et al 2015, David et al in review). To better understand potential impacts of changing sea ice habitats for Arctic ecosystems, the HGF Young Investigators Group *Iceflux* in cooperation with IMARES (*Iceflux-NL*) and AWI's PEBCAO group aim to quantify the trophic carbon flux from sea ice into the under-ice community and to investigate physiological capacities of abundant Arctic copepods to adapt to environmental conditions. This should be achieved by 1) quantitative sampling of the in-ice, under-ice and pelagic community in relation to environmental parameters; 2) using molecular and isotopic biomarkers to trace sea ice-derived carbon in pelagic food webs; 3) studying the diet of sea ice-associated organisms, and 4) an experimental study on the resilience of *Calanus* spp to a changing food regime.

Work at sea

SUIT sampling

A Surface and Under-Ice Trawl (SUIT: van Franecker et al 2009) was used to sample the meso- and macrofauna down to 2 m under the ice. The SUIT had two nets, a 0.3 mm mesh plankton net, and a 7 mm mesh shrimp net. During SUIT trawls, data from the physical environment were recorded, e.g. water temperature, salinity, fluorescence, ice thickness, and multi-spectral light transmission. Fifteen SUIT deployments were completed in the closed pack-ice between the Svalbard shelf and the Yermak Plateau (Table 8.1). An overview of the sampling locations is given in Fig. 8.1. Macrofauna samples from the SUIT shrimp net were sorted to the lowest possible taxonomic level. The catch was entirely preserved frozen (-20°C / -80°C), on ethanol (70 % / 100 %), or on 4 % formaldehyde/seawater solution, depending on analytical objectives. In euphausiids, the composition of size and sexual maturity stages was determined 48 hrs after initial preservation in formaldehyde solution.

Tab. 8.1: Summary statistics of SUIT hauls conducted during PS92

Station	Date	Start Time (UTC)	Latitude (North)	Longitude (East)	Bottom depth (m)
19-1	27-05-15	15:22	19.907	81.007	188.5
27-1	31-05-15	4:16	17.767	81.368	827.9
28-4	2-06-15	13:13	19.417	81.513	928.2
31-1	3-06-15	4:41	19.575	81.552	1050.5
32-12	7-06-15	17:00	19.702	81.180	335.6
38-1	9-06-15	15:46	16.311	81.317	2249.1
39-17	12-06-15	18:53	11.817	81.652	1954.7
43-23	16-06-15	15:23	7.0983	82.152	793.6
43-24	16-06-15	17:21	7.068	82.148	799.4
44-1	17-06-15	7:23	9.258	81.942	814.4
45-1	17-06-15	12:26	9.802	81.912	921.5
47-1	19-06-15	7:00	13.650	81.380	2139.1
48-1	21-06-15	6:59	12.963	81.013	2046.9
49-1	21-06-15	13:23	12.848	81.030	2083.1
56-2	23-06-15	12:02	8.190	81.015	848.8

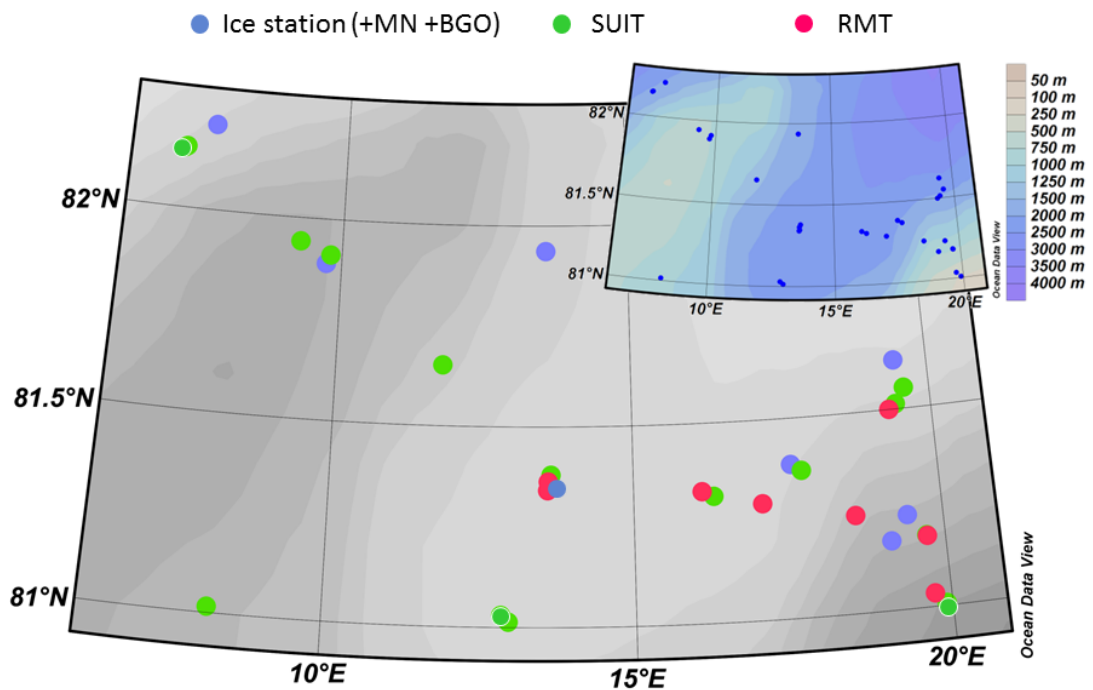


Fig. 8.1: Overview of stations sampled by the Iceflux/PEBCAO team during PS92 BGO: Bongo net; MN: Multinet

Pelagic sampling

A Multiple opening Rectangular Midwater Trawl (M-RMT) was used to sample the pelagic community. During trawling, sampling depth, water temperature and salinity were recorded with a CTD probe attached to the bridle of the net. The standard sampling strata in offshore waters were 1000-200 m, 200-50 m, and 50 m to the surface. In shallow waters or when heavy ice limited the length of the trawl, the lowest depth stratum varied between 100 and 800 m. We conducted 8 depth-stratified hauls with the M-RMT. The catch was sorted by depth stratum and taxon. Sample collection and size measurements on euphausiids were performed in the analogue procedure described above for SUIT sampling.

Tab. 8.2: Summary statistics of RMT hauls conducted during PS92

Station	Date	Start Time (UTC)	Latitude (North)	Longitude (East)	Bottom depth (m)	Lower limits of depth strata sampled
19-2	27.05.15	18:16	81.033	19.737	173	25 m, 50 m, 100 m
24-2	30.05.15	14:37	81.245	18.592	477.6	50 m, 200 m, 400 m
27-17	1.06.15	14:47	81.292	17.100	866.2	50 m, 200 m, 300 m
28-5	2.06.15	16:04	81.500	19.295	908.1	50 m, 100 m, 200 m
32-11	7.06.15	14:48	81.178	19.710	320	50 m, 200 m, 290 m
38-2	9.06.15	17:58	81.330	16.123	2273.8	50 m, 200 m, 500 m
47-2	19.06.15	9:35	81.363	13.607	2145.4	50 m, 200 m, 300 m
47-23	20.06.15	22:37	81.342	13.593	2175.4	50 m, 200 m, 1000 m

The pelagic mesozooplankton community was sampled with a Multinet at each ice station. The Multinet had an opening of 0.25 m² and a mesh size of 150 µm. Sampling was performed over 5 discrete depth layers: 1500-1000 m, 1000-500 m, 500-200 m; 200-50 m, and 50 m to the surface. At stations shallower than 1500 m, the lowest depth stratum extended to 30 m above bottom depth. In total, 9 Multinet stations were completed, including one day/night comparison (Tab. 8.3).

Tab. 8.3: Summary statistics of Multinet hauls conducted during PS92

Station	Date	Time	Latitude (North)	Longitude (East)	Bottom Depth [m]
19-11	2015-05-28	16:48	81.192	19.013	412.3
27-9	2015-05-31	17:17	81.358	17.475	821.3
31-8	2015-06-03	20:17	81.593	19.075	1421
32-9	2015-06-07	9:19	81.212	19.605	447
39-13	2015-06-12	5:58	81.787	12.570	1741.1
43-18	2015-06-15	22:48	82.207	7.142	871.4
46-8	2015-06-18	6:06	81.888	9.852	929.3
46-11	2015-06-18	8:49	81.878	9.863	942.1
47-10	2015-06-19	21:15	81.338	13.600	2184.1
47-18	2015-06-20	11:51	81.348	13.688	2175.5

At each ice station, Bongo nets with a mesh size of 500 µm were used to sample the mesozooplankton community from 200 m depth to the surface. Samples were taken for respiration measurements in collaboration with N Morata and for fecal pellet production experiments in collaboration with C Dybwad. At the last two stations, in total 3 additional Bongo net hauls were conducted for the sampling of living copepods for experiments at the AWI (Table 8.4).

Tab. 8.4: Summary statistics of Bongo net hauls conducted during PS92

Station	Date	Time	Latitude (East)	Longitude (North)	Bottom Depth [m]	Purpose
19-16	2015-05-29	8:29	81.210	18.655	438.6	on-board experiments
20-2	2015-05-29	23:30	81.033	19.342	178.1	on-board experiments
27-11	2015-05-31	19:41	81.353	17.433	814.7	on-board experiments
31-5	2015-06-03	16:13	81.605	19.257	1451.9	on-board experiments
32-17	2015-06-08	8:05	81.098	19.642	209	on-board experiments
32-18	2015-06-08	8:52	81.102	19.690	196.1	on-board experiments
39-12	2015-06-12	4:27	81.800	12.648	1731	on-board experiments
43-10	2015-06-15	11:43	82.208	7.410	812.7	on-board experiments
43-11	2015-06-15	12:13	82.208	7.393	806.3	on-board experiments
46-6	2015-06-18	4:30	81.892	9.820	924.5	on-board experiments
46-7	2015-06-18	5:02	81.892	9.832	924.7	on-board experiments
46-12	2015-06-18	9:47	81.873	9.853	943	on-board experiments
46-13	2015-06-18	10:19	81.870	9.847	948.2	on-board experiments
47-8	2015-06-19	19:14	81.338	13.610	2176	on-board experiments
47-9	2015-06-19	19:43	81.338	13.608	2177.3	on-board experiments
47-13	2015-06-20	6:15	81.345	13.673	2175.8	AWI experiments
47-14	2015-06-20	6:45	81.345	13.683	2176.8	AWI experiments
56-6	2015-06-23	16:31	81.015	8.292	853.9	AWI experiments

Polarstern's EK60 echosounder recorded the distribution of acoustic targets continuously during sailing, only paused during geological surveys of bottom sediments. Our sampling frequencies were 38 kHz, 70 kHz, 120 kHz, and 200 kHz All EK60 data were backed up on the ship's mass storage server.

For biomarker analysis, Particulate Organic Matter (POM) was collected from filtered seawater obtained from the CTD rosette at each ice station.

Sea ice work

Our sea ice work was conducted in close collaboration with the AWI sea ice physics group (T Krumpfen et al.). A total of 8 sea ice stations were sampled during PS92 (Table 8.5) Depending on time availability and weather conditions, the following sampling procedure was completed during sea ice stations:

- a) We conducted measurements of the under-ice light field using a RAMSES spectroradiometer attached to an L-arm, sampling light spectra under the sea ice well away from the drilling hole. At each L-arm site, a bio-optical core was taken straight above one RAMSES measurement point. Additional bio-optical cores were sampled above RAMSES measurement points along ROV transect of the sea ice physics group.
- b) Ice cores were taken for biomarker analysis and sea ice infauna, respectively.
- c) We lowered a CTD probe equipped with a fluorometer through a hole down to 50 m depth, thus obtaining vertical profiles of temperature, salinity and chlorophyll a content in the upper 50 m under the sea ice.
- d) We collected under-ice water for the analysis of the microzooplankton composition with a handheld Kemmerer water sampler lowered to approximately 1 m under the ice.

In bio-optical cores, the bottom 10 cm were separated from the rest of the core, and both retained sections were processed for chlorophyll a content in order to determine the relationship of ice algal biomass with the under-ice spectral light properties. Additionally, subsamples from the melted bio-optical core sections were taken for pigment analysis (HPLC), POM, and microscopic analysis. In cores for sea ice infauna, 10 cm sections from the bottom, the top and the inner part of the core were retained for sample collection. Retained sections of sea ice infauna cores were carefully melted at 4°C in the ship's temperature-controlled laboratory container. 200 ml filtered sea water per cm core section were added to melting sections of sea ice infauna cores. Filters for POM and pigment analysis obtained from melted ice core sections and water samples were frozen at -80°C. Microscopy samples from bio-optical cores, under-ice microzooplankton and sea ice infauna were stored at 4°C on 4 % formaldehyde/seawater solution.

Tab. 8.5: List of the ice stations sampled, and number of ice cores, L-arm measurements and CTDs taken at each sampling site. For each ice station it is specified if there have been conducted under ice radiation measurements (L-arm), and the number of under-ice CTD profiles conducted

Ice st. no	Station	Cores	L-arm	CTD
01	19-6	7	1	2
02	22-1	7	1	2
03	31-2	7	1	2
04	32-4	5	1	1
05	39-9	5	1	1
06	43-6	5	1	2
07	46-3	3	-	1
08	47-5	4	-	1

Preliminary (expected) results

SUIT sampling

SUIT sensors data: All 15 SUIT hauls were conducted under sea ice. Bio-environmental profiles were obtained from each SUIT haul (Fig. 8.2) The average ice coverage of the under-ice hauls was 51 %. Preliminary mean ice draft calculated based on pressure measurements of the SUIT's CTD ranged between 175 cm and 394 cm in heavy sea ice (Fig. 8.3). In a first analysis of surface water chlorophyll-a content, a characteristic pattern could not be identified.

More insight on the biological productivity of the system, however, can be expected as soon as spectral data from the SUIT's RAMSES sensor can be related to the chlorophyll a content of sea ice derived from our L-arm measurements and associated ice core sampling.

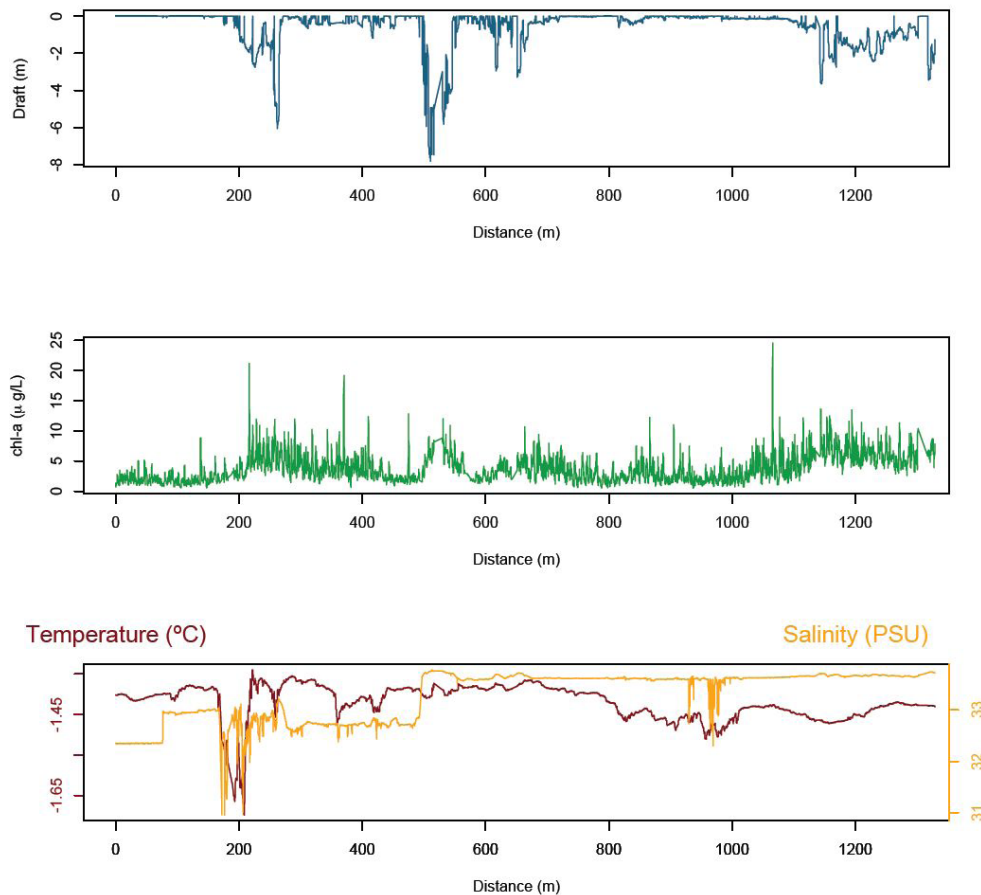


Fig. 8.2: Example of environmental data profiles obtained from the SUIT's sensor array at station 27-1.

SUIT catch composition: A large part of the catch from the 7 mm mesh shrimp net was counted and sorted on board. Several abundant taxa, however, were excluded from this preliminary analysis due to time limitations. These include the often dominant chaetognaths (mainly *Sagitta* spp), *Calanus* spp, and appendicularians. Fig. 8.3 shows an overview of the taxa quantified. In terms of abundance, the catch was heavily dominated by amphipods. The under-ice amphipod *Apherusa glacialis* was the most abundant species over all SUIT hauls. Other ice amphipods, such as *Onisimus* spp, *Eusirus holmii* and *Gammarus wilkitzkii*, were practically omnipresent, albeit at lower abundances. The catch composition in the eastern part of the survey area was clearly dominated by *A glacialis* and other ice amphipods. In this region, low numbers of polar cod *Boreogadus saida* were caught at stations deeper than 1,000 m. In the western part of the investigation area, the pelagic amphipod *Themisto libellula* co-dominated. In this region, several stations also had high abundances of the krill *Thysanoessa* spp, and the sea angel *Clione limacina* (Fig. 8.3). Increased numbers of *Thysanoessa* spp and appendicularians (data not shown) may indicate a higher Atlantic influence in the western part of the survey area.

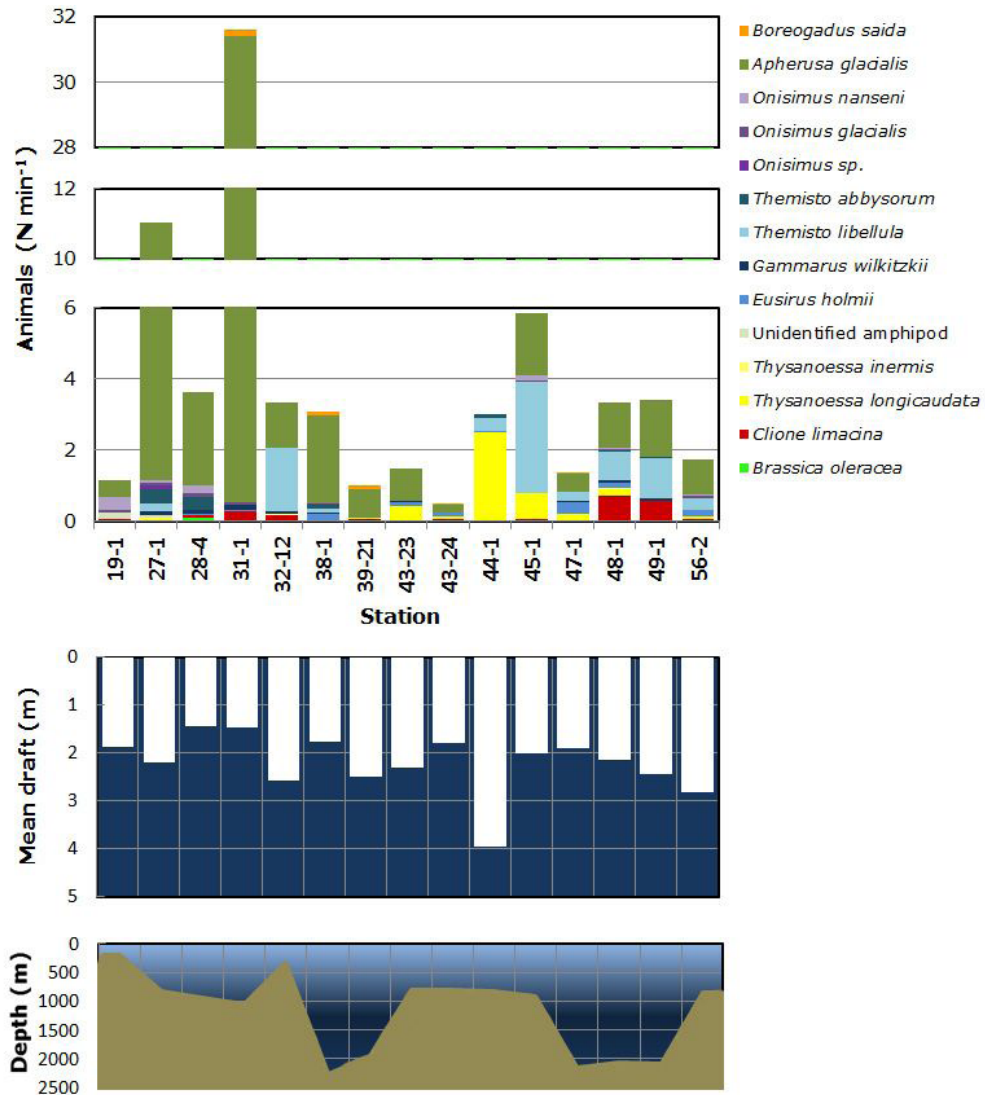


Fig. 8.3: SUIT catch composition, sea ice draft and bottom depth during trawling. The top panel shows the abundance of major taxa at each SUIT station in numbers per minute trawled. In the center panel, the white bars represent the modal ice draft during each haul. The lower panel shows the bottom depth at each SUIT station. Depths between SUIT sampling stations were interpolated and do not represent the actual depth profile of the cruise track.

RMT sampling

We completed in total 8 M-RMT hauls, mostly in close proximity to SUIT sampling locations. However, no RMT hauls were conducted in the western part of the survey area due to heavy ice and time limitations (Fig. 8.1). In this report we present preliminary data on macrozooplankton and micronekton collected by the RMT-8 nets of the upper 200 m of the water column. Data on cnidarians, ctenophores, copepods, chaetognaths and appendicularians were not included in this preliminary analysis.

Macrozooplankton communities: The catch composition was heavily dominated by euphausiids ('krill') at each station (Fig. 8.4). *Thysanoessa longicaudata* and *T. inermis* co-dominated in terms of abundance, whereas the considerably larger *Meganyctiphanes norvegica* probably dominated in terms of biomass (Fig. 8.5). At several stations, the more temperate *Nematocelis megalops* was present. After the euphausiids, pelagic amphipods *Themisto* spp represented the second most abundant taxon (Fig. 7.4). High abundances were also obtained by the copepod *Calanus hyperboreus*, and the chaetognath *Sagitta* spp (both not quantified) Ctenophores (not quantified) and sea angels *Clione limacina* were regularly present, but in lower numbers. We caught several squid larvae and one lanternfish (Myctophidae). Due to the lack of sampling locations in the western part of the survey area, no spatial pattern similar to the SUIT catch composition was apparent from the RMT data.

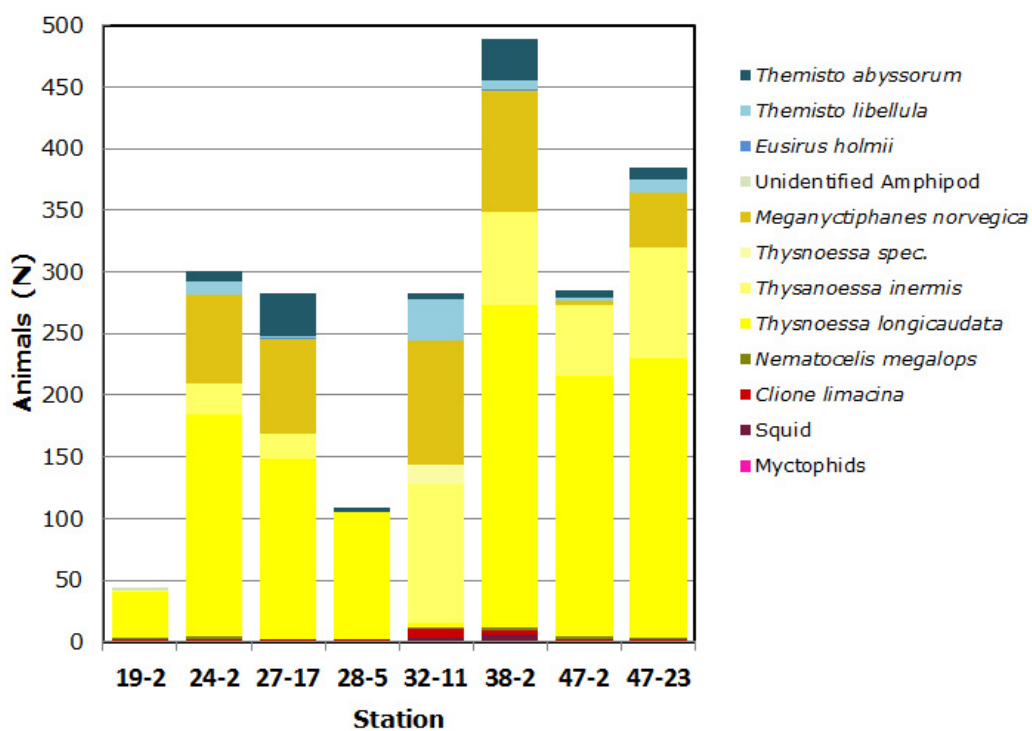


Fig. 8.4: RMT catch composition of the upper 200 m

Euphausiid size distribution: The size of *Meganyctiphanes norvegica* ranged between 12 and 40 mm, with a mode at 25 mm. Most animals were adults, with an approximately equal proportion of females and males. The majority of females were in maturity stage 2; whereas about 60 % of the males were in maturity stage 3A, and each about 20 % in stage 2 and 3B, respectively. The length distribution of *Thysanoessa inermis* reached from 10 to 32 mm. It had two modes at 16 and 25 mm, respectively. The 16 mm-mode was dominated by juveniles. Krill over 20 mm length were predominantly adults. About 80 % of the females were in maturity stage 2 and 3A. Only 20 % of the females were in maturity stage 3B. In males, about 40 % were in stage 3A and 3B, respectively. The size of *Thysanoessa longicaudata* ranged from 7 to 17 mm. The size distribution was bimodal, with modes at 10 and 13 mm. Less than 5 % of the sampled krill were juveniles. About 25 % of the females and 35 % of the males were in maturity stage 3A. In both sexes, about 15 % of the animals were in maturity stage 3B, and less than 10 % were in maturity stage 2.

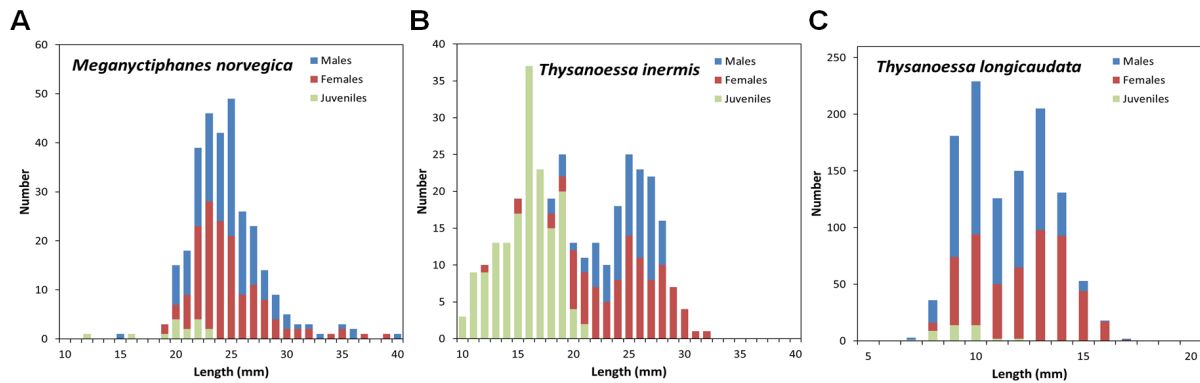


Fig. 8.5: Length-frequency distributions of the three most abundant krill species *Meganyctiphanes norvegica* (A), *Thysanoessa inermis* (B), and *T. longicaudata* (C) in the upper 200 m of the water column

Sea ice work

The basic parameters of each sea ice station and their sampling sites were summarised in the sea ice biology section of this report. Table 8.6 lists the number of ice cores taken for the bio-optical work, sea ice infauna, and biomarker analysis.

Tab. 8.6: Numbers of ice cores taken at each ice station for bio-optical, biomarker (LSI) and sea ice meiofauna analysis

<i>Ice</i>	<i>Station</i>	<i>Meiofauna</i>	<i>LSI</i>	<i>BioOptical</i>
01	19-6	2	2	3
02	22-1	2	2	3
03	31-2	2	2	3
04	32-4	2	2	1
05	39-9	2	2	1
06	43-6	2	2	1
07	46-3	2	0	1
08	47-5	2	0	2

The CTD profiles provided information on the water characteristics at the ice stations. The temporal variability of CTD profiles at one station could significantly exceed between-station variability, both in physical parameters and chlorophyll *a* concentrations (Fig. 8.6).

At most ice stations we performed under-ice light field measurements. The high variability of the sampled ice floes offers the possibility to study light transmission through ice of different types and thicknesses as well as through different snow covers. This will help to parameterize the under-ice radiation in relation to different sea-ice physical conditions and, once the further analysis on the chlorophyll *a* will be completed, with different biomass content.

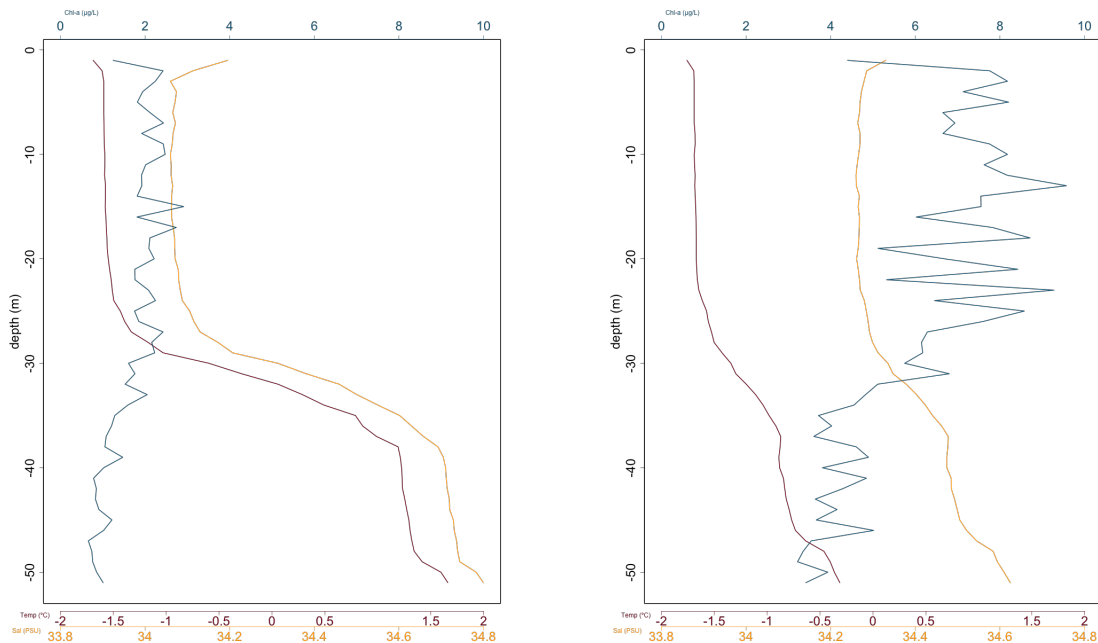


Fig. 8.6: Repeated CTD profiles in the top 50 m of the water column at ice station 31-2. The period between the two measurements was approximately 24 hours.

Data management

Almost all sample processing will be carried out in the home laboratories at AWI and IMARES. This may take up to three years depending on the parameters as well as analytical methods (chemical measurements and species identifications and quantifications). As soon as the data are available they will be accessible to other cruise participants and research partners on request. Metadata will be shared at the earliest convenience; data will be published depending on the finalization of PhD theses and publications. Metadata will be submitted to PANGAEA, and will be open for external use.

References

- van Franeker JA, Flores H, Van Dorssen M (2009) The Surface and Under Ice Trawl (SUIT), in: Flores, H (Ed), *Frozen Desert Alive - The Role of Sea Ice for Pelagic Macrofauna and its Predators* PhD thesis University of Groningen, pp 181–188
- David C, Lange B, Rabe B and Flores H (2015) Community structure of under-ice fauna in the Eurasian central Arctic Ocean in relation to environmental properties of sea-ice habitats, *Marine Ecology-Progress Series*, 522, pp 15-32 doi:10.3354/meps11156
- David C, Lange B, Krumpfen T, Schaafsma F, van Franeker JA, Flores H (2015) Under-ice distribution of polar cod *Boreogadus saida* in the central Arctic Ocean and their association with sea ice habitat properties *Polar Biology* doi: 10.1007/s00300-015-1774-0

9. ECOSYSTEMS

9.1 Nutrients, primary production and nitrogen cycling (GREENEDGE)

Marie-Amélie Blais¹, Maxime Fradette², Marieke
Beaulieu²

¹Takuvik/UnL

²UnS

not on board: Marcel Babin¹, Jean-Eric Tremblay¹,
Flavienne Bruyant¹, Yannick Huot²

Grant No AWI_PS92_00

Objectives

The objectives of our team on board line up with the general objectives of the ANR funded "Green-Edge" project: to understand the processes that control the Arctic phytoplankton spring bloom (PSB) as it expands northward and to determine its fate in the ecosystem by investigating its related carbon fluxes.

Marine biological productivity in the Arctic is highly constrained by sea ice, which limits the penetration of sunlight and air-sea interactions. The September extent of the Arctic Ocean icepack has decreased by nearly 40 % over the last 3 decades (Stroeve et al 2012) It is expected by many that the resulting increase in the penetration of sunlight in the water column will boost primary production (PP) of phytoplankton and, possibly, increase the overall biological productivity in the Arctic Ocean. Several arctic surveys using ocean color remote sensing do confirm an increase in PP by about 20 % between 1998 and 2009 (Pabi et al 2008, Arrigo et al 2008, 2011, Bélanger et al 2013). Over longer time periods, the trajectory of PP is however uncertain. As in most parts of the World Ocean, the PSB provides a large fraction of the annual PP and, most importantly, nearly all of the new primary production exportable through the food chain and toward the bottom sediments. In the Arctic Ocean, the PSB often develops around the ice-edge (Sakshaug 2004). This highly transient phenomenon lasts about 3 weeks at any given location in the seasonal ice zone (SIZ). According to Perrette et al (2011), ice-edge blooms represent most of the annual PP in the Arctic Ocean. The SIZ is currently increasing in size and may cover the entire Arctic Ocean as of the 2030s (Wang and Overland 2009). Therefore, one may expect ice-edge blooms to cover a much larger area than they use to through a significant northward expansion. However, we currently do not know what will be the fate of this additional phytoplankton biomass built up along the retreating ice cover.

The study conducted during Transsiz was perfect to improve our understanding of the key physical, chemical and biological processes that govern the PSB in the Arctic Ocean and identify key phytoplankton species involved and model their growth under various environmental conditions.

Work at sea

The Imaging Flow Cytobot (IFCB) was deployed on the flow-through system during the entire cruise. This instrument takes images of phytoplankton in a 5 mL water sample. It had taken water samples every 20 minutes between the 20th May and the 26th June except during the processing of the CTD samples.

9.1 Nutrients, primary production and nitrogen cycling (GREENEDGE)

We have sampled water from the CTD at each station and each bio-cast (see Tab. 9.1.1). On these samples, we have done filtration for protein analysis, imaging of phytoplankton with the IFCB, measurements of Quantum efficiency of photochemistry in PSII and Functional absorption cross-section of PSII using the FIRE. In addition, primary production measurements were taken for each depth. For each of the selected depths, 28 incubations (volume of 1.5 mL) were conducted with varying light intensities, which allow determining the P vs E parameters with accuracy.

Tab. 9.1.1: Water column sampling effort during PS92 cruise *phytoplankton*

Station	Depth [m]	Protein	IFCB	FIRE	Primary production
PS92/19-05	5, 10, 20, 40, 75	x	x	x	x
PS92/21-01	2, 5, 20, 50, 100	x	x	x	
PS92/24-01	2, 10, 25, 50, 100	x	x	x	
PS92/27-02	2, 5, 10, 20, 30, 50	x	x	x	x
PS92/28-01	2.5, 10, 15, 30, 50	x	x	x	
PS92/29-01	1.5, 5, 10, 20, 50	x	x	x	
PS92/31-03	1.5, 5, 10, 25, 40, 75	x	x	x	x
PS92/32-05	1.5, 5, 10, 25, 30, 50	x	x	x	x
PS92/36-01	2, 5, 10, 20, 30, 50	x	x	x	x
PS92/39-08	1.3, 5, 10, 35, 50, 75	x	x	x	x
PS92/43-05	1.7, 5, 10, 20, 40, 75	x	x	x	x
PS92/46-02	2, 10, 20, 30, 40, 75	x	x	x	x
PS92/47-04	2.1, 5, 10, 15, 30, 50	x	x	x	x
PS92/52-01	1.8, 10, 20, 30, 40, 75	x	x	x	x
PS92/56-03	2.7, 10, 17, 30, 50, 100	x	x	x	

The same measurements were also taken for ice cores and subsurface water samples with the exception of the first ice station where the ice productivity measurements were not processed (see Tab. 9.2.2). When sampling of the ice occurred on the same day as chlorophyll measurements, a deep chlorophyll sample was also taken from the ice.

Tab. 9.1.2: Ice sampling effort during PS92 cruise; (under-ice surface water (UIW); under-ice water deep chlorophyll maximum (UIW-DCM), ice core (IC))

Station	Depth [m]	Protein (only water, no core)	IFCB	FIRE	Primary Production
PS92/27-03	UIW, bottom 1 cm of ice core, bottom 5 cm of IC	x	x	x	x
PS92/31-02	UIW, bottom 1 cm of ICs	x	x	x	x
PS92/32-04	UIW, UIW-DCM, bottom 1 cm of ICs	x	x	x	x
PS92/39-06	UIW, UIW-DCM, bottom 1 cm of ICs	x	x	x	x
PS92/43-04	UIW, bottom 1 cm of ICs	x	x	x	x
PS92/46-01	UIW, UIW-DCM, bottom 1 cm of ICs	x	x	x	x
PS92/47-03	UIW, UIW-DCM, bottom 1 cm of ICs	x	x	x	x

For the ice samples, the bottom 1 cm was taken on duplicate ice cores from the sampling grid 50 mL of filtered (0.2 µm) surface water were added to the ice core that was rapidly thawed by continuously shaking. The final volume was of approximately 100 mL. Samples were generally processed within an hour of sampling. From here on, ice samples were processed, as were the water column samples.

We have also deployed the Underwater Video Profiler (UVP) on ice station 3 and 4. This instrument takes images of particles and zooplankton in the water column. It allows knowing the particles size and abundance distribution in the water column.

Samples for nutrients were either stored frozen (nitrate, nitrite, phosphate, silicate) for analysis at the home laboratory or analysed fresh onboard (ammonium). Incubations were performed in deck boxes using trace additions of 15-N labeled ammonium and nitrate to determine rates of new and regenerated production. Total primary production was determined simultaneously with the addition of 13-C labeled bicarbonate. Incubations were terminated by filtration; the filters were dried and subsequently analyzed by continuous flow Isotope-ratio-mass-spectrometry at the home laboratory (Tab 9.1.3).

Tab. 9.1.3: Water column sampling effort during PS92 cruise for nutrients

Station	Depth [m]	Nutrients	NH ₄	Incubations (deck)	Incubations (in-situ)
PS92/19-05	350, 150, 100, 75, 50, 40, 30, 20, 10, 5, surf	x	x		75, 50, 40, 30, 20, 10, 5, surf
PS92/21-01	Bottom, 150, 100, 75, 50, 40, 30, 20, 10, 5, surf	x	x		
PS92/24-01	500, 300, 200, 150, 100, 75, 50, 40, 30, 25, 10, 5, surf	x	x		
PS92/27-03	150, 100, 75, 50, 40, 30, 20, 10, 5, surf	x	x		75, 50, 40, 30, 20, 10, 5, surf
PS92/27-04	200, 100, 75, 50, 40, 30, 15, 5	x	x	100, 75, 50, 30, 15, 5	
PS92/27-07	800, 500, 300	x	x		
PS92/28-01	Bottom, 500, 300, 200, 150, 100, 75, 50, 40, 30, 15, 10, surf	x	x		
PS92/29-01	Bottom, 1000, 500, 300, 200, 150, 100, 75, 50, 40, 30, 20, 10, 5, surf	x	x		
PS92/31-03	Bottom, 500, 300, 200, 150, 100, 75, 50, 40, 30, 25, 10, 5, surf	x	x		75, 50, 40, 30, 25, 10, 5, surf
PS92/31-04	100, 75, 50, 30, 25, 5	x	x	x	
PS92/31-12	Bottom, 800, 600, 500, 400, 300, 250, 200, 150, 100, 75, 50, 25, surf	x	x		
PS92/32-05	Bottom, 300, 200, 150, 100, 75, 50, 40, 30, 20, 10, 5, surf	x	x		75, 50, 40, 30, 20, 10, 5, surf
PS92/32-06	100, 75, 50, 30, 20, 5	x	x	x	
PS92/32-14	Bottom, 200, 150, 100, 75, 50, 25, surf	x	x		

9.1 Nutrients, primary production and nitrogen cycling (GREENEDGE)

Station	Depth [m]	Nutrients	NH ₄	Incubations (deck)	Incubations (in-situ)
PS92/33-01	Bottom, 300, 200, 150, 100, 75, 50, 40, 30, 25, 10, 5, surf	x	x		
PS92/35-01	Bottom, 500, 300, 200, 150, 100, 75, 50, 40, 30, 20, 15, 10, 5, surf	x	x		
PS92/36-01	Bottom, 1000, 500, 300, 200, 150, 100, 75, 50, 40, 30, 20, 10, 5, surf	x	x		
PS92/37-01	Bottom, 1000, 500, 150, surf	x	x		
PS92/39-08	Bottom, 1000, 500, 300, 200, 150, 100, 75, 50, 40, 35, 30, 10, 5, surf	x	x		75, 50, 40, 35, 30, 10, 5, surf
PS92/39-09	Bottom, 1000, 800, 700, 600, 500, 400, 300, 250, 200, 150, 100, 75, 50, 40, 10, surf	x	x		
PS92/39-11	100, 75, 50, 30, 20, 5	x	x	x	
PS92/40-04	Bottom, 600, 500, 400, 300, 250, 200, 150, 100, 75, 60, 50	x	x		
PS92/43-01	Bottom, 600, 500, 400, 300, 250, 200, 150, 100, 75, 50, 30, surf	x			
PS92/43-05	Bottom, 500, 300, 200, 150, 100, 75, 50, 40, 30, 20, 10, 5, surf	x	x		75, 50, 40, 30, 20, 10, 5, surf
PS92/43-06	100, 75, 50, 30, 20, 5	x	x	x	
PS92/46-02	Bottom, 500, 300, 200, 150, 100, 75, 50, 40, 30, 20, 10, 5, surf	x	x		75, 50, 40, 30, 20, 10, 5, surf
PS92/46-03	100, 75, 50, 30, 20, 5	x	x	x	
PS92/46-14	Bottom, 600, 500, 400, 300, 250, 200, 150, 100, 75, 50, 30, surf	x	x		
PS92/47-04	1000, 500, 300, 200, 150, 100, 75, 50, 40, 30, 15, 10, 5, surf	x	x		75, 50, 40, 30, 15, 10, 5, surf
PS92/47-06	100, 75, 50, 25, 10, 5	x	x	x	
PS92/47-19	Bottom, 800, 600, 500, 400, 300, 250, 200, 150, 100, 75, 65, 50, 10, surf	x	x		
PS92/52-01	Bottom, 1000, 500, 300, 200, 150, 100, 75, 50, 40, 30, 20, 10, 5, surf	x	x		
PS92/55-01	Bottom, 500, 300, 200, 150, 100, 75, 50, 40, 30, 20, 10, 5, surf	x	x		
PS92/56-03	Bottom, 500, 300, 200, 150, 100, 75, 50, 40, 30, 17, 10, 5, surf	x	x		

Preliminary (expected) results

The Imaging Flow Cytobot (IFCB) in conjunction with the UVP, will allow the precise identification and quantification of phytoplankton species encountered during the cruise. It is critical to see which species are involved in PP as a shift in environmental conditions may trigger a shift in species succession and therefore PP rates.

PP rates and photosynthetic parameters in conjunction with variable fluorescence assessment will give an estimation of photosynthetic efficiency of the phytoplankton spring bloom species encountered as well as an estimation of PP.

Our results will provide information on the current (incubations) and prior (nutrient drawdown) distribution of primary production across the survey area and contribute to the interpretation of spatial patterns in the other variables measured by our group (assemblage composition of phytoplankton and zooplankton) and others (sedimentation, benthic fluxes). Estimates of nitrate and ammonium assimilation will complement those of another group measuring N₂ fixation, providing a detailed overview of nitrogen cycling and new biological productivity in the area (i.e. the quantity of organic matter available for export to the higher food web or the Deep Ocean and sediments).

Data management

Data treatment for the UVP and the IFCB is quite time demanding. Raw data will be processed using a Matlab™ based custom software for image interpretation and cross-controlled using images from real taxonomical samples. Data will be given access to in due time when processing is finished and stored in PANGAEA latest after 3 years.

Data from P vs E curves are not yet available, as samples need to be recounted at AWI. When dpm radioactivity counts will be made available to us, we will process the data mathematically and apply our PP model in order to estimate the photosynthetic parameters. After getting the HPLC data and particulate absorption data photosynthetic parameters will be ready within 6 months. Overall the data will be ready to submit to PANGAEA after 5 years.

For nutrients and incubations the sample analysis and data processing will be done at Laval University and the final results will be made available to other participants. Depending on the finalization of student theses and publications, data will be submitted to PANGAEA, and will be open for external use after 5 years.

References

- Arrigo K R, P A Matrai and G L Van Dijken (2011) Primary productivity in the Arctic Ocean: Impacts of complex optical properties and subsurface chlorophyll maxima on large-scale estimates *J Geophys Res-Oceans* 116
- Arrigo K R, G Van Dijke, and S Pabi (2008) Impact of a shrinking Arctic ice cover on marine primary production *Geophys Res Lett* 35: DOI: 10.1029/2008GL035028
- Belanger S, M Babin and J E Tremblay (2013) Increasing cloudiness in Arctic damps the increase in phytoplankton primary production due to sea ice receding *Biogeosciences* 10: 4087-4101
- Pabi S, G L Van Dijken and K R Arrigo (2008) Primary production in the Arctic Ocean, 1998-2006 *J Geophys Res-Oceans* 113
- Sakshaug E (2004) Primary and secondary production in the Arctic Seas, p 57–82 In R Stein and R W MacDonald [eds], *The organic carbon cycle in the Arctic Ocean* Springer
- Stroeve J C, M C Serreze, M M Holland, J E Kay, J Malanik, and A P Barrett (2012) The Arctic's rapidly shrinking sea ice cover: a research synthesis *Climatic Change* 110: 1005-1027
- Wang MY, and J E Overland (2009). A sea ice free summer Arctic within 30 years? *Geophys Res Lett* 36

9.2 Distribution patterns of protists with special emphasis on toxic dinoflagellates in the North Atlantic and Arctic Waters

Johanna Hessel¹
not on board: Katja Metfies¹

¹AWI

Grant No AWI_PS92_00

Objectives

Climate induced changes in the Arctic such as the drastic decrease in sea ice, ice-thickness or the increase in temperature are expected to impact the biodiversity in pelagic ecosystems. A shift in species composition is expected to occur in all phytoplankton size classes. Within the marine phytoplankton there are toxic micro-algal species (mainly dinoflagellates) known to have the potential to form Harmful Algal Blooms, the so called HABs. Impacts of toxic algae species appear to have increased on a global basis in frequency, intensity and geographic distribution over the past decades (e.g. Zingone and Enevoldsen 2000; Moestrup 2004). Incidences of harmful bloom events in Norwegian waters moved northwards during the past 40 years (Okoldkov 2005). The distribution ranges of HAB-species into or within the Arctic Ocean might further expand northwards due to ongoing temperature increase and larger ice-free regions during summer (e.g. Hallegraeff 2010). This might impact Arctic ecosystems due to toxin production, and their accumulation in higher trophic levels. For coastal areas of the Eurasian Arctic there are records of 14 toxic and potentially toxic dinoflagellate species including *Dinophysis sp* or *Alexandrium sp* (Okoldkov 2005). However, information on abundance and distributional patterns of these species in the Arctic Oceans is still scarce.

We aim to identify current distributional patterns of toxic dinoflagellates in the Norwegian Sea and Arctic Waters in July 2015. In a recent study highest abundances of toxic dinoflagellates were observed during July in the North Atlantic (Taylor et al 2013). Therefore, the timing of the current cruise is well suited to assess the spatial distribution of toxic dinoflagellates in the North Atlantic and Arctic Waters. In addition to surveillance of toxic dinoflagellates, we will characterize the phytoplankton background population in detail in order to establish structural community linkages between toxic algae and the surrounding phytoplankton community. The study will be based on collecting samples from surface waters on a regular basis throughout the whole cruise using a newly developed automated filtration system and sampling different depths in the water column at the main stations via CTD. We will carry out the following genetic analyses to describe distributional patterns of protist communities and the abundance of toxic microalgae in the observation area:

- Automated Ribosomal Intragenic Sequence Analysis (ARISA) in order to get information on spatial variability of protist communities in the observation area.
- Quantification of toxic algae using an automated rRNA biosensor in order to get information on the abundance of toxic algae in the observation area.
- Quantitative PCR in order to evaluate the data generated with the automated nucleic acid biosensor.
- Next generation sequencing (Illumina) to get information on the protist community structure in selected samples.

Within the arctic long-term observatory FRAM (Frontiers in Arctic Marine Monitoring) we will furthermore operate a nutrient analyzer for continuous measurements of nitrate (NO₃), nitrite (NO₂), phosphate (PO₄) and silicate (SiO₂) in surface waters (~10m). The analyzer device is provided by the HZG Geesthacht. The operation will start during cruise PS92 and will be continued during the whole arctic expedition to enable the recording of nutrient data in high temporal and spatial resolution.

Work at sea

Automatic filtration system for marine microbes

During the ships progress to the Arctic sea ice zone, phytoplankton samples were collected using a newly developed automatic filtration system for marine microbes (AutoFiM, Fig. 9.2.1). Therefore 2000 – 3000 ml of seawater was filtrated through 0.4 µm membrane filters mostly every 1° latitude/longitude. AutoFiM is connected to the ships pump system thus sampled seawater correspond to water depths of around 10 meters. In total 40 filters were generated with this automatic device covering latitude positions from 58° to 81° North and longitude positions from 03° to 19° East. Filters were preserved with 600µl of lysis buffer each and stored at -20°C (long term at -80°C) for further molecular analysis at AWI.

CTD/Rosette Sampling

In addition to the sample collection by AutoFiM, water column samples were collected by a CTD/rosette sampler (Seabird, Typ SBE 911plus) at selected stations and depths for vertical phytoplankton community investigations and in order to evaluate the quality of the automatic sampling performance (Table 9.2.1). Mostly these stations represented the official ice stations during the cruise. Seawater was collected at three different depths: surface water (5 - 10m), fluorescence maximum depth and 50m. Fractionated filtration with volumes up to 2,000 ml was done using a plastic filtration unit with 500 ml attachment (Nalgene Bottle-Top-Filter) and polycarbonate membrane filters (Millipore) with pore sizes of 10 µm, 3 µm and 0.4 µm, alternatively 0.2 µm mainly for additional bacteria analysis. At 8 ice stations 186 filters have been prepared in total 27 filters were collected for exclusiv chlorophyll A analysis. All samples are stored at -80°C until further molecular genetic analysis in the home laboratory.

Furthermore 100 ml of seawater from the three different sample depths were stored in brown glass bottles for microscopic analysis (24 samples in total). The water samples were preserved with 1 ml of lugol solution (2 %) and stored dark at 4°C.

Additionally, unfractional filters were prepared for exclusive RNA extraction. Therefore up to 2,000 ml seawater from the surface and fluorescence maximum water depths have been directly filtrated through 0.4 µm membrane filters, preserved with 600 µl lysis buffer and stored at -80°C. At least 25 RNA filters were prepared for further analysis at AWI.



Fig. 9.2.1: Automatic filtration system for marine microbes (AutoFiM) Sample reservoir could be filled with up to 5L of seawater. Filters are provided in a filter magazine and automatically placed under the filtration unit. When filtration is finished, generated filters are preserved with lysis buffer and stored in a rondell. Filtration operation is performed automatically

Nutrient analysis

During the whole cruise the four main nutrients nitrate (NO_3), nitrite (NO_2), phosphate (PO_4) and silicate (SiO_2) were measured using the automatic analyzing device named $\mu\text{MAC-C}$. The nutrient analyzer is operated in connection with the automatic flow through system Ferrybox and allows continuous measurement (approximately every hour) of the nutrient concentrations in the upper water column. Measurements are based on colorimetric reactions and resulting values measured as optical densities (ODEs) can be used for concentration calculation ($\mu\text{mol/L}$)

Table 9.2.1: Water column sampling effort using a CTD sampler during PS92 cruise DNA and chlorophyll a filters were generated by fractional filtration with 10, 3 and 0.4/2 µm filters RNA filters were generated by unfractional filtration using 0.4 µm filters.

Station	Depth [m]	DNA	Microscopy	RNA	Chl a
PS92/19	5	x	x	x	
	20	x	x	x	x
	50	x	x		
PS92/27	10, 20, 50	x	x	x	
	20				x
PS92/31	5, 25, 50	x	x	x	
	25				x
PS92/32	5	x	x	x	
	25	x	x	x	x
	50	x	x		
PS92/39	5	x	x	x	
	35.5	x	x	x	x
	50	x	x	x	
PS92/43	5.2	x	x	x	
	20	x	x	x	x
	50	x	x		
PS92/46	5	x	x	x	
	40	x	x	x	x
	50	x	x		
PS92/47	5	x	x	x	
	15	x	x	x	x
	49.9	x	x		
PS92/53	5.1	x	x	x	
	20.1	x	x	x	x
	50	x	x		

Preliminary results

Preliminary AutoFiM evaluation

During this cruise we successfully tested the automatic filtration system AutoFiM on *Polarstern* for its applicability on board ships. In general the system operates effectively during the ship's progress to the arctic sea ice zone. At each selected position 2000 – 3000 ml were filtered within 20-60 minutes depending on water profile and quality. The sampling quality will be evaluated at AWI by molecular methods. AUTOFiM provides the technical background for automated high resolution collection of marine samples for molecular analyses and allows rapid and economizing filtration of seawater samples without permanent attendance of a scientist.

Parameter setting and operation of AutoFiM could to date be done via the VNC-Viewer basically at every place on the ship. For future work it is also planned to control the filtration performance and programme via satellite communication.

9.2 Distribution patterns of protists with special emphasis on toxic dinoflagellates

The most serious hardware problem was the operation of AutoFiM during the ships time in the sea ice as the ships pump system was shut down due to freezing problems in this zone. As AutoFiM is connected to this pump system at some point it could not be ensured anymore that there is a continuous and accurate flow through of seawater. Therefore we recommend to configure AutoFiM with flow sensors to control the quantity and performance of the seawater flow through. For further and long term performance we also aim to connect the filtration system to another continuous sampling device, e.g. the Ferrybox.

Nutrient analysis

Optical densities of main nutrients nitrate (NO_3), nitrite (NO_2), phosphate (PO_4) and silicate (SiO_2) were measured continuously during the whole cruise in the upper seawater column. First calculations on concentrations (raw values) indicate high temporal and spatial variability of concentrations during the ships progress to the north-east (e.g. NO_3 , Fig. 9.2.3). Concentrations ranged from 0.00 – 0.34 $\mu\text{mol/l}$ NO_2 , 0.00 – 6.62 $\mu\text{mol/l}$ NO_3 , 0.03 – 0.47 PO_4 and 0.00 – 3.86 $\mu\text{mol/l}$ SiO_2 .

For preliminary evaluation concentration averages were precalculated for 7 (out of 8) ice stations, reaching highest values at the far north-east ice stations 39 – 46 (Fig. 9.2.4). Data still needs to be processed for final values.

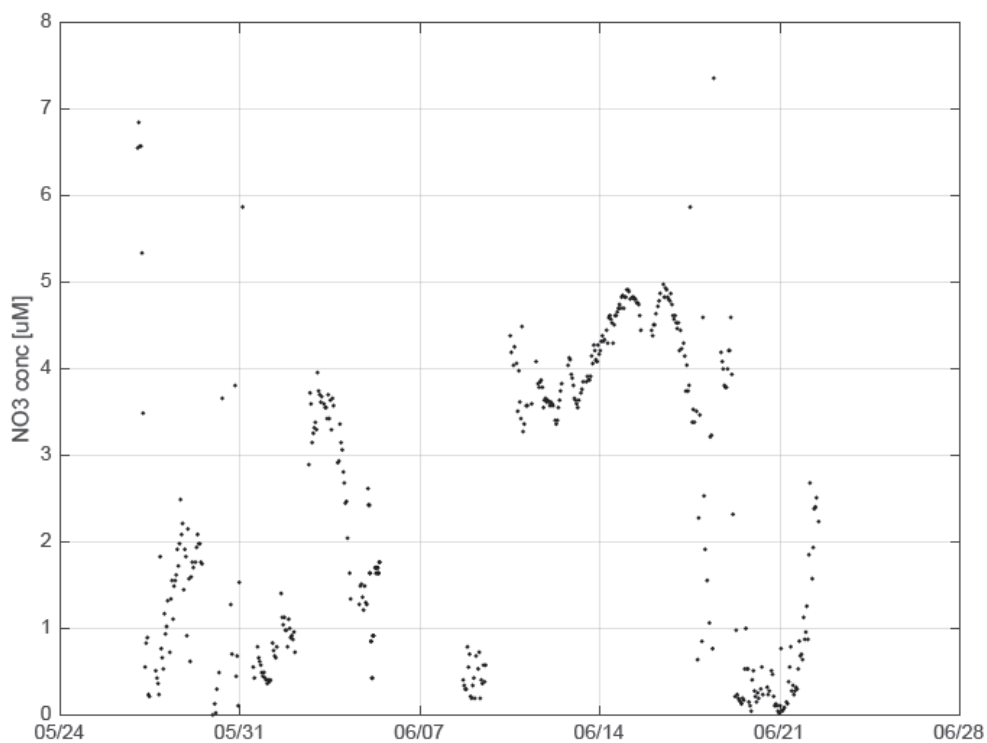


Fig. 9.2.3: Plot of nitrate concentrations X-axis represents dates. Uncorrected raw value data (Graphic: A Randelhoff).

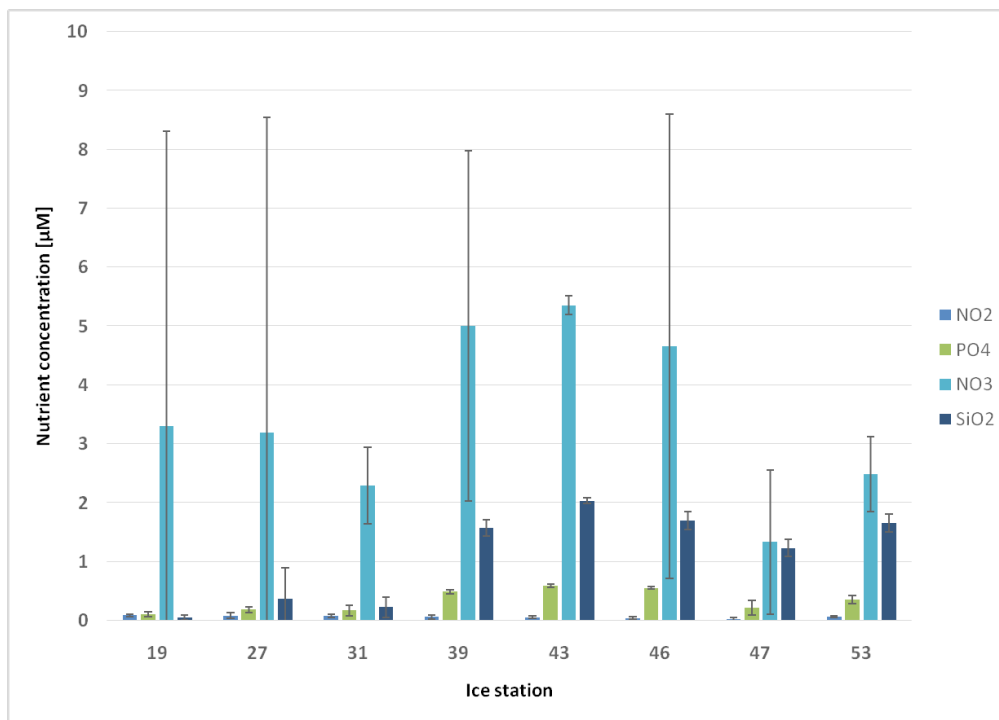


Fig. 9.2.4: Average of nutrient concentration in μM at seven ice stations. Averages are mainly based on raw optical density (ODE) values within two days. Bars indicate error deviation.

Data management

Most molecular data will be obtained through laboratory analyses after the cruise. Samples are stored at the AWI and will be analyzed within 6-36 months. Molecular genetic data generated from samples collected during the expedition will be stored either in the information system PANGAEA at the AWI (<http://www.pangaea.de>), or in public sequence repositories. Nutrient concentration data will be available after processing and publishing by the HZG Geesthacht.

References

- Hallegraeff GM (2010) Ocean Climate Change, Phytoplankton Community Responses, And Harmful Algal Blooms: A Formidable Predictive Challenge *Journal of Phycology*, 46(2), 220-235
- Moestrup O (2004) IOC Taxonomic reference list of toxic algae, In O Moestrup [ed], IOC reference list of toxic algae Intergovernmental Oceanographic Commission of UNESCO
- Okoldkov YB (2005) The Global Distributional Patterns of Toxic, Bloom Dinoflagellates recorded from the Eurasian Arctic, *Harmful Algae*, 4, 351-369
- Taylor JD, Berzano M, Percy L, Lewis J (2013) Evaluation of the MIDTAL Microarray Chip for Monitoring Toxic Microalgae in the Orkney Islands, *UK Environmental Science and Pollution Research*, 20(10), 6765-6777
- Zingone A, Enevoldsen HO (2000) The diversity of harmful algal blooms: a challenge for science and management, *Ocean Coast Management*, 43, 725-748

9.3 Nitrogen cycling and microbial ecology in the Arctic: measurements of dinitrogen fixation rates, characterization of diazotroph assemblages, and *nifH* gene expression

Allison Fong¹

¹AWI

not on board: Susanne Spahic¹, Anya Waite¹

Grant No AWI_PS92_00

Objectives

The process of biological dinitrogen fixation is the conversion of dinitrogen gas to ammonia. Dinitrogen fixation is an energetically expensive process and iron is required in nitrogenase enzyme complex. Additionally, *in vitro*, the nitrogenase enzyme is sensitive to inactivation by oxygen. Classically, biological dinitrogen fixation is believed to be limited to subtropical and tropical regions of the world's oceans, with waters warmer than 25°C and depleted in inorganic nitrogen, such as nitrate. Recent work has shown a greater geographical extent and more diverse *nifH* phylogeny than previously believed, with low, but measureable rates of dinitrogen fixation and recovery of *nifH* genes from polar regions.

Biological nitrogen fixation in aquatic habitats is limited to organisms possessing the *nif* operon. The *nifH* gene is the most common *nif* gene used to identify and quantify the community and expression of nitrogen-fixing organisms. Additionally, dinitrogen fixation rates can be measured by applying a ¹⁵N₂ tracer technique, in which microbial communities are incubated with ¹⁵N₂-enriched seawater.

We plan to use a combination of experiments and techniques to measure dinitrogen fixation rates, characterize the diazotroph community, and measure *nifH* gene expression. Our aim is to broadly sample multiple Arctic environments and link rates of nitrogen fixation to the portion of the microbial assemblages responsible for this process. We will coordinate our efforts with others who are making measurements of ammonia and nitrate uptake rates, so together these rate measurements will provide a comprehensive understanding of nitrogen cycling processes in the Arctic.

Work at sea

Discrete water column samples from 5, the chlorophyll maximum layer, 50, 75, 100, and 200 meters were subsampled from Niskin bottles attached to the CTD-rosette. On average, 24-36 liters were subsampled from each depth for nitrogen fixation rate measurements, particulate carbon and nitrogen (PCPN), and collections of microbial DNA and RNA. Eight incubation experiments with ¹⁵N₂-labeled seawater were performed to measure dinitrogen fixation rates at each of the ice stations. Duplicate nitrogen fixation rate measurement incubations were performed in 4.5 and 2.3 L clear polycarbonate bottles from each depth. Bottles were spiked with ¹⁵N-N₂ gas enriched artificial seawater to a final concentration of ~ 1.1%, and with ¹³C-bicarbonate solution to a final concentration of ~ 10 μmol L⁻¹. The Tremblay group conducted parallel measurements of nitrate and ammonium assimilation. All bottles were shaded with neutral density mesh, and incubated in on-deck incubators plumbed with surface seawater for 24 hours. Initial measurements were collected from 5 and 100 m.

Additionally, 2-4 liters of seawater were in-line size-fractionated (> 10 μm and 0.2 μm) for DNA and RNA collections. Genomic, transcriptomic, and functional gene analysis will be performed on these samples to assess the active diazotroph community and nitrogen fixation rates (Table 9.3.1). Subsamples from the sediment trap array were sampled for DNA. DNA from traps were collected at 6 of the 8 stations. Trap DNA samples were not collected at 2 ice stations.

due to very low biomass. In total, 254 DNA/RNA filters were collected and will be extracted at the AWI onshore laboratory (Table 9.3.2).

Additionally, triplicate 2 mL flow cytometry samples were collected from 10 depths spanning the full water column, but concentrated in the upper 100 meters, in parallel to nutrient and primary production samples. Flow cytometry samples were preserved to a final concentration of 0.2 % PFA. Flow cytometry samples were also collected on the BIO-CTD casts. In total, 124 unique flow cytometry samples were collected on the cruise (Table 9.3.1).

At the 8 sea-ice stations, 10 cm length sections from the top, middle, and bottom of ice cores were collected in triplicate. Ice core sections are stored at -20 C and will be used to test the development of methods of primary production and nitrogen fixation rate measurements. Additionally, cores will be processed for prokaryotic DNA and RNA to characterize the microbial diversity (Bacteria and Archaea). In total 72 ice core sections and 24 snow sampled were collected.

Tab. 9.3.1: PS92 water column sampling

Station	Depths (m)	Micro-bial DNA	Micro-bial RNA	FCM	¹³ C & ¹⁵ N natural abundance	N ₂ fixation rates	¹³ C-derived PP
PS92/19-5	5, 10, 20, 30, 40, 50, 75, 100, 150, 354			X			
PS92/19-8	5, 20, 50, 100, 350	X	X		X	X	
PS92/21-1	5, 10, 20, 50, 100, 200			X			
PS92/24-1	5, 20, 50, 100, 200, 510			X			
PS92/27-3	5, 10, 20, 30, 40, 50, 75, 100, 150, 200			X			
PS92/27-4	5, 15, 50, 75, 100, 200	X	X		X	X	X
PS92/29-1	5, 10, 20, 40, 50, 75, 100, 150, 200, 500, 1000			X			
PS92/31-3	5, 10, 25, 50, 75, 100, 150, 200, 500, 1000			X			
PS92/31-4	5, 25, 50, 75, 100, 200	X	X		X	X	X
PS92/32-5	10, 25, 30, 40, 50, 75, 100, 150, 200, 500, 1000			X			
PS92/32-6	5, 25, 50, 75, 100, (200)	X	X		X	X	X
PS92/36-1	10, 30, 40, 50, 75, 100, 150, 200, 500, 1000			X			
PS92/37-1	45	X	X				
PS92/39-8	10, 35, 40, 50, 75, 100, 150, 200, 500, 1000			X			
PS92/39-11	5, 20, 50, 75, 100, 200	X	X		X	X	X
PS92/43-1	10, 30, 50, 100, 200, 300, 500, 764	X	X				
PS92/43-5	10, 20, 40, 50, 75, 100, 150, 200, 500, 790			X			
PS92/43-6	5, 20, 50, 75, 100, (200)	X	X		X	X	X
PS92/46-2	10, 20, 40, 50, 75, 100, 150, 200, 500, 874			X			
PS92/46-3	5, 20, 50, 75, 100, 200	X	X		X	X	X

9.3 Nitrogen cycling and microbial ecology in the Arctic

Station	Depths (m)	Micro-bial DNA	Micro-bial RNA	FCM	¹³ C & ¹⁵ N natural abundance	N ₂ fixation rates	¹³ C-derived PP
PS92/47-4	10, 15, 40, 50, 75, 100, 150, 200, 500, 1000			X			
PS92/47-6	5, 25, 50, 75, 100, 200	X	X		X	X	X
PS92/47-flow through	Flow through intake	X					
PS92/52-1	10, 20, 40, 50, 75, 100, 150, 200, 500, 1000			X			

Tab. 9.3.1: PS92 sea ice and sediment trap sampling

Station	Depth (m)	Microbial DNA	Microbial RNA	NifH gene	Snow	¹³ C & ¹⁵ N natural abundance
PS92/19	Top 10 cm of core, 10 cm of middle core, bottom 10 cm of core	X	X	X	X	
PS92/19-Traps	30, 40, 60 90					X
PS92/27	Top 10 cm of core, 10 cm of middle core, bottom 10 cm of core	X	X	X	X	
PS92/27-Traps	30, 40, 60, 90, 200	X				X
PS92/31	Top 10 cm of core, 10 cm of middle core, bottom 10 cm of core	X	X	X	X	
PS92/31-Traps	30, 40, 60, 90, 200	X				X
PS92/32	Top 10 cm of core, 10 cm of middle core, bottom 10 cm of core	X	X	X	X	
PS92/32-Traps	30, 40, 60, 90, 200	X				X
PS92/39	Top 10 cm of core, 10 cm of middle core, bottom 10 cm of core	X	X	X	X	
PS92/39-Traps	30, 40, 60, 90, 200					X-no replicates
PS92/43	Top 10 cm of core, 10 cm of middle core, bottom 10 cm of core	X	X	X	X	
PS92/43	30, 40, 60, 90, 200					X-no replicates
PS92/46	Top 10 cm of core, 10 cm of middle core, bottom 10 cm of core	X	X	X	X	

Station	Depth (m)	Microbial DNA	Microbial RNA	NifH gene	Snow	¹³ C & ¹⁵ N natural abundance
PS92/46-Traps	30, 40, 60, 90, 200					X-no replicates
PS92/47	Top 10 cm of core, 10 cm of middle core, bottom 10 cm of core	X	X	X	X	
PS92/47-Traps	30, 40, 60, 90, 200	X				X

Expected results

Sampling is expected to result in measurements of the spatial distributions of nitrogen fixation rates, *nifH* gene expression patterns, and characterizations of microbial assemblages across the study region and within different sampling environments (water column, sea-ice, and sinking particulate matter). A majority of samples will be analysed at the AWI onshore laboratory. Rates, expression patterns, and assemblage composition will be analysed in the context of hydrographic and biogeochemical data.

Data management

Sample analyses will occur at shore-based laboratories. Stable isotope measurements to measure ¹³C and ¹⁵N natural abundances on particulate matter and constrain nitrogen fixation rates will be processed via elemental analyzers and isotope ratio mass spectrometry (EA-IRMS). Processing time of these samples will take from 12 – 16 months for completion and quality control. Upon completion and publication by primary researchers, this data will be available through the information system PANGAEA (<http://www.pangaea.de>) at the World Data Center for Marine Environmental Sciences (WDC-MARE) operated by the Alfred Wegener Institute for Polar and Marine Research, Bremerhaven (AWI) and the MARUM, Bremen.

Nucleic acid sequence data derived from microbial DNA and RNA samples will be archived in the publicly available database, GenBank (<http://www.ncbi.nlm.nih.gov/genbank/>). Processing time of these samples will take from 12 - 30 months for completion. Archived microbial DNA and RNA samples will be stored frozen at the AWI within the Polar Biological Oceanography section and can be made available to other research parties upon request.

All data will be made available to the scientific community through the databases after publication and latest 5 years post-cruise

9.4 Vertical export

Christine Dybwad¹

¹UiT

Not on board: Camilla Svensen¹, Marit Reigstad¹

Grant No AWI_PS92_00

Objectives

The objective of the work is to quantify the vertical export of biogenic matter under the ice at a vertical gradient ranging from 30 to 200 m depth (Reigstad et al 2008). Faecal pellet (FP) production by larger mesozooplankton (i.e. *Calanus* spp.) will be experimentally determined on board. Export is dependent on the available organic material as well as the retention by pelagic consumers. FP production rates will be used as a measure of *Calanus* grazing activity, and by comparing the FP production to the vertical FP export we will obtain an indication of the retention efficiency (Wexels Riser et al 2008).

Subsamples from the sediment traps will be analysed for pigment composition, and also provide material for collaborative projects involving phytoplankton composition and bacterial characterisation focusing on N cycling.

Vertical export will be related to the quality and quantity of the suspended material in the water column <200 m depth, with respect to particulate organic carbon and nitrogen as well as phytoplankton pigments.

Additionally, by interpreting results in light of information from cooperating participants on nutrients and productivity, aspects on the fate of carbon from primary production related to the plankton community and vertical export can be addressed (Reigstad et al 2011).

Work at sea

At all of the ice stations, the samples were collected from the water column suspended profile using the CTD/rosette 8 depths were sampled in a vertical profile of 0-200 m, and filtered for POC, PON, size fractionated chlorophyll *a* (total and >10 µm), and nutrients (Tab. 9.4.1). Additional CTD casts were sampled during transit in order to provide core measurements of POC, PON and size fractionated chlorophyll *a* for the region.

Exported organic material was sampled by deploying KC Denmark double-cylinder sediment traps, without preservatives. The traps were deployed from the ship and anchored to the ice floe at the first 2 ice stations, and deployed through the ice at the remaining 6 ice stations. The sediment trap cylinders were deployed at 5 depths from 30 to 200 m for roughly 24 hours, to catch the daily amount of particles exported under the ice. Upon retrieval, the exported material in the traps were subsampled and filtered or preserved for analysis of POC, PON, size fractionated chlorophyll *a* (total and >10 µm) and faecal pellets (Tab. 9.4.2). Subsamples for bacterial characterizations and phytoplankton were also taken, for collaborative partners.

Bottles prepared for primary production incubation (by MABlais) were deployed on the sediment trap mooring at 8 predefined depths, in order to measure *in-situ* primary production, such as nitrate and ammonium uptake. Finally, at each ice station, *Calanus* were collected using a WP-2 net or a Bongo net (provided by H Flores, Tab. 8.4). Faecal pellet (FP) experiments were subsequently performed on healthy, late stage *Calanus* spp 5 individuals were incubated in water from the chlorophyll maxima for 6 hours, in special double-mesh FP production chambers. The copepods and FP material was preserved for later analysis.

Tab. 9.4.1: Water column sampling during PS92 cruise

Station	Depth [m]	POC/ PON	CHL A	CHL A >10µm	Nutrients
<i>PS92/19-05</i>	10, 20, 30, 40, 50, 75, 100, 150	x	x	x	x
<i>PS92/21-01</i>	5, 20, 50, 100, 192 7	x	x		
<i>PS92/24-01</i>	5, 25, 50, 100, 200, 496*	x	x		
<i>PS92/27-02</i>	10, 20, 30, 40, 50, 75, 100, 200	x	x	x	x
<i>PS92/29-01</i>	10, 20, 50, 100, 200, 500*, 1000*	x	x		
<i>PS92/31-03</i>	10, 25, 30, 40, 50, 75, 100, 200	x	x	x	x
<i>PS92/32-05</i>	10, 25, 30, 40, 50, 75, 100, 200	x	x	x	x
<i>PS92/36-01</i>	10, 30, 50, 100, 200, 500*, 1000*, 1490*	x	x		
<i>PS92/39-08</i>	10, 30, 34, 40, 50, 75, 100, 200, 500*, 1000*	x	x	x	x
<i>PS92/43-05</i>	10, 20, 30, 40, 50, 75, 100, 200, 500*, 780*	x	x	x	x
<i>PS92/46-02</i>	10, 20, 30, 40, 50, 75, 100, 200, 500*, 870*	x	x	x	x
<i>PS92/47-04</i>	10, 15, 30, 40, 50, 75, 100, 200, 500*, 1000*	x	x	x	x
<i>PS92/47-19</i>	63 6	x			
<i>PS92/52-01</i>	10, 20, 30, 50, 100, 200, 500*, 1000*	x	x		
<i>PS92/56-03</i>	10, 17, 30, 50, 100, 200	x	x		

*Note: For all depths >200m, Chl a (total and >10µm) was not sampled

Tab. 9.4.2: Sediment trap sampling during PS92 cruise

Station	Depth [m]	POC/ PON	CHL A	CHL A >10µm	Faecal Pellets	Phyto- plankton**
<i>PS92/19</i>	30, 40, 60, 90	x	x	x	x	x
<i>PS92/27</i>	30, 40, 60, 90, 200	x	x	x	x	x
<i>PS92/31</i>	30, 40, 60, 90, 200	x	x	x	x	x
<i>PS92/32</i>	30, 40, 60, 90, 200	x	x	x	x	x
<i>PS92/39</i>	30, 40, 60, 90, 200	x	x	x	x	x
<i>PS92/43</i>	30, 40, 60, 90, 200	x	x	x	x	x

9.4 Vertical export

Station	Depth [m]	POC/ PON	CHL A	CHL A >10µm	Faecal Pellets	Phyto- plankton**
<i>PS92/46</i>	30, 40, 60, 90, 200	x	x	x	x	x
<i>PS92/47</i>	30, 40, 60, 90, 200	x	x	x	x	x

**Note: samples for collaborative use

Preliminary results

A total of 14 suspended profiles were sampled from the CTD, including the 8 ice stations. Along with the 8 exported profiles collected with the sediment traps and the 8 FP production experiments at the ice stations, a quantification of the vertical carbon export the change in export rates with depth and an estimate of the fraction contributed by mesozooplankton faecal pellets will be generated. All analysis will be performed post-cruise in home laboratories.

Data management

The data will be analysed at UiT after the cruise, and used for student thesis (MSci) and subsequent publication. The data will be interconnected with other partners on board to utilise the synergy of relevant information available Metadata can be made available after the cruise. Data of biogeochemistry (POC, Chl a) from water column and sediment trap will be made available at a protected site, in the PANGAEA database, within 24 months. The data will be made public after publication, maximum 5 years, according to the data-handling plan.

References

- Reigstad M, Wexels Riser C, Wassmann P, Ratkova T (2008) Vertical export of particulate organic carbon: Attenuation, composition and loss rates in the northern Barents Sea Deep Sea Research Part II: Topical Studies in Oceanography, 55, 2308-2319
- Reigstad M, Carroll J, Slagstad D, Ellingsen I, Wassmann P (2011) Intra-regional comparison of productivity, carbon flux and ecosystem composition within the northern Barents Sea Progress in Oceanography, 90, 33-46
- Wexels Riser C, Wassmann P, Reigstad M, Seuthe L (2008) Vertical flux regulation by zooplankton in the northern Barents Sea during Arctic spring Deep Sea Research Part II: Topical Studies in Oceanography, 55, 2320-2329

9.5 Watercolumn biogeochemistry

Sarah Zwicker^{1,2}, Ilka Peeken¹

¹AWI

²HS-BRV

Grant No AWI_PS92_00

Objectives

Acknowledging the sensitivity of the Arctic to environmental change, the project PEBCAO (Plankton Ecology and Biogeochemistry in a Changing Arctic Ocean) is dedicated to study plankton communities and microbial processes relevant for biogeochemical cycles of in the Arctic Ocean. It is expected that the Arctic is facing rising temperatures, a decline of sea ice and/or a decrease in seawater pH in the future. In order to understand and track potential consequences for the pelagic ecosystem in the Arctic Ocean both long-term field observations of Arctic plankton species are needed to gain knowledge about the biological feedback potential of pelagic communities in the future Arctic Ocean. The current data set will improve the long term observation in the Fram Strait and the Central Arctic.

Work at sea

Sea water was sampled of 6-8 depths by a CTD/rosette sampler at all ice and biogeochemistry stations (Tab 9.5.1). Samples for HPLC were filtered on 25 mm GF/F filters (Whatman) and immediately frozen in liquid nitrogen and thereafter stored at -80°C. Samples for bPSi were filtered on cellulose nitrate filters (0,45 µm) and stored at -20°C. For Utermöhl samples 200 ml of sea water were placed in brown glas bottles and preserved with Formaldehyde (final solution 2 %).

Tab. 9.5.1: Sample list from biogeochemistry CTD cast for pigments (HPLC), particulate biogenic silicate (bPSi) and Utermöhl samples (UT)

Station	Depth [m]	HPLC	bPSi	UT
PS92/19-05	2, 5, 10, Chl Max 20, 30, 40, 50, 100	x	x	x
PS92/21-01	2, 10, Chl Max 20, 30, 50, 100	x	x	x
PS92/24-01	2, 10, Chl Max 25, 30, 50, 100	x	x	x
PS92/27-02	2, 10, Chl Max 20, 30, 40, 50, 100, 200	x	x	x
PS92/29-01	2, Chl Max 10, 20, 30, 50, 100	x	x	x
PS92/31-03	5, 10, Chl Max 25, 30, 40, 50, 100, 200	x	x	x
PS92/32-05	2, 5, 10, Chl Max 25, 30, 40, 50, 100	x	x	x
PS92/36-01	2, 10, 20, Chl Max 30, 50, 100	x	x	x
PS92/39-08	2, 5, 10, Chl Max 30, 40, 50, 100	x	x	x
PS92/43-05	2, 5, 10, Chl Max 20, 30, 40, 50, 100	x	x	x
PS92/46-02	2, 5, 10, Chl Max 20, 30, 40, 50, 100	x	x	x
PS92/47-04	2, 5, Chl Max 15, 10, 30, 40, 50, Chl Max II 63 5, 100	x	x	x
PS92/52-01	2, 10, Chl Max 20, 30, 50, 100	x	x	x
PS92/56-03	2, 10, Chl Max 17, 30, 50, 100	x	x	x

Preliminary (expected) results

The samples will be integrated into the long term data set of the PEBCAO group to address changes in the phytoplankton community and biogeochemistry in the changing Arctic. Pigment data will further be used for the validation of satellite data. In collaboration with the Green Edge group these data serve for modelling purposes.

Data management

Samples

Except for the microscopy all samples taken during the cruise will be processed within one year after the cruise. Leftovers of the microscopic samples and the DNA will be stored at the Polar Biological Oceanography at the AWI for approximately 10 years.

Data

As soon as the data are available they will be accessible to other cruise participants and research partners on request. Except for the microscopy the entire data set will be submitted to PANGAEA within 2-3 years.

9.6 Benthos ecology

Monika Kędra¹, Nathalie Morata², Maeve McGovern²

not on board: Katarzyna Grzelak¹, Paul Renaud²,
Emma Michaud³

¹IOPAN

²APN

³LEMAR

Grant No AWI_PS92_00

Objectives

Arctic shelf seas are often characterized by tight benthic-pelagic coupling and the total and proportional annual primary production of ice algae and phytoplankton will likely change with shifts in the sea ice extent, thickness and duration. This will likely have critical consequences for the benthic populations in the Arctic Ocean. Thus, the main objective was to investigate how benthic communities structure and function change spatially as a function of environmental conditions and food inputs during the spring bloom, along the sea ice and depth gradient.

Work at sea

Box corer sampling was conducted at 9 stations. At station *PS92/43* Box coring was repeated at the end of sea ice station. In total 17 box corer samples were taken: 2 box corers per station except from stations *PS92/39* and *PS92/46* where only 1 box corer was taken. First box corer sample was used for respiration and bioturbation measurements. In order to characterize the inputs of fresh phytodetritus to the seafloor, at each station, except from station *PS92/39* where no core sampling was conducted, 2 or 3 replicates sediment cores were collected and sliced every 0.5 cm until 2 cm, and every 1 cm until 10 cm for "initial conditions". Samples were frozen on board, and analyses of pigments, diatom frustules, total organic matter, carbon and nitrogen contents, and granulometry, will be carried out back at the laboratory. In order to characterize the activities from the overall community (including macro-, meio- and micro-

fauna), 3 to 5 sediment cores were incubated for 48 to 72h in order to measure respiration and nutrient fluxes (in collaboration with Christian März) of the overall community as indicator of metabolic activities (Tab. 9.6.1).

Two subsamples from second boxcorer were taken for studies of macrofauna community structure including species identification, abundances, biomass, function and production. If only one boxcorer sample was taken, macrofauna was either sieved from single subsample or from sediment corer collected for respiration measurements. Four replicates sediment cores were collected and sliced from surface to 1 cm, 1 cm to 2 cm, and from 2 cm to 5 cm. Three replicates were taken for the community analysis and one (surface to 2 cm) for genetic studies. All fauna samples for taxonomic identification were preserved in 10 % formaldehyde solution and samples for genetic studies were preserved in 96 % ethanol. Samples will be analysed in the laboratory at the later stage (Tab. 9.6.1).

Separately, animal tissues of benthic organisms were taken for the analysis of food web structure based on stable isotopes composition of organic carbon ($\delta^{13}\text{C}$) and nitrogen ($\delta^{15}\text{N}$). Animals were picked up from the remaining sediment, identified on-board and frozen. To determine food sources, the origin of particulate organic matter (POM) was assessed with use of $\delta^{13}\text{C}$ analyses. For that water collected at the chlorophyll maximum and near bottom was filtered and filters were frozen, and later dried (Tab. 9.5.2). Additionally, to determine the organic matter transformation in the water column, water samples collected from sediment trap (30 m, 40 m, 60 m, 90 m, and 200 m) were filtered and filters were frozen, and later dried (in collaboration with Allison Fong/Christine Dybwad/Marit Reigstad. Tab. 9.5.3)

Preliminary (expected) results

Benthic communities' species composition, trophic relations and functioning (including respiration rates), was expected to change along the depth gradient. Other parameters, like amount and source of food are likely important factors structuring benthic communities functioning.

Preliminary results suggest that despite the expectation to have very low respiration at the deepest stations, respiration rates were higher than expected, in particular at station PS92/47, where an important ice algae bloom seemed to be occurring, reaching the seafloor even at more than 2000 m.

Data management

Data will be published in peer reviewed journals and presented on international conferences. After the data are quality accessed by the P I they will be made available for all project partners and in the indicated data bases with a pass word protection to allow the own right of publication for the P I s. Data will subsequently be made available to the scientific community through the data bases after publication and finalization of PhD theses: after that, data will be submitted to PANGAEA, and will be open for external use.

Tab. 9 6 1: Benthic sampling effort during PS92 cruise

Station	Depth [m]	Number of meio-fauna sub-samples	Number of macrofauna subsamples	Samples for sediment characteristics	Number of sediment cores sliced for initial conditions	Number of sediment cores incubated for respiration	Number of sediment cores incubated for bioturbation
PS92/19-20	448	4	2	x	3	5	5
PS92/20-4	172	4	2	x	3	5	5
PS92/27-15	832	4	2	x	3	5	5
PS92/28-2	927	4		x		5	5
PS92/31-17	1656	4		x	3	5	5
PS92/32-2	309	4	2	x	2	4	
PS92/39-4	1499	4	2	x			
PS92/43-2	790	4	1	x			
PS92/43-21	792	4	2	x	3	4	
PS92/46-16	867	4	1	x	2	4	
PS92/47-21	2129	4	2	x	3	4	

Tab. 9.6.2: Water column sampling effort during PS92 cruise; first water depth for chl max is given, next bottom water depth; * - no chl max; if one depth is given – chl max

Station	Depth sampled [m]	POM
PS92/0019-5	20.4; 354.8	x
PS92/0019-15	15.2; 412	x
PS92/0020-1	25.5; 163	x
PS92/0027-2	20; 760	x
PS92/0027-13	23	x
PS92/0028-1	15	x
PS92/0031-6	25	x
PS92/0031-12	25; 1651	x
PS92/0032-1	25; 301	x
PS92/0037-1	30; 2220	x
PS92/0039-9	40; 1552	x
PS92/0040-4	40; 781	x
PS92/0043-1	30	x
PS92/0046-14	30*; 871	x
PS92/0047-19	10*; 2157	x

Tab. 9.6.3: Sediment trap sampling effort during PS92 cruise – samples collected for stable isotopes of carbon and nitrogen analysis in POM

Station	Depth sampled [m]	POM
PS92/19	30; 40; 60; 90	x
PS92/27	30; 40; 60; 90; 200	x
PS92/31	30; 40; 60; 90; 200	x
PS92/32	30; 40; 60; 90; 200	x
PS92/39	30; 40; 60; 90; 200	x
PS92/43	30; 40; 60; 90; 200	x
PS92/46	30; 40; 60; 90; 200	x
PS92/47	30; 40; 60; 90; 200	x

10. GEOLOGY AND PALEOCEANOGRAPHY

Matt O'Regan¹, Jens Matthiessen², Christian März³, Michael Nairn⁴, Clara Stolle², Chao Weng-Si⁵, Kirstin Werner⁶, Jutta Wollenburg², Eunmi Park²,
not on board: Kirsten Fahl², Matthias Forwick⁷, Kate Hendry⁸, Caroline Lear⁴, Ludvig Löwemark⁵, Juliane Müller², Rüdiger Stein²

¹SUn
²AWI
³NUn
⁴CUn
⁵NTU
⁶BPCRC
⁷UiT
⁸UBr

Grant No AWI_PS92_00

General Objectives

Arctic perennial sea-ice cover is an important and unique component of the global climate system. Reconstructions of sea ice and how it interacted with changing ocean and atmospheric circulation patterns in the past are needed to evaluate modern changes in the Arctic marine system. Sedimentary records collected during previous expeditions provide a few key sedimentary records that underpin our understanding of late Quaternary paleoceanographic conditions in the Eurasian Arctic. However, advances during the past decade(s) in the analytical techniques and climate proxy indicators (proxies) used to reconstruct sea ice and water mass properties from marine sediment archives provide an opportunity to significantly improve these reconstructions. The geology program on TRANSIZ was developed to calibrate and test different sedimentary proxies for sea ice and ocean circulation; establish how they are preserved in the sedimentary records; and use the results to improve Arctic paleoceanographic and paleoenvironmental reconstructions during the last one to two glacial cycles.

Of particular interest is the evaluation of the spatial variation in proxies used in Arctic paleoceanography, including how surface ocean and sedimentary signals (co-)vary a) laterally, across the changing ice margin and in the underlying sediments, and b) vertically, within different water masses that intersect the continental slope.

The objectives of the expedition can be subdivided into 2 broad themes;

1. Proxy calibration and validation
2. Late Quaternary paleoceanography (0-200 kyrs)

Specific aims of the original proposal were:

- Improve paleo-reconstructions by calibrating, comparing and validating established and emerging proxies for sea ice and water mass indicators/properties
- Decipher the history/properties of Atlantic Water (AW) inflow during the last 2 glacial cycles (200 kyr), specifically during periods of potentially reduced sea ice extent in the central Arctic Ocean

- Reconstruct changes in vertical stratification in water masses across the last 2 glacial cycles and its relation to changes in sea ice extent
- Investigate the response of planktonic and benthic ecosystems to changes in AW inflow and sea ice during interglacial and interstadial periods in the late Quaternary

In addition to these aims, *J Wollenburg* (AWI) will use surface sediments collected during TRANSSIZ to culture benthic foraminifera in newly developed high-pressure aquaria (under in-situ pressures and differing temperature, pH and water carbonate chemistry) to establish the first species-specific trace metal calibration curves for the Arctic Ocean Core top analyses will verify the experimental results.

Overview of work at sea

The geology component of the TRANSSIZ proposal was built around a shelf to basin transect along 30°E, crossing the position of sediment core PS2138. The initial plan was to re-occupy this site and acquire a kastenlot core that could be used for paleoenvironmental reconstructions during the last 2 glacial cycles. Impenetrable ice conditions during the expedition prevented us from reaching the planned transect at 30°E. Instead we worked mainly east of 20°E, and were unable to complete a downslope coring transect along the path of inflowing Atlantic Water. However, a kastenlot core was acquired in close proximity to another well-studied sediment core from the Yermak Plateau (PS1533; Nowaczyk et al., 1994; Spielhagen et al., 2004), that should allow detailed paleoceanographic reconstructions for the last 2 glacial cycles.

At each of the ~36 hour ice stations, the multicore, equipped with a live broadcasting video system (TV-MUC), was deployed for geological investigations of surface sediments. Sediments obtained by the TV-MUC were specifically sampled for studies related to proxy calibration and validation. At some key locations, and where Parasound data indicated sufficient accumulations of acoustically stratified sediments, one or more of the Giant Box Corer (GKG), Gravity Corer (SL) and Kastenlot Corer (KAL) were deployed to acquire longer time series for paleoceanographic work (Fig. 10.1). A separate series of 3 multicores were deployed on the western side of the Yermak Plateau to collect sediments for the culturing experiments of *J Wollenburg* (AWI).

In addition to the multicores, plankton net samples, sea ice samples, and water column samples were collected at all of the ice stations. On 2 occasions, special excursions were made (1 by helicopter, and 1 by zodiac) to sample dirty ice floes.

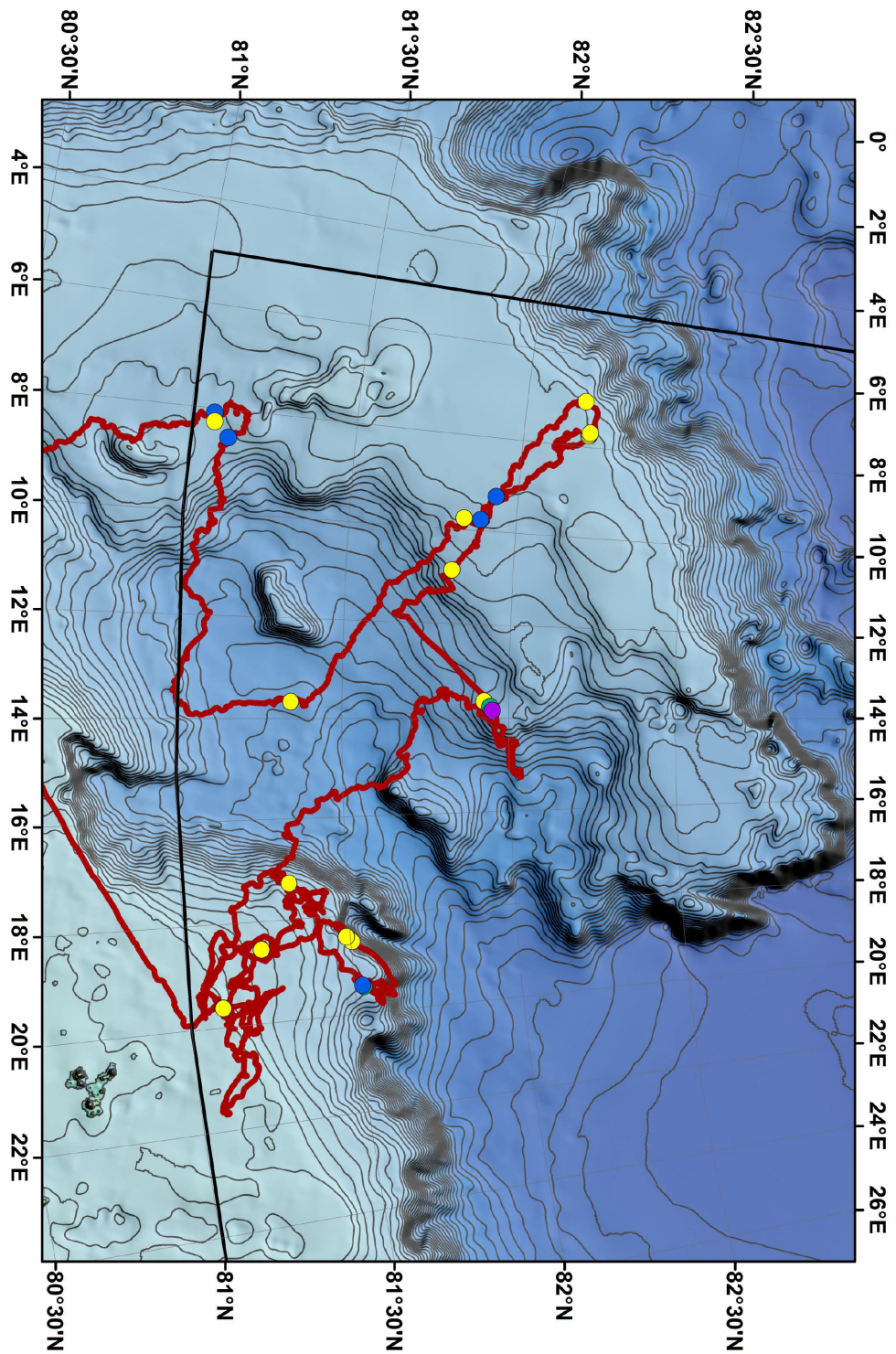


Fig. 10.1: Ship track and geology station map for PS92, TRANSSIZ. Symbols indicate location of gravity cores (blue dots), kastenlot core (purple dot), multi cores (yellow dots) and box cores (green dots).

10.1 Parasound and Hydrosweep

Clara Stolle and Jens Matthiessen AWI

Objectives

In the research area of PS92, hydroacoustic surveys were conducted during limited time periods with the ATLAS Hydrographic Hydrosweep DS3 multibeam echosounder and sediment echosounder Parasound to obtain information on the sea floor topography and the sub-bottom acoustic stratigraphy. Since work with the SIMRAD echosounder EK60 had priority during the expedition, both the Hydrosweep and Parasound were only used to enable identification of coring sites based on the bathymetry and sub-bottom acoustic pattern and reflection amplitude.

Work at sea

Technical specifications and settings used during the expedition were extensively described in the expedition report of PS87 in 2014. Data quality was extremely affected by heavy sea ice conditions in the research area, while the survey in mostly open waters off northwestern Svalbard yielded a data set of high quality. The Hydrosweep system was partly run in parallel with the EK 60 echosounder using the Kongsberg K-Sync synchronization unit to obtain at least basic bathymetric data in regions that have not been systematically surveyed in the past decades.

Since the upgrade of the Hydrosweep system to DS3 resulted in a substantial increase in the acquisition of data (beam width 4 to 5 times of water depth) a full 24/7 watch system is required to fully process the data, in particular when working in ice covered regions. Because of these time limitations, the collected bathymetric data was not systematically cleaned and processed shipboard. Initial analysis was mainly restricted to visual inspection of data to obtain information on coring sites and for track planning.

The Parasound system was operated less extensively than Hydrosweep to allow better acquisition of EK60 data, and was mainly restricted to areas of potential coring locations.

Preliminary results

During PS92, an area of about 4000 km² was mapped Fig. 10.2 shows an overview of the acquired multibeam data coverage.

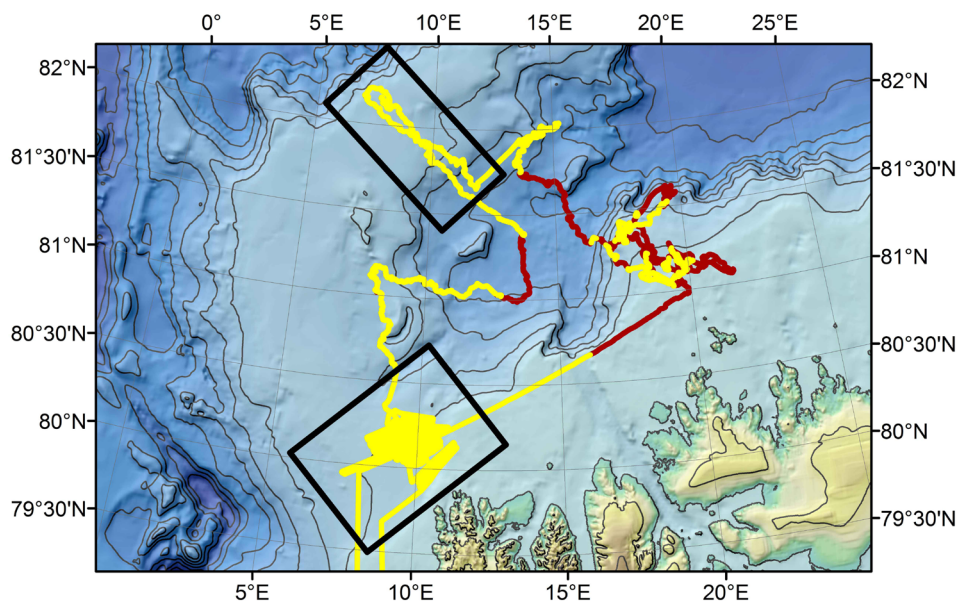


Fig. 10.2: Overview map of the multibeam data coverage for PS92 Yellow lines indicate regions where Hydrosweep data was collected

Outside the research area, an extensive bathymetric and sediment echosounding survey was performed on the southern Yermak Plateau to study the depositional environment and history during the middle to late Pleistocene. The survey was conducted under ice-free conditions, with a total duration of 63 hours (Fig. 10.3, Tab. 10.1).

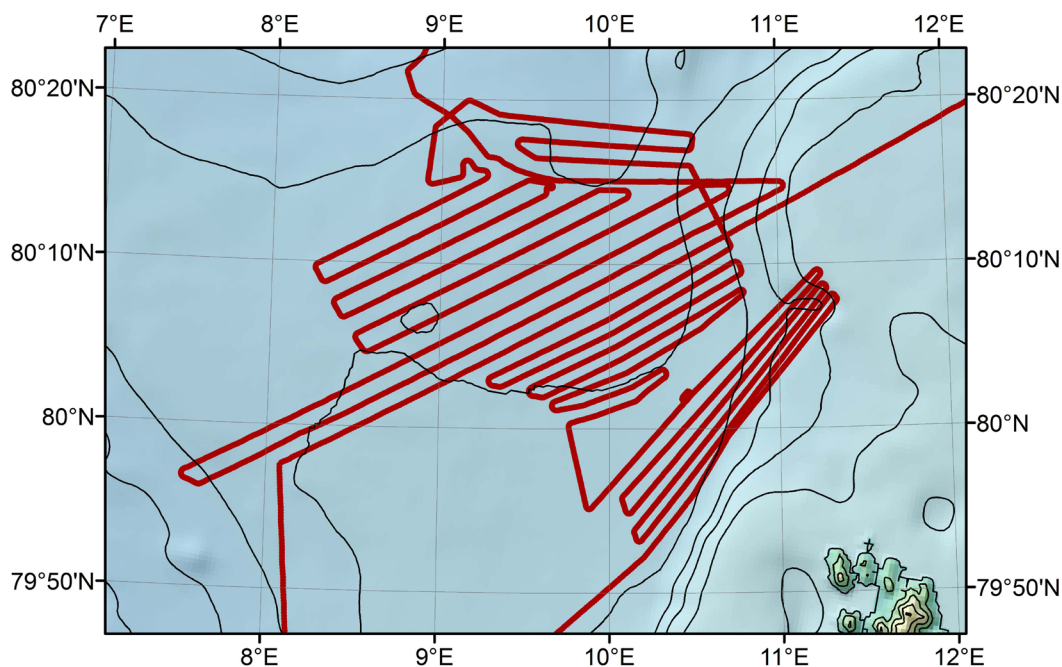


Fig. 10.3: Bathymetric survey PS92/059

Tab. 10.1: Bathymetric survey times and coverage

Station PS92/059		
Start Survey Date and Time [UTC]	24.06.2015	13:00
End Survey Date and Time [UTC]	27.06.2015	04:30
Duration [h]	63.5	
Coverage [km ²]	2200	

Data management

The acquired raw data will be stored in the long-term archive PANGAEA and will be available on request. The processed data will be archived in the bathymetric archive of the AWI bathymetry group. Furthermore, the data will contribute to global datasets such as IBCAO (International Bathymetric Chart of the Arctic Ocean) and GEBCO (General Bathymetric Chart of the Oceans).

10.2 Sediment coring

Matt O'Regan¹, ¹SUn
 Jens Matthiessen² ²AWI

Objectives

Sediment cores were collected for 2 objectives;

- 1 Paleoceanographic proxy calibration and validation using surface sediments,
- 2 Paleoenvironmental reconstructions during the last 2 glacial cycles.

Multicores were collected at each of the ice stations (Fig. 10.1) to reach objective 1, while gravity cores and a kastenlot core, aimed to meet objective 2, were acquired when Parasound data indicated a promising sediment drape, and ice conditions and ship operations allowed time for deployment.

Work at sea

A total of 5 gravity cores, 1 kastenlot core, and 13 Multicores were collected during TRANSSIZ (Fig. 10.1; Tab. 10.2, Tab. 10.3).

Tab. 10.2: Summary of coring stations during PS92

Date	Time (UTC)	Station	Gear	Lat.	Lon.	Depth (m)
29/05/2015	13:35:00	PS92/0019-19	TVMUC	81° 13.79' N	18° 33.04' E	481
01/06/2015	06:58:00	PS92/0027-14	TVMUC	81° 19.55' N	17° 16.87' E	795
02/06/2015	10:43:00	PS92/0028-2	BC	81° 31.71' N	19° 27.39' E	940
02/06/2015	12:00:00	PS92/0028-3	GC	81° 31.45' N	19° 25.91' E	933
04/06/2015	10:30:00	PS92/0031-13	TVMUC	81° 30.20' N	18° 31.72' E	1852
04/06/2015	12:38:00	PS92/0031-14	TVMUC	81° 29.27' N	18° 25.56' E	1829
08/06/2015	06:15:00	PS92/0032-15	TVMUC	81° 5.98' N	19° 36.95' E	219
08/06/2015	07:18:00	PS92/0032-16	TVMUC	81° 6.01' N	19° 37.50' E	220
11/06/2015	05:44:00	PS92/0039-2	KAL	81° 56.99' N	13° 49.70' E	1464
11/06/2015	07:18:00	PS92/0039-3	BC	81° 56.61' N	13° 44.72' E	1493
11/06/2015	11:00:00	PS92/0039-5	TVMUC	81° 55.50' N	13° 37.98' E	1523
13/06/2015	11:55:00	PS92/0040-1	TVMUC	81° 49.04' N	10° 52.06' E	1158
14/06/2015	19:12:00	PS92/0042-1	TVMUC	82° 11.67' N	7° 45.11' E	781
14/06/2015	20:25:00	PS92/0042-2	TVMUC	82° 11.76' N	7° 43.19' E	792
14/06/2015	21:40:00	PS92/0042-3	TVMUC	82° 11.85' N	7° 41.12' E	802
16/06/2015	10:53:00	PS92/0043-20	TVMUC	82° 10.45' N	7° 0.53' E	817
17/06/2015	09:32:00	PS92/0044-3	GC	81° 56.02' N	9° 15.14' E	800
17/06/2015	14:04:00	PS92/0045-2	GC	81° 53.60' N	9° 46.13' E	915
18/06/2015	17:24:00	PS92/0046-15	TVMUC	81° 50.62' N	9° 45.48' E	886
20/06/2015	16:07:00	PS92/0047-20	TVMUC	81° 20.68' N	13° 39.94' E	2175
22/06/2015	14:31:00	PS92/0054-1	GC	81° 7.38' N	8° 27.97' E	1145
23/06/2015	10:58:00	PS92/0056-1	GC	81° 1.19' N	8° 14.27' E	855
23/06/2015	15:45:00	PS92/0056-5	TVMUC	81° 0.94' N	8° 17.05' E	854

Tab. 10.3: Curated section lengths for the gravity cores and the kastenlot core

Core	Type	Section	Top (cmbsf)	Base (cmbsf)
PS92/0028-3	GC	1	0	28
		2	28	128
		3	128	228
		4	228	328
		5	328	428
PS92/0039-2	KAL	N/A	0	860
PS92/0044-3	GC	1	0	58.5
		2	58.5	159
		3	159	258
		4	258	357.5
		5	357.5	458
PS92/0045-2	GC	1	0	39
		2	39	120.5
		3	120.5	220
		4	220	319.5
		5	319.5	419.5
		6	419.5	519.5
PS92/0054-1	GC	1	0	21.5
		2	21.5	114.5
		3	114.5	214.5
		4	214.5	314.5
		5	314.5	414.5
		CC		
PS92/0056-1	GC	1	0	58
		2	58	158
		3	158	258
		4	258	359
		5	359	459
		CC	459	477

Multicores were collected at each of the ice stations. The rationale for the remaining cores is given below.

PS92/28-03-GC: Collected from 933 mbsl, on a relatively flat section of the continental shelf, before a steep slope extends down into the Sophia Basin. Here the Parasound data revealed the first thickening of a sediment drape located below the core of Atlantic Water. The intention was to continue with additional cores downslope to generate a depth transect. Ice conditions prevented us from acquiring additional cores. A box core (PS92/28-02) was also collected to acquire a more complete modern and Holocene sequence.

PS92/39-2-KC: Collected from 1464 mbsl, the site was selected on-route to the location of core PS-1533, on the eastern flank of the Yermak Plateau (Fig. 10.1). Tough ice conditions, and generally poor acoustic stratification of sediments nearing site PS1533, prompted us to turn back and core at the selected location. A box core (PS92/39-03) was also collected to acquire a more complete modern and Holocene sequence.

PS92/0044-3-GC, PS92/0045-2-GC: The location for these gravity cores were selected from Parasound data collected after leaving coring station PS92/39-2, and enroute to the western flank of the Yermak Plateau. PS92/45-2 (915 mbsl) targeted a similar acoustically stratified drape as PS92/39-2. PS92/0044-3 (800 mbsl) was selected because of the thin sedimentary

10.2 Sediment coring

drape that lay at this site (and imaged across the Yermak Plateau), which likely sits on top of a glacially scoured surface. The intention was, through correlation to PS92/0045-2, to date the erosional unconformity that appears to be of a regional nature.

PS92/0054-1-GC: This core was collected on the way to the Sverdrup Bank region of the Yermak Plateau. Having been prevented from reaching the western slope of the Yermak Plateau, where sediments purportedly thicken below 900-1000 mbsl, the Sverdrup Bank was our last attempt to recover current influenced sediments (drift deposits) that may capture paleoenvironmental changes during the last 2 glacial cycles. This core penetrated a region where the sedimentary drape thinned, perhaps because of current winnowing. The intention was to complement it with core(s) from regions of thickened sediments after performing an overnight Parasound and Bathymetric survey. However, progress through the ice was very slow, and in the morning all operations were cancelled, and the ship headed towards more open water areas. Drift sediments were therefore not recovered.

PS92/0056-1-GC: Prior to leaving the research permissions area (Fig. 10.1) a final ice station was performed. This core was simply collected opportunistically, and was not positioned in a strategic position.

Preliminary results

Sampling of the multicores was performed on the ship immediately upon recovery. After water samples were collected from the top of the multicores, the 8 tubes were sampled for pore water chemistry, benthic and planktonic foraminifera, organic and inorganic geochemistry, and an archive core that was to be stored at AWI (Tab. 10.4).

Tab. 10.4: Sampling outline for the multicores

#Tubes	Sample	Contact Person	Sampling Interval	Storage
1	Rhizoms	März/Nairn	0-End of Core	Vials
	Bulk Org Matter	März	0-5 or 10 cm	Plastic Bags
3	Benthic Foraminifers	Wollenburg/Nairn	0-End of Core	Kautex 1000ml/500 ml
	Organic Geochemistry	Park	0-End of Core	Glas Petri Dishes
1	Planktonic Foraminifers	Werner	0-End of Core	Nasco Bags
1	In Geochemistry (Sedimentology)	März	0-End of Core	Plastic Bags
1	Archive/ Palynology	AWI/ Matthiessen	0-EOC/ 0 10cc	Nasco Bags/ Kautex 100ml

The gravity cores were split onboard. X-ray slabs were taken from each core, and were sent back to AWI for storage and analysis. They will be used for sedimentological descriptions and available for post cruise studies on bioturbation and trace fossils (*L Löwemark*). Pore waters were extracted from all the gravity cores (*see inorganic geochemistry section*). Once opened, ~20 cc samples were taken at a downcore resolution of 25 cm for geochemical characterization (*C März*). An initial assessment of foraminifera bearing horizons in cores PS92/28-03-GC and PS92/39-02-KC was conducted by *J Wollenburg* (Tab. 10.5, 10.6.)

Core PS92/28-03-GC was sampled continuously using paleomagnetic cubes with dimensions of 2x2x2 cm (*M O'Regan*). U-channels were taken from Cores PS92/0044-3, PS92/0045-2 and PS92/0054-1 for shorebased paleomagnetic studies (*M O'Regan*).

The kastenlot core (PS92/39-02-KC) was sampled in 4 series. These were;

1. Continuous sampling with paleomagnetic cubes (*M O'Regan*) and x-ray slabs
2. 2 sets of 100x8 plastic boxes; 1 for MSCS core logging (shipboard) and, and 1 for colour

scanning and high-resolution magnetic susceptibility measurements (shorebased at AWI)

3. 1 set of 100x10 plastic boxes for organic geochemical work (*R Stein*)
4. 2 sets of 100x15 plastic boxes
5. Bag samples were collected from the remainder of the kastenlot core at a resolution of 5 cm in the upper 2 m, and then 10 cm for the remainder of the core

Tab. 10.5: PS92/28-3 Initial foram abundance inventories A=abundant, R=rare, Ab=absent .

Depth (cmbsf)	Planktonic forams			Calcareous benthic forams			Agg benthic forams			BF Remarks	
	A	R	Ab	A	R	Ab	A	R	Ab		
20	X			X					X	<i>P bulloides</i>	
75		X				X		X			
103		X			X				X		
220			X			X			X		
270		X				X			X		
330		X				X			X		
335			X			X			X		
340			X			X			X		
350			X			X			X		
370		X			X				X		
375		X			X				X		
400		X			X				X		<i>B marginata</i>
404			X		X				X		
415			X		X				X	<i>M zaandami</i>	
420			X			X			X		

Tab. 10.6: PS92/39-2 Initial foram abundance inventories A=abundant, R=rare, Ab=absent, BF Remains = benthic foram fragments

Depth (cmbsf)	Planktonic forams			Calcareous benthic forams			Agg benthic forams			BF Remarks
	A	R	Ab	A	R	Ab	A	R	Ab	
14-16	X			X			X			
19-21		X			X		X			
24-26		X			X		X			
32-34		X			X		X			
37-39		X			X		X			
42-44		X			X		X			
47-49		X			X		X			
52-54		X			X		X			
62-64			X			X	X			
67-69			X			X	X			
72-74			X			X	X			
77-79			X			X			X	
82-84									X	
87-89	X			X					X	
107-109	X			X					X	

10.2 Sediment coring

Depth (cmbstf)	Planktonic forams			Calcareous benthic forams			Agg benthic forams			BF Remarks
	A	R	Ab	A	R	Ab	A	R	Ab	
127-129	X			X					X	
142-144	X			X					X	
147-149	X			X					X	
157-159		X			X				X	
167-169		X				X	X			
187-189		X			X				X	
207-209	X			X					X	
227-229	X			X					X	
247-249			X			X			X	
257-259			X			X			X	
267-269			X			X			X	
297-299	XXX			XX					X	N labradorica
327-329			X			X			X	
357-359	X			X					X	
387-389	XX			X					X	P bulloides
417-419		X				X			X	
447-449			X			X			X	
477-479			X			X			X	
507-509			X			X			X	
537-539		X				X			X	
547-549			X			X			X	
557-559			X			X			X	
567-569		X			X				X	
577-579	XXXXX			XXX					X	Phytod spp
587-589			X			X			X	
621-623			X			X			X	
624-626			X			X			X	
627-629			X			X			X	
631-633	XX				X				X	B aculeata
634-636	XXXXX			XX					x	C neat , O ten
638-640	XX			XX					x	C neat
657-659	XX			XX					x	subpol PF
687-689	XX			XX					X	
717-719	XXXXX			XXXX					x	CT,OT,ELP
747-749	X			X					X	
777-779	X			X					X	CT,OT
807-809	X			X					X	CT,OT
837-839	X			X					X	CT,OT

Data management

Working and archive halves of all sediment cores will be returned and stored at AWI. A post-cruise sampling party is anticipated to bring together shore-based and shipboard participants of the Geology and Paleoceanography team to distribute some of the shipboard multicore samples, and further sample the gravity and kastenlot cores.

10.3 Multi-sensor core logging

Matt O'Regan SUn

Objectives

Shipboard core logging was performed for rapid and detailed quantification of sediment physical properties. The data allows for an evaluation of lithologic variations within and between cores, and provides a tool for correlating acquired cores to other dated records from the region.

Work at sea

A standard MSCL track (GEOTEK Ltd , UK, Ser No 25) was used to measure temperature, core diameter, gamma-ray attenuation, and magnetic susceptibility. The principle of logging cores is described in more detail in the GEOTEK manual "Multi-Sensor Core Logging", which can be downloaded from the web (<http://www.geotek.co.uk>). The MSCL was configured in the horizontal position, and the gravity cores were logged unsplit .

Compressional wave velocity measurements were attempted on the first gravity core (PS92/28-03), but a suitable gate and delay time could not be found using the oscilloscope P-wave measurements were not made on subsequent cores. The last gravity core was not logged on the MSCL due to a problem with the stepper motor that developed in the last days of the cruise. Data can be acquired on shore using a split core MSCL system Acquisition settings for all logged cores are found in Tab. 10.7.

Tab. 10.7: Acquisition settings on the MSCL.

Core	Measurement Resolution	Gamma Dens. (count time)	Gamma Dens. (Collimator)	Mag. Susc. (Sensitivity)
PS92/0028-3	0.5 cm	10 seconds	2.5 mm	x0.1
PS92/0039-2	0.5 cm	10 seconds	2.5 mm	x0.1
PS92/0044-3	0.5 cm	10 seconds	5 mm	x0.1
PS92/0045-2	1 cm	10 seconds	5 mm	x0.1
PS92/0054-1	1 cm	10 seconds	5 mm	x0.1
PS92/0056-1	<i>Not logged</i>			

Bulk density was derived from the attenuation of gamma rays passing through the cores. Calibration pieces made of aluminium with varying thicknesses were used to convert gamma-ray attenuation into bulk density. The aluminium calibration standards were placed in 1-m long piece of cylindrical core liner for the gravity core, and a 1-m plastic sampling box for the kastenlot core. These were filled with water and allowed to equilibrate to room temperature before the standards were logged. The aluminium standards had thicknesses of 0, 0.83, 1.65, 2.47, 3.29, 4.11, 4.93, 5.76, 6.6, 7.03 cm (for the kasten core) and 10, 9.01, 8.01, 7.01, 6.00, 5.01, 4.00, 3.01, 2.00, 1.01, 0 cm (for the gravity core).

Magnetic susceptibility was measured with a Bartington MS-2 loop sensor with a diameter of 110 mm. The MS-2 meter zeroed 20 cm before the core reached the sensor. No drift or volume corrections were applied to magnetic susceptibility measurements.

Preliminary results

Bulk density and magnetic susceptibility profiles for cores PS92/39-02-KC, PS92/45-02-GC and PS92/54-01-GC (Fig. 10.4), show similar patterns of downhole variability (Fig. 10.5).

10.3 Multi-sensor core logging

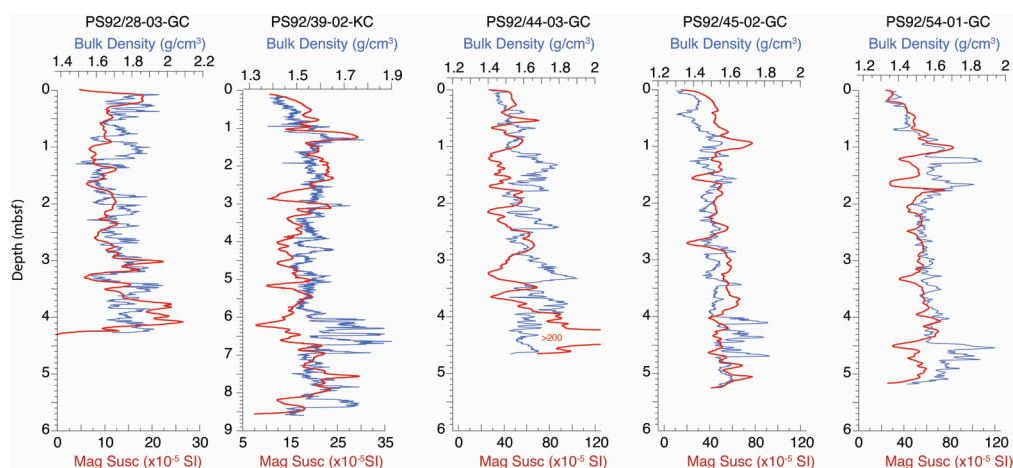


Fig. 10.4: Bulk density and magnetic susceptibility records for the gravity cores and kastenlot core from PS92

Downcore variations in magnetic susceptibility within these cores are similar to those seen in PS1533 (Fig. 10.5). Further correlation of these records should be possible using high-resolution point susceptibility measurements, XRF data, and magnetic stratigraphy, all to be performed onshore. The existing correlation can provide a preliminary age model and will be further tested through direct dating using biostratigraphy, ^{14}C , isotope stratigraphy and paleomagnetism.

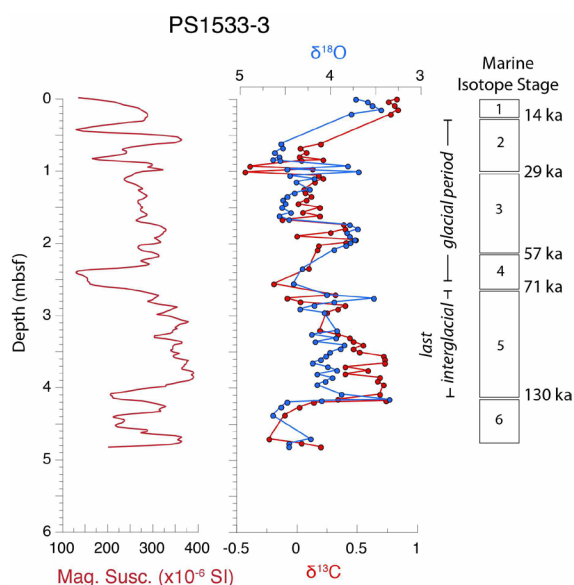


Fig. 10.5 : Magnetic susceptibility, isotope stratigraphy, and age model for PS-1533 (Age model from Spielhagen et al., 2004).

Data management

The MSCL data will be made available to all shipboard and shorebased participants after a final cleaning, and submitted to PANGAEA for long-term storage.

References

Spielhagen RF, Baumann K-H, Erlenkeuser H, Nowaczyk NR, Norgaard-Pedersen N, Vogt C, Weiel D (2004) Arctic Ocean deep-sea record of northern Eurasian ice sheet history: *Quaternary Science Reviews* 23, 1455–1483 doi: 10.1016/j.quascirev.2003.12.015.

10.4 Inorganic geochemistry

Christian März¹, Marie-Amelie Blais²,
Michael Nairn³

¹NUn
²Takuvik/UnL
³CUn

Objectives

The objectives of the inorganic geochemical studies during this expedition were to sample, analyse and conserve pore waters and sediments for the determination of dissolved and sedimentary concentrations of major and minor elements and element species. In the pore waters, a particular interest is in dissolved nutrients (PO_4^{3-} , NO_3^- , NH_4^+ , H_4SiO_4 etc.), metals (Fe^{2+} , Mn^{2+} , Mg^{2+} , Ba^{2+} etc.), and inorganic carbonate species (DIC, alkalinity). In the sediments, bulk contents of major (Al, Si, Fe, Ca, Mg etc.) and minor (Mn, Co, Mo, Ba, Sr etc.) elements as well as different iron species (carbonates, oxides, sulphides, silicates) will be investigated. This will provide insights into depositional processes and transport energies, terrigenous sediment provenance, primary productivity and nutrient availability, and early diagenetic processes (including the benthic recycling of nutrients to the bottom waters). A further interest is in the effect of early diagenetic processes and element mobilisations on the chemical composition of foraminifera tests preserved in the sediment.

Work at sea

During this expedition, pore water samples were taken for shipboard and shore-based inorganic-geochemical analyses. Pore waters were extracted in the scientific cool room (4°C) from pre-drilled Multicorer tubes using rhizone samplers and 12 mL plastic syringes. From gravity cores, the ~1 m long segments were transferred into the cool room as well, and rhizones were inserted through holes drilled into the plastic liner. Samples from the supernatant bottom waters, at the sediment-water interface, were taken from the Multicorer tubes at 1 cm resolution between 0 and 10 cm depth, 2 cm resolution between 10 and 20 cm depth, and 5 cm intervals below 20 cm depth. Gravity cores were sampled in regular intervals of 25 cm. No Box cores or kastenlot cores were sampled with rhizones. All stations, analysed parameters, and pore water splits are listed in Tab. 10.7.

Tab. 10.7: All stations with pore water samples, parameters determine onboard, and pore water splits for shore-based analysis MUC = Multicorer, GC = Gravity Corer, NUT = nutrients, TM = trace metals, DIC = dissolved inorganic carbon.

Station	Instrument	pH	Nutrient split	Metal split	DIC split	Ammonium	Sediments
19-19	MUC	X	X	X	X	X	X
27-14	MUC	X	X	X	X	X	X
28-3	GC		X	X		X	X
31-13	MUC	X	X	X	X	X	X
39-5	MUC	X	X	X	X	X	X
40-1	MUC	X	X	X	X	X	X
43-20	MUC	X	X	X	X	X	X
44-3	GC		X	X		X	X
45-2	GC		X	X		X	X
46-15	MUC	X	X	X	X	X	X
47-20	MUC	X	X	X	X	X	X

Station	Instrument	pH	Nutrient split	Metal split	DIC split	Ammonium	Sediments
54-1	GC		X	X		X	X
56-1	GC		X	X		X	X
56-5	MUC	X	X	X	X	X	X

Extracted pore water volumes ranged from ~8 to 12 mL (with maximum extraction times reaching from ~2 to 8 hours), and each sample was split into three aliquots for later analysis. Around 4-6 mL were stored in plastic centrifuge tubes for shipboard analysis of NH₄⁺ (see below) and shore-based analysis of other nutrients (PO₄³⁻, NO₃⁻, H₄SiO₄ etc). Around 3-4 mL were stored in cryogenic plastic vials for shore-based analysis of dissolved metal concentrations (Fe²⁺, Mn²⁺, Mg²⁺, Ba²⁺ etc) and metal over Calcium ratios (Mg/Ca, Li/Ca, B/Ca etc). Around 2 mL were stored in glass vials for shore-based analysis of inorganic carbonate parameters (DIC, alkalinity). Samples were conserved with either HgCl₂ (nutrient and carbonate splits) or concentrated HCl (metal splits), and stored at 4°C. Ammonium was analysed spectrophotometrically on board at 1:10 to 1:14 dilution with distilled water (Fig. 10.6).

Parallel to pore water sampling, sediment samples were taken from multicorer tubes, gravity and kastenlot cores using plastic and stainless steel devices. Multicorer tubes (from the same cast as the pore water tubes) were sampled within 1 hour after recovery at a continuous 1 cm downcore resolution. Before sampling, the pH value in each interval was analysed using a punch-in pH electrode (Fig. 10.7). In addition, the top 10 cm of the pore water tubes were taken as whole samples following pore water extraction. Gravity and kastenlot cores were sampled within 1 hour after splitting at a 10 cm downcore resolution, apart from intervals with marked lithology or colour changes that were sampled at 5 cm resolution. Sediment samples were stored in plastic zip-lock bags at -20°C, only the top 10 cm pore water tube samples were stored at 4°C.

Preliminary results

From the shipboard data, some initial interpretations can be made. In most of the studied sediment cores, there is a clear increase in NH₄⁺ concentrations with sediment depth (Fig. 10.6), while pH values decrease (Fig. 10.7). In the case of NH₄⁺, the pore water trends can be explained by increasing degrees of organic matter remineralization with sediment depth, releasing NH₄⁺ as one of the main degradation products. This NH₄⁺ diffuses towards the sediment-water interface and into the overlying water column, contributing to overall nitrogen cycling in the studied benthic environments. Differences in NH₄⁺ concentrations reflect different degrees of early diagenetic processes, driven by different amounts or reactivities of buried organic material. In some of the studied Multicorer tubes, for example, the NH₄⁺ concentrations are indistinguishable from the bottom water values down to 25 cm sediment depth; in other locations, NH₄⁺ concentrations reach ~70 µmol/L at the same depth interval. The pH trend is also related to early diagenetic processes, and can largely be explained by the generation of acidity (mostly carbonic acid formed by microbial CO₂ generation and its solution in the pore waters) as organic matter is degraded by microbes. These degradation processes are usually most intense in the top 5 cm of the sediment column, and this is where the steepest decline in pH values is typically found. Deeper than ~5 cm, pH values tend to stabilize at values around 7.4 to 7.5.

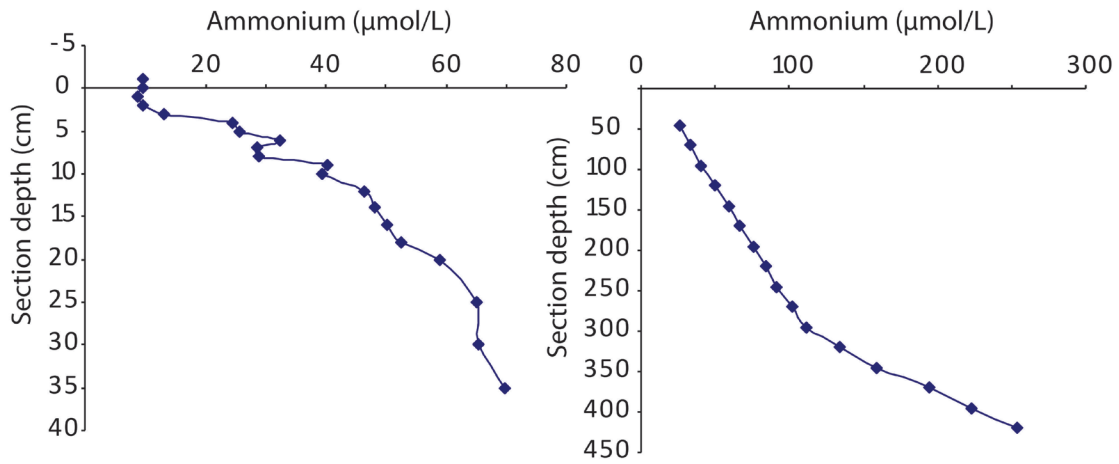


Fig. 10.6: Examples of NH_4^+ profiles

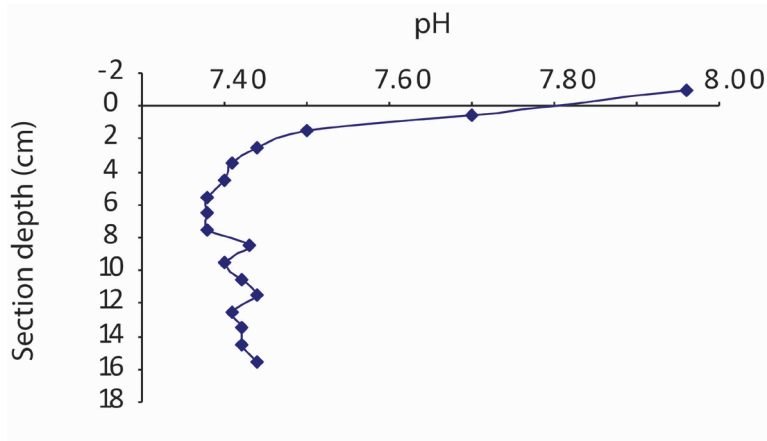


Fig. 10.7: Examples of a pH profile

Data management

Raw and processed data (shipboard and shorebased) will be made available in PANGAEA

10.5 Water column and sea ice studies

Kirstin Werner¹, Marie-Amelie Blais²,
Jutta Wollenburg³, Eunmi Park³ and Matt
O'Regan⁴

¹BPCRC
²Takuvik/UnL
³AWI
⁴SUn

Objectives

The objectives of using plankton tows during this expedition was to sample different depth intervals of the water column to investigate the abundance and distribution of foraminifera and pteropoda in the (sub-)surface waters, as well as their stable isotope and trace metal ratios. For comparison also sea ice samples have been taken. Geological records from the Arctic Ocean provide invaluable insights to climate and oceanographic changes in the high northern latitudes well beyond the period of historical and observational data acquisition. Uncertainties, however, often arise in paleoceanographic reconstructions due to a yet imperfect understanding of the living proxy's characteristics under certain ambient conditions. This study contributes to improving the modern-based proxy-to-ocean calibration and verification in the Arctic Ocean. An accurate understanding of the regional variability of proxy characteristics to modern seawater and sea ice conditions may facilitate reliable multiproxy geological reconstructions and conclusions on past Arctic environmental conditions.

Work at sea

Multinet studies

To complement micropaleontological investigations on planktonic microorganisms in the sediment records, 12 multinet casts were carried out collecting planktonic foraminifers, pteropods and ostracods from Polar Surface Water, Atlantic Layer and Upper Polar Deep Water (Tab. 10.8, Tab. 10.9). Five nets with a mesh size of 55 µm were used to catch plankton samples at different water intervals according to preceding CTD casts from the same station. Samples were sieved through 250 and 63 µm sieves and stained with a Rose Bengal/ethanol mixture to allow a differentiation between zooplankton that lived in a certain water column and those of allochthonous origin.

Tab. 10.8: Date, location and water depths of the multinet casts for the geology programme

Site	Date	Latitude	Longitude	Depth [m]
PS92/019-12	28.05.15	81° 11.55' N	18° 58.81' E	416.6
PS92/027-10	31.05.15	81° 21.39' N	17° 27.15' E	816.2
PS92/031-9	03.06.15	81° 35.08' N	18° 58.94' E	1356.4
PS92/032-10	07.06.15	81° 12.79' N	19° 36.55' E	452.4
PS92/039-14	12.06.15	81° 46.06' N	12° 27.48' E	1776.4
PS92/043-14	15.06.15	82° 12.78' N	7° 18.12' E	841.7
PS92/043-15	15.06.15	82° 12.83' N	7° 15.99' E	864.5
PS92/046-9	18.06.15	81° 53.09' N	9° 51.92' E	922.9
PS92/046-11	18.06.15	81° 52.73' N	9° 51.81' E	942.1
PS92/047-11	19.06.15	81° 20.29' N	13° 35.41' E	2184.7
PS92/047-12	20.06.15	81° 20.30' N	13° 35.50' E	2183.8
PS92/056-7	23.06.15	81° 0.94' N	8° 18.18' E	855.5

Tab. 10.9: Sampling intervals of the multinet casts

Station	Depth intervals [m]
PS92/19-12	0-20. 20-60. 60-100. 100-220. 220-301
PS92/27-10	0-20. 20-60. 60-100. 100-200. 200-515
PS92/31-09	0-30. 30-45. 45-100. 100-300. 300-500
PS92/32-10	0-35. 35-50. 50-100. 100-200. 200-400
PS92/39-14	0-40. 40-75. 75-120. 120-200. 200-750
PS92/43-14	0-20. 20-100. 100-200. 200-300. 300-750
PS92/43-15	0-20. 20-100. 100-200. 200-300. 300-750
PS92/46-09	0-20. 20-90. 90-150. 150-300. 300-750
PS92/46-10	0-60. 60-90. 90-150. 150-300. 300-750
PS92/47-11	0-25. 25-35. 35-80. 80-120. 120-850
PS92/47-12	0-35. 35-80. 80-120. 120-500. 500-850
PS92/56-07	0-40. 40-100. 100-250. 250-450. 450-700

Under-ice water and plankton sampling

Water under sea-ice floes (under-ice surface, under-ice chlorophyll a maximum, sackhole and meltpond water) were sampled by *K. Werner*. Water samples will be analysed for $d^{13}C$ and $d^{18}O$. In addition, the same samples have been filtered through 45 μm filters in order to investigate the potential abundance of planktonic foraminifera in water from and under the sea ice (Tab. 10.10). During the last four sea-ice stations *K. Werner* also sampled under-ice waters for plankton (uppermost 20 m) using a small hand net (mesh size 20 μm). Samples were stained with a Rose Bengal/Ethanol mixture. Filters and samples will be systematically studied under the microscope at home institutions.

Tab. 10.10: List of filtered water samples, ¹ as determined from fluorescence maximum

Site	Date	Latitude (N)	Longitude (E)	Filters
PS92/019-06	28.05.15	81° 11.55'	18° 58.81'	<ul style="list-style-type: none"> • Sackhole (ca 50 cm) • Under-ice surface • Under-ice chl a max.¹ • Ice core GEO1-1 • Ice core GEO1-2 (0-45 cm)
PS92/027-02	31.05.15	81° 21.39'	17° 27.15'	<ul style="list-style-type: none"> • Sackhole • Under-ice surface • Under-ice chl a max. (8 m)¹ • Mummy chair dirty ice sample
PS92/031-02	03.06.15	81° 35.08'	18° 58.94'	<ul style="list-style-type: none"> • Sackhole • Under-ice surface • Under-ice chl a max.¹ • Ice core GEO bottom (1 3-1 1m) • Ice core GEO (1 1-0 9 m) • Ice core GEO1 (1 02 m) • Ice core GEO2

Site	Date	Latitude (N)	Longitude (E)	Filters
PS92/032-04	07.06.15	81° 12.79'	19° 36.55'	<ul style="list-style-type: none"> • Sackhole • Under-ice surface • Under-ice chl a max.¹ • Ice core GEO • Ice core GEO2
PS92/039-06	12.06.15	81° 46.06'	12° 27.48'	<ul style="list-style-type: none"> • Sackhole • Under-ice surface • Under-ice chl a max. (3 m)¹ • Ice core GEO bottom • Ice core GEO top
PS92/043-04	15.06.15	82° 12.78'	7° 18.12'	<ul style="list-style-type: none"> • Sackhole • Under-ice surface • Under-ice chl a max.¹ • Ice core GEO complete • Dirty ice core 1-1 • Dirty ice core 1-2 • Dirty ice core #3 • Dirty ice Zodiac
PS92/046-01	18.06.15	81° 53.09'	9° 51.92'	<ul style="list-style-type: none"> • Sackhole • Under-ice surface • Under-ice chl a max.¹ • Ice core GEO complete
PS92/047-03	19.06.15	81° 20.29'	13° 35.41'	<ul style="list-style-type: none"> • Sackhole • Under-ice surface • Under-ice chl a max.¹ • meltpond • Ice core GEO complete

Sea ice and dirty ice sampling

Sea-ice cores were obtained from each of the sea-ice stations. The melted cores were filtered through a 0.45 µm filter. In addition, dirty ice was obtained from three stations during the cruise (Tab. 10.10), 2 by zodiac, and one large dirty ice flow visited by helicopter (Fig. 10.8). Samples from the dirty ice floes and filters will be systematically studied at home institutions.

Preliminary results

Treatment of samples will be carried out in home laboratories by *K. Werner* and *J. Wollenburg*, who will collaborate on micropaleontological assemblages of planktonic foraminifera. In addition, *J. Wollenburg* will analyse pteropods caught in the nets. *K. Werner* will furthermore investigate the geochemical composition of calcareous planktonic foraminifer shells for stable oxygen and carbon isotopes, trace metals, and, if applicable, radiogenic isotopes and compare results from living planktonic foraminifera to geochemical signatures in the water column and the sediment surface. Expected results will help understanding regional understanding and calibration of climate proxy indicators used in marine geology.



Fig. 10.8: Helicopter retrieval of diamict containing bolder size material on top of ice flow. Date of sampling was on 20.06.2015 at 81° 20.33' N and 13° 53.84' E.

Data management

Raw and processed data will be made available to all shipboard and shorebased, and submitted to PANGAEA for long-term storage.

10.6 Benthic foraminifera culturing experiments

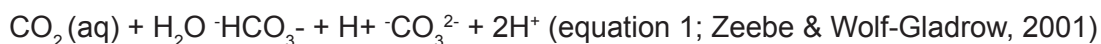
Jutta Wollenburg AWI

The environmental controls of trace metal (Mg/Ca, B/Ca, U/Ca) and boron isotope ratios recorded in calcareous tests of Arctic deep-sea benthic foraminifera – Culture experiments, modern field data and the long-term geological record

Objectives

The Arctic Ocean shows a strong positive feedback to climate change. Hereby, a rise in northern hemisphere air temperature is amplified in the Arctic Ocean by a factor of 2 to 4 (Miller et al., 2010; Seereze & Barry, 2011). This so-called Arctic amplification is the result of a collection of positive feedbacks to temperature rise with the strongest and quickest being melt of sea-ice and snow coverage, one of the slowest the melting of continental ice sheets (Seereze & Barry, 2011). As consequence of seasonal sea-ice retreat, primary production and via the continental shelf pump the uptake and export of CO₂ increases (Anderson et al., 2010). Exchange of carbon dioxide (CO₂) between atmosphere and ocean is a critical process of the polar oceans carbon cycle (Orr et al., 2009; McNeill et al., 2008) and an important determinant of past and future climate change (Tripathi et al., 2005). The polar oceans are the global sites of deep-water formation. Here production of dense water is supposed to occur preferably on the broad continental shelves where water not only is cooled to its freezing point, but also increases its salinity due to the accumulation of brine rejected during freezing of sea ice (Rudels & Quadfasel, 1991). This dense water flows down the slope and contributes to and ventilates the respective deep and bottom waters. Since ice-free surface waters are in equilibrium with the atmosphere large areas of ice-free water, sea-ice formation and deep convection are favourable for a high CO₂ uptake/deep-water storage in the polar oceans.

The present increase in anthropogenic CO₂ emissions and attendant increase in ocean acidification and sea ice melt decrease the pH and saturation state of carbonate ion concentrations in the Arctic Ocean (Orr et al., 2009; McNeill et al., 2008; Tanahua et al., 2009; Hauck et al., 2010). Hereby, the uptake of CO₂ by seawater increases the concentration of hydrogen ions, which lowers pH and, in changing the chemical equilibrium of the inorganic carbon system, reduces the concentration of carbonate ions (CO₃²⁻). If the CO₂ concentration changes, the carbonate ion concentration and pH change as a result of shifts in the equilibrium (see equation 1).



Since the boron isotope composition (¹¹B) is a pH-proxy (Hemming and Hanson, 1992) and the B/Ca, a proxy of bicarbonate ion concentration (Yu and Elderfield, 2007), the carbonate chemistry of the ocean can be reconstructed by analysis of these proxies in foraminiferal calcite. These parameters are master variables to reconstruct changes in surface to deep ocean carbon gradient and identify the natural carbon storage place in the glacial ocean.

However, for the Arctic Ocean deep-sea benthic foraminifer calibration curves for these proxies constrained by either core-top samples or culture experiments are lacking. Newly developed high-pressure aquaria have recently facilitated the first efficient cultivation (producing offspring) of our most trusted paleodeep-water recorder *Cibicides wuellerstorfi* (Wollenburg et al., 2015). The surface sediment samples collected during this cruise will be used to cultivate deep-water foraminifers at different pH values, pressures and in waters with different carbonate chemistries to establish the first species-specific trace metal and boron isotope calibration curves for the Polar Oceans. Core top analyses (0-15cm) of the collected multicorer samples will verify the experimental results.

Work at sea/preliminary results

For culturing we have successfully operated three multiple corer cast and transferred the surface sediments into push-cores for the transport in the cold lab at the AWI. Here push cores will be transferred into high-pressure aquaria running at 130 to 500bar and mesocosms running at atmospheric pressure (Table 10.11). We will culture these sediments for 5 months in calcein-tagged water. Hereby, new experimental offspring can be visualised by fluorescence analyses. The cultures will be kept at site-alike environmental conditions, and different but within the individual experiment stable pH-values of 7.9 to 8.5. Analyses on newly formed tests will start approximately 6 months after the expedition. The obtained results will be compared to results of comparable experiments from the last 4 years and from the Arctic and Antarctic Ocean

Trace metal and boron isotope analyses on foraminifera from surface samples from 10 additional multiple corer casts accomplish the data set (Table 10.12). From each cast 3 tubes were sampled, each with 10 cm diameter. Samples interval was 1 cm and samples from the upper 15 cm were treated with Rose Bengal to allow for the distinction of foraminifers that were recently alive. Working collaboratively with other shipboard and shore based scientists, these results will be related to DIC and alkalinity analyses on water samples from CTD casts and additional samples from the water covering the sediments in the respective multiple corer tubes.

Tab. 10.11: Location of dedicated Multicores collected for culturing experiments

Date	Site	Gear	Latitude	Longitude	Depth [m]
14.06.2016	PS92/42-1.2.3	Multi corer	82° 11.67 N	17° 45.11' E	1303.1

Tab. 10.12: List of sampled multicores for trace metal and boron analyses on forams.

Date	Site	Latitude	Longitude	Depth
29.05.2015	PS92/019-18	81°13.69'N	18°33.78'E	470.3m
29.05.2015	PS92/019-19	81°13.79'N	18°33.04'E	481.3m
01.06.2015	PS92/027-14	81°19.77'N	17°18.01'E	793.4m
04.06.2015	PS92/031-13	81°30.20'N	18°31.72'E	1851.3m
04.06.2015	PS92/031-14	81°29.27'N	18°25.56'E	1828.8m
08.06.2015	PS92/032-15	81°05.98'N	19°36.95'E	218.8m
08.06.2015	PS92/032-16	81°06.02'N	19°37.43'E	223.4m
11.06.2015	PS92/039-05	81°55.50'N	13°37.98'E	1522.6m
13.06.2015	PS92/040-01	81°49.04'N	10°52.06'E	1158m
14.06.2015	PS92/042-01	82°11.67'N	07°45.11'E	780.5m
16.06.2015	PS92/043-20	82°10.45'N	07°00.53'E	816.7m
18.06.2015	PS92/046-15	81°50.62'N	09°45.48'E	886.1m
20.06.2015	PS92/047-20	81°20.68'N	13°39.94'E	2174.7m
23.06.2015	PS92/056-05	81°00.94'N	08°17.05'E	853.8m

Acknowledgement: The culturing study is funded by DFG grant WO 742/2-1 of SPP 1158

References

- Anderson L G, Tanhua, T, Björk G, Hjalmarsson S, Jones E P, Jutterströma S, Rudels B, Swift J H, Wåhlistöma I (2010) Arctic ocean shelf basin interaction: An active continental shelf CO₂ pump and its impact on the degree of calcium carbonate solubility, *Deep-Sea Research I* 57, 869–879
- Hauck J, M Hoppema, R G J Bellerby, C Völker, Wolf-Gladrow, D (2010), Data-based estimation of anthropogenic carbon and acidification in the Weddell Sea on a decadal timescale, *J Geophys Res* 115, C03004, doi:10.1029/2009JC005479
- Hemmin N G, Hanson G N (1992), Boron isotopic composition and concentration in modern marine carbonates *Geochimica et Cosmochimica Acta* 56, 537–543
- Miller G H, Alley E B, Brigham-Grette J, Fitzpatrick J J, Polyak L, Serreze, M C White J W C (2010) Arctic amplification: can the past constrain the future? *Quatern Sci Rev* 29, 1779–1790
- McNeil B I, Matear, R J (2008), Southern Ocean acidification: A tipping point at 450-ppm atmospheric CO₂, *PNAS* 105(48), 18860-18864
- Nowaczyk R N, Freerichs T W, Eisenhauer A, Gard G (1994) Magnetostratigraphic data from late Quaternary sediments from the Yermak Plateau, Arctic Ocean: evidence for four geomagnetic polarity events within the last 170Ka of the Brunhes Chron *Geophys J Int*, 117, 453-471
- Orr, J C et al (2009), Amplified acidification of the Arctic Ocean, *IOP Conf Series: Earth and Environmental Science* 6, doi: 10.1088/1755-1307/6/6/462009
- Rudels B, Quadfasel D (1991), Convection and deep water formation in the Arctic Ocean-Greenland Sea system, *Journal of Marine Systems* 2, 3-4, 435-450
- Serreze M C, Barry R G (2011), Processes and impacts of Arctic amplification: A research synthesis *Global and Planetary Change* 77 (2011) 85–96
- Spielhagen R F, Baumann K -H, Erlenkeuser H, Nowaczyk N R, Norgaard- Pedersen N, Vogt C, Weiel D (2004) Arctic Ocean deep-sea record of northern Eurasian ice sheet history: *Quaternary Science Reviews* 23, 1455–1483 doi: 10.1016/j.quascirev.2003.12.015
- Stein R (with contributions of the participants, 2015) The Expedition PS87 of the Research Vessel *POLARSTERN* to the Arctic Ocean in 2014: *Berichte zur Polar- und Meeresforschung* 688,279p doi:10.2312/BzPM_0688_2015
- Tanhua T et al (2009), Ventilation of the Arctic Ocean: Mean ages and inventories of anthropogenic CO₂ and CFC-11, *J Geophys Res* 114, C01002, doi: 10.1029/2008JC004868
- Tripathi, S N, Dey, S, Tare, V, Satheesh, S K (2005) Aerosol black carbon radiative forcing at an industrial city in northern India *Geophysical Research Letters* 32: doi: 10.1029/2005GL022515 issn: 0094-8276
- Wollenburg J E, Raitzsch M, Tiedemann R (2015), Novel high-pressure culture experiments on deep-sea benthic foraminifera — Evidence for methane seepage-related $\delta^{13}\text{C}$ of *Cibicides wuellerstorfi*, *Marine Micropaleontology* 117, 47–64
- Yu J, Elderfield H (2007), Benthic foraminiferal B/Ca ratios reflect deep water carbonate saturation state, *Earth Planetary Sci Lett* 258, 73 – 86
- Zeebe R, Wolf-Gladrow D (2001), CO₂ in seawater: Equilibrium, kinetics, isotopes, *Elsevier Oceanogr Ser Vol 65*, Elsevier, Amsterdam

Data Management

After culturing and measuring the B/Ca ratios and B isotopes data will be published in peer reviewed journals and presented on international conferences. Final data will be submitted to a public data center (PANGAEA) after publication, after 5 years by the latest. Before this, for any data request, please contact Jutta Wollenburg.

APPENDIX

A.1 TEILNEHMENDE INSTITUTE / PARTICIPATING INSTITUTIONS

A.2 TEILNEHMER / PARTICIPANTS

A.3 SCHIFFSBESATZUNG / SHIP'S CREW

A.4 STATIONSLISTE PS92 / STATION LIST

A 1 TEILNEHMENDE INSTITUTE / PARTICIPATING INSTITUTIONS

	Address
AWI	Alfred-Wegener-Institut Helmholtz-Zentrum für Polar- und Meeresforschung Postfach 120161 27515 Bremerhaven Germany
ABWR	AquaBiota Water Research Löjtnantsgatan 25 SE-11550 Stockholm Sweden
APN	Akvaplan-niva AS Fram Centre 9296 Tromsø Norway
BPCRC	Byrd Polar & Climate Research Center 1090 Carmack Road The Ohio State University 43210-1002 Columbus USA
CAU	Christian-Albrechts-Universität zu Kiel Christian-Albrechts-Platz 4 D-24098 Kiel Germany
CUn	Cardiff University School of Earth and Ocean Sciences Main Building, Park Place CF10 3AT, Cardiff United Kingdom
DFO	Fisheries and Oceans Canada Freshwater Institute (FWI) 501 University Crescent R3T 2N6 Winnipeg Canada
DWD	Deutscher Wetterdienst Geschäftsbereich Wettervorhersage Seeschiffahrtsberatung Bernhard Nocht Str 76 20359 Hamburg Germany

A.1 Teilnehmende Institute / Participating Institutes

	Address
FMI	Finnish Meteorological Institute P O BOX 503 FI-00101 HELSINKI FINLAND
GEOMAR	Helmholtz-Zentrum für Ozeanforschung Kiel Wischhofstr 1-3 24119 Kiel Germany
HS-B	Hochschule Bremen Werderstraße 73 28199 Bremen Germany
HS-BRV	Hochschule Bremerhaven An der Karlstadt 8 27568 Bremerhaven Germany
IMARES	Institute for Marine Resources & Ecosystem Studies P O Box 167 1790 AD Den Burg (Texel) The Netherlands
IOPAN	Institute of Oceanology Polish Academy of Sciences Powstańców Warszawy 55 81-712 Sopot Poland
LEMAR	Laboratoire des sciences de l'Environnement MARin 20 avenue Le Gorgeu 29200 Brest France
LSCE	Laboratoire des Sciences du Climat et de l'Environnement, Unité mixte CEA-CNRS-UVSQ CE Saclay Orme des Merisiers F-91191, Gif-Sur-Yvette France
NTU	National Taiwan University Department of Geosciences No 1 Sec 4 Roosevelt Road P O Box 13-318 Da'an District, Taipei City Taiwan 10617

	Address
NPI	Norwegian Polar Institute Fram Centre, P O BOX 6606 Langnes N-9296 Tromsø Norway
NUn	Newcastle University School for Civil Engineering and Geosciences (CEG) Newcastle upon Tyne, NE1 7RU United Kingdom
PML	Plymouth Marine Laboratory Prospect Place The Hoe Plymouth, PL1 3DH United Kingdom
SUn	Stockholm University Department of Geological Sciences Svante Arrhenius väg 8 SE-106 91, Stockholm Sweden
UBr	University of Bristol Senate House Tyndall Avenue Bristol, BS8 1TH United Kingdom
UH	University of Helsinki Yliopistonkatu 4 00100 Helsinki Finland
UHB	University of Bremen Bibliothekstraße 1 28359 Bremen Germany
UHH	University of Hamburg Martin-Luther-King Platz 3 20146 Hamburg Germany
UiT	University of Tromsø Hansine Hansens veg 18 N-9019 Tromsø Norwegen

A.1 Teilnehmende Institute / Participating Institutes

	Address
UnS	Université de Sherbrooke, Faculté des lettres et Sciences Humaines, Département de Géomatique 2500 Boulevard de l'Université Sherbrooke QC J1K 2R1 Canada
UTR	Universität Trier Universitätsring 15 54286 Trier Germany
Takuvik/UnL	Takuvik Joint International Laboratory, Université Laval (Canada) - CNRS (France) Département de Biologie and Québec-Océan Pavillon Alexandre Vachon 1045, Avenue de la Médecine Université Laval Québec QC G1V 0A6 Canada
v D Met	Van Dorssen Metaalbewerking bv Schilderend 113 1791 BE Den Burg (Texel) The Netherlands

A. 2 FAHRTTEILNEHMER / CRUISE PARTICIPANTS

Name/ Last name	Vorname/ First name	Institut/ Institute	Beruf/Profession
Peeken	Ilka	AWI	Chief scientist, Sea ice ecology
Beaulieux	Marieke	UnS	Student, Green-Edge
Belter	Jakob	GEOMAR	Student, Sea ice physics
Blais	Marie-Amélie	Takuvik/UnL	Student, Green-Edge
Büttner	Stefan	GEOMAR	Student, Biogeochemistry
Castellani	Giulia	AWI	Scientist, Under Ice & zooplankton ecology
Dietrich	Ulrike	UHB	Student, Sea ice ecology
Dybwad	Christine	UiT	Student, Plankton ecology
Flores	Hauke	AWI/UHH	Group leader, Under ice and zooplankton ecology
Fong	Allison	AWI	Group leader, Plankton ecology
Fradette	Maxime	UnS	Student, Green-Edge
Gros	Valérie	LSCE	Group leader, Trace Gases
Hessel	Johanna	AWI	Student, Plankton ecology
Hölemann	Jens	AWI	Scientist, Oceanography
Immerz	Antonia	AWI	Student, Under ice and zooplankton ecology
Janout	Markus	AWI	Scientist, Oceanography
Juhls	Bennet	GEOMAR	Student, Oceanography
Katlein	Christian	AWI	Student, Sea ice physics
Kedra	Monika	IOPAN	Group leader, Benthos ecology
Korhonen	Meri	FMI/UH	Student, Oceanography
Kruppen	Thomas	AWI	Group leader, Sea ice physics
MacPhee	Shannon	DFO	Scientist, Sea ice ecology
März	Christian	NUn	Scientist, Geology
Matthießen	Jens	AWI	Scientist, Geology
McGovern	Maeve	APN/UiT	Student, Benthos ecology
Meler	Justyna	IOPAN	Technician, Biogeochemistry
Morata	Nathalie	APN/LEMAR	Scientist, Benthos ecology
Nairn	Michael	CUn	Student, Geology
Nikolopoulos	Anna	ABWR	Group leader, Oceanography
O'Regan	Matt	SUn	Group leader, Geology

A. 2 Fahrtteilnehmer / Cruise Participants

Name/ Last name	Vorname/ First name	Institut/ Institute	Beruf/Profession
Park	Eunmi	AWI	Student, Biogeochemistry
Randelhoff	Achim	NPI/UiT	Student, Oceanography
Sarda-Esteve	Roland	LSCE	Engineer, Trace Gases
Schaafsma	Fokje	IMARES	Student, Under ice and zooplankton ecology
Schulte-Kortnack	Sebastian	HS-B	Scientist, Sea ice physics
Stolle	Clara	AWI	Student, Geology
Ungermann	Mischa	AWI	Student, Sea ice ecology
van Dorssen	Michiel	v D Met	Technician, Under ice and zooplankton ecology
Vortkamp	Martina	AWI	Technician, Under ice and zooplankton ecology
Weng-si	Chao	NTU	Student, Geology
Werner	Kirstin	BPCRC	Scientist, Geology
Willmes	Sascha	UTR	Scientist, Sea ice physics
Wollenburg	Jutta	AWI	Scientist, Geology
Zablocka	Monika	IOPAN	Group leader, Biogeochemistry
Zwicker	Sarah	AWI	Student, Plankton ecology
Sonnabend,	Hartmut	DWD	Meteorology
ScientMiller	Max	DWD	Meteorology
Vaupel	Lars	HeliService	Helicopter
Brauer	Jens	HeliService	Helicopter
Rothenburg	Mark	HeliService	Helicopter
Richter	Roland	HeliService	Helicopter

A.3 SCHIFFSBESATZUNG / SHIP'S CREW

No	Name	Rank
1	Wunderlich, Thomas	Master
2	Spilok, Norbert	Doctor
3	Lauber, Felix	1.Offc.
4	Fallei, Holger	2.Offc.
5	Kentges, Felix	2.Offc.
6	Stolze, Henrik	2.Offc.
7	Westphal, Henning	Ch. Eng.
8	Buch, Erik-Torsten	2.Offc.
9	Rusch, Torben	2.Offc.
10	Schnürch, Helmut	2.Offc.
11	Brehme, Andreas	Elec.Tech.
12	Hofmann, Jörg	Comm.Offc.
13	Dimmler, Werner	ELO
14	Feiertag, Thomas	ELO
15	Ganter, Armin	ELO
16	Nasis, Ilias	ELO
17	Schröter, René	Boatsw
18	Neisner, Winfried	Carpenter
19	Burzan, Gerd-Ekkeh	A B
20	Clasen, Nils	A B
21	Gladow, Lothar	A B
22	Hartwig-Lab , Andreas	A B
23	Kretzschmar, Uwe	A B
24	Leisner, Bert	A B
25	Müller, Steffen	A B
26	Schröder, Norbert	A B
27	Sedlak, Andreas	A B
28	Beth, Detlef	Storek
29	Dinse, Horst	Mot-man
30	Klein, Gert	Mot-manM
31	Krösche, Eckard	Mot-man
32	Plehn, Markus	Mot-man
33	Watzel, Bernhard	Mot-man
34	Meißner, Jörg	Cook
35	Tupy, Mario	Cooksmate
36	Luoto, Eija	1 Steward
37	Wartenberg, Irina	2 Stwdss
38	Schwitzky-Schwarz, Carmen	Stwdss/Nurse

No	Name	Rank
39	Chen, Quan	2 Steward
40	Duka, Maribel	2nd
41	Hischke, Peggy	2nd
42	Hu, Guo Yong	2 Steward
43	Kelling, Elke	2nd
44	Ruan, Hui Guang	Laundrym.

A.4 STATIONS LISTE PS92 / STATION LIST

Station	Date	Time (UTC)	GEAR	Action	Position Lat	Position Lon	Water Depth (m)
PS92/0001-1	22 05 2015	12:12	TEST	on ground/ max depth	65° 15 65' N	3° 37 20' E	1266
PS92/0002-1	23 05 2015	20:30	FLOAT	on ground/ max depth	69° 55 45' N	4° 13 72' E	3266
PS92/0002-2	23 05 2015	20:38	XCTD	on ground/ max depth	69° 55 76' N	4° 18 05' E	3267
PS92/0003-1	24 05 2015	19:25	CTD/UW	on ground/ max depth	70° 52 41' N	13° 41 18' E	2340
PS92/0004-1	25 05 2015	6:24	CTD/UW	on ground/ max depth	72° 46 64' N	12° 33 41' E	1635
PS92/0005-1	25 05 2015	10:53	CTD/UW	on ground/ max depth	73° 35 73' N	12° 2 52' E	1936
PS92/0006-1	25 05 2015	14:26	CTD/UW	on ground/ max depth	74° 11 87' N	11° 38 85' E	2280
PS92/0007-1	25 05 2015	16:34	CTD/UW	on ground/ max depth	74° 35 04' N	11° 23 23' E	2429
PS92/0008-1	25 05 2015	19:27	CTD/UW	on ground/ max depth	75° 6 27' N	11° 1 54' E	2457
PS92/0009-1	26 05 2015	5:12	CTD/UW	on ground/ max depth	76° 45 97' N	9° 46 90' E	2300
PS92/0010-1	26 05 2015	7:40	CTD/RO	on ground/ max depth	77° 4 30' N	9° 30 88' E	2197
PS92/0011-1	26 05 2015	9:21	CTD/UW	on ground/ max depth	77° 14 55' N	9° 22 72' E	2104
PS92/0012-1	26 05 2015	14:26	CTD/UW	on ground/ max depth	78° 12 18' N	8° 42 33' E	1567
PS92/0013-1	26 05 2015	16:31	CTD/UW	on ground/ max depth	78° 35 41' N	8° 34 52' E	886
PS92/0014-1	26 05 2015	19:30	CTD/UW	on ground/ max depth	79° 9 76' N	8° 22 45' E	461
PS92/0015-1	26 05 2015	22:14	CTD/UW	on ground/ max depth	79° 41 88' N	8° 10 75' E	631
PS92/0016-1	27 05 2015	5:00	CTD/UW	on ground/ max depth	80° 25 35' N	13° 13 18' E	230
PS92/0017-1	27 05 2015	8:54	XCTD	on ground/ max depth	80° 43 06' N	16° 39 46' E	182
PS92/0018-1	27 05 2015	12:18	XCTD	on ground/ max depth	80° 53 11' N	18° 37 30' E	134
PS92/0019-1	27 05 2015	15:38	SUIT	on ground/ max depth	81° 0 70' N	19° 53 12' E	189
PS92/0019-2	27 05 2015	18:31	RMT	profile start	81° 2 48' N	19° 42 98' E	173
PS92/0019-3	27 05 2015	22:42	SEP	profile start	81° 9 73' N	19° 6 85' E	367
PS92/0019-5	28 05 2015	6:28	CTD/RO	on ground/ max depth	81° 10 43' N	19° 8 07' E	377
PS92/0019-6	28 05 2015	6:29	ICE	start of ice activities	81° 10 43' N	19° 8 07' E	377
PS92/0019-8	28 05 2015	10:45	CTD/RO	on ground/ max depth	81° 11 03' N	19° 6 89' E	392
PS92/0019-9	28 05 2015	12:28	ZODIAK	on ground/ max depth	81° 11 32' N	19° 6 08' E	417
PS92/0019-10	28 05 2015	13:31	ISP	on ground/ max depth	81° 11 43' N	19° 5 46' E	411
PS92/0019-11	28 05 2015	16:48	MN	on ground/ max depth	81° 11 53' N	19° 0 84' E	412

A.4 Stationsliste PS92 / Station List

Station	Date	Time (UTC)	GEAR	Action	Position Lat	Position Lon	Water Depth (m)
PS92/0019-12	28 05 2015	17:50	MN	on ground/ max depth	81° 11 55' N	18° 58 81' E	417
PS92/0019-13	28 05 2015	18:29	WP2	on ground/ max depth	81° 11 57' N	18° 57 49' E	412
PS92/0019-14	28 05 2015	19:10	CTD/RO	on ground/ max depth	81° 11 60' N	18° 56 15' E	411
PS92/0019-15	29 05 2015	7:26	CTD/RO	on ground/ max depth	81° 12 44' N	18° 41 03' E	432
PS92/0019-16	29 05 2015	8:29	BONGO	on ground/ max depth	81° 12 64' N	18° 39 36' E	439
PS92/0019-6	29 05 2015	11:10	ICE	end of ice activities	81° 12 75' N	18° 38 60' E	439
PS92/0019-18	29 05 2015	12:58	TVMUC	on ground/ max depth	81° 13 69' N	18° 33 78' E	470
PS92/0019-19	29 05 2015	13:35	TVMUC	on ground/ max depth	81° 13 79' N	18° 33 04' E	481
PS92/0019-20	29 05 2015	16:18	BC	on ground/ max depth	81° 14 08' N	18° 29 18' E	462
PS92/0019-21	29 05 2015	17:29	BC	on ground/ max depth	81° 14 23' N	18° 26 78' E	461
PS92/0020-1	29 05 2015	22:52	CTD/RO	on ground/ max depth	81° 1 91' N	19° 21 22' E	178
PS92/0020-2	29 05 2015	23:30	BONGO	on ground/ max depth	81° 2 04' N	19° 20 58' E	178
PS92/0020-3	30 05 2015	0:27	BC	on ground/ max depth	81° 2 23' N	19° 19 04' E	167
PS92/0020-4	30 05 2015	1:09	BC	on ground/ max depth	81° 2 33' N	19° 18 92' E	170
PS92/0021-1	30 05 2015	7:26	CTD/RO	on ground/ max depth	81° 4 35' N	18° 55 54' E	209
PS92/0022-1	30 05 2015	8:36	ICE	start of ice activities	81° 6,40' N	18° 42,77' E	307
PS92/0023-1	30 05 2015	10:36	CTD/RO	on ground/ max depth	81° 9 52' N	18° 29 46' E	393
PS92/0024-1	30 05 2015	13:18	CTD/RO	on ground/ max depth	81° 16 59' N	18° 40 22' E	516
PS92/0024-2	30 05 2015	14:50	RMT	profile start	81° 15 02' N	18° 35 45' E	478
PS92/0025-1	30 05 2015	17:35	CTD/RO	on ground/ max depth	81° 21 31' N	18° 8 68' E	712
PS92/0026-1	31 05 2015	0:43	CTD/RO	on ground/ max depth	81° 25 20' N	17° 28 97' E	918
PS92/0027-1	31 05 2015	5:33	SUIT	on ground/ max depth	81° 23 70' N	17° 43 38' E	882
PS92/0027-2	31 05 2015	6:26	ICE	start of ice activities	81° 23 18' N	17° 35 66' E	877
PS92/0027-3	31 05 2015	6:52	CTD/RO	on ground/ max depth	81° 23 13' N	17° 35 13' E	876
PS92/0027-4	31 05 2015	10:55	CTD/RO	on ground/ max depth	81° 22 53' N	17° 31 83' E	855
PS92/0027-5	31 05 2015	12:29	ZODIAK	on ground/ max depth	81° 22 28' N	17° 31 31' E	845
PS92/0027-6	31 05 2015	13:10	WP2	on ground/ max depth	81° 22 16' N	17° 31 13' E	842
PS92/0027-7	31 05 2015	14:30	CTD/RO	on ground/ max depth	81° 21 95' N	17° 30 67' E	835

Station	Date	Time (UTC)	GEAR	Action	Position Lat	Position Lon	Water Depth (m)
PS92/0027-8	31 05 2015	15:27	UVP	on ground/ max depth	81° 21 80' N	17° 30 12' E	830
PS92/0027-9	31 05 2015	17:17	MN	on ground/ max depth	81° 21 55' N	17° 28 56' E	821
PS92/0027-10	31 05 2015	18:37	MN	on ground/ max depth	81° 21 39' N	17° 27 15' E	816
PS92/0027-11	31 05 2015	19:41	BONGO	on ground/ max depth	81° 21 28' N	17° 26 06' E	815
PS92/0027-12	31 05 2015	20:27	ISP	on ground/ max depth	81° 21 21' N	17° 25 35' E	813
PS92/0027-13	01 06 2015	4:23	CTD/RO	on ground/ max depth	81° 20 07' N	17° 20 17' E	790
PS92/0027-14	01 06 2015	6:01	TVMUC	on ground/ max depth	81° 19 77' N	17° 18 01' E	793
PS92/0027-14	01 06 2015	6:58	TVMUC	on ground/ max depth	81° 19 55' N	17° 16 87' E	795
PS92/0027-15	01 06 2015	12:15	BC	on ground/ max depth	81° 18 30' N	17° 8 95' E	842
PS92/0027-2	01 06 2015	13:00	ICE	end of ice activities	81° 18 15' N	17° 7 82' E	851
PS92/0027-16	01 06 2015	13:19	BC	on ground/ max depth	81° 18 09' N	17° 7 37' E	854
PS92/0027-17	01 06 2015	14:58	RMT	profile start	81° 17 79' N	17° 6 17' E	866
PS92/0028-1	02 06 2015	9:46	CTD/RO	on ground/ max depth	81° 31 69' N	19° 27 32' E	939
PS92/0028-2	02 06 2015	10:43	BC	on ground/ max depth	81° 31 71' N	19° 27 39' E	940
PS92/0028-3	02 06 2015	12:00	GC	on ground/ max depth	81° 31 45' N	19° 25 91' E	933
PS92/0028-4	02 06 2015	13:26	SUIT	on ground/ max depth	81° 31 10' N	19° 24 93' E	928
PS92/0028-5	02 06 2015	16:15	RMT	profile start	81° 30 25' N	19° 18 11' E	908
PS92/0029-1	02 06 2015	19:11	CTD/RO	on ground/ max depth	81° 34 75' N	19° 49 04' E	1412
PS92/0030-1	03 06 2015	1:03	CTD/RO	on ground/ max depth	81° 36 99' N	19° 39 25' E	2287
PS92/0031-1	03 06 2015	4:55	SUIT	on ground/ max depth	81° 33 24' N	19° 34 06' E	1047
PS92/0031-2	03 06 2015	11:00	ICE	start of ice activities	81° 37 37' N	19° 26 92' E	2050
PS92/0031-3	03 06 2015	11:44	CTD/RO	on ground/ max depth	81° 37 20' N	19° 25 64' E	1963
PS92/0031-3	03 06 2015	14:09	ZODIAK	on ground/ max depth	81° 36 00' N	19° 20 00' E	1700
PS92/0031-4	03 06 2015	14:54	CTD/RO	on ground/ max depth	81° 36 54' N	19° 18 67' E	1524
PS92/0031-5	03 06 2015	16:13	BONGO	on ground/ max depth	81° 36 34' N	19° 15 45' E	1452
PS92/0031-6	03 06 2015	17:27	CTD/RO	on ground/ max depth	81° 36 17' N	19° 12 47' E	1409
PS92/0031-7	03 06 2015	18:47	UVP	on ground/ max depth	81° 35 96' N	19° 8 94' E	1347
PS92/0031-8	03 06 2015	20:17	MN	on ground/ max depth	81° 35 65' N	19° 4 58' E	1421
PS92/0031-9	03 06 2015	22:11	MN	on ground/ max depth	81° 35 08' N	18° 58 94' E	1356

A.4 Stationsliste PS92 / Station List

Station	Date	Time (UTC)	GEAR	Action	Position Lat	Position Lon	Water Depth (m)
PS92/0031-10	03 06 2015	23:14	ISP	on ground/ max depth	81° 34 72' N	18° 55 89' E	1366
PS92/0031-11	04 06 2015	7:01	ZODIAK	on ground/ max depth	81° 31 94' N	18° 40 63' E	1620
PS92/0031-12	04 06 2015	7:42	CTD/RO	on ground/ max depth	81° 31 61' N	18° 39 15' E	1714
PS92/0031-13	04 06 2015	10:30	TVMUC	on ground/ max depth	81° 30 20' N	18° 31 72' E	1852
PS92/0031-14	04 06 2015	12:38	TVMUC	on ground/ max depth	81° 29 27' N	18° 25 56' E	1829
PS92/0031-2	04 06 2015	16:38	ICE	end of ice activities	81° 28 18' N	18° 16 81' E	1576
PS92/0031-15	04 06 2015	18:23	BC	on ground/ max depth	81° 27 92' N	18° 15 10' E	1460
PS92/0031-16	04 06 2015	20:20	BC	on ground/ max depth	81° 28 47' N	18° 12 00' E	0
PS92/0031-17	04 06 2015	21:22	BC	on ground/ max depth	81° 28 19' N	18° 10 45' E	1656
PS92/0032-1	06 06 2015	8:12	CTD/RO	on ground/ max depth	81° 9 48' N	20° 0 89' E	320
PS92/0032-2	06 06 2015	8:49	BC	on ground/ max depth	81° 9 38' N	20° 0 76' E	312
PS92/0032-3	06 06 2015	9:29	BC	on ground/ max depth	81° 9 24' N	20° 0 62' E	290
PS92/0032-4	06 06 2015	16:45	ICE	start of ice activities	81° 14 16' N	19° 25 52' E	462
PS92/0032-5	06 06 2015	17:39	CTD/RO	on ground/ max depth	81° 14 00' N	19° 25 84' E	481
PS92/0032-6	06 06 2015	20:04	CTD/RO	on ground/ max depth	81° 13 76' N	19° 26 63' E	453
PS92/0032-7	07 06 2015	6:24	ISP	on ground/ max depth	81° 12 71' N	19° 35 01' E	438
PS92/0032-9	07 06 2015	9:19	MN	on ground/ max depth	81° 12 75' N	19° 36 31' E	447
PS92/0032-10	07 06 2015	10:28	MN	on ground/ max depth	81° 12 79' N	19° 36 55' E	452
PS92/0032-8	07 06 2015	10:39	ZODIAK	on ground/ max depth	81° 12 79' N	19° 36 61' E	453
PS92/0032-4	07 06 2015	13:30	ICE	end of ice activities	81° 12 58' N	19° 38 26' E	440
PS92/0032-11	07 06 2015	15:16	RMT	profile start	81° 10 21' N	19° 43 77' E	320
PS92/0032-12	07 06 2015	17:17	SUIT	on ground/ max depth	81° 10 59' N	19° 42 52' E	336
PS92/0032-13	08 06 2015	4:33	UVP	on ground/ max depth	81° 6 06' N	19° 35 22' E	250
PS92/0032-14	08 06 2015	5:07	CTD/RO	on ground/ max depth	81° 6 04' N	19° 35 38' E	246
PS92/0032-15	08 06 2015	6:15	TVMUC	on ground/ max depth	81° 5 98' N	19° 36 95' E	219
PS92/0032-16	08 06 2015	7:09	TVMUC	on ground/ max depth	81° 6 02' N	19° 37 43' E	223
PS92/0032-16	08 06 2015	7:18	TVMUC	on ground/ max depth	81° 6 01' N	19° 37 50' E	220
PS92/0032-17	08 06 2015	8:05	BONGO	on ground/ max depth	81° 5 98' N	19° 38 51' E	209

Station	Date	Time (UTC)	GEAR	Action	Position Lat	Position Lon	Water Depth (m)
PS92/0032-18	08 06 2015	8:52	BONGO	on ground/ max depth	81° 6 11' N	19° 41 43' E	196
PS92/0032-19	08 06 2015	9:20	ISP	on ground/ max depth	81° 6 12' N	19° 41 66' E	192
PS92/0033-1	09 06 2015	4:46	CTD/RO	on ground/ max depth	81° 8 98' N	17° 45 99' E	514
PS92/0034-1	09 06 2015	7:08	CTD/RO	on ground/ max depth	81° 12 56' N	17° 14 34' E	785
PS92/0035-1	09 06 2015	8:57	CTD/RO	on ground/ max depth	81° 15 51' N	17° 3 12' E	925
PS92/0036-2	09 06 2015	11:11	ZODIAK	on ground/ max depth	81° 20 40' N	16° 45 99' E	1505
PS92/0036-1	09 06 2015	11:23	CTD/RO	on ground/ max depth	81° 20 48' N	16° 46 22' E	1506
PS92/0037-1	09 06 2015	14:24	CTD/RO	on ground/ max depth	81° 19 37' N	16° 20 64' E	2253
PS92/0038-1	09 06 2015	16:55	SUIT	on ground/ max depth	81° 20 15' N	16° 19 53' E	2278
PS92/0038-2	09 06 2015	18:16	RMT	profile start	81° 20 21' N	16° 6 77' E	2274
PS92/0039-1	11 06 2015	1:10	SEP	profile start	82° 1 89' N	15° 15 71' E	2094
PS92/0039-2	11 06 2015	5:44	KAL	on ground/ max depth	81° 56 99' N	13° 49 70' E	1464
PS92/0039-3	11 06 2015	7:18	BC	on ground/ max depth	81° 56 61' N	13° 44 72' E	1493
PS92/0039-4	11 06 2015	9:00	BC	on ground/ max depth	81° 56 25' N	13° 41 59' E	1507
PS92/0039-5	11 06 2015	11:00	TVMUC	on ground/ max depth	81° 55 50' N	13° 37 98' E	1523
PS92/0039-6	11 06 2015	12:49	ICE	start of ice activities	81° 56 23' N	13° 34 20' E	1571
PS92/0039-7	11 06 2015	13:18	ZODIAK	on ground/ max depth	81° 55 99' N	13° 32 87' E	1572
PS92/0039-8	11 06 2015	15:05	CTD/RO	on ground/ max depth	81° 55 04' N	13° 27 55' E	1589
PS92/0039-9	11 06 2015	18:19	CTD/RO	on ground/ max depth	81° 53 24' N	13° 15 99' E	1609
PS92/0039-10	11 06 2015	20:06	UVP	on ground/ max depth	81° 52 28' N	13° 9 33' E	1624
PS92/0039-11	11 06 2015	21:03	CTD/RO	on ground/ max depth	81° 51 79' N	13° 5 80' E	1630
PS92/0039-12	12 06 2015	4:27	BONGO	on ground/ max depth	81° 48 00' N	12° 38 90' E	1731
PS92/0039-13	12 06 2015	5:58	MN	on ground/ max depth	81° 47 28' N	12° 34 27' E	1741
PS92/0039-14	12 06 2015	8:13	MN	on ground/ max depth	81° 46 06' N	12° 27 48' E	1776
PS92/0039-15	12 06 2015	9:31	CTD/RO	on ground/ max depth	81° 45 40' N	12° 23 60' E	1827
PS92/0039-16	12 06 2015	12:18	ISP	on ground/ max depth	81° 44 04' N	12° 14 76' E	1872
PS92/0039-6	12 06 2015	17:57	ICE	end of ice activities	81° 41 34' N	11° 53 46' E	1917
PS92/0039-17	12 06 2015	19:04	SUIT	on ground/ max depth	81° 39 18' N	11° 48 89' E	1972
PS92/0040-1	13 06 2015	11:50	TVMUC	on ground/ max depth	81° 49 04' N	10° 52 06' E	1158

A.4 Stationsliste PS92 / Station List

Station	Date	Time (UTC)	GEAR	Action	Position Lat	Position Lon	Water Depth (m)
PS92/0040-1	13 06 2015	11:55	TVMUC	on ground/ max depth	81° 49 04' N	10° 52 06' E	1158
PS92/0040-2	13 06 2015	12:39	XCTD	on ground/ max depth	81° 48 88' N	10° 50 69' E	1157
PS92/0040-3	13 06 2015	12:51	XCTD	on ground/ max depth	81° 48 88' N	10° 50 01' E	1155
PS92/0040-4	13 06 2015	13:25	CTD/RO	on ground/ max depth	81° 48 79' N	10° 47 96' E	1151
PS92/0041-1	14 06 2015	11:04	XCTD	on ground/ max depth	82° 7 40' N	7° 47 89' E	775
PS92/0041-2	14 06 2015	11:14	XCTD	on ground/ max depth	82° 7 23' N	7° 50 96' E	760
PS92/0042-1	14 06 2015	19:12	TVMUC	on ground/ max depth	82° 11 67' N	7° 45 11' E	781
PS92/0042-2	14 06 2015	20:25	TVMUC	on ground/ max depth	82° 11 76' N	7° 43 19' E	792
PS92/0042-3	14 06 2015	21:40	TVMUC	on ground/ max depth	82° 11 85' N	7° 41 12' E	802
PS92/0043-1	14 06 2015	23:18	CTD/RO	on ground/ max depth	82° 12 01' N	7° 39 45' E	796
PS92/0043-2	15 06 2015	0:51	BC	on ground/ max depth	82° 12 32' N	7° 38 06' E	797
PS92/0043-3	15 06 2015	1:56	BC	on ground/ max depth	82° 12 54' N	7° 37 46' E	806
PS92/0043-4	15 06 2015	4:00	ICE	start of ice activities	82° 12 70' N	7° 35 70' E	806
PS92/0043-5	15 06 2015	4:45	CTD/RO	on ground/ max depth	82° 12 67' N	7° 35 30' E	804
PS92/0043-6	15 06 2015	7:25	CTD/RO	on ground/ max depth	82° 12 63' N	7° 31 86' E	809
PS92/0043-7	15 06 2015	8:06	UVP	on ground/ max depth	82° 12 57' N	7° 30 87' E	811
PS92/0043-8	15 06 2015	10:00	ZODIAK	on ground/ max depth	82° 12 50' N	7° 27 99' E	819
PS92/0043-9	15 06 2015	10:51	CTD/RO	on ground/ max depth	82° 12 51' N	7° 26 40' E	822
PS92/0043-10	15 06 2015	11:43	BONGO	on ground/ max depth	82° 12 54' N	7° 24 67' E	813
PS92/0043-12	15 06 2015	12:08	ZODIAK	on ground/ max depth	82° 12 57' N	7° 23 80' E	806
PS92/0043-11	15 06 2015	12:13	BONGO	on ground/ max depth	82° 12 58' N	7° 23 62' E	806
PS92/0043-13	15 06 2015	13:25	MN	on ground/ max depth	82° 12 67' N	7° 21 08' E	816
PS92/0043-14	15 06 2015	14:55	MN	on ground/ max depth	82° 12 78' N	7° 18 12' E	842
PS92/0043-15	15 06 2015	16:15	MN	on ground/ max depth	82° 12 83' N	7° 15 99' E	865
PS92/0043-16	15 06 2015	17:17	UVP	on ground/ max depth	82° 12 83' N	7° 14 41' E	880
PS92/0043-17	15 06 2015	17:43	ISP	on ground/ max depth	82° 12 81' N	7° 13 87' E	869
PS92/0043-18	15 06 2015	22:48	MN	on ground/ max depth	82° 12 47' N	7° 8 55' E	871
PS92/0043-19	16 06 2015	6:37	ZODIAK	on ground/ max depth	82° 11 71' N	7° 5 56' E	842

Station	Date	Time (UTC)	GEAR	Action	Position Lat	Position Lon	Water Depth (m)
PS92/0043-20	16 06 2015	10:53	TVMUC	on ground/ max depth	82° 10 45' N	7° 0 53' E	817
PS92/0043-4	16 06 2015	11:17	ICE	end of ice activities	82° 10 34' N	6° 59 98' E	816
PS92/0043-21	16 06 2015	12:27	BC	on ground/ max depth	82° 10 06' N	6° 58 49' E	0
PS92/0043-22	16 06 2015	13:22	BC	on ground/ max depth	82° 9 89' N	6° 57 39' E	804
PS92/0043-23	16 06 2015	16:20	SUIT	on ground/ max depth	82° 9 85' N	7° 1 12' E	806
PS92/0043-24	16 06 2015	17:34	SUIT	on ground/ max depth	82° 9 06' N	7° 3 23' E	796
PS92/0044-1	17 06 2015	7:36	SUIT	on ground/ max depth	81° 56 31' N	9° 15 79' E	808
PS92/0044-2	17 06 2015	8:41	XCTD	on ground/ max depth	81° 55 49' N	9° 16 29' E	813
PS92/0044-3	17 06 2015	9:32	GC	on ground/ max depth	81° 56 02' N	9° 15 14' E	800
PS92/0045-1	17 06 2015	12:41	SUIT	on ground/ max depth	81° 54 56' N	9° 48 21' E	914
PS92/0045-2	17 06 2015	14:04	GC	on ground/ max depth	81° 53 60' N	9° 46 13' E	915
PS92/0046-1	17 06 2015	15:44	ICE	start of ice activities	81° 53 48' N	9° 43 95' E	907
PS92/0046-2	17 06 2015	16:15	CTD/RO	on ground/ max depth	81° 53 44' N	9° 43 69' E	906
PS92/0046-3	17 06 2015	18:52	CTD/RO	on ground/ max depth	81° 53 39' N	9° 42 13' E	898
PS92/0046-4	17 06 2015	20:29	CTD/RO	on ground/ max depth	81° 53 37' N	9° 41 43' E	891
PS92/0046-5	17 06 2015	21:12	ISP	on ground/ max depth	81° 53 37' N	9° 41 33' E	890
PS92/0046-6	18 06 2015	4:30	BONGO	on ground/ max depth	81° 53 54' N	9° 49 24' E	925
PS92/0046-7	18 06 2015	5:02	BONGO	on ground/ max depth	81° 53 50' N	9° 49 99' E	925
PS92/0046-8	18 06 2015	6:06	MN	on ground/ max depth	81° 53 38' N	9° 51 11' E	929
PS92/0046-9	18 06 2015	7:32	MN	on ground/ max depth	81° 53 09' N	9° 51 92' E	923
PS92/0046-10	18 06 2015	7:45	ZODIAK	on ground/ max depth	81° 53 03' N	9° 51 98' E	924
PS92/0046-11	18 06 2015	8:49	MN	on ground/ max depth	81° 52 73' N	9° 51 81' E	942
PS92/0046-12	18 06 2015	9:47	BONGO	on ground/ max depth	81° 52 42' N	9° 51 21' E	943
PS92/0046-13	18 06 2015	10:19	BONGO	on ground/ max depth	81° 52 24' N	9° 50 84' E	948
PS92/0046-14	18 06 2015	16:16	CTD/RO	on ground/ max depth	81° 50 72' N	9° 46 19' E	889
PS92/0046-1	18 06 2015	17:00	ICE	end of ice activities	81° 50 65' N	9° 45 76' E	888
PS92/0046-15	18 06 2015	17:24	TVMUC	on ground/ max depth	81° 50 62' N	9° 45 48' E	886
PS92/0046-16	18 06 2015	18:28	BC	on ground/ max depth	81° 50 55' N	9° 44 65' E	883

A.4 Stationsliste PS92 / Station List

Station	Date	Time (UTC)	GEAR	Action	Position Lat	Position Lon	Water Depth (m)
PS92/0047-1	19 06 2015	7:15	SUIT	on ground/ max depth	81° 22 77' N	13° 39 11' E	2139
PS92/0047-2	19 06 2015	9:50	RMT	profile start	81° 21 42' N	13° 36 66' E	2155
PS92/0047-3	19 06 2015	11:20	ICE	start of ice activities	81° 20 89' N	13° 36 75' E	2169
PS92/0047-4	19 06 2015	12:03	CTD/RO	on ground/ max depth	81° 20 80' N	13° 36 56' E	2171
PS92/0047-5	19 06 2015	12:47	ZODIAK	on ground/ max depth	81° 20 71' N	13° 36 43' E	2169
PS92/0047-6	19 06 2015	14:52	CTD/RO	on ground/ max depth	81° 20 50' N	13° 36 52' E	2175
PS92/0047-7	19 06 2015	17:57	CTD/RO	on ground/ max depth	81° 20 34' N	13° 36 87' E	2174
PS92/0047-8	19 06 2015	19:14	BONGO	on ground/ max depth	81° 20 32' N	13° 36 69' E	2176
PS92/0047-9	19 06 2015	19:43	BONGO	on ground/ max depth	81° 20 31' N	13° 36 57' E	2177
PS92/0047-10	19 06 2015	21:15	MN	on ground/ max depth	81° 20 30' N	13° 36 03' E	2184
PS92/0047-11	19 06 2015	23:07	MN	on ground/ max depth	81° 20 29' N	13° 35 41' E	2185
PS92/0047-12	20 06 2015	0:34	MN	on ground/ max depth	81° 20 30' N	13° 35 50' E	2184
PS92/0047-13	20 06 2015	6:15	BONGO	on ground/ max depth	81° 20 74' N	13° 40 49' E	2176
PS92/0047-14	20 06 2015	6:45	BONGO	on ground/ max depth	81° 20 79' N	13° 41 01' E	2177
PS92/0047-15	20 06 2015	6:46	ZODIAK	on ground/ max depth	81° 20 79' N	13° 41 02' E	2177
PS92/0047-16	20 06 2015	7:27	ISP	on ground/ max depth	81° 20 85' N	13° 41 54' E	2178
PS92/0047-17	20 06 2015	8:11	ZODIAK	on ground/ max depth	81° 20 90' N	13° 41 87' E	2176
PS92/0047-18	20 06 2015	11:51	MN	on ground/ max depth	81° 20 92' N	13° 41 35' E	2176
PS92/0047-19	20 06 2015	13:53	CTD/RO	on ground/ max depth	81° 20 79' N	13° 40 56' E	2177
PS92/0047-20	20 06 2015	16:07	TVMUC	on ground/ max depth	81° 20 68' N	13° 39 94' E	2175
PS92/0047-3	20 06 2015	16:41	ICE	end of ice activities	81° 20 67' N	13° 39 79' E	2174
PS92/0047-21	20 06 2015	18:20	BC	on ground/ max depth	81° 20 64' N	13° 39 22' E	2168
PS92/0047-22	20 06 2015	19:49	BC	on ground/ max depth	81° 20 64' N	13° 38 32' E	2167
PS92/0047-23	20 06 2015	23:11	RMT	profile start	81° 19 79' N	13° 36 39' E	2173
PS92/0048-1	21 06 2015	7:10	SUIT	on ground/ max depth	81° 0 90' N	12° 57 28' E	2048
PS92/0048-2	21 06 2015	8:18	XCTD	on ground/ max depth	81° 1 63' N	12° 50 33' E	2075
PS92/0049-1	21 06 2015	13:43	SUIT	on ground/ max depth	81° 1 73' N	12° 47 88' E	2080
PS92/0050-1	21 06 2015	19:38	CTD/RO	on ground/ max depth	81° 1 00' N	11° 26 59' E	2096

PS92 (ARK-XXIX/1)

Station	Date	Time (UTC)	GEAR	Action	Position Lat	Position Lon	Water Depth (m)
PS92/0051-1	22 06 2015	1:03	CTD/RO	on ground/ max depth	81° 4 89' N	10° 12 97' E	1786
PS92/0052-1	22 06 2015	4:42	CTD/RO	on ground/ max depth	81° 7 07' N	9° 44 66' E	1507
PS92/0053-1	22 06 2015	8:46	CTD/RO	on ground/ max depth	81° 5 50' N	9° 14 57' E	1057
PS92/0054-1	22 06 2015	14:31	GC	on ground/ max depth	81° 7 38' N	8° 27 97' E	1145
PS92/0055-1	22 06 2015	17:48	CTD/RO	on ground/ max depth	81° 10 07' N	8° 9 75' E	892
PS92/0055-2	22 06 2015	18:27	SEP	profile start	81° 10 12' N	8° 9 39' E	885
PS92/0056-1	23 06 2015	10:58	GC	on ground/ max depth	81° 1 19' N	8° 14 27' E	855
PS92/0056-2	23 06 2015	12:16	SUIT	on ground/ max depth	81° 0 97' N	8° 12 11' E	849
PS92/0056-3	23 06 2015	14:14	CTD/RO	on ground/ max depth	81° 0 98' N	8° 16 26' E	854
PS92/0056-4	23 06 2015	14:35	ZODIAK	on ground/ max depth	81° 0 97' N	8° 16 43' E	854
PS92/0056-5	23 06 2015	15:45	TVMUC	on ground/ max depth	81° 0 94' N	8° 17 05' E	854
PS92/0056-6	23 06 2015	16:31	BONGO	on ground/ max depth	81° 0 94' N	8° 17 51' E	854
PS92/0056-7	23 06 2015	17:27	MN	on ground/ max depth	81° 0 94' N	8° 18 18' E	856
PS92/0057-1	24 06 2015	09:18	XCTD	on ground/ max depth	80° 26 67' N	8° 59 53' E	861
PS92/0058-1	24 06 2015	10:31	XCTD	on ground/ max depth	80° 19 59' N	8° 56 69' E	645
PS92/0059-1	24 06 2015	13:00	HS_PS	profile start	80° 14 83' N	11° 2 33' E	235
PS92/0060-1	24 06 2015	13:33	XCTD	on ground/ max depth	80° 12 71' N	10° 39 90' E	411
PS92/0061-1	24 06 2015	19:20	XCTD	on ground/ max depth	79° 59 23' N	7° 55 39' E	525
PS92/0062-1	25 06 2015	09:09	XCTD	on ground/ max depth	80° 9 28' N	8° 40 27' E	537
PS92/0064-1	26 06 2015	02:50	XCTD	on ground/ max depth	80° 4 49' N	9° 44 94' E	528
PS92/0065-1	26 06 2015	07:45	CTD/UW	on ground/ max depth	80° 5 53' N	10° 17 28' E	524
PS92/0066-1	26 06 2015	10:33	CTD/UW	on ground/ max depth	80° 1 25' N	9° 45 20' E	498
PS92/0067-1	26 06 2015	13:22	CTD/UW	on ground/ max depth	79° 56 77' N	10° 1 86' E	476
PS92/0068-1	26 06 2015	16:31	CTD/UW	on ground/ max depth	80° 8 06' N	11° 8 60' E	210
PS92/0069-1	26 06 2015	20:16	XCTD	on ground/ max depth	80° 3 20' N	10° 47 80' E	406
PS92/0059-1	27 06 2015	03:00	HS_PS	profile end	80° 3 82' N	11° 2 10' E	260

Gear abbreviations:

BC	Box corer		RMT	Rectangular Midwater Trawl
BONGO	Bongo net		SEP	Sediment Profile Imaging
CTD/RO	CTD/Rosette water sampler		SUIT	Surface Under Ice Trawl
CTD/UW	UNDERWAY-CTD		TEST	Test
FLOAT	FLOAT		TVMUC	Television Multicorer
GC	Gravity corer		UVP	Underwater Video Profiler
HS_PS	HydroSweep/ParaSound		WP2	WP-2 Bucket Net
ICE	Ice station profile			
ISP	In situ Pump		XCTD	Expendable CTD
KAL	Kastenlot		ZODIAK	Rubber boat, Zodiac
MN	Multiple Net			

Die **Berichte zur Polar- und Meeresforschung** (ISSN 1866-3192) werden beginnend mit dem Band 569 (2008) als Open-Access-Publikation herausgegeben. Ein Verzeichnis aller Bände einschließlich der Druckausgaben (ISSN 1618-3193, Band 377-568, von 2000 bis 2008) sowie der früheren **Berichte zur Polarforschung** (ISSN 0176-5027, Band 1-376, von 1981 bis 2000) befindet sich im electronic Publication Information Center (**ePIC**) des Alfred-Wegener-Instituts, Helmholtz-Zentrum für Polar- und Meeresforschung (AWI); see <http://epic.awi.de>. Durch Auswahl "Reports on Polar- and Marine Research" (via "browse"/"type") wird eine Liste der Publikationen, sortiert nach Bandnummer, innerhalb der absteigenden chronologischen Reihenfolge der Jahrgänge mit Verweis auf das jeweilige pdf-Symbol zum Herunterladen angezeigt.

The **Reports on Polar and Marine Research** (ISSN 1866-3192) are available as open access publications since 2008. A table of all volumes including the printed issues (ISSN 1618-3193, Vol. 377-568, from 2000 until 2008), as well as the earlier **Reports on Polar Research** (ISSN 0176-5027, Vol. 1-376, from 1981 until 2000) is provided by the electronic Publication Information Center (**ePIC**) of the Alfred Wegener Institute, Helmholtz Centre for Polar and Marine Research (AWI); see URL <http://epic.awi.de>. To generate a list of all Reports, use the URL <http://epic.awi.de> and select "browse"/ "type" to browse "Reports on Polar and Marine Research". A chronological list in declining order will be presented, and pdf icons displayed for downloading.

Zuletzt erschienene Ausgaben:

Recently published issues:

694 (2016) The Expedition PS92 of the Research Vessel POLARSTERN to the Arctic Ocean in 2015, edited by Ilka Peeken

693 (2015) The Expedition PS93.2 of the Research Vessel POLARSTERN to the Fram Strait in 2015, edited by Thomas Soltwedel

692 (2015) Antarctic Specific Features of the Greenhouse Effect: A Radiative Analysis Using Measurements and Models by Holger Schmithüsen

691 (2015) Krill in the Arctic and the Atlantic Climatic Variability and Adaptive Capacity by Lara Kim Hünlerlage

690 (2015) High latitudes and high mountains: driver of or driven by global change? 26th Intern. Congress on Polar Research, 6 – 11 September 2015, Munich, Germany, German Society for Polar Research, edited by Eva-Maria Pfeiffer, Heidemarie Kassens, Christoph Mayer, Mirko Scheinert, Ralf Tiedemann and Members of the DGP Advisory Board

689 (2015) The Expedition PS89 of the Research Vessel POLARSTERN to the Weddell Sea in 2014/2015, edited by Olaf Boebel

688 (2015) The Expedition PS87 of the Research Vessel POLARSTERN to the Arctic Ocean in 2014, edited by Rüdiger Stein

687 (2015) The Expedition PS85 of the Research Vessel POLARSTERN to the Fram Strait in 2014, edited by Ingo Schewe

686 (2015) Russian-German Cooperation CARBOPERM: Field campaigns to Bol'shoy Lyakhovsky Island in 2014, edited by Georg Schwamborn and Sebastian Wetterich

685 (2015) The Expedition PS86 of the Research Vessel POLARSTERN to the Arctic Ocean in 2014, edited by Antje Boetius

684 (2015) Russian-German Cooperation SYSTEM LAPTEV SEA: The Expedition Lena 2012, edited by Thomas Opel



ALFRED-WEGENER-INSTITUT
HELMHOLTZ-ZENTRUM FÜR POLAR-
UND MEERESFORSCHUNG

BREMERHAVEN

Am Handelshafen 12
27570 Bremerhaven
Telefon 0471 4831-0
Telefax 0471 4831-1149
www.awi.de

